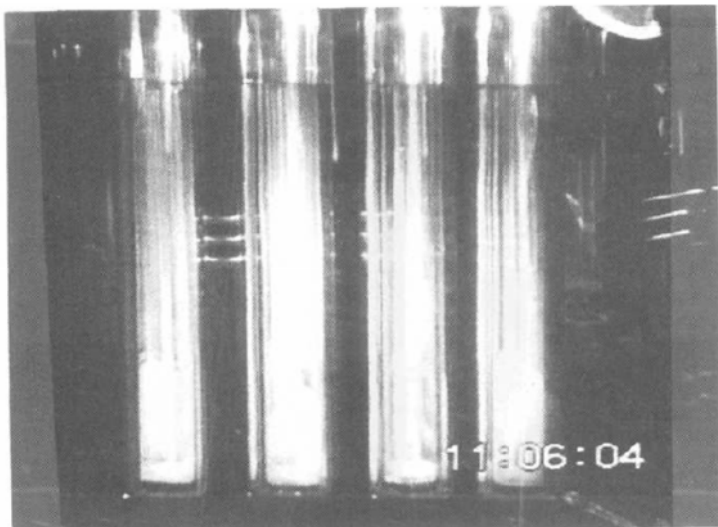
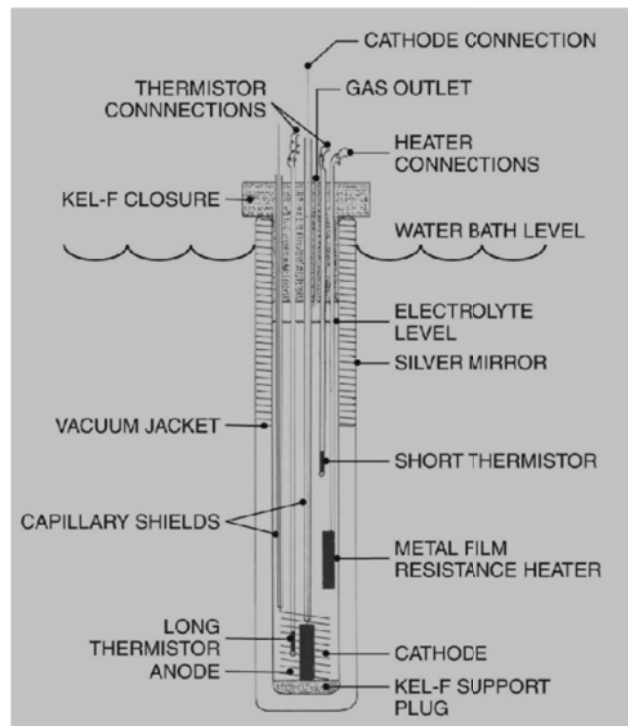
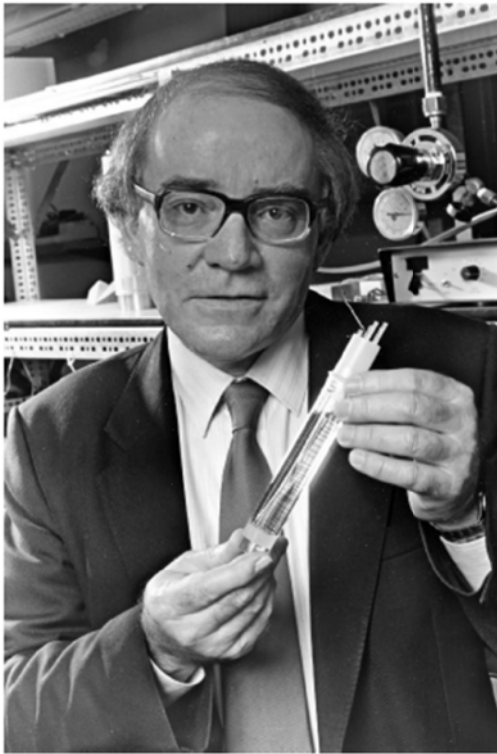


Thermal Behavior Of the Polarized Pd/D-D₂O System



CONTRIBUTORS

Dr. Martin Fleischmann
Bury Lodge, Duck Street
Tisbury, Salisbury, Wilts, SP36LJ, UK

Dr. Melvin H. Miles
University of LaVerne,
LaVerne, CA USA

EDITOR

Dr. Pamela A. Mosier-Boss
Research Laboratory of Electronics
Massachusetts Institute of Technology
Cambridge, MA USA

Table of Contents

Chapter I: More About Thermal Behavior of Polarized Pd/D-D ₂ O System.....	1
Our Penultimate Papers on the Isoperibolic Calorimetry of the Pt/D ₂ O and Pd/ D ₂ O Systems.....	2
Our Penultimate Papers on the Isoperibolic Calorimetry of the Pt/D ₂ O and Pd/ D ₂ O Systems Part II: the Pd/B and Pd-B-Ce Systems.....	52
Our Penultimate Papers on the Isoperibolic Calorimetry of the Pt/D ₂ O and Pd/ D ₂ O Systems Part III: the Pd/D Codeposition System.....	91
Our Penultimate Papers on the Isoperibolic Calorimetry of the Pt/D ₂ O and Pd/ D ₂ O Systems Part IV: an Experiment with a Pd-Cathode in 0.1 M LiOD/ D ₂ O Carried Out in 1989.....	117
The “Instrument Function” of Isoperibolic Calorimeters: Excess Enthalpy Generation due to Parasitic Reduction of Oxygen.....	151
More about Positive Feedback; More about Boiling.....	176
Chapter II: An Example of Difficulties in Publishing LENR-Related Results.....	189
The Precision and Accuracy of Isoperibolic Calorimetry as Applied to the Pt/D ₂ O System.....	190
Letter to Cold Fusion Authors Dated 9-5-2006.....	239
Letter to the Editor Dated 11-1-2005.....	241
E-mail Message to Dr. Fleischmann Dated 3-5-2006 with Comments from Reviewers 69 and 65.....	242
Letter to the Editor Dated 3-14-2007 Rebutting Comments of Reviewers.....	248
E-mail Message to Dr. Miles Dated 3-30-2006 Containing Replies by the Two Reviewers.....	250
E-mail Messages Between the Editor and Dr. Miles Dated 4-17-2006.....	251
Letter to the Editor Dated 6-4-2006 Containing Full Rebuttals to Each Reviewer.....	252
E-mail Message Dated 7-19-2006 Asking that Reviewers Respond to Dr. Miles’ Rebuttal.....	258
E-mail Dated 7-21-2006 Rejecting Submitted Paper.....	259

Chapter I: More about Thermal Behavior of Polarized Pd/D-D₂O System.

The research in the thermal behavior of the polarized Pd/D-D₂O system was, and still is, directed towards determining the conditions maximizing excess enthalpy production. At the present time, a sustained low grade heat source can be maintained for considerable periods of time.

Although the excess enthalpy production in these systems is generally accepted, there are still instances of misunderstanding even among seasoned scientists. In the series of papers entitled “Our penultimate papers on the isoperibolic calorimetry of the Pt/D₂O and Pd/D₂) systems”, Prof. Fleischmann (and his collaborators) deals with the correct and incorrect interpretation of calorimetric data.

In a separate paper “More about positive feedback; more about boiling “Prof. Fleischmann discusses aspects of this system of interest to practical applications, *viz* the design of an effective energy source.

Our Penultimate Papers on the Isoperibolic Calorimetry of the Pt/D₂O and Pd/D₂O systems

Part I: The Pt/D₂O Blank System

M. Fleischmann, Bury Lodge, Duck Street, Tisbury, Salisbury, Wilts., SP3 6LJ, U.K.

M.H.Miles, Department of Chemistry, University of La Verne, La Verne, CA 91750

U.S.A.

Abstract

The precision and accuracy of “open cell” isoperibolic calorimetry are evaluated using a series of “blank experiments” unlikely to show any major excess enthalpy generation (Pt cathodes polarised in 0.1 M LiOD/D₂O). The differential and integral heat transfer coefficients are evaluated and it is shown that the latter based on backward integration of the data sets should be used in accurate evaluations of the experimental data. It is shown that the precision is better than 99.99% while the accuracy is close to this figure.

The high precision and accuracy allow the determination of the excess enthalpy generation due to the reduction of electrogenerated oxygen. It is shown that this was ~ 0.0011 W for the experiments in question whereas the input enthalpy to the cell was ~ 0.8 W for these particular experiments.

By way of explanation:

In recent years we have commented extensively on the investigation of these systems using isoperibolic calorimetry. In view of these and related commentaries one might be led to believe that it would be possible to publish papers in the normal literature about the use of such calorimetric methods to investigate excess enthalpy production in the Pd/D₂O system (and in systems closely related to this original design (1), (2)). This expectation has not been realised.

This situation prompts us to examine once again the precision and accuracy of isoperibolic calorimetry. We do this by carrying out a comparative analysis of a series of “blank experiments” using the Pt / 0.1 M LiOD-D₂O system polarised in an ICARUS -2 cell and using the ICARUS -2 system (3). Succeeding parts of this paper will deal with a comparative evaluation of the Pd / D₂O, Pd-B / D₂O, Pd-B-Ce / D₂O and, especially the Pd-D / D₂O codeposition systems (4).

This division of the present investigation into a number of Parts will also explain our choice of the somewhat strange title “Our Penultimate Paper on the Isoperibolic Calorimetry of the Pt/D₂O and Pd/D₂O systems”. It has been our view that the only paper on this topic which would be justified at the present time would be a comparative evaluation of the various studies of “Cold Fusion” systems, paying due attention to the precision and accuracy of the various studies. We would regard such a paper as being “Our Ultimate Paper -” which might, however, well mark the beginning of a new phase of the investigation of Cold Fusion. However, we have been unable to secure the release of the prime sets of the raw data for any of the investigations which we regard as being central to such an investigation. We have therefore been forced to restrict attention to the measurements on the Pd/D₂O, Pd-B/D₂O, Pd-B –Ce/D₂O and Pd-D/D₂O codeposition systems carried out by one of us (M.H.M) during his stay at N.H.E. Laboratories in Sapporo, Japan with the proviso that we regard this as a “Penultimate Study”.

Some preliminary considerations about the design of calorimetric systems.

If we consult any of the classical texts of Chemical Engineering (e.g. see (5)) we find that reactors in which there are both chemical and thermal changes should be classified as being “ideal” and “non-ideal”. The “well-stirred tank” and “plug flow reactor” are pre-eminently examples of the “ideal” type whereas “dispersive plug flow” should be regarded as being “non-ideal”. It should be evident that “isoperibolic calorimetry” might be classified as being “ideal” (we have to justify some additional criteria to satisfy this description). Although it might well be possible to design calorimetric systems which would satisfy the criteria of a “an ideal plug flow reactor” (e.g. research on fluidised beds of Pd particles) such research has not been carried out hitherto, to the best of our

knowledge. Research on the fashionable flow reactors is governed by “dispersive plug flow” and should therefore be classified under the “non-ideal” heading.

Fig. 1 illustrates the type of single compartment isoperibolic calorimeter which we have adopted for most of the research on “Cold Fusion” including the present paper, the comparative study to be presented in Part II (6) and the investigation of the Pd-D codeposition system (4) to be presented in Part III, (7). We make the following additional observations about the operation of this calorimeter:

(i) heat transfer is controlled by radiation across the vacuum gap of the Dewar cells, this heat transfer being predominantly due to the lower, unsilvered parts of the cells. The heat transfer coefficient is therefore given by the product of the Stefan-Boltzmann coefficient and the radiant surface area as has been confirmed in numerous studies. Deviation from this predicted value of the heat transfer coefficient indicates malfunctions of the cells and/or mistakes in the data analyses.

(ii) Adjustments of the relative extents of the silvered and unsilvered portions allows the change of the heat transfer coefficient by about one order of magnitude; larger changes require changes in the dimensions of the cells.

(iii) As heat transfer is controlled by heat transfer across the vacuum gap, the thermal impedance has no “memory”. It is therefore possible to examine the non-steady state behaviour of the systems in a straightforward manner which affects especially the response of the systems to calibration pulses supplied by the Joule resistive heaters. It is evident that this crucially important design criterion has not been understood by the many critics of “Cold Fusion” (e.g. see (8)).

(iv) The long and narrow design of the calorimeters ensures that the contents are well-mixed by the gas sparging induced by the gas evolution at the anodes and cathodes. The radial and axial mixing times of the system (as revealed by tracer experiments) are ~3 s and ~20 s whereas the thermal relaxation time of the ICARUS -2 cell investigated in the present paper is ~5000 s (see Footnotes (1) and (2)).

Footnote (1) The differential equation representing the model of the calorimeter is non-linear and inhomogeneous (see equation A.2 of the Appendix) The estimate of a “thermal relaxation time” is therefore approximate.

Footnote (2) The calorimeters used in the initial studies (1), (2) had heat transfer coefficients which exceeded the value given by the product of the Stefan-Boltzmann coefficient and the radiant surface area. We attributed the conductive contribution to conductance across the nominal vacuum gap due to inadequate evacuation of the Dewar cells. It was therefore not clear whether the system should have been modelled as being “pseudoradiative” or “pseudoconductive” (depending on whether the conductive or radiative contribution was neglected; for an alternative strategy see (9)); the thermal relaxation time of these cells was ~ 3000 s.

(v) in view of (iv) the contents of the calorimeter have always been at a uniform temperature.

(vi) equally, the temperature of the heat sinks (water baths) surrounding the calorimeters have always been at a uniform temperature. This has been ensured by using a combined rejection of heat to the surrounding ambient room temperature coupled to thermostatic control of the water baths. The room temperature has always been itself controlled using two independent temperature controllers operated in parallel i.e. the overall system used two thermal impedances operated in series.

(vii) the cells have always been operated in the “open mode” i.e. the products of electrolysis have been vented to the ambient [see Footnote (3)]. N.M.R. measurements confirmed that this strategy (imposing continuous isotopic separation of H) ensured the maintenance of the initial isotopic composition of the electrolyte.

Footnote (3) It should be noted that this strategy avoids the introduction of large localised and fluctuating sources of enthalpy in the gas spaces (which is a characteristic of the use of cells fitted with catalytic recombiners).

(viii) measurements have usually been made using 0.1 M LiOD/D₂O. The use of this electrolyte ensured that there were no parasitic reactions which could affect the thermal balances of the system.

(ix) it was confirmed that the volumes of the gases evolved agreed to within ~ 1% of those calculated assuming 100% Faradaic efficiency of the electrolytic reactions (neglecting the initial part of the measurement sequences during which there is charging of the Pd-based systems by hydrogen isotopes). The volumes of D₂O required to maintain the levels of electrolyte in the cells also agreed with those calculated by Faraday's Laws i.e. there is no possibility of involving large-scale recombination of the electrolytically formed gases to explain excess enthalpy production.

(x) measurements of cell and calibration currents of cell and bath temperatures and of the cell potentials and potentials across the resistive calibration heaters were made every 300 s [see Footnote (4)]

Footnote (4) A limit on the rate of data acquisition is set by the time lags induced by the thin glass shields surrounding the thermistors, ~ 10 s (see also further below). Furthermore, it would be possible to exceed this rate of acquisition if the time lags in the glass shields were taken into account.

(xi) three calorimetric cells were maintained in each thermostat tank.

(xii) in view of the small extent of the head spaces (which contained no exposed bare metal parts), the systems could be operated in absolute safety.

Measurements and Interpretation.

Fig. 2 gives a plot of the “raw data” (the cell temperature and input enthalpy for days 9 and 10 of the measurement cycles) carried out on a Pt cathode ($\phi = 1$ mm, $l = 2$ cm). It can be seen that with increasing time following each perturbation of the system, both these time series show a small progressive decrease with time. This decrease of temperature with time is due to the progressive increase of the electrolyte concentration due to electrolysis; this in turn causes an increase of the conductance and hence a fall in the input power. The fall in the input power leads to a decrease of the cell temperature with time.

Four times are of special interest; $t = 0$ following the “topping-up” of the cell after the previous measurement cycle; $t = t_1$, the start of the calibration period; $t = t_2$, the cessation of the calibration period and $t = T$, the end of the measurement cycle. Estimates of the pseudo-radiative lower bound heat transfer coefficient, $(k_R')_1$, and of the pseudo-radiative true heat transfer coefficient, $(k_R')_2$, can be conveniently made near $t = t_2$, equations A.4 and A.6 in Appendix A. In the first of these estimates we assume that there is no generation of any excess enthalpy, hence the designation of “lower bound”; the presence of any known source of excess enthalpy would increase the enthalpy input and, hence, decrease the heat transfer coefficient. In the second estimate of the pseudo-radiative true heat transfer coefficient, $(k_R')_2$, we also have to estimate the input power and cell temperature which would have been reached in the absence of the heater calibration. We can do this conveniently by interpolating the time series for the regions $t < t_1$ and $t_2 < t < T$: the reason for stipulating $t_1 = 12$ hours, $t_2 = 24$ hours and $T = 48$ hours will be all too self-evident. Contraction of these times say to $t_1 = 6$ hours, $t_2 = 12$ hours and $T = 24$ hours leads to an inevitable lowering of the precision of $(k_R')_1$ and accuracy of $(k_R')_2$. Unfortunately, such a contraction of the measurement cycles has been the norm in most of the investigations carried out by other research groups.

The values of these “robust” estimates of $(k_R')_1$ and $(k_R')_2$ (made from A-3 sized plots of the “raw data”) are shown in Columns 2 and 3 of Table 1 for a series of 7 measurement cycles. The values of $(k_R')_1$ and $(k_R')_2$ were the first estimates of the heat transfer coefficients which we made from the “raw data” (hence their designation) and were used as starting values for more precise and accurate evaluations using non-linear regression [see Footnote(5)]

Footnote (5) In the original investigation (2), $(k_R')_2$ was estimated near $t = t_1$ in an attempt to eliminate one of the required interpolations. Although this procedure was explained in (2) (as was the subsequent application of non-linear regression; for further explanation see (10)) the basis of our estimates was clearly not understood e.g. see (11). As we could not make the non-linear regression methodology “user friendly” with the computing power available to us in 1992, we based all further analyses on the application of linear regression (for further explanation, see (12)) Linear regression was also the basis of the statistical treatments incorporated in the ICARUS -1 and ICARUS -2 packages (3) and is the methodology which we have adopted in all investigations after October 1989.

It is important that $(k_R')_1$ and $(k_R')_2$ are respectively the least precise and least accurate estimates of the heat transfer coefficient which we can make from the data. Furthermore, they are subject to errors due to the refilling of the cells to make up for losses in D_2O due to electrolysis (see further below). The means of the values derived are also shown in Columns 2 and 3 of Table 1. (see also further below).

The next stage of the analysis is the evaluation of the differential lower bound heat transfer coefficients $(k_R')_{11}$, throughout the time range of the measurement cycle. Here the subscript 11 denotes that we are evaluating a differential coefficient and that we are also considering a lower bound value. We have always used a second order central difference in the estimates of the differentials of the temperature-time series. Fig. 3 shows the 11-point means, $(\overline{k_R'})_{11}$, of $(k_R')_{11}$ and the further 6-point means, $(\overline{\overline{k_R'}})_{11}$, of $(\overline{k_R'})_{11}$ for days 1

and 2 of the measurement cycles; (there was no calibration of the system during this particular cycle).

We can use the differential lower bound heat transfer coefficients in several ways to assess the performance of the instrumentation. Thus, we can estimate the true heat transfer coefficient from the mean of the values in Column 3, Table 1 or else, we can assume that the true heat transfer coefficient varies in the same way with time as does the lower bound value $(k_R')_{11}$, Fig. 3 (a better assumption is to base this variation on the integral heat transfer coefficient, $(k_R')_{21}$, Fig. 6 and see further below). We can then evaluate the differential rates of excess enthalpy generation using

$$\text{differential rate of excess enthalpy generation} = [(k_R')_2 - (k_R')_{11}] f_1(\theta) \quad (1)$$

$$\text{where } f_1(\theta) = (\text{cell temperature})^4 - (\text{bath temperature})^4 \quad (2)$$

(see also Appendix A)

Fig. 4 gives the upper and lower tail distributions for Day 3- 16 of the data sets (c.a. 4000 measurements) using the second set of assumptions (i.e. allowing for the variation of $(k_R')_2$ with time). We can see that the data are consistent with a normal distribution of errors (due principally to errors in the temperature measurements) on which is superimposed a small steady state of excess enthalpy production (which accounts for the positive deviations of the plots from those for purely normal distribution of errors especially in the region of the upper tail distribution).

We can also evaluate the corresponding rates of excess enthalpy generation in a variety of ways. The methodology which we adopted in 1991-1993 (and which we have also used here) is to evaluate the total excess enthalpy as a function of time and then to divide the relevant excess enthalpy by the time elapsed since the start of the measurement cycles (here $t = 0$ on Day 3). The results for the two limiting sets of assumptions (allowing for the variation of $(k_R')_2$ with time or using a single value of $(k_R')_2$ at $t = 86,400$ s) are given in Figs. 5A and 5B. We can see that the effects of the random variations in the differential lower bound heat transfer coefficient, Fig. 3, are gradually suppressed with increasing time, the rate approaching ~ 1.3 mW. The significance of this value will be

discussed below. At the same time, we can see that the magnitudes of the excess rates given in Figs. 5A and 5B are affected by the assumptions made about the time dependence of the true heat transfer coefficients and that the evaluation requires very long integration intervals in order to reduce the effects of random errors to acceptable levels. [see Footnote (6)].

Footnote (6) The evaluations carried out in 1991-93 were restricted to the first measurement cycle calculated with allowance of the variation of the true heat transfer coefficient with time, as in Fig. 5A. This led in turn to the erroneous conclusions that the accuracy of $(k_R')_2$ was about one order of magnitude below the precision of $(k_R')_1$ and that the rates of excess enthalpy production were about one tenth of the rate which could be attributed to the reduction of electrogenerated oxygen (in turn attributed to a degassing of this species from the solution adjacent to the cathode by the electrogenerated bubbles of deuterium). It can be seen that these conclusions were incorrect: the accuracy of $(k_R')_2$ must be comparable to the precision of $(k_R')_1$; the question of the reduction of electrogenerated oxygen is discussed further below.

These difficulties are avoided by basing the evaluation on the integral rather than the differential heat transfer coefficients. We can distinguish two types of heat transfer coefficient denoted by the symbols $(k_R')_{i,j,l}$ where $i = 2$ signifies backward integration (i.e. typically starting from $t = T$, $t = t_2$ or $t = t_1$), $i = 3$ signifies forward integration (starting typically from $t = 0$, $t = t_1$ or $t = t_2$), $j = 5, 6, 7$ or 8 denotes the region adjacent to $t = 0$, $t = t_1$, $t = t_2$ or a combination of the regions adjacent to $t = t_1$ and $t = t_2$, $l = 1$ signifies “lower bound” and $l = 2$ signifies “true”. In this scheme of description $i = 1$ stands for “differential”; omission of the central subscript, j , denotes that we are considering the whole measurement cycle $0 < t < T$.

It can be seen that we can base the evaluation on many versions of the heat transfer coefficients (which of course, are all related to each other) so that it is necessary to standardise on the usage of a sensible subset of these coefficients.

Fig. 6 gives a comparison of the integral coefficients $(k_R')_{2I}$ (see equation A. 8) and $(k_R')_{3I}$ (see equation A. 9) with the differential coefficient $(k_R')_{1I}$. It can be seen that if we exclude the first ~ 100 data points adjacent to $t = T$ in the evaluation of $(k_R')_{2I}$ and the first ~ 100 data points adjacent to $t = 0$ in the evaluation of $(k_R')_{3I}$ (time zones in which the benefits of using the integral procedure are established) the variability of $(k_R')_{2I}$ and $(k_R')_{3I}$ is actually much smaller than the variability of the double mean of the differential lower bound coefficient, $(k_R')_{1I}$. The interrelation of these coefficients can be understood as follows :

the variation of $(k_R')_{1I}$ with time can be represented to the first order by

$$(k_R')_{1I} = (k_R')^0 (1 - \gamma t) \quad (3)$$

where $(k_R')^0_{1I}$ is the value of $(k_R')_{1I}$ at $t = 0$. On the other hand, in the evaluation of the integral heat transfer coefficients, these coefficients are initially regarded as being constant in time, so that we obtain equations (A.8), (A.9), (A.11) and (A.12) (and similar expressions for other heat transfer coefficients which may be used in the interpretation). If, instead, the time dependence of the heat transfer coefficients is included in the differential equation (A.1) representing the calorimeter, we obtain, for example, equation (A. 13). If we now regard $f_1(\theta)$ as being constant throughout a measurement cycle (which is a rough approximation for the case of the “lower bound heat transfer coefficients” as there is no calibration pulse) we obtain

$$(k_R')_{2I} = (k_R')^0_{2I} \left[1 + \frac{\gamma(T-t)}{2} \right] \quad (A. 14)$$

and

$$(k_R')_{3I} = (k_R')^0_{3I} \left[1 - \frac{\gamma t}{2} \right] \quad (A. 15)$$

where $(k_R')^0_{2I}$ and $(k_R')^0_{3I}$ are respectively the values of $(k_R')_{2I}$ and $(k_R')_{3I}$ at $t = T$ and $t = 0$. It follows that the slopes of the plots of $(k_R')_{2I}$ and $(k_R')_{3I}$ versus time are roughly one

half of the corresponding plot for $(k_R')_{11}$ and hence of those for $(k_R')_{11}$ and $(k_R')_{11}$ as is shown by Fig. 6.

An alternative approach towards the evaluation of accurate values of the heat transfer coefficients can be based on the application of equations such as (A.8), (A.9), (A.11) and (A.12). Such evaluations give $(k_R')^0_{i,j,l}$ which are the intercepts at the chosen origins of the abscissae of $C_p M d\Delta\theta / dt$ (note that the values of the intercepts are independent of the value of $C_p M$) ; the water equivalents, $C_p M$, are derived from the slopes of the plots.

Figs. 7A and 7B are anomalous in this sequence because they are based on the responses of the systems to the “topping up” of the cells to make up for losses of D_2O due to electrolysis in the previous measurement cycles (rather than the response due to the calibration pulse). Fig. 7A illustrates the determination of $(k_R')^0_{251}$ where the origin has been set at $t = 14,000$ s whereas this origin is at $t = T$ for the evaluation illustrated in Fig. 7B. It was found that the values of $(k_R')^0_{251}$ determined in this way agreed with the value of $(k_R')_{11}$ evaluated at $t = 14,000$ s (e.g. see Fig. 6) and these values are listed for this series of measurement cycles in Column 4 of Table1. However, although the values of $(k_R')^0_{251}$ determined with the time origin set at $t = T$ were smaller than those determined with the origin set at $t = 14,000$, (e.g. compare Figs. 7A and B), this decrease was, in general, too small. We therefore concluded that it would not be possible to use this methodology to determine $(k_R')^0_{251}$ with the time origin set to t_2 i.e. that the most sought after heat transfer coefficient could not be determined in this way. Furthermore, we were unable to develop this methodology to allow the determination of the “true integral heat transfer coefficients, $(k_R')^0_{252}$ ”. This particular methodology was therefore excluded from the ICARUS Systems and we have not used it in the intervening years. See Footnote (7).

Footnote 7) We note, however, that this particular method for determining the heat transfer coefficients requires further investigation. “Topping-up” of the cells with heated D₂O could be made to produce perturbations of the same amplitude as those achieved using the resistive heaters. This would improve the precision of the evaluation of $(k_R')^o_{251}$ which could then probably be determined at $t = t_2$. It might also allow the determination of $(k_R')^o_{252}$ and would certainly lead to a considerable simplification of the experiment design.

Figs. 8A, 8B and 9 illustrate the determination of $(k_R')^o_{261}$ and $(k_R')^o_{262}$ with the start and end of the integration procedures being set at $t = t_2$ and $t = t_1$ (for Figs. 8A and 9) and $t = T$ and $t = t_1$ (for Fig. 8B). It should be noted that the origin for the plots in Figs. 8A and 9 is well-defined near $t = t_2$ (where $d\Delta\theta/dt \simeq 0$) which is the point in time at which we require the heat transfer coefficients. The small values of the abscissae should be especially noted as should be the degradation of the performance when setting the origin at $t = T$ (Fig. 8B) compared to $t = t_1$ (Fig. 8A). The evaluation of these heat transfer coefficients (with the origin set at $t = t_2$) became one of the targets of the ICARUS procedures; the values determined for these sets of measurements are listed in Columns 6-9 of Table 1. The values of $(k_R')^o_{261}$ determined in this way are somewhat larger than the values of $(k_R')_{21}$ determined at the same point in time listed in Column 10 of Table 1. This is expected as the extrapolations in these Figures determine $(k_R')_{11}$ at $t = t_2$ (rather than $(k_R')_{21}$).

We would expect the means of $(k_R')^o_{261}$ and $(k_R')^o_{262}$ (Columns 6 and 8 of Table 1) to be close to the means of $(k_R')_1$ and $(k_R')_2$, (Columns 2 and 3 of Table 1). Table 1 shows that this is indeed the case.

Fig. 10 illustrates the determination of $(k_R')^o_{271}$ and Columns 11 and 12 of Table 1 list the derived values. The determination of the heat transfer coefficient at $t = T$ is not of

any particular significance and this particular method of evaluation was not included in the ICARUS package.

Figs. 11-14 illustrate the determination of $(k_R')^0_{361}$ and $(k_R')^0_{362}$ based on forward integration of the data from $t = t_1$. Here Figs. 11 and 12 use the first 33 data points adjacent to $t = t_1$ while Figs. 13 and 14 use the 33 data points adjacent to $t = T$. It can be seen that these evaluations are unsatisfactory from several different points of view. In the first place, the origin of the plots is not well-defined ($d\Delta\theta/dt \neq 0$ as $t \rightarrow t_1$); secondly, the range of the extrapolations required is too long (see especially Figs. 11, 13 and 14); thirdly, the values of the abscissae are large and comparable to the ordinates (see especially Fig. 12). It is not surprising therefore that the determination of the heat transfer coefficients using these particular procedures fails (see Columns 12-16 of Table 1). It was pointed out that evaluations near the end of the calibration pulse (Figs. 13 and 14 and Columns 17-20 of Table 1) would be more satisfactory than those based on the region close to the start of this pulse, $t = t_1$ (Figs. 11 and 12 and Columns 13-16 of Table 1). As the time at which the derived heat transfer coefficients might apply was uncertain, the procedures based on the forward integration of the data sets was excluded from the ICARUS Systems [see Footnote (8)]. However, the evaluation of $(k_R')^0_{31}$ near $t = t_2$, Column 21 of Table 1, was included to serve as a check on the evaluation procedures.

Footnote (8) However, we believe that the evaluations carried out by the group at the New Hydrogen Energy Laboratories have been based on such forward integrations, see Part II [8].

It is important to point out a major limitation of these data analyses. It can be seen that the time-dependence of the evaluated heat transfer coefficients e.g. see Figs. 3 and 6, is entirely in accord with the expected behaviour, equations (A.1) and (A.2). It was therefore hoped that the derived values of the water equivalents, $C_p M$, could be used to provide the minor corrections to the level of the electrolyte required to allow the

presentation of the derived heat transfer coefficients on a single plot versus the electrolyte content of the cells. However, this hope could never be realised; the water equivalents are derived from the slopes of the plots such as those in Fig. 7A-10. Inevitably, this introduces errors into the estimations of C_pM and the accuracy of these water equivalents is therefore insufficient to allow the corrections of the heat transfer coefficients for changes in the level of the electrolyte between the successive measurement cycles.

In view of this deficiency, a level controller was added to the ICARUS -1 system in the development of the further ICARUS -2 instrumentation. The principle of this level controller is illustrated in Fig. 15B and it was estimated that this would reduce the errors of the heat transfer coefficients between successive measurement cycles to $\sim 0.04\%$. However, these level controllers were never used. It was also apparent that it was necessary to control the level of the water baths surrounding the calorimeters, but such level controllers were never constructed.

Fig. 15B also illustrates a further feature of the instrumentation: the proposed use of the cell currents to drive the resistive calibration heaters. This aspect is discussed further below, see Fig. 20.

It is also necessary to assess the errors inherent in the various evaluations of the heat transfer coefficients which can be conveniently carried out by using the relevant standard deviations. Thus Fig. 16 shows the standard deviations of $10^9 (k_R')_{11}$ and $10^9 (\overline{k_R'})_{11}$ as a function of time for Days 1 and 2 of the measurement cycles. The second is lower than the first by about $(6)^{1/2}$ as would be expected if these differential coefficients show normally distributed random errors (due principally to errors in the temperature measurements cf. Fig. 4).

Next, Fig. 17 shows the standard deviations of the integral lower bound heat transfer coefficients $(k_R')_{21}$ and $(\overline{k_R'})_{21}$. Note first of all that $\sigma(k_R')_{21}$ is much smaller than $\sigma(k_R')_{11}$ which illustrates the benefits of using the integral rather than the differential coefficients. However, we find that $\sigma(\overline{k_R'})_{21} > \sigma(k_R')_{21}$ which is clearly impossible. This

result is, in fact, due to the systematic decrease of $(k_R')_{21}$ (and of all the other heat transfer coefficients) with time.

The effects of these systematic variations with time can be taken into account by evaluating the standard deviations about the median centre lines. The effects on the results in Fig. 16 are entirely negligible (of order 10^{-14} i.e. 0.00001 on the scale of Fig. 16) confirming that the fluctuations are due to random errors. The effects on the standard deviations of the integral heat transfer coefficients are shown in Fig. 18. We see that $\sigma(\overline{k_R'})_{21}$ is now of the same order as $\sigma(k_R')_{21}$. We would expect it to be much smaller but, evidently, we now reach the limit of the evaluation procedures: we cannot investigate random or systematic errors in these coefficients if these are less than $0.00001 \times 10^9 (k_R')$ as this is the cut-off limit of the interpretation. [see Footnote (9)]

Footnote (9) However, we see that the integral heat transfer coefficients in Figs. 6-10 are not statistically independent as the process of integration uses all the preceding values of the coefficients. Fig. 19 shows we can get round this difficulty in principle; we section the data (here into sectors of 28,650 s duration) so that we obtain a series of statistically independent values of $(k_R')_{21}$. However, note that these values will converge onto the relevant plot of $(k_R')_{11}$ versus time. A realistic application of this methodology would require a raising of the rate of data acquisition (desirable for other reasons). A practical limit is set by the time-lags in the glass shields surrounding the thermistors-say ~ 10 s. This would allow the making of ~ 60 measurements of statistically independent values of $(k_R')_{21}$ over a two day period. However, it is debatable whether such an investigation would be useful as these values of $(k_R')_{21}$ would converge onto the $(k_R')_{11}$ median line.

An alternative way of testing the errors of the integral heat transfer coefficients is to apply equation (A.13) to the data and to then evaluate the standard deviations of the derived values of $(k_R')^0_{21}$. This method has the advantage that it simultaneously tests the

applicability of the differential equation modelling the calorimeters by testing whether the heat transfer coefficients can be represented by a single, time-independent value.

Fig. 20 gives the results for days 1 and 2 and for days 9 and 10 of the measurement cycles. If we exclude the first ~ 100 points in the integration procedure, we find that the relative standard deviations $\sigma (k_R')_{21} / (k_R')_{21}$ is just 0.0056% for the measurements on Days 1 and 2 (i.e. better than the specification 0.01% for the instrumentation). The comparable relative standard deviation for Days 9 and 10 is 0.015% which is actually better than the 0.1% which was specified for the instrumentation. However, closer inspection of the data in Fig. 20 shows that the results for $(k_R')_{21}$ actually fall into two groups separated by the cessation of the calibration pulse. The relative standard deviations on the two sides of this dividing line are 0.0023%. The mismatch of the kind observed for Days 9 and 10 is presumably due to errors in the power delivered by one or both of the polarising circuits used to drive the cell and the calibration heater. The circuit illustrated in Fig. 15B was therefore devised to use the same current supply to drive both the cell and the calibration heater. However, this feature of the switching boxes was never put into use.

We observe that notwithstanding the errors illustrated in Fig. 20, the relative standard deviations are so small that it should be possible to make thermal balances to within 0.1 mW for a typical input of 1 W to the calorimeters. The analysis presented above indicates that such balances should be made using the integral heat transfer coefficients $(k_R')_{22}$ estimated at $t = 0$. Table 2 illustrates such a calculation made using the seven applicable measurement cycles. We can see that the rate of excess enthalpy generation shown in Column 8 is 0.0011 W. These rates, also shown in Figs. 5A and B in comparison with those calculated using the differential heat transfer coefficients $(k_R')_{12}$, are approximately equal to the rates which may be calculated for the reduction of electrogenerated oxygen present in the cell (compare[15]). It will be clear that we must regard the rates as being constant during each measurement cycle, an assumption which is evidently justified. The data shown in Column 8 of Table 2 confirm that such rates can be estimated to within ± 0.0001 W which requires that the accuracy of the true integral heat transfer coefficient is nearly equal to the precision of the lower bound values, i.e. that the errors are $\sim \pm 0.01\%$.

Discussion

The material presented in this paper shows that exact data analyses should be based on the evaluation of the true integral heat transfer coefficient, $(k_R')_{22}$, coupled to the integral lower bound heat transfer coefficient $(k_R')_{21}$. Accurate and precise estimates of these coefficients can be obtained from $(k_R')_{262}^0$ and $(k_R')_{261}^0$, the values that apply to the calibration period $t_1 < t < t_2$. The procedure which we have illustrated here was part of that incorporated in the ICARUS-Systems methodology (3).

The accuracy of $(k_R')_{22}$ and precision of $(k_R')_{21}$ are very nearly equal with errors of $\sim \pm 0.01\%$. Such errors can in fact be estimated from the errors in the temperature measurements coupled to the averaging procedures which have been described in this paper. The accuracy and precision which can be achieved should be compared to the rather wild statements have been made in the literature about the accuracy of this type of instrumentation. Such statements can be seen to be the outcome of inadequate experiments coupled to inadequate and incomplete interpretations.

It will be seen that the application of the integral heat transfer coefficients requires that the rates of any excess enthalpy generation be constant in time. In turn this requires that the experiments be carried out using suitable “blank systems “. If the rates of excess enthalpy generation vary with time, we will inevitably conclude that the instrumentation has enhanced errors. Moreover, such a conclusion will apply to any calorimetric system which we might propose. The lack of execution of “blank experiments” is undoubtedly a contributory factor to the confusing statements which have been made in the literature.

The wild statements made in the literature extend also to the effects of the rates of reduction of electrogenerated oxygen. These rates can be estimated perfectly adequately by carrying out suitable “blank experiments”. We note that if the precision and accuracy of the experimentation is lowered to say 1%, it will then be impossible to measure such rates; equally, it will be impossible to monitor the build-up of excess enthalpy generation until

this has reached specific rates in the range $0.1\text{-}1\text{ Wcm}^{-3}$. Such deficiencies are no doubt at the root of many of the further confusing results and statements which have been made in the literature.

We observe also that the calibration of the cells could be based equally well on the determination of the lower bound heat transfer coefficients for suitable “blank experiments”. The use of such heat transfer coefficients in the data analysis for Pd-based cathodes in D_2O -based electrolytes will then automatically discriminate against the contribution of the reduction of electrogenerated oxygen to the total rates of excess enthalpy generation.

Appendix Part I

It has been established that at low to intermediate cell temperatures (say $30^\circ < \theta < 80^\circ$) the behaviour of the calorimeters is modelled adequately by the differential equation

$$\begin{aligned}
 C_p M (d\Delta\theta/dt) &= [E_{\text{cell}}(t) - E_{\text{thermoneutral, bath}}] I + Q_f(t) \\
 &\quad \text{change in the enthalpy content of the calorimeter} \quad \text{enthalpy input due to electrolysis} \quad \text{rate of excess enthalpy generation} \\
 &\quad + \Delta QH(t-t_1) - \Delta QH(t-t_2) - (3I/4F[P/\{P^*-P\}])[C_{p,D_2O,g} - C_{p,D_2O,l}]\Delta\theta + L] \\
 &\quad \text{calibration pulse} \quad \text{rate of enthalpy removal by the gas stream with } E_{\text{thermoneutral}} \text{ referred to the bath temperature} \\
 &\quad - (k_R^0)\theta_{\text{bath}}^3[1-\gamma t] \{f_1(\theta)/\theta_{\text{bath}}^3 + 4\phi\Delta\theta\} \quad (A.1) \\
 &\quad \text{time dependent heat transfer coefficient} \quad \text{effect of radiation} \quad \text{effect of conduction}
 \end{aligned}$$

With the calorimeters supplied with the ICARUS Systems, the conductive contribution to heat transfer is very small. This term could therefore be “lumped” into the radiative term by allowing for a small increase in the radiative heat transfer coefficient:

$$\text{Radiative heat transfer} = (k_R')^0[1-\gamma t][(\theta_{\text{bath}} + \Delta\theta)^4 - \theta_{\text{bath}}^4] \quad (A.2)$$

The values of the pseudoradiative “heat transfer coefficient, $(k_R')^0[1-\gamma t]$, derived are close to those calculated from the Stefan-Boltzmann coefficient and the radiative surface area. If the time dependence of the heat transfer coefficient is not included explicitly in equation (A.2) then

$$\text{Radiative heat transfer} = (k_R')[(\theta_{\text{bath}} + \Delta\theta)^4 - \theta_{\text{bath}}^4] \quad (A.3)$$

where the pseudoradiative heat transfer coefficient, (k_R') , now shows a weak time-dependence.

The simplest starting point is to assume that there is no excess enthalpy generation in the calorimeter and to evaluate a corresponding “differential lower bound heat transfer coefficient” at a time just before the end of the calibration pulse, $t = t_2$:

$$(k_R')_1 = [(E_{\text{cell}}(t) - E_{\text{thermoneutral, bath}})I - \Delta H_{\text{evap}}(t) - C_p M(d\Delta\theta/dt) + \Delta QH(t-t_1)]/f_1(\theta) \quad (A.4)$$

This was the first heat transfer coefficient used in our investigations, hence the designation $(k_R')_1$. It will be apparent that the differential lower bound heat transfer coefficient $(k_R')_{11}$, may be evaluated at other points of the measurement cycle, by changing the enthalpy input due to the calibration pulse to

$$\Delta QH(t-t_1) - \Delta QH(t-t_2) \quad (A.5)$$

It is next necessary to evaluate a “true heat transfer coefficient”. The simplest procedure giving $(k_R')_2$ near the end of the calibration period at $t=t_2$ is obtained by including the calibration pulse

$$(k_R')_2 = \{ \Delta Q + [E_{\text{cell}}(\Delta\theta_2, t_2) - E_{\text{cell}}(\Delta\theta_1, t_2)]I - \Delta H_{\text{evap}}(\Delta\theta_2, t_2) + \Delta H_{\text{evap}}(\Delta\theta_1, t_2) - C_p M[(d\Delta\theta/dt)_{\Delta\theta_2, t_2} - (d\Delta\theta/dt)_{\Delta\theta_1, t_2}] \} / f_2(\theta) \quad (\text{A.6})$$

where we now have

$$f_2(\theta) = [\theta_{\text{bath}} + (\Delta\theta_2, t_2)]^4 - [\theta_{\text{bath}} + (\Delta\theta_1, t_2)]^4 \quad (\text{A.7})$$

It can be seen that we need to estimate the cell potential, the cell temperature and the differential of this temperature at the time $t=t_2$ which would have been reached in the absence of the calibration pulse [see footnote (A.1)]

Footnote (A.1) This evaluation was carried out in a somewhat different manner in the initial studies (1), (2), (10) in an attempt to avoid the disadvantages of such interpolation procedures. The values of $(k_R')_{11}$ and $(k_R')_{12}$ obtained were used as starting values for the non-linear regression procedure used at that time (2). As we could not make this procedure “user friendly” with the computing power then available to us and as, more especially, the methodology which we adopted was evidently not understood (11). (for a further example of such misunderstanding see (8)) we adopted the methodology described in the present paper. This methodology was also the basis of the ICARUS Systems (3).

As is explained in the main text, it is preferable to base the evaluation of the “raw data” on the integrals of the enthalpy input and of the temperature functions rather than to lower the precision and accuracy of the evaluations by using the differentials of the inherently noisy temperature-time series.

For the backward integrals starting from $t \approx T$ we obtain

$$(k_R')_{21} = \frac{\int_T^t \text{net enthalpy input } (\tau) d\tau}{\int_T^t f_1(\theta) d\tau} - \frac{C_p M [\Delta\theta(t) - \Delta\theta(T)]}{\int_T^t f_1(\theta) d\tau} - \frac{Q_d [t - T]}{\int_T^t f_1(\theta) d\tau} \quad (\text{A.8})$$

while forward integration from the start of the measurement cycle

$$(k_R')_{31} = \frac{\int_0^t \text{net enthalpy input } (\tau) d\tau}{\int_0^t f_1(\theta) d\tau} - \frac{C_p M [\Delta\theta(t) - \Delta\theta(0)]}{\int_0^t f_1(\theta) d\tau} - \frac{Q_d [t]}{\int_0^t f_1(\theta) d\tau} \quad (\text{A.9})$$

The evaluation of the heat transfer coefficients applicable to particular time regions ($j = 5, 6, 7, 8$) simply requires changes in the lower limits of the relevant integrals.

The evaluation of the “true heat transfer coefficients” requires the combination of the enthalpy inputs in equations (A.8) and (A.9) with the thermal inputs made at one or a series of points. This can be carried out in a number of ways; we confine attention here to the procedure originally suggested in the handbook for the ICARUS - 1 System (3). If we consider $(k_R')_{362}$ and if we make a thermal balance just before the application of the calibration pulse, then if the system has relaxed adequately so that we can set $d\Delta\theta \approx 0$

$$0 = [\text{Net enthalpy input } (t_1)][t - t_1] + Q_f[t - t_1] - (k_R')_{32} \{[(\theta_{\text{bath}} + \Delta\theta(t_1))^4 - \theta_{\text{bath}}^4]\} [t - t_1] \quad (\text{A.10})$$

Combination with equation (A.9) (with the appropriate change in the lower limit of the integration) gives

$$(k_R')_{362} = \frac{\int_{t_1}^t \text{net enthalpy input } (\tau) d\tau - [\text{net enthalpy input } (t_1)][t - t_1] - C_p M [\Delta\theta(t) - \Delta\theta(t_1)]}{\int_{t_1}^t f_1(\theta) d\tau} \quad (\text{A.11})$$

The corresponding equation for $(k_R')_{262}$ follows from (A.11) on replacing t_1 by t_2 . It is convenient to write all the equations for the determination of the relevant heat transfer coefficients in the “straight line form” e.g.

$$\begin{aligned} & \frac{\int_{t_2}^t \text{net enthalpy input } (\tau) d\tau - [\text{net enthalpy input } (t_1)][t - t_2]}{\int_{t_2}^t f_1(\theta) d\tau} \\ &= \frac{C_p M [\Delta\theta(t) - \Delta\theta(t_2)]}{\int_{t_2}^t f_1(\theta) d\tau} + (k_R')_{262}^0 \end{aligned} \quad (\text{A.12})$$

where $(k_R')_{262}^0$ can be seen to be the value of the integral heat transfer coefficient at $t = t_2$. The value of t_2 should be chosen to be the mid-point of the measurement cycle as $(k_R')_{262}^0$ is the most useful (and well defined) value of the true heat transfer coefficient. It should be noted that extrapolations such as (A.12) automatically remove the effects of $C_p M$ on the value of the derived heat transfer coefficient (a desirable feature because the water equivalents of the cells have the highest errors).

The integral lower bound heat transfer coefficient, $(k_R')^o_{261}$ (equation (A.8) with T replaced by t_2) and the integral true heat transfer coefficient, $(k_R')^o_{262}$, (equation (A.12)) were the “target procedures” for the ICARUS -style evaluations of the experimental data (3).

It should be noted that the definitions of the integral heat transfer coefficients given in this Appendix have regarded these coefficients as being constant in time whereas we would, in fact, anticipate a weak time dependence e.g. equation (A.2) or Fig.6. This weak time-dependence causes an equally weak time-dependence of the derived heat transfer coefficients. Use of the more exact equation (A.2) gives for example for the derived values of $(k_R')_{21}$ in (A.8)

$$(k_R')_{21} = (k_R')^o_{21} [1 - \gamma(t-T) + \gamma \int_T^t \int_T^t f_1(\theta) d\tau d\tau / \int_T^t f_1(\theta) d\tau] \quad (A.13)$$

where $(k_R')^o_{21}$ is the value of $(k_R')_{21}$ at $t = T$. An ultimate test of the validity of the representation of the calorimeters by the differential equation (A.1) is therefore the question of whether the heat transfer can be represented by a single time-dependence coefficient, here $(k_R')^o_{21}$. This question is discussed further in the main text.

We also note that if we regard $f_1(\theta)$ as being constant throughout the measurement cycle (which is a rough approximation for the case of the “lower bound heat transfer coefficients”) then (A.13) becomes

$$(k_R')_{21} = (k_R')^o_{21} [1 + \gamma(T - t)/2] \quad (A.14)$$

Similarly, we obtain

$$(k_R')_{31} = (k_R')^o_{31} [1 - \gamma t/2] \quad (A.15)$$

where $(k_R')^o_{31}$ is now the value of $(k_R')_{31}$ at $t = 0$. It follows that the slopes of the plots of $(k_R')_{21}$ and $(k_R')_{31}$ versus time are roughly one half of the plot of $(k_R')_{11}$ versus time (cf. Fig. 6)

For a more complete discussion see (13), (14).

TABLE 1 Summary of some important values of the heat transfer coefficients.

1	ICARUS METHOD		4	5	6	ICARUS METHOD		9	10	11	12	13	14	15
	2	3				7	8							
Days	$10^9(k_R')_1$ /WK ⁻¹	$10^9(k_R')_2$ /WK ⁻⁴	$10^9(k_R')_{251}^0$ /WK ⁻⁴	$C_p M$ /JK ⁻¹	$10^9(k_R')_{261}^0$ /WK ⁻⁴	$C_p M$ /JK ⁻¹	$10^9(k_R')_{262}^0$ /WK ⁻⁴	$C_p M$ /JK ⁻¹	$10^9(k_R')_{21}^0$ /WK ⁻⁴	$10^9(k_R')_{271}^0$ /WK ⁻⁴	$C_p M$ /JK ⁻¹	$10^9(k_R')_{361}^0$ /WK ⁻⁴	$C_p M$ /JK ⁻¹	$10^9(k_R')_{362}^0$ /WK ⁻⁴
	near $t=t_2$	near $t=t_2$	near $t=0$	r	near $t=t_2$	r	near $t=t_2$	r	at 129,000s		r	evaluation	r	evaluation
1 and 2			0.6215	-349.8 -0.99961					0.619035			near $t=t_1$		near $t=t_1$
3 and 4	0.61913	0.61706	0.62179	-331.6 -0.99955	0.61953	-348.6 -0.99975	0.6196	-397.4 -0.99977	0.618326	0.61884	-322.5 -0.99993	0.63367	-282.1 -0.98786	0.8132
5 and 6	0.62056	0.62016	0.62177	-348.2 -0.99961	0.62115	-340.2 -0.99991	0.62124	-339.1 -0.99993	0.619428	0.61976	-327.7 -0.99999	0.62719	-310.2 -0.99862	0.70098
7 and 8	0.62043	0.62202	0.62205	-349.6 -0.99987	0.62123	-340.7 -0.99993	0.62111	-340.2 -0.99992	0.61979	0.61916	-326.8 -0.99998	0.64828	-211.4 -0.88512	1.15002
9 and 10	0.62049	0.62446	0.62192	-356.9 -0.99838	0.62087	-341.1 -0.99993	0.62085	-341.1 -0.99994	0.619579	0.61977	-330 -0.99999	0.62242	-341.2 -0.98509	0.53265
11 and 12	0.62075	0.62139	0.62207	-355.6 -0.9998	0.62135	-339.8 -0.9999	0.62133	-339.7 -0.99991	0.619157	0.61951	-329.7 -0.99998	0.63371	-273.5 -0.9667	0.94799
13 and 14	0.61972	0.6185	0.62172	-362.3 -0.9995	0.62071	-337.5 -0.99994	0.62101	-336.1 -0.99994	0.61874	0.61913	-325 -0.99997	0.64916	-205.2 -0.96089	0.94681
15 and 16	0.61985	0.62051	0.62172	-348.3 -0.99964	0.62065	-339 -0.9999	0.62064	-338.9 -0.99994	0.618502	0.61885	-321.8 -0.99907	0.61047	-408.6 -0.90565	-0.33424
	mean	mean			mean		mean							
	0.62013	0.62059			0.62078		0.62083							

					ICARUS METHOD
16	17	18	19	20	21
$C_p M$ /JK ⁻¹	$10^9(k_R')_{361}^0$ /WK ⁻⁴	$C_p M$ /JK ⁻¹	$10^9(k_R')_{362}^0$ /WK ⁻⁴	$C_p M$ /JK ⁻¹	$10^9(k_R')_{31}$ /WK ⁻⁴
r	evaluation near $t=t_2$	r	evaluation near $t=t_2$	r	near $t=t_2$
-281.4	0.62032	-321.6	0.62331	-323.4	0.61886
-0.99827		-0.99891		-0.99914	
-310.9	0.62094	-341.1	0.62017	-340.6	0.62028
-0.9997		-0.99927		-0.99941	
-181.1	0.62086	-347.9	0.61934	-347.5	0.62063
-0.969		-0.99782		-0.99819	
-363.3	0.62099	-338.7	0.62131	-339.4	0.62102
-0.99973		-0.99951		-0.99952	
-242.5	0.62094	-375.7	0.61925	-375	0.62704
-0.99231		-0.99921		-0.99933	
-211	0.62041	-328.9	0.62007	-320	0.61704
-0.98956		-0.99926		-0.99808	
-580.7	0.62044	-329.9	0.61872	-332.6	0.61734
-0.98163		-0.99978		-0.99964	

Table 2								
Thermal balances using the integral heat transfer coefficient based on backward integration of the data sets.								
1	2	3	4	5	6	7	8	
Days	input $d\tau$	$10^{-9} f_1(\theta)d\tau$	$10^9(k_R')_{262}$	$10^9(k_R')_{262}$	thermal	output	equivalent	
	/J	K^4s	ΔWK^{-4}	ΔWK^{-4}	output	- input $d\tau$	excess rate	
			near $t=t_2$	near $t=0$	/J	/J	/W	
3 and 4	140501.1	226640.2	0.6187	0.6195	140403.6	181.313	0.00109	
5 and 6	141849	228529.4	0.62034	0.62114	141948.8	182.824	0.00110	
7 and 8	141774.4	228484.3	0.62021	0.62101	141891	182.788	0.00110	
9 and 10	143166.6	230672.1	0.61995	0.62075	143189.7	184.538	0.00111	
11 and 12	143956.7	231844.2	0.62043	0.62123	144028.6	185.476	0.00112	
13 and 14	145003.8	233772.4	0.62011	0.62091	145151.6	187.018	0.00113	
15 and 16	144858	233584.8	0.61974	0.62054	144948.7	186.868	0.00113	

References

- 1) M. Fleischmann, S. Pons and M. Hawkins, J. Electroanal Chem., 261 (1989) 301; 263 (1989) 187.
 - 2) M. Fleischmann, S. Pons, M.W. Anderson, L.J. Li and M. Hawkins, J. Electroanal Chem., 287 (1990) 293
 - 3) ICARUS -2; Isoperibolic Calorimetry : Acquisition, Research and Utilities System. Document Version 2.0 (February, 1995), TECHNOVA INC., 13th Floor, Fukoku Seimei Building, 2-2-2 Uchisaiwai-cho, Chiyoda-Ku, Tokyo 100, Japan.
- The ICARUS -1 System is described in:
- The ICARUS Systems; Isoperibolic Calorimetry : Acquisition, Research and Utilities System, Version 1 (December 1993), Low Power Measuring System for Three Cells, TECHNOVA INC., 13th Floor, Fukoku Seimei Building, 2-2-2 Uchisaiwai-cho, Chiyoda-Ku, Tokyo 100, Japan.
- 4) P.A. Mosier-Boss and S. Szpak, Nuovo Cimento, 112A (1999) 577.
 - 5) O. Levenspiel, "Chemical Reaction Engineering" (1972) Wiley, London.
 - 6) M.H. Miles, M.A. Imam and M. Fleischmann, " Our Penultimate Paper on the Calorimetry of the Pt/D₂O and Pd/D₂O Systems Part II : A Comparison of the Pt/D₂O, Pd-B-Ce/D₂O and Pd-B/D₂O systems", paper submitted for publication.
 - 7) "Thermal Behaviour of Polarised Pd/D Electrodes prepared by Co-deposition", submitted for publication.
 - 8) Frederick T. Wagner, Thomas E. Moylan, Michael E. Hayden, Ulrike Narger and James L. Booth, J. Electroanal Chem., 295 (1990) 393.
 - 9) Wilford N. Hansen, Proceedings of the Second Conference on Cold Fusion, Conference Proceedings of the Italian Physical Society, Editors: Tullio Bressani, Emilio Del Giudice, Giuliano Preparata, Como, Italy. 33 (1991) 491; ISBN 88-7794-045-X. see also Michael E. Melich and Wilford N. Hansen, Proceedings of the Third International Conference on Cold Fusion, Universal Academy Press, Frontiers of Science Series N° 4, Editor : H. Ikegami, Tokyo, Japan, (1993) 397; ISBN 4-946443-12-6.
 - 10) M. Fleischmann and S. Pons, J. Electroanal Chem., 332 (1992) 33.
 - 11) R.H. Wilson, J.W. Bray, P.G. Kosky, H.B. Vakil and F.G. Will, J. Electroanal Chem., 332 (1992) 1.
 - 12) M. Fleischmann, S. Pons, Monique Le Roux and Jeanne Roulette, Trans. Fusion Technol., 26 (1994) 323.

13) M. H. Miles, M. Fleischmann and M. A. Imam, Report NRL / MR / 6320—01—8526, Naval Research Laboratory, Washington, DC 20375-5320, March 2001.

14) S. Szpak and P. A. Mosier-Boss, Technical Report 1862, Volume 2, SPAWAR Systems Centre, San Diego, February 2002.

15) Fritz G. Will, J. Electroanal Chem., 426 (1997) 177.

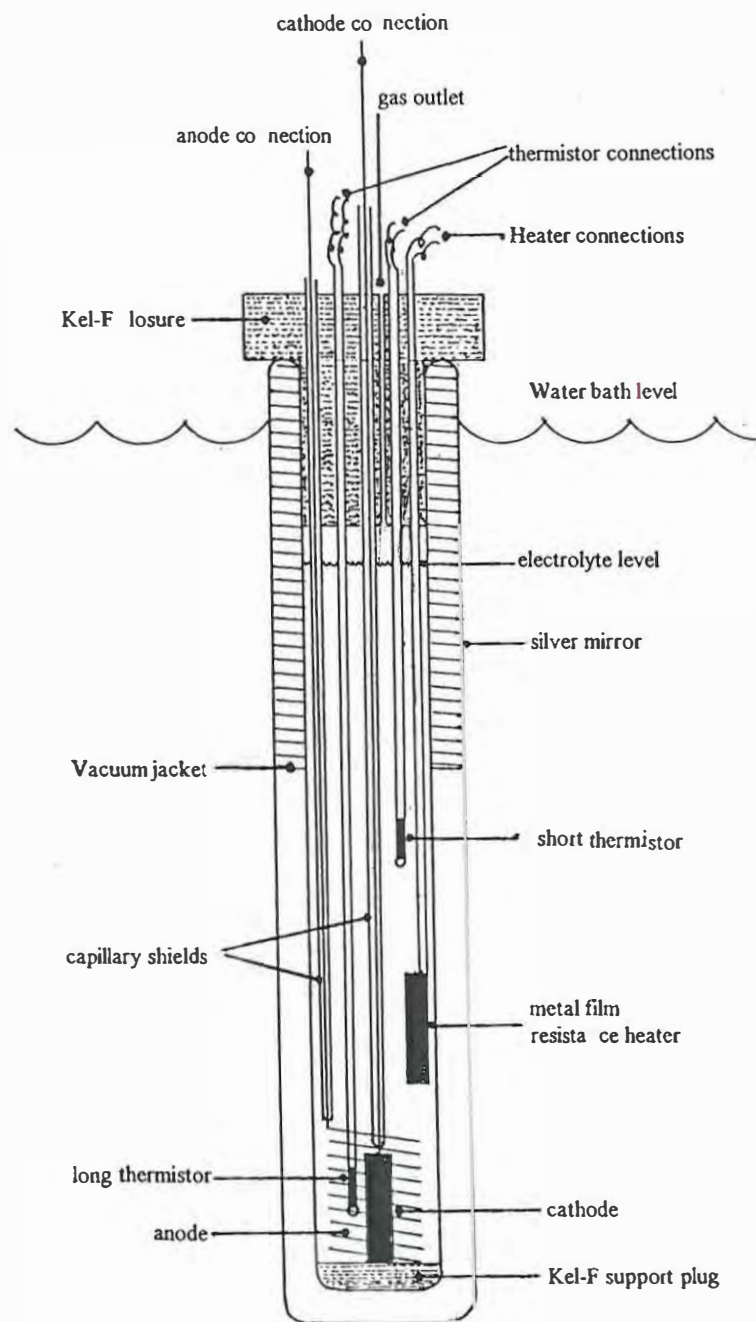


Fig. 1 The Isoperibolic Calorimetric Cell.

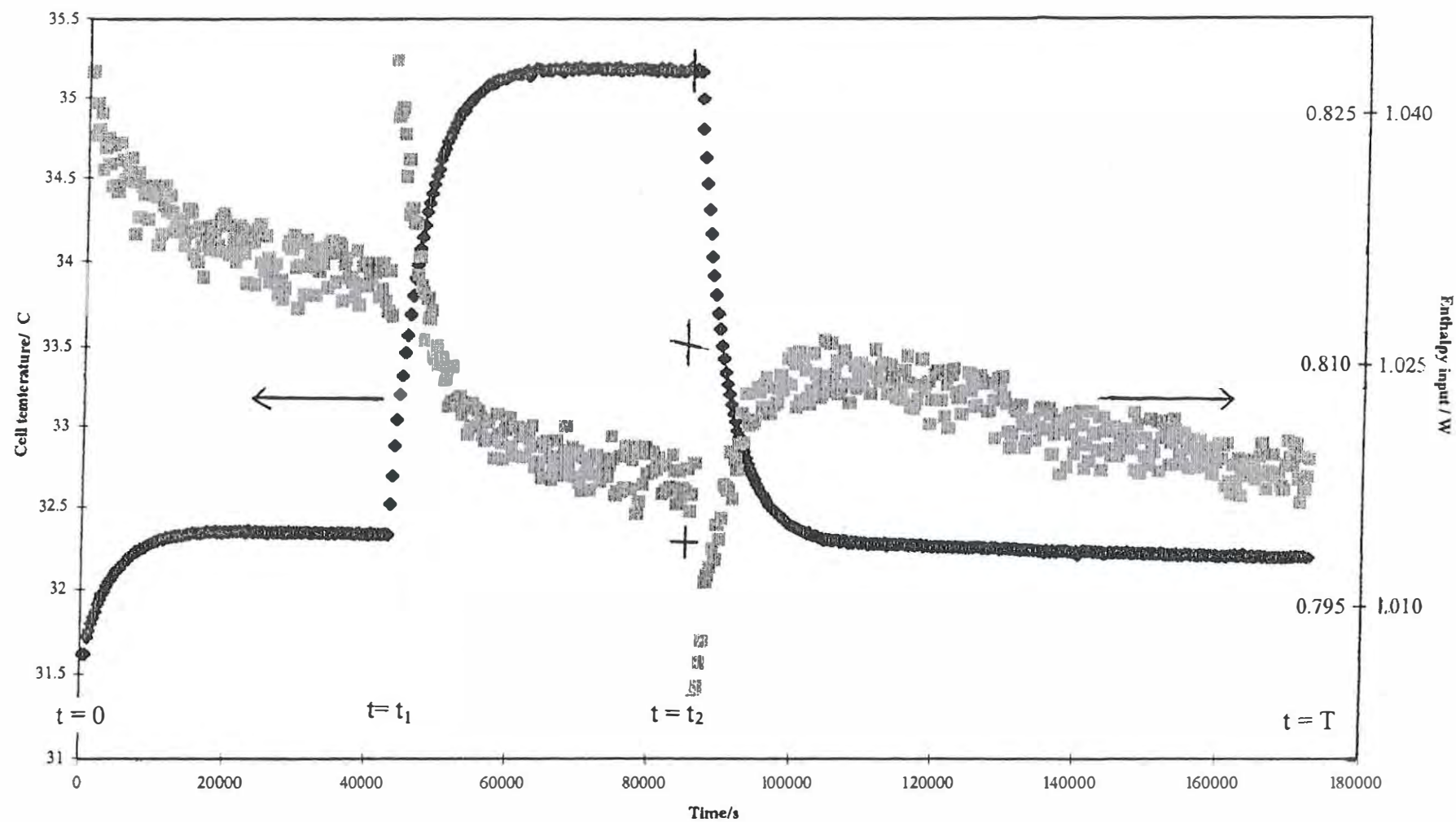


Fig. 2 Plot of the “raw data” for days 9 and 10 of the “blank experiment”.
 Pt cathode ($\phi = 1\text{mm}$, $\ell = 2\text{cm}$) polarised at 0.2A in $0.1\text{ M LiOD/D}_2\text{O}$.
 Estimates of the pseudo-radiative lower bound heat transfer coefficient, $(k_R')_1$, and of the pseudo-radiative true heat transfer coefficient, $(k_R')_2$, can be made near the end of the calibration period at $t = t_2$.

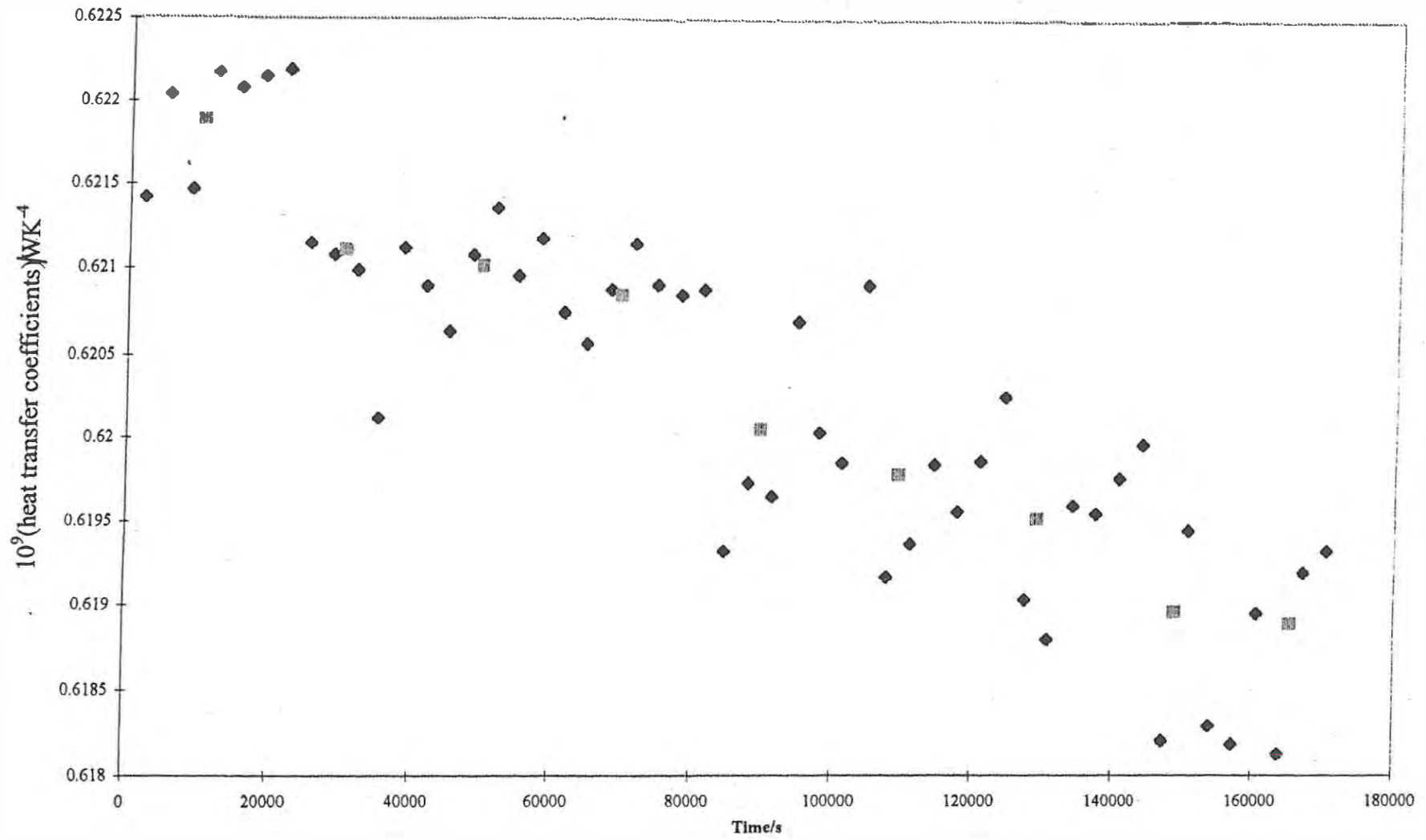


Fig. 3 The values of $(\overline{k_R})_{11}$ \blacklozenge , and of $(\overline{k_R}')_{11}$ \square , for days 1 and 2 of the measurement cycles.

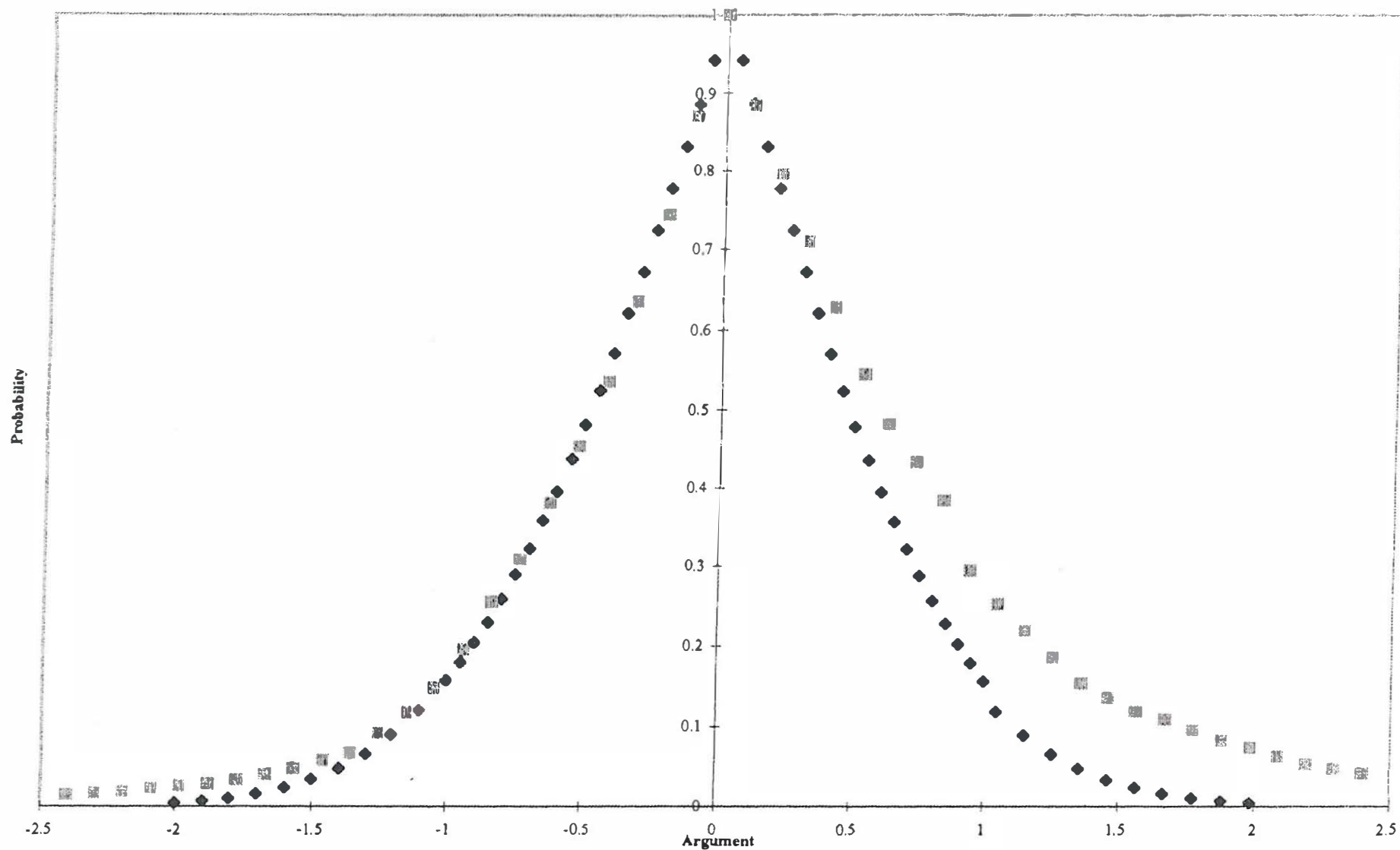


Fig. 4 The upper and lower tail distributions of the differential rates of excess enthalpy generation for days 3-16 of the measurement cycles, ▣; comparison with a normal distribution of errors, ◆.

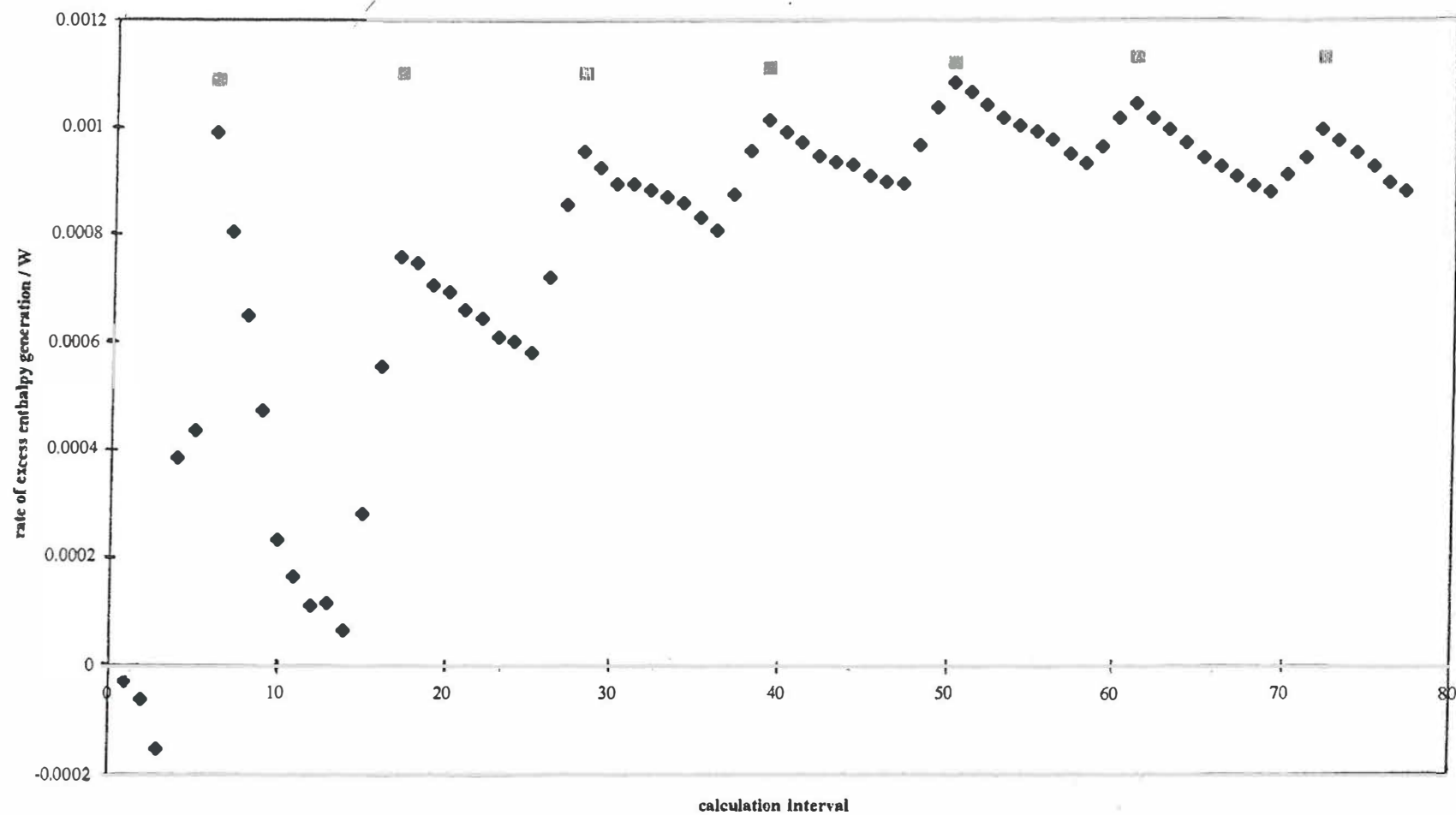


Fig. 5A The differential rates of excess enthalpy generation calculated with a true heat transfer coefficient varying with time, ◆. The figure also shows rates calculated using the integral value of the heat transfer coefficient ◻, see table 2 below.

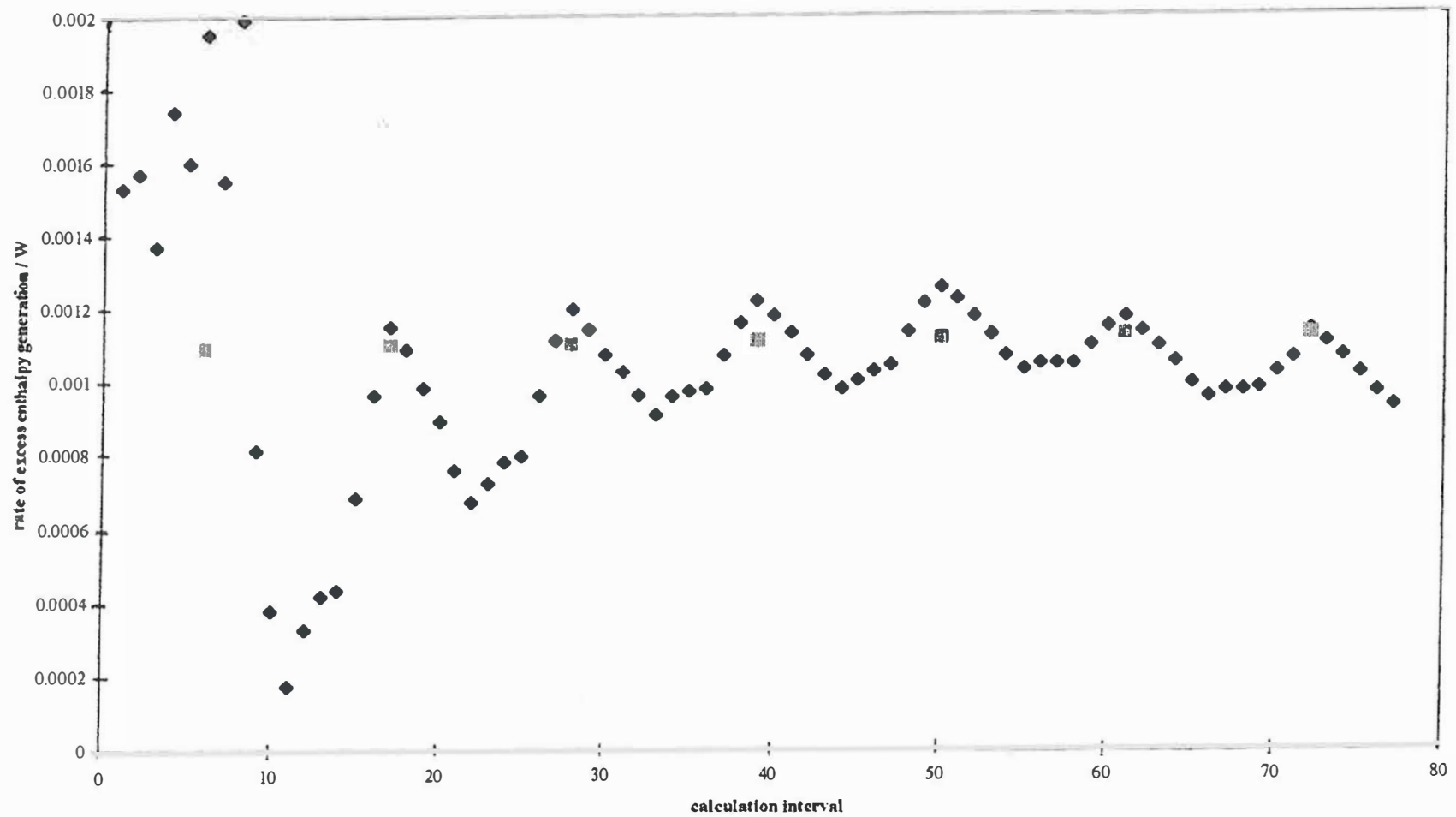


Fig. 5B The differential rates of excess enthalpy generation calculated using a single value of the true heat transfer coefficient at $t = 86,400\text{s}$, \blacklozenge . The figure also shows rates calculated using the integral value of the heat transfer coefficients, \blacksquare , see Table 2 below.

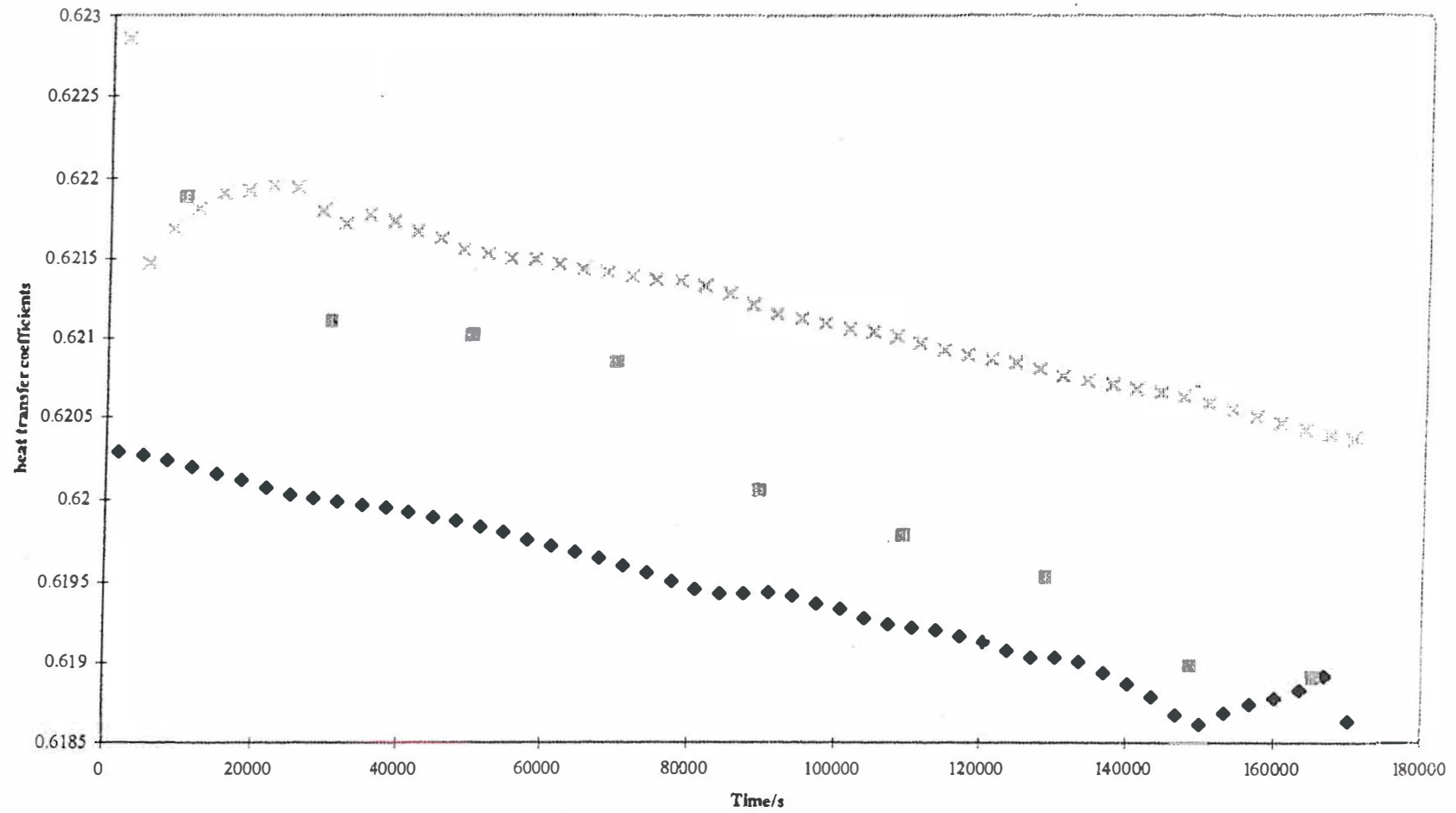
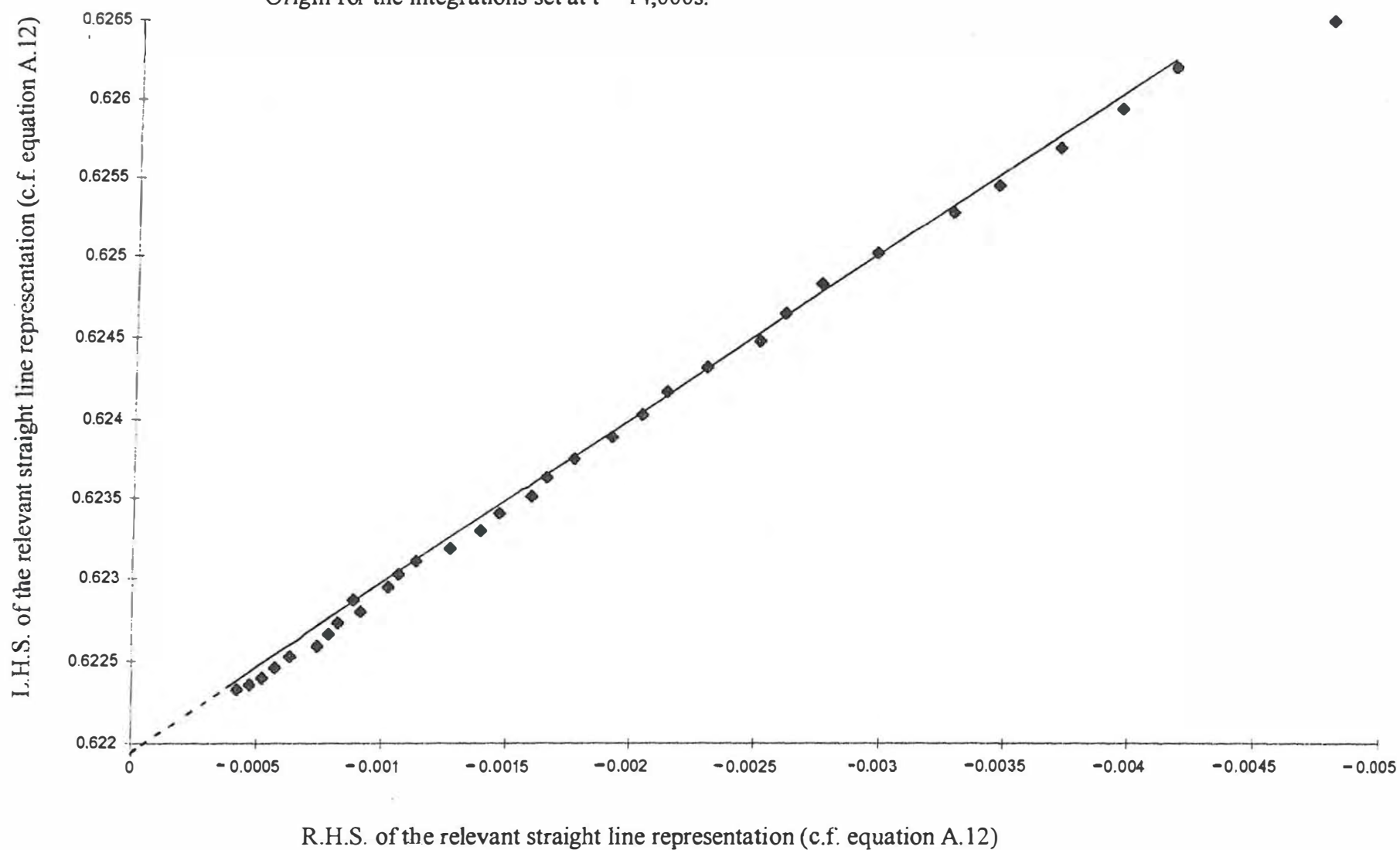


Fig. 6 Comparison of the variation with time of the integral heat transfer coefficients, $(k_R')_{31}$ and $(k_R')_{21}$ x, ◆, with the differential lower bound heat transfer coefficient, $(k_R)_{11}$ ■ Days 1 and 2 of the measurement cycles.

Fig. 7A Evaluation of $(k_R')^0_{251}$ and C_pM for Days 9 and 10 of the measurement cycles.
Origin for the integrations set at $t = 14,000s$.



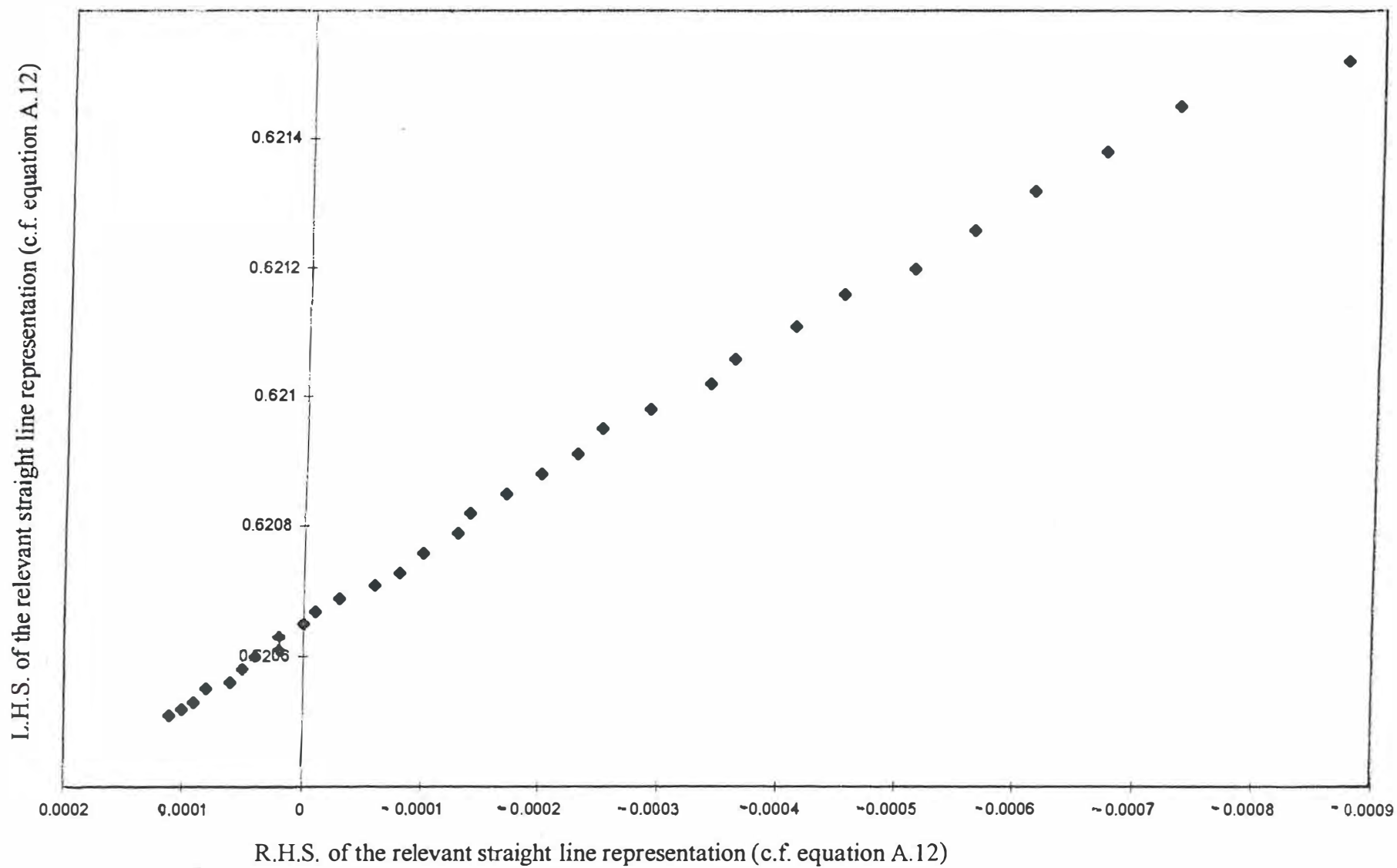


Fig. 7B Evaluation of $(k_R')_{251}^0$ and CpM for Days 9 and 10 of the measurement cycles. Origin for the integrations set at $t = T$.

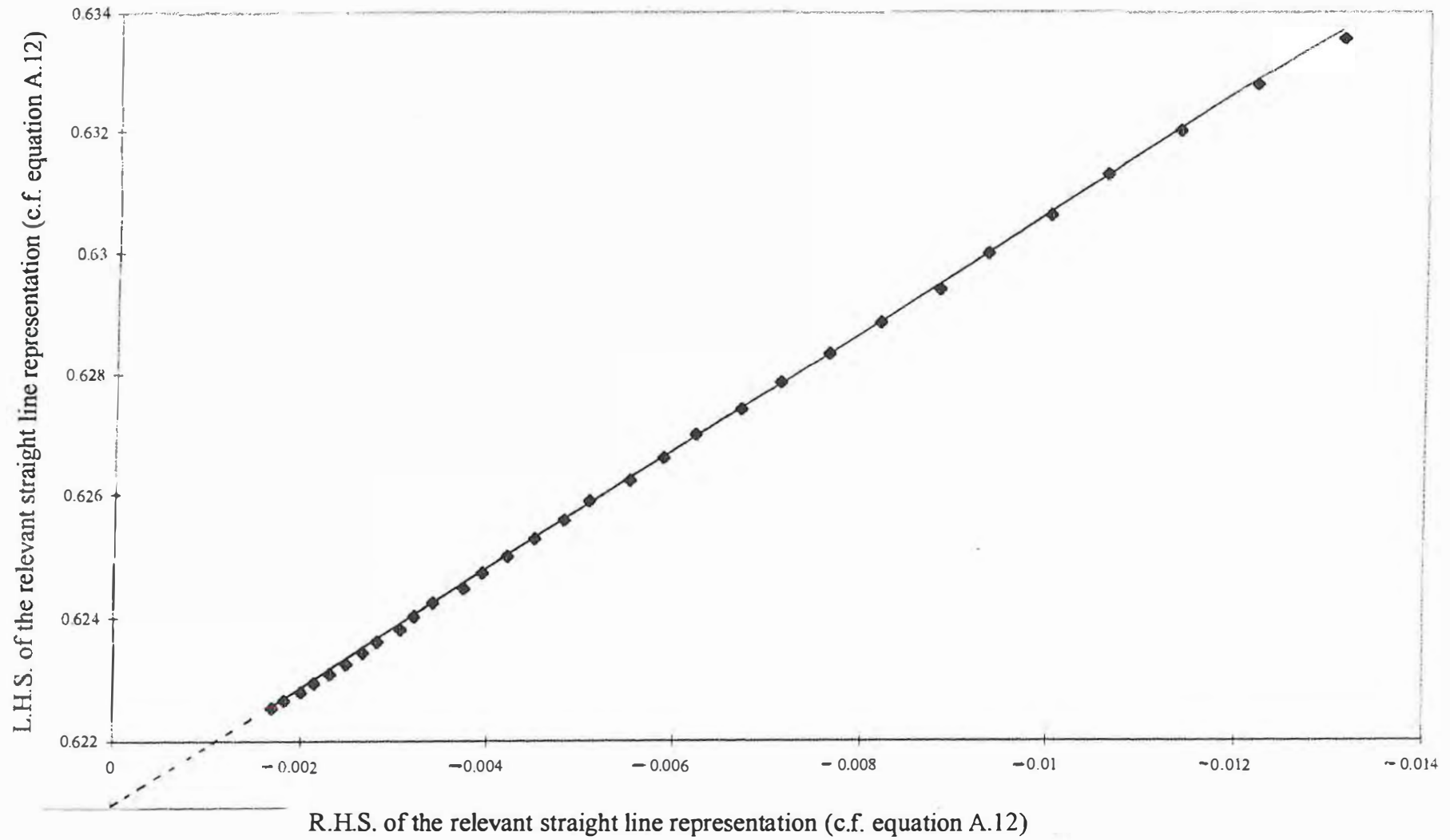


Fig. 8A Evaluation of $(k_R')_{261}^0$ and C_{pM} for Days 9 and 10 of the measurement cycles. Origin for the integrations set at $t = t_2$.

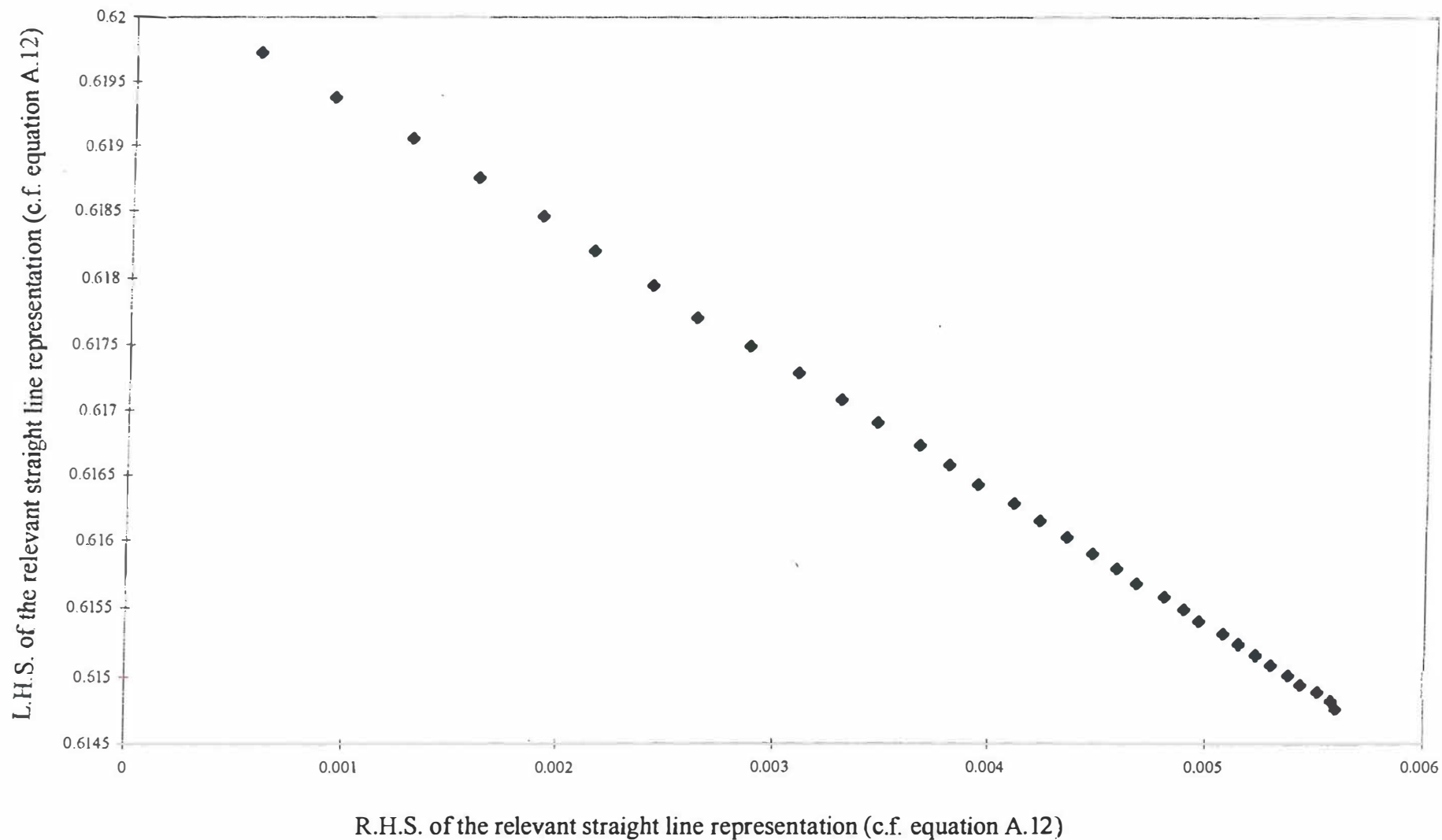


Fig. 8B Evaluation of $(k_R')_{261}^\circ$ and C_pM for Days 9 and 10 of the measurement cycles. Origin for the integrations set at $t = T$.

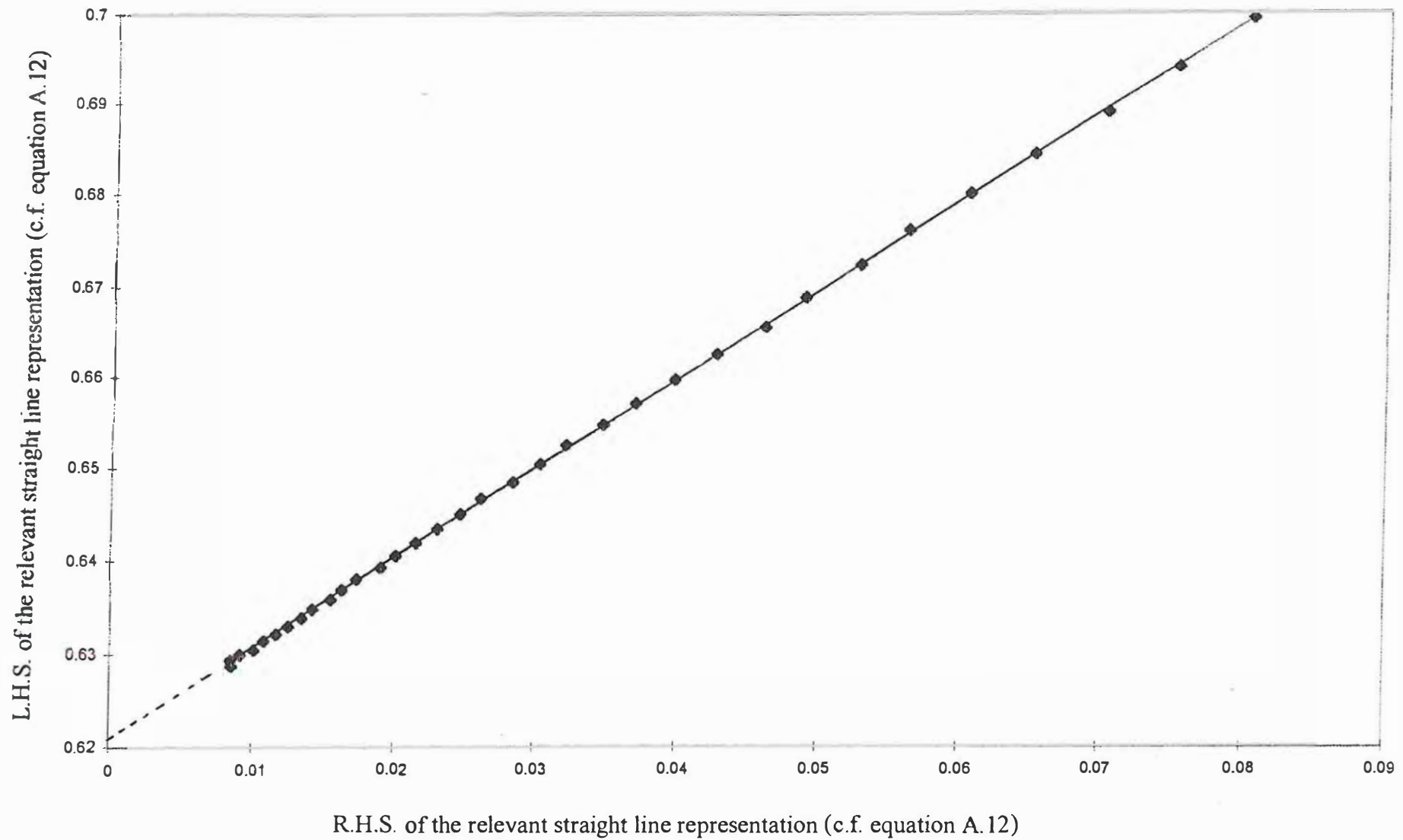


Fig. 9 Evaluation of $(k_R')_{262}^0$ and C_pM for Days 9 and 10 of the measurement cycles. Origin for the integrations set at $t = t_2$.

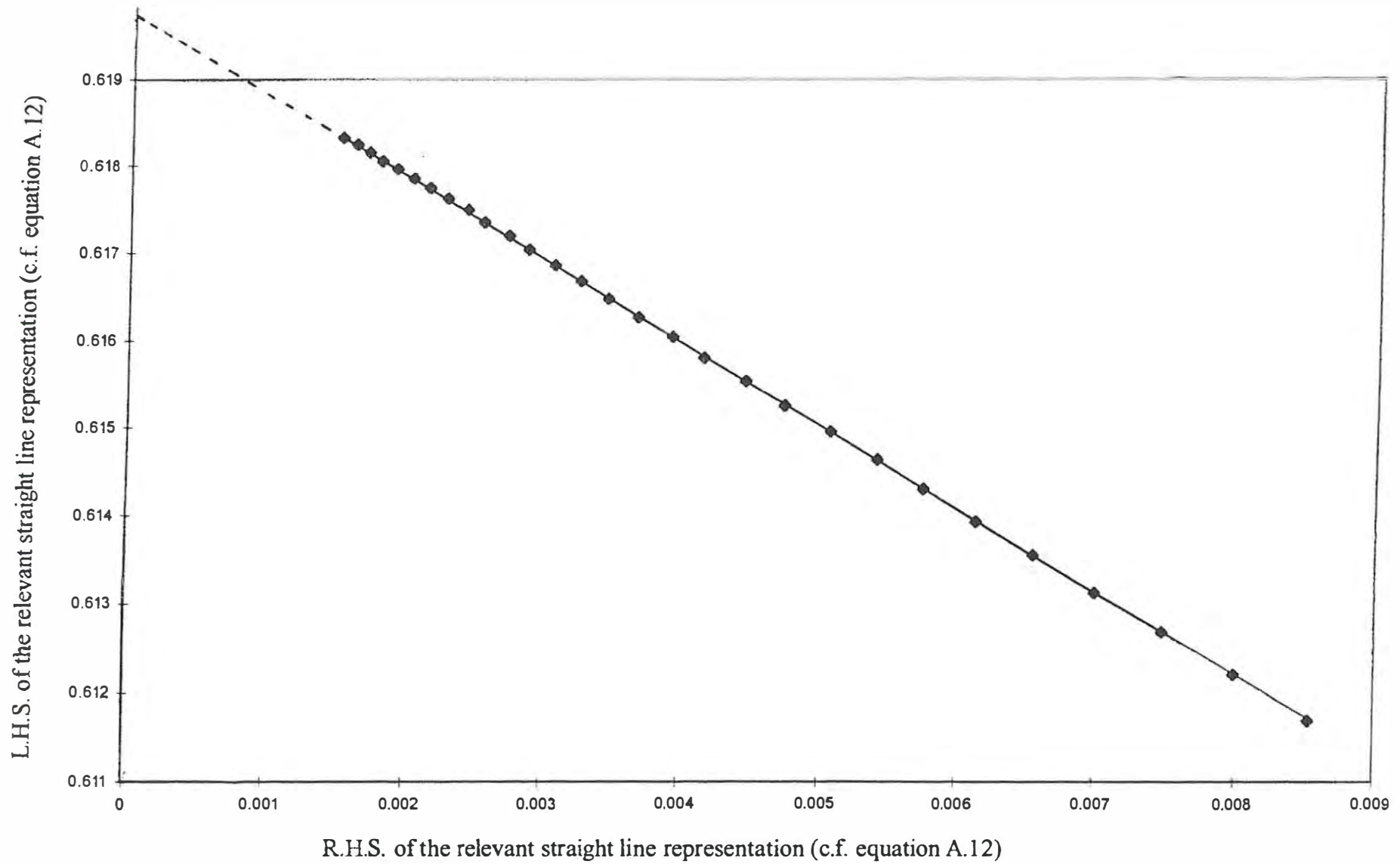


Fig. 10 Evaluation of $(k_R')_{271}^0$ and CpM for Days 9 and 10 of the measurement cycles. Origin for the integrations set at $t = T$.

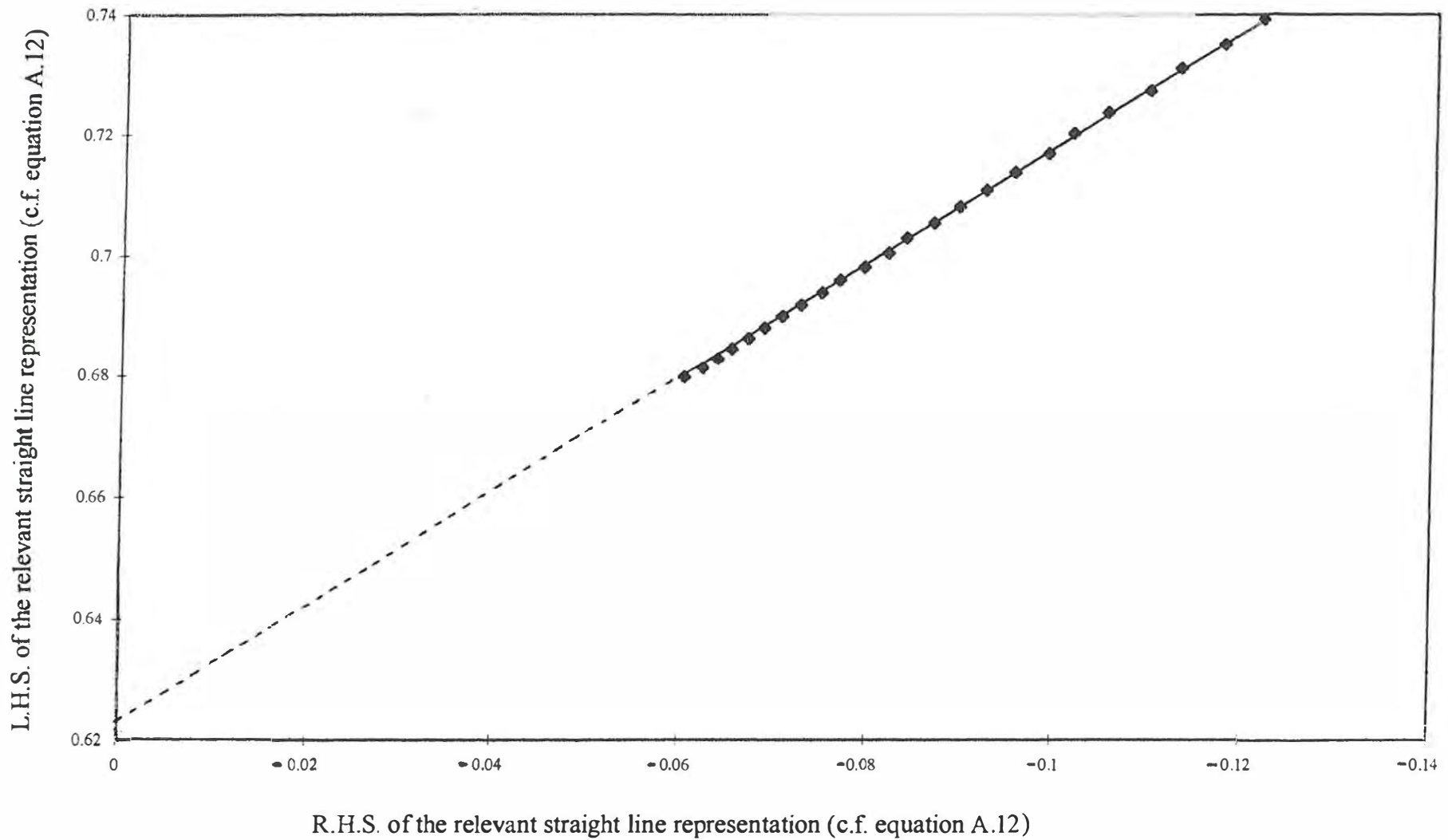


Fig. 11 Evaluation of $(k_R')_{361}^0$ and $C_p M$ for days 9 and 10 of the measurement cycles
origin for the integrations set at $t = t_1$. Use of the 33 measurement intervals adjacent to $t = t_1$

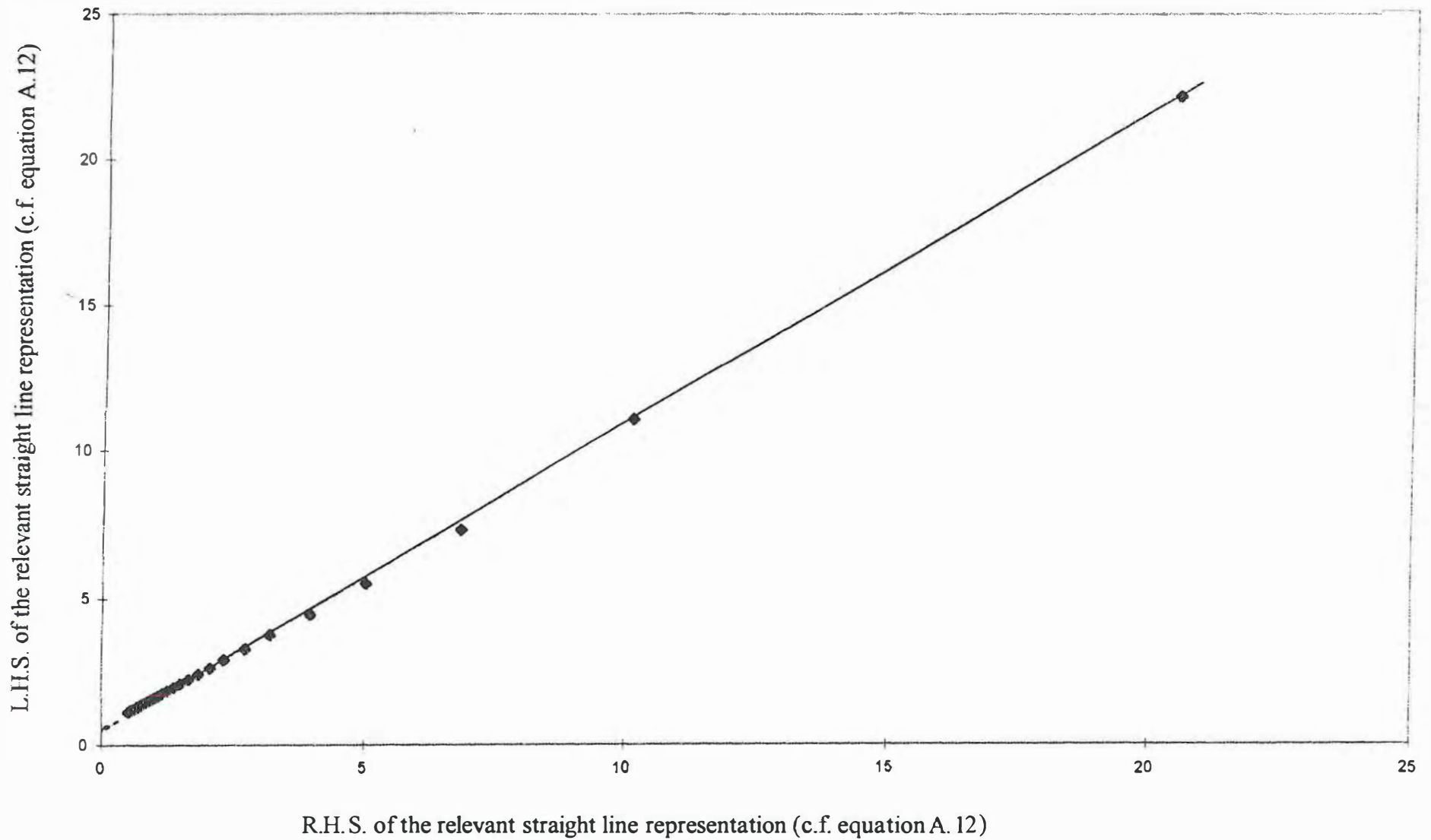


Fig. 12 Evaluation of $(k_R')_{362}^0$ and $C_p M$ for days 9 and 10 of the measurement cycles origin for the integrations set at $t = t_1$. Use of the 33 measurement intervals adjacent to $t = t_1$.

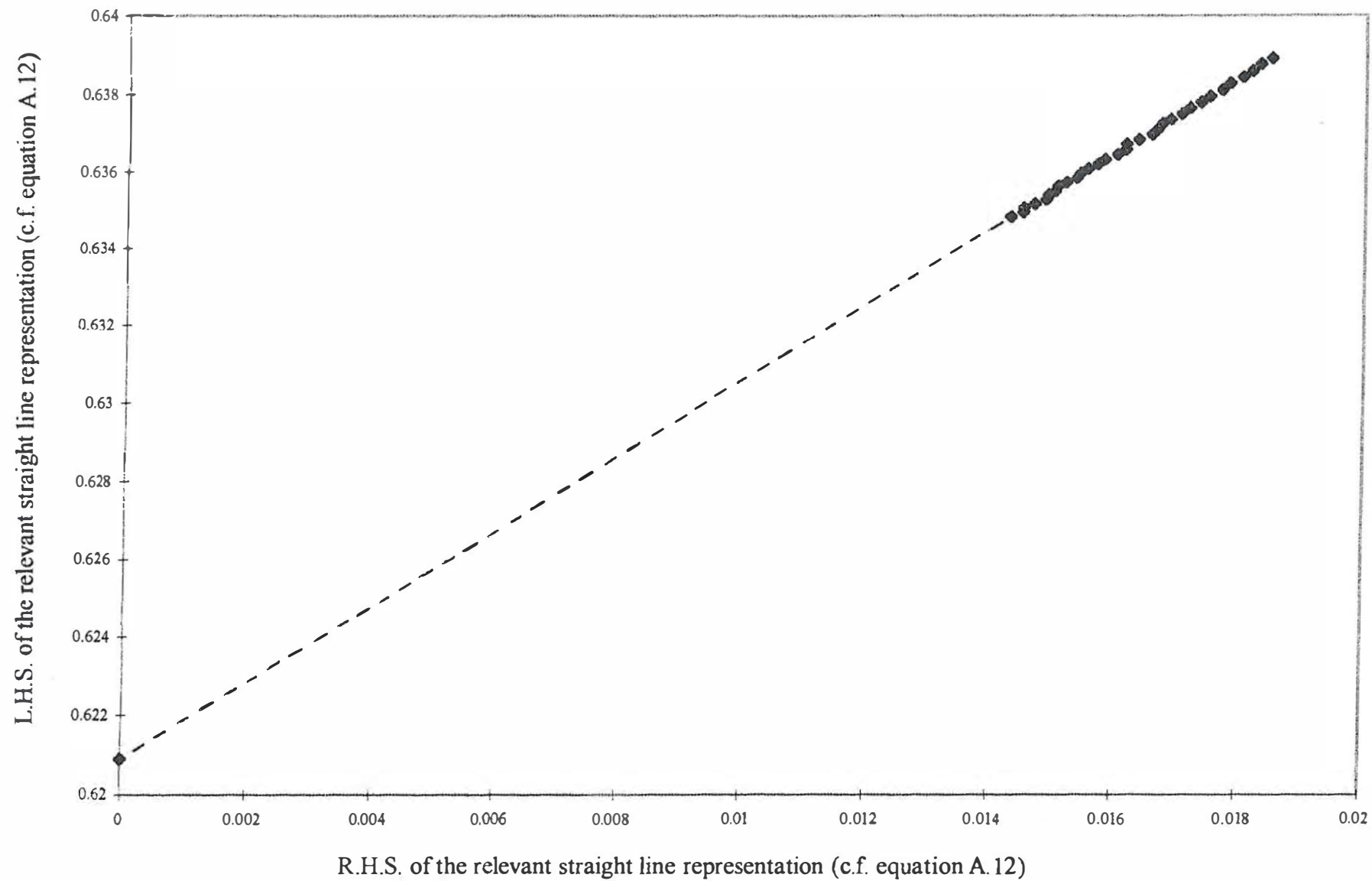


Fig. 13 Evaluation of $(k_R')^0_{361}$ and $C_p M$ for days 9 and 10 of the measurement cycles origin for the integrations set at $t = t_1$. Use of the 33 measurement intervals adjacent to $t = t_2$

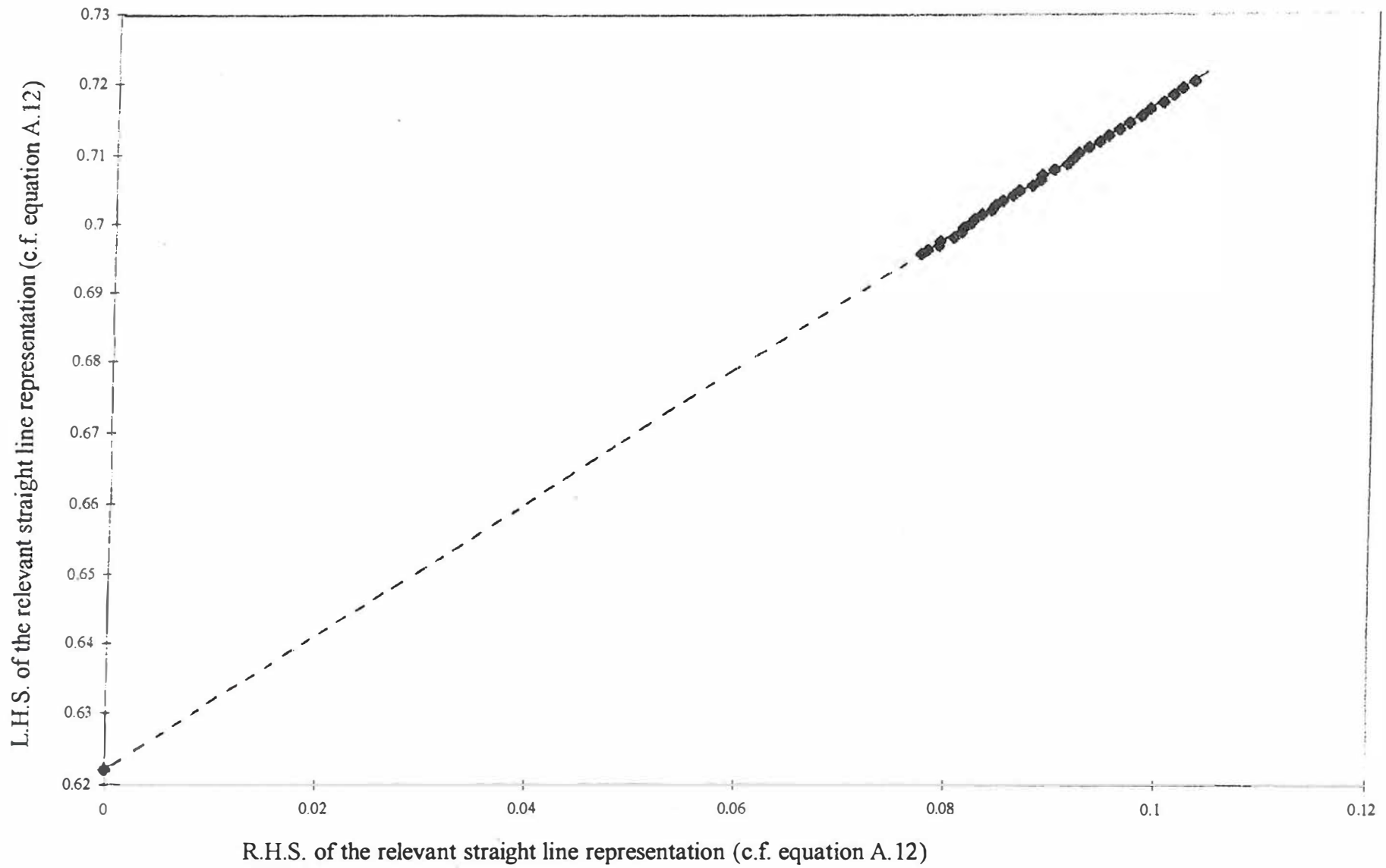


Fig. 14 Evaluation of $(k_R')^0_{362}$ and $C_p M$ for days 9 and 10 of the measurement cycles origin for the integrations set at $t = t_1$. Use of the 33 measurement intervals adjacent to $t = t_2$

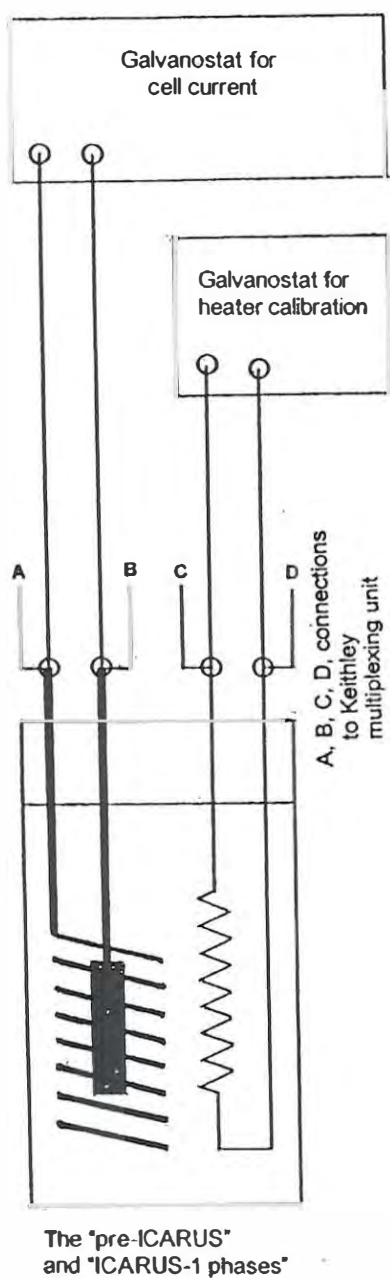


Fig. 15A Schematic of the polarising circuit used with the ICARUS -1 System.

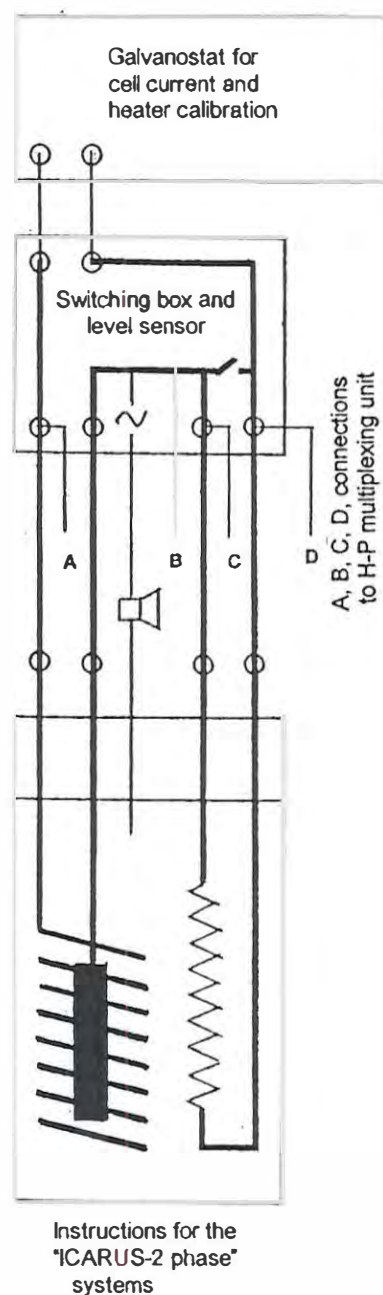


Fig. 15B Schematic of the polarising circuit used with the ICARUS -2 System. The figure shows the provision of the means of using the cell current to calibrate the system as well as the means for testing the level of the electrolyte in the cell.

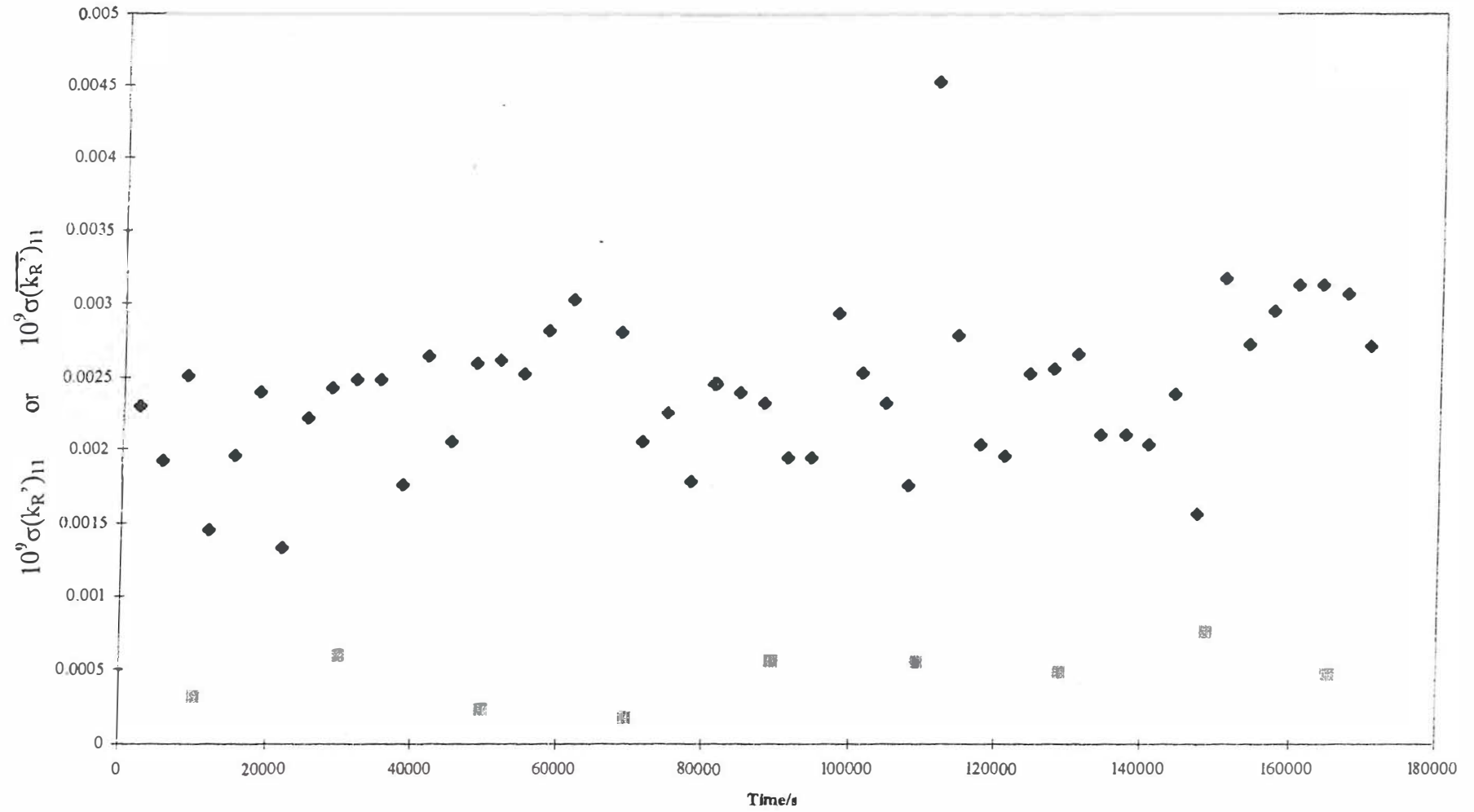


Fig. 16 The standard deviations of the differential lower bound heat transfer coefficients $10^9 (k_R')_{II}$, ◆, and $10^9 (\overline{k_R})_{II}$, ■, Days 1 and 2 of the measurement cycles.

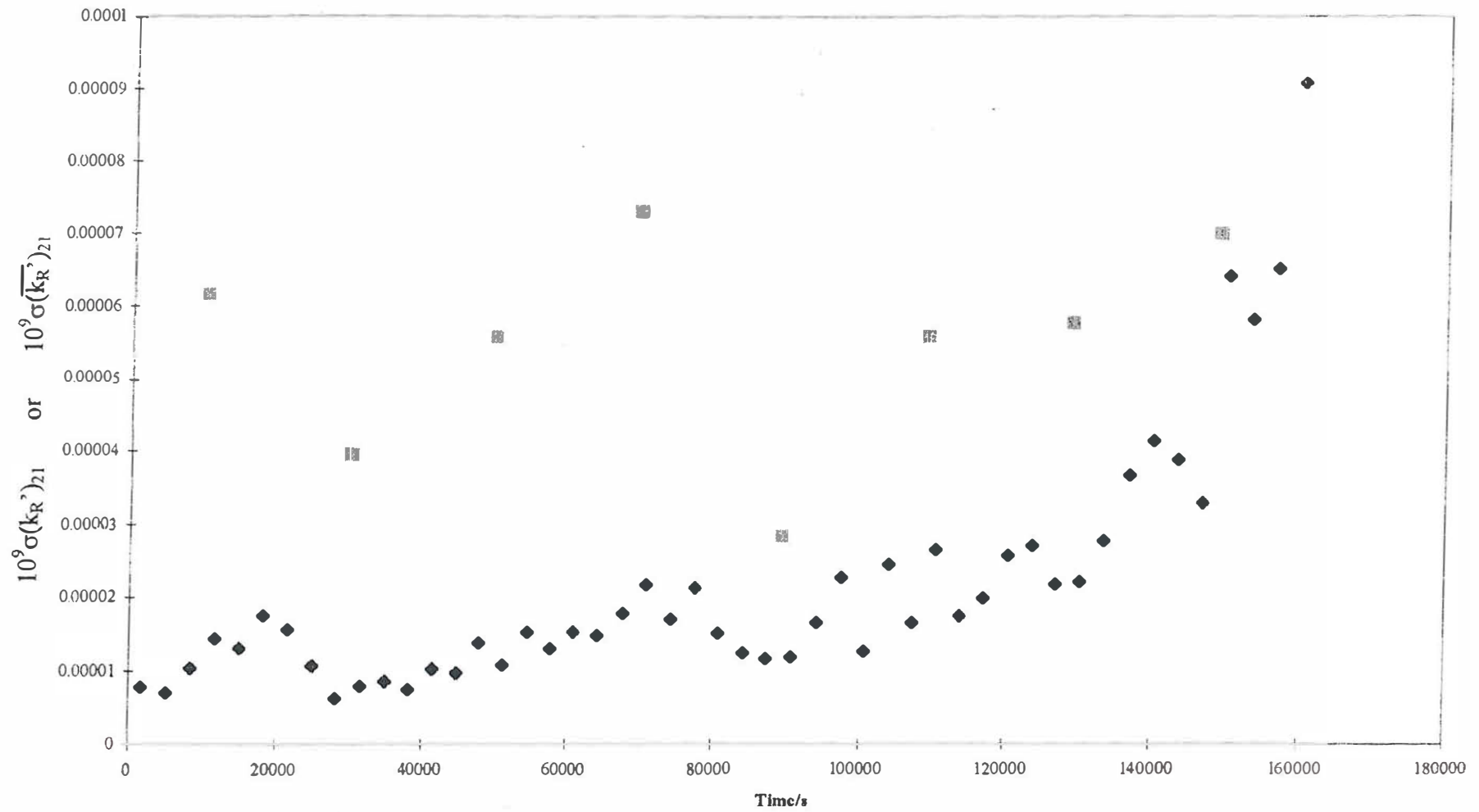


Fig. 17 The standard deviations of the integral lower bound heat transfer coefficients $10^9 (k_R')_{21}$, ◆, and $10^9 (\overline{k_R}')_{21}$, ■, Days 1 and 2 of the measurement cycles.

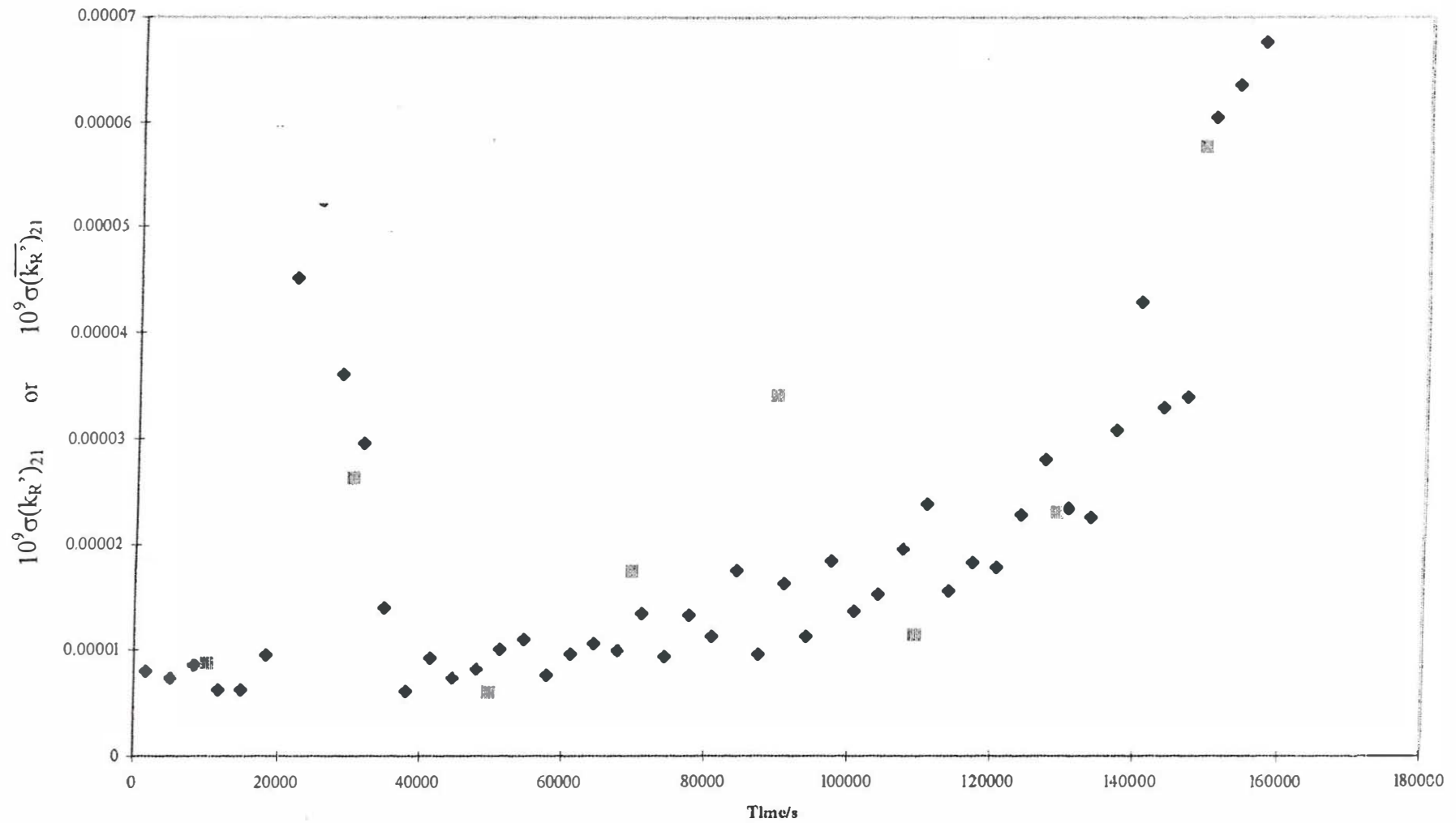


Fig. 18 The standard deviations of the integral lower bound heat transfer coefficients $10^9 (k_R')_{21}$, ◆, and $10^9 (\overline{k_R'})_{21}$, ■, evaluated about the median centre lines. Days 1 and 2 of the measurement cycles.

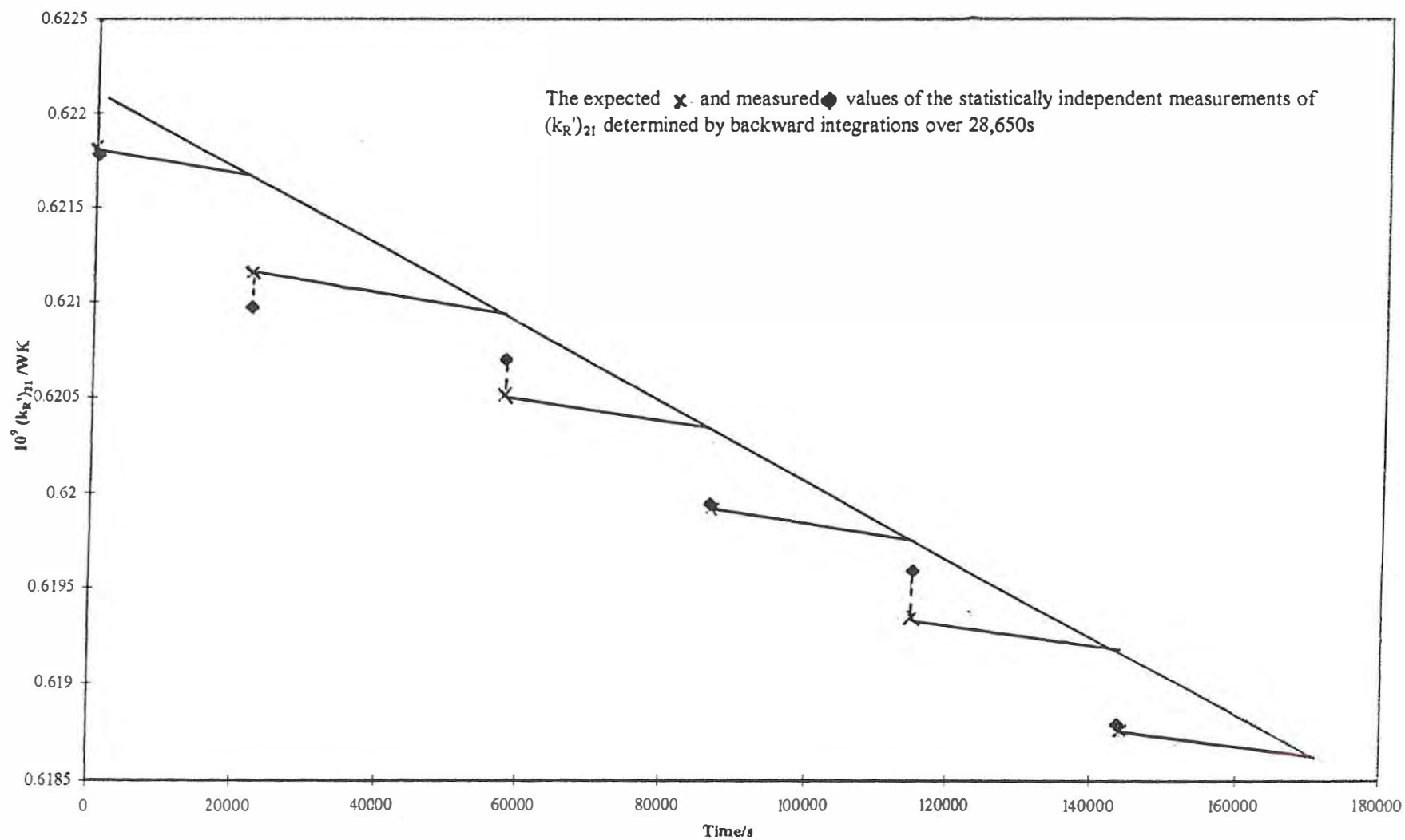


Fig. 19 The expected, \times , and measured \blacklozenge values of the statistically independent measurements of $(k_R')_{21}$, determined by backward integrations over 28,650s time intervals.

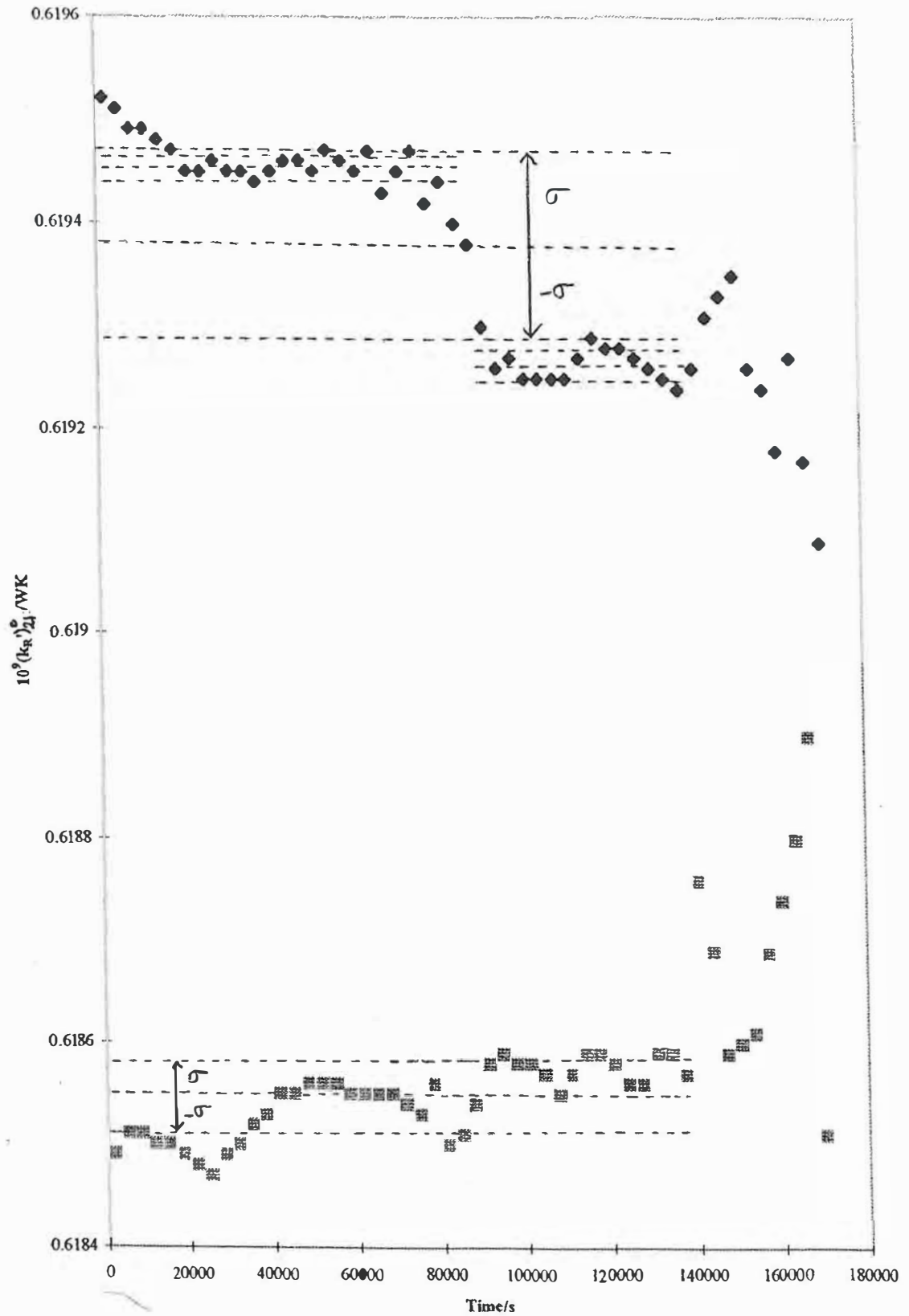


Fig. 20 The variation of derived value of $(k_R')_{21}$, with time (equation (A.13)). Data for days 9 and 10, ♦, and for days 1 and 2, ■

Our Penultimate Paper on the Isoperibolic Calorimetry of the Pt/D₂O and Pd/D₂O Systems

Part II : the Pd/B and Pd-B-Ce Systems

M. Fleischmann, Bury Lodge, Tisbury, Salisbury, Wilts., SP3 6LJ, U.K.

M.H. Miles, Department of Chemistry, University of La Verne, La Verne, CA 91750
U.S.A.

M.A. Imam, Naval Research Laboratory, Washington, DC 20375-5320, U.S.A.

Abstract

The generation of excess enthalpy for Pd-B and Pd-B-Ce cathodes polarised in 0.1M LiOD/D₂O is investigated using the preliminary methods of data analysis of the ICARUS-1 (1) and ICARUS-2 (2) Systems. Comparisons are made with the complete ICARUS-style data analysis of a series of measurement cycles for the Pt-D₂O “blank” system (3) and with the preliminary analysis of a short data section (6 days) for the same system carried out during 1994 (4).

It is shown that there was only a low level of excess enthalpy generation for the Pd-B-Ce system ; however, the use of this system in lieu of a “blank” has failed presumably because of low and variable rates of excess enthalpy production. For the Pd-B system the “lower bound” heat transfer coefficient, $(k_R')_{11}$, showed an abnormally large variation with time following the “topping up” of the cell with D₂O to make up for losses due to electrolysis in the open cell. We attribute such variations to contamination of the heavy water by light water (see further below). This variation prevents the application of the complete ICARUS -style data analysis, (3), which must therefore remain restricted to the preliminary methods used in this analysis scheme.

The onset of excess enthalpy generation as well as the intervention of “positive feedback” was established at short times for the Pd-B system and, in contrast to the behaviour of Pd electrodes (5), there is no evidence for any threshold value of the current

density for the onset of this excess enthalpy generation. Furthermore, there is evidence for “positive feedback” throughout the time range of this experiment which must be attributed to differences in the protocols used in this experiment in comparison to the earlier studies (e.g. see (6)).(in particular, to the low current densities used in the present experiment). It is also shown that the quoted powers delivered to the Joule heater used to calibrate the cell were in error and this was a contributory factor preventing the use of the full ICARUS evaluation strategy for this experiment (contrast (3)).

A comparison is made between the levels of excess enthalpy generation reached in the initial study, (5), and the values achieved in the present investigation which remain restricted due to the limited range of current densities used.

Introduction

As has already been explained, (3), the present series of papers has been prompted by the continued opposition to the publications on the topic of “Cold Fusion” in the Scientific Literature. The objective of the present papers is to demonstrate the evaluation of the precision and accuracy of the isoperibolic calorimetry used in the initial investigation of the phenomenon, (e.g. see (5)), followed by the illustration of the answer to the question : “why were we so certain that there is excess enthalpy generation during the cathodic polarisation of Pd-based electrodes ?”

In Part I of this series, (3), we have presented a complete ICARUS -style analysis, (1), (2), of the behaviour of the Pt- D₂O “blank system”. The generation of excess enthalpy in such systems is restricted to that due to the reduction of electrogenerated oxygen which, moreover, generates an excess rate which is constant in time. We have therefore been able to carry out accurate evaluations of both the differential and integral heat transfer coefficients and to use these coefficients to determine the rates of excess enthalpy generation (for a description of these coefficients, see the Appendix). In line with earlier assessments ((1), (2), (6), (7), (8)) we have shown that the optimal precision and accuracy is achieved when using the integral heat transfer coefficients based on backward integration of the time series (i.e. integration from long to short times) such as $(k_R')_{261}$ and $(k_R')_{262}$. The precision and accuracy of these coefficients is characterised by relative errors < 0.01%. In consequence it is possible to evaluate the excess rates to within 0.1 mW, these rates being due to the reduction of electrogenerated oxygen. An alternative strategy is to carry

out appropriate signal averaging when using the less precise and accurate differential heat transfer coefficients $(k_R')_{11}$ and $(k_R')_{12}$, (3). The low values of these rates (of order 1 mW) may be contrasted with the extreme statements which have been made in the literature.¹

The present paper is restricted to evaluations of calorimetric experiments using Pd-B and Pd-B-Ce cathodes carried out by one of us (M.H.M.) in the Laboratories of the New Hydrogen Energy Group (N.H.E.) in Sapporo, Japan. It will be shown that these evaluations have to be confined to the initial assessment of the “lower bound” heat transfer coefficient, $(k_R')_1$, and the “true” coefficient, $(k_R')_2$, carried out near the ends of the calibration periods $t = t_2$, Fig. 1, as well as the differential “lower bound” heat transfer coefficients $(k_R')_{11}$, $(\overline{k_R'})_{11}$ and $(\overline{\overline{k_R'}})_{11}$ evaluated throughout the time range of the measurement cycles (the bars denote averaging procedures, see the Appendix). The evaluation of a restricted set of these measurement cycles has already been given previously. (9), (10), (11).

This division of the present investigation into a number of Parts will also explain the somewhat strange title “Our Penultimate Paper on the Isoperibolic Calorimetry of the Pt/D₂O and Pd/ D₂O Systems”. It has been our view that the only paper which would be justified at the present time would be a comparative evaluation of the various studies of “Cold Fusion” systems, paying due attention to the precision and accuracy of the various studies. We would regard such a paper as being “Our Ultimate Paper on the Isoperibolic Calorimetry of the Pt/D₂O and Pd/ D₂O Systems” which might, however, well mark the beginning of a new phase of the investigation of “Cold Fusion”.

We have identified nine studies which could form the basis of such an “Ultimate Paper” but, for a variety of reasons, we have been unable to secure the release of the prime sets of the raw data for all but two of the investigations. We have therefore had to restrict attention to the measurements on the Pd-B / D₂O and Pd-B-Ce / D₂O and the Pd-D

¹ We note that such extreme statements have been based on suppositions rather than measurements; it is perfectly possible to evaluate such rates quantitatively by carrying out experiments at sufficiently high precision and accuracy when using appropriate “blank systems”.

We note also that the extreme statements about the generation of excess enthalpy are frequently accompanied by equally extreme statements about the accuracy of the heat transfer coefficients. In this case one can usually trace the origin of these statements to the use of inappropriate experiment designs, inadequate execution of the experiment or incomplete evaluations of the experimental data. One may ask : “how would it be possible for the “lower bound” heat transfer coefficients to show the large errors which have been attributed to such coefficients ?”

codeposition (see (12)) systems carried out by one of us (M.H.M.) during his stay at the N.H.E. laboratories in Sapporo, Japan, with the proviso that we regard this as a “Penultimate Study”

Experimental

The Pd-B and the Pd-B-Ce electrodes were prepared by one of us (M.A.I.) at the Naval Research Laboratory, Washington, D.C. The Pd-B electrode was in the form of a cylindrical rod having a 4.71 mm diameter and 20.1 mm length. This gives :

$$\text{Volume of electrode} = 0.350 \text{ cm}^3$$

$$\text{Area of electrode} = 3.15 \text{ cm}^2$$

The composition of this electrode was 99.5% Pd + 0.5% B (weight %).

The Pd-Ce-B rod was of 4.40 mm diameter and 20.05 mm length giving

$$\text{Volume of electrode} = 0.305 \text{ cm}^3$$

$$\text{Area of electrode} = 2.92 \text{ cm}^2$$

The Pt - wire used in (3) was supplied by Johnson Matthey PLC.

The experimental details have been given in a number of publications most recently in (1), (2), (3), (9), (10) and (11).

Measurements and Interpretation.

The first step in the ICARUS - style evaluation of the experimental data is the plotting of A-3 sized graphs of the experimental temperature - time and cell potential - time series for each measurement cycle of the experimental sequence e.g. see Fig.1² The “straight line” averaging of the plots near the end of the calibration period at $t = t_2$ gives immediately the “robust” estimate of the “lower bound” heat transfer coefficient, $(k_R')_l$.

² In the initial development of this methodology we used a variety of different sized plots ranging from A -4 to A - 0. For a variety of reasons we eventually recommended the use of the A - 4 size (1). However, we now believe that the A - 3 sized plots are to be preferred.

Interpolation of the temperature-time and cell potential-time series between the time regions $t < t_1$ and $t_2 < t < T$ gives the cell temperatures and cell voltages which would be reached at the time $t = t_2$ in the absence of the calibration pulse, Q . These lead to the “robust” estimates of the “true” heat transfer coefficient, $(k_R')_2$. The values of $(k_R')_1$ and $(k_R')_2$ obtained are listed in Table 1 and are considered further below.

In the next step of the evaluation, we consider the values of the “lower bound” heat transfer coefficient, $(k_R')_{11}$, throughout the measurement cycles. As the evaluation of the differential heat transfer coefficients magnifies the “noise” of the derived coefficients (due to the differentiation of the temperature-time series), it is desirable to take suitable averages of $(k_R')_{11}$; we have found the 11-point average, $(\overline{k_R'})_{11}$, of $(k_R')_{11}$ and the further 6-point average $(\overline{\overline{k_R'}})_{11}$, of $(\overline{k_R'})_{11}$ to be useful in this regard³ This process also has the advantage of successively compressing the data set (from 19,296 to 1754 and then to 292 values for the 67 days spanning the experiment with the Pd-B electrode; day 68 is excluded because the cell boiled dry on that day).

The production of the so-called $(k_R')_{11}$ -spreadsheet by the ICARUS software is an useful intermediate step in this process of data reduction. Table 2 illustrates an extract of these spreadsheets produced by the N.H.E. group whereas Table 3 is an extract for the same data section produced as in the original ICARUS version. (Tables 2 and 3 cover the region of the onset of the calibration pulse at $t = t_1 = 94167775$ s). We can see an immediate shortcoming of the spreadsheets used by N.H.E.: the rate of enthalpy input by the calibration heater has been entered as zero throughout the time range (column 10 of Table 2). In consequence it is not possible to interpret the derived values of $(k_R')_{11}$ (columns 13 and 19 of Table 2) nor to assess whether the enthalpy inputs delivered by the polarising circuit of the cell and by the calibration heater have been given correctly. On the other hand, the original ICARUS-style spreadsheets illustrate these points immediately. Thus Table 3 shows that the derived values of $(k_R')_{11}$ which apply to the time region before the application pulse i.e. $t < t_1$ (column 15 of Table 3) differ from the values for $t > t_1$ (column 16 of Table 3). Alternatively, we can consider the values of $(k_R')_{11}$ shown in heavy type in Table 3. We can conclude at the outset that there has (or have) been one (or several) mistakes in the execution of the experiment. Thus the powers delivered by the

³ Averaging beyond the level of $(\overline{\overline{k_R'}})_{11}$ is not useful as the “noise” then becomes dominated by the systematic decrease of $(k_R')_{11}$ with time (due to the progressive fall of the level of the electrolyte).

polarising circuit or to the calibration heater (0.2500 W) may have been incorrectly given and/or the experiments may have been wired up incorrectly (using the wires supplied with the ICARUS-1 system for the ICARUS -2 system). We will consider these points further below⁴ We have therefore used the original ICARUS approach in carrying out our evaluation of this experiment. We note that we have used the values $E_{\text{thermoneutral, cell}} = 1.527$ V and $C_p M = 490 \text{ JK}^{-1}$ in the calculations. The second assumption would certainly have to be changed in more exact evaluations (compare (3)).

We consider next the values of $(k_R')_{II}$ at short times, Fig. 2. We have to ask. “what can be the cause(s) of the remarkable differences between the time dependence observed for the Pd-B electrode and that for the Pt/D₂O blank system ?” The figure also shows $(k_R')_{II}$ for the Pd-B-Ce electrode where the values of $(k_R')_{II}$ have been averaged over the whole data set so as to remove the effects of random fluctuations. We note that $(k_R')_{II}$ for the Pd-B system is initially low which we attribute (as in 6)) to excess enthalpy generation due to the absorption of D⁺ in the Pd lattice (an exothermic process). On saturation of the electrode, the value of $(k_R')_{II}$ then rises to $\sim 0.845 \times 10^{-9} \text{ WK}^{-4}$ which we assume to be close to the “true” value of the heat transfer coefficient for a system showing little or no excess enthalpy generation. However, the “lower bound” heat transfer coefficient then falls due to the onset of such excess enthalpy generation⁵ The behaviour for $t < 172,800 \text{ s}$ (i.e. Days 1 and 2) is closely similar to that which has been discussed previously (6).

At still longer times (Day 3) we observe the development of “positive feedback” signalled by the progressive decrease of $(k_R')_{II}$ induced by the heater calibration pulse and the delayed relaxation of $(k_R')_{II}$ following the termination of this pulse. We note that the measurements for the Pt/D₂O “blank system”, (3), do not show any of the effects seen in the Pd-B/ D₂O system which can be explained entirely by the intervention of excess enthalpy generation.

Fig. 3 shows the behaviour of $(k_R')_{II}$ for the polarisation of the Pd-B electrode for Days 1-67 of the measurement cycles ; we have excluded Day 68 during which the cell

⁴ It appears that the group at N.H.E. wanted to assess whether the power input delivered to the calibration heater could be correctly recovered from the rate of excess enthalpy generation shown in columns 12 and 18 of Table 2. It does not appear to be sensible though to combine a term, ΔQ , which is known exactly, with a term which is subject to the fluctuations introduced by the “lower bound” heat transfer coefficient. There are also further objections to the procedure adopted by N.H.E. (10), (11).

⁵ Note that the rate of decrease of $(k_R')_{II}$ with time at the cell current $\sim 0.15 \text{ A}$ is more rapid than that of $(k_R')_{II}$ for the Pd-B-Ce system at the higher mean cell current $\sim 0.42 \text{ A}$

boils to dryness. In this case $\overline{(k_R')}_{11}$ is the scrolling 6-point mean of $(\overline{k_R'})_{11}$.⁶ The figure also shows the variations of $(k_R')_{11}$ for the Pt/D₂O “blank experiment” (3) as well as the predicted changes $\Delta(k_R')_{11}$ at the centre point ($t = t_2$) of each measurement cycle. These are based on the known effects of changes in the electrolyte level within the cells (using both the data for the Pt/D₂O “blank experiment” and the changes observed when using the Pd-B-Ce electrode, Fig. 2) coupled to the schedule of additions of D₂O to the cell.

We observe that the changes in $(k_R')_{11}$ for the Pd-B electrode are much larger than any which could be attributed to changes in the electrolyte level and, furthermore, that the amplitudes of these changes do not correlate with the amplitudes of $\Delta(k_R')_{11}$. However, some of the repeated increases of $(k_R')_{11}$ for the Pd-B experiment do correlate with the addition of D₂O to make up the electrolyte following losses of D₂O due to the combined effects of electrolysis and evaporation into the gas stream leaving the cell. We believe, therefore, that some of these additions “quench” excess enthalpy production, the most likely reason being contamination of some of the samples of D₂O used to make up the electrolyte by HDO. The continued electrolysis in the “open” cell then progressively removes the added light water⁷ so that the excess enthalpy production is somewhat restored. Nevertheless, excess enthalpy production remains restricted.

These effects can also be seen very clearly from the values of the specific rates of excess enthalpy generation as a function of time for the experiment using the Pd-B cathode, Figs. 4A-C and 5. The values shown have been calculated using the product

$10^9 \overline{(k_R')}_{11} \cdot \overline{f_1(\theta)}$.⁸ We also need the value of the “true” heat transfer coefficient,

$10^9 (k_R')_{12}$, but, unfortunately, this cannot be determined from the experiments principally because the quoted power delivered to the Joule heater used to calibrate the system is incorrect (see further below). We have therefore used the value $10^9 (k_R')_2 = 0.855 \text{ WK}^{-4}$ which ensures that the estimates of the specific excess enthalpy are positive at all times up to Day 61.⁹ However, the evaluation on Day 61 shows that $10^9 (k_R')_2$ must have been at

⁶ We have used the scrolling rather than the simple mean of $(k_R')_{11}$ so as to adequately illustrate the time-dependence of the heat transfer coefficient.

⁷ The H/D separation factor on Pd cathodes is very large (13).

⁸ A better estimate would be based on $10^9 \overline{(k_R')}_{11} \cdot \overline{f_1(\theta)}$ but the difference between these two estimates is within the error limits of the experiment.

⁹ It is impossible to derive excess enthalpies which are negative because this would require the cell to operate as a spontaneous refrigerator (compare (6)). The endothermicity of the cell reaction has already been fully taken into account by using the thermoneutral potential, 1.527 V.

least 0.950 WK^{-4} to ensure that the excess enthalpies on that day would also be positive. The estimates based on $10^9 (k_R')_{12} = 0.855 \text{ WK}^{-4}$ therefore give a “lower bound” for the specific rate of excess enthalpy generation; nevertheless, we can see that there is excess enthalpy generation throughout the time range Day 1 - Day 60 and Day 61 - Day 68 even when using this low estimate of the value of the true heat transfer coefficient.

We note that there are just three periods (Days 4-10, 16-21 and 26-31) during which the electrode was polarised for a sufficiently long time at constant current to allow valid estimates of the rates of excess enthalpy generation to be made. This specification of the length of time required to achieve a reasonably stable rate of excess enthalpy production is influenced by the effects of “quenching” of these rates due to the “topping-up” of the cells (see further below). However, it is possible that the measurements on Days 22-24, 36-38 and 41-45 can also be used to make viable estimates of the rates of excess enthalpy production. The rates we derive are naturally dependent on the chosen value of the “true” heat transfer coefficient. For the two values $10^9 (k_R')_{12} = 0.855$ and 0.950 WK^{-4} we obtain

Time	$\log_{10}(\text{current density})$ /mA cm ⁻²	$10^9 (k_R')_{12} = 0.855 \text{ WK}^{-4}$ $\log_{10}(\text{specific excess})$ /Wcm ⁻³	$10^9 (k_R')_{12} = 0.950 \text{ WK}^{-4}$ $\log_{10}(\text{specific excess})$ /Wcm ⁻³
Days 4-10	1.68	-0.921	-0.523
Days 16-21	2.20	-0.102	0.224
Days 22-24	2.10	-0.244	0.0974
Days 26-31	1.80	-0.745	-0.351
Days 36-38	2.10	-0.366	0.0624
Days 41-45	2.20	-0.356	0.187

We believe that the values calculated with $10^9 (k_R')_{12} = 0.950 \text{ WK}^{-4}$ are more representative of the behaviour of the system than the values calculated with $10^9 (k_R')_{12} = 0.855 \text{ WK}^{-4}$. In Fig. 5 we compare the former values with the specific rates of excess enthalpy generation determined in the Preliminary Investigation under a wider range of conditions (5).

We note that one important step in the production of the electrodes used in the Preliminary Investigation was the melting of the palladium in the presence of calcium boride (so as to ensure a low level of the oxygen activity in the system). The close

agreement of the two sets of results is perhaps therefore not surprising; however, one should not attach undue significance to the numerical values because the level of the specific rates of excess enthalpy reached is evidently dependent on the protocols adopted for the experiments. Thus prolonged polarisation leads to a marked increase in the level of excess enthalpy generation, Fig. 4C, leading to the “boiling to dryness” of the cell.¹⁰ There is evidently a complex interplay between the level of the rates of excess enthalpy generation and the cell temperature which is also illustrated by the persistence of the effects of “positive feedback” shown in Fig. 4.^{11 12}

We also need to consider further the variation of $(k_R')_{11}$ with time, Fig. 3, and relationships between $(k_R')_1$, $(k_R')_2$ and $\Delta(k_R')$, Table 1. The lack of any quantitative correlation between $(k_R')_{11}$ for the Pd-B electrode with the predicted values of $\Delta(k_R')_{11}$ raises the question whether such a correlation might be observed for the “true” heat transfer coefficients such as $(k_R')_2$. Fig. 6 shows that whereas the changes in $(k_R')_2$ are essentially within the range of the changes in $\Delta(k_R')$, the correlation is very poor : we simply obtain essentially a “scatter diagram”. The major reason for the high degree of scatter is the contraction of the measurement cycle from the recommended 2-day duration to 1-day so that the duration following each perturbation was insufficient to allow an adequate

¹⁰ The values of the rates of specific excess enthalpy generation shown in Fig. 4 are averages over 3,300 s. The rate reaches $\sim 280 \text{ Wcm}^{-3}$ in the measurement intervals (each lasting 300 s) immediately preceding the “boiling to dryness”

The experiment was observed closely by one of us (M.H.M.) during this phase. The Pd-B electrode was obviously the hottest part of the cell and vigorous boiling and swirling action was centred around the electrode. The group at N.H.E. were evidently not interested in the phenomenon. The whole experiment was conducted during this period Dec. 5 (1997) - Feb. 10 (1998) (Day 68 of the measurements).

¹¹ The persistence of these effects is due to the protocol used in this experiment (polarisation of the cell at low current densities which were in the region required for the onset of the phenomenon, (8)). By contrast, in the earlier studies, the current density was raised once the effects of “positive feedback” could be detected so as to drive the cell towards the boiling point. It was found that prolonged operation of the cell in the region for the onset of “positive feedback” could destroy the phenomenon of excess enthalpy generation. It may well be that the operation of the cell on Day 48 is an illustration of these effects.

¹² The ICARUS -2 system was designed so as to allow the injection of much higher levels of Joule heat using the resistive heater compared to the levels used in the Preliminary Investigation and in the ICARUS -1 system. It was intended that this should lead to a systematic investigation of the effects of temperature on the level of excess enthalpy generation. However, the facilities installed were never put into use. (see also the Discussion)

It was also envisaged that the rate of data acquisition should be increased say, to a measurement point every 11 s. This limit is set by the time-lags in the thin glass shields surrounding the thermistors. However, such time-lags could also be taken into account in a more elaborate data analysis scheme.

The benefits in increasing the rate of data acquisition will be apparent (improvements to the precision and accuracy of the evaluations) although such benefits are largely in the nature of “gilding the lily”.

relaxation of the time-series. This inadequate relaxation of the time-series is aggravated by the fact that the duration of the calibrations, $(t_2 - t_1)$ in the systems used by N.H.E. was only 6 hours. Elimination of the most inadequate calibrations leaves a set of just 22 measurement cycles and Fig. 7 shows that there is now a reasonable correlation between $(k_R')_2$ and $\Delta(k_R')$.¹³

A further surprising feature of the evaluations of $(k_R')_1$ and $(k_R')_2$, Table 1, is that $(k_R')_2$ is systematically lower than $(k_R')_1$ throughout nearly the whole time range of the measurement cycles. We note again that it is not possible for the “lower bound” heat transfer coefficient to be larger than the “true” value because this would require the cell to be a spontaneous refrigerator which contravenes the Second Law of Thermodynamics : the endothermicity of the cell reaction has already been taken into account by using the thermoneutral potential in the modelling of the cell. Observation of restricted time ranges in which the “lower bound” heat transfer coefficients exceed the “true” values may be explained by the intervention of “positive feedback” (14) and this may well account for some of the reports of such effects (15) (see also the effects illustrated in Fig. 2 and 4). However, the extended observation of such effects, Table 1, points to a malfunction of the experiment which is also indicated by the changes in the “lower bound” heat transfer coefficient in the region of the application of the heater calibration pulse, $t_1 < t < t_2$, Table 3. The most likely explanation is that the value of ΔQ given is incorrect ; we note that an increase of ΔQ from 0.2500 W to ~ 0.2725 W would remove the anomaly and would give $(k_R')_2$ in the neighbourhood of $0.850 \times 10^{-9} \text{ WK}^{-4}$ over the whole experiment duration (within the limits set by $\Delta(k_R')$).

We have already noted that the experiments on the Pt/D₂O “blank system” show that the “true” heat transfer coefficient is slightly larger than the “lower bound” value (based on the much more precise and accurate evaluations using the integral heat transfer coefficients (3)). This would, of course, be expected as there is only a low level of excess enthalpy generation in this system due to the reduction of electrogenerated oxygen. Bearing in mind the nature of the results given in Table 1, a comparable evaluation of experiments carried out by the N.H.E. group is highly desirable. Unfortunately, it appears that this group

¹³ This correlation is as good as one can reasonably expect bearing in mind that $(k_R')_2$ is the least accurate way of calibrating the calorimeter as well as the marked variation of the rate of excess enthalpy production with time (e.g. see Fig.3 and 4) due to the contamination of the electrolyte by HDO

never carried out these essential “blank” experiments. We do, however, have the preliminary details of some “blank” experiments carried out at the beginning of 1994 which were strictly in accord with the ICARUS-protocols. An example of the time series for one of the measurement cycles of experiment 4141 is shown in Fig. 8 ¹⁴ We obtain the following values of $(k_R')_1$ and $(k_R')_2$;

$$\text{Days 1 and 2} \quad 10^9(k_R')_1 = 0.75350 \text{ WK}^{-4} \quad 10^9(k_R')_2 = 0.75368 \text{ WK}^{-4}$$

$$\text{Days 3 and 4} \quad 10^9(k_R')_1 = 0.75408 \text{ WK}^{-4} \quad 10^9(k_R')_2 = 0.75455 \text{ WK}^{-4}$$

$$\text{Days 5 and 6} \quad 10^9(k_R')_1 = 0.75300 \text{ WK}^{-4} \quad 10^9(k_R')_2 = 0.75321 \text{ WK}^{-4}$$

We believe therefore that the ICARUS-1 system installed in 1993 (and , presumably therefore, the ICARUS-2 system installed in 1994) behaved exactly as predicted by the modelling of the calorimeters outlined in the Appendix. This confirms our conclusion that the strange behaviour observed in Table 1 is due to the use of an incorrect value of the power delivered to the calibration heater. The marked variation of the rate of excess enthalpy generation implied by Fig. 3 as well as the uncertainty as to the magnitude of the power delivered to the calibration heater prevent the application of the full ICARUS-style evaluation procedures (e.g. see(3)) to the data sets for the Pd-B system.

Discussion

The evaluations presented in this and one of the companion papers, Part I of the series (3), show that the calorimeter behaves exactly as predicted by the differential equation, (A.1), modelling the equipment provided we restrict attention to suitable “blank systems”. For the particular system chosen, the polarisation of Pt-cathodes in D₂O based electrolytes, the only process which can lead to the generation of excess enthalpy is the

¹⁴ As far as we can tell, this experiment was discontinued after Day 6. We note that if the “blank experiments” set up at the end of 1993 had been completed and, if the $(k_R')_1$ -spreadsheets for these experiments were available, it would have been possible to carry out the complete evaluations which have been illustrated in Part I of the present series (3).

reduction of electrogenerated oxygen. This is a small term (giving an excess enthalpy of order ~ 1 mW) which, moreover, is constant in time. In consequence it is possible to use the full analysis developed for the ICARUS-systems (1), (2), (6), (7), (8) and, in particular, the highly precise and accurate integral heat transfer coefficients $(k_R')_{261}$ and $(k_R')_{262}$; these have a precision and accuracy characterised by relative errors $< 0.01\%$ and it has been possible to estimate the excess enthalpy to within 0.1 mW.

The situation is rather different for the Pd-B system considered in the present paper,. In this case there is an evident major excess term (as indicated by the “lower bound” heat transfer coefficient, $(k_R')_{11}$, Fig. 3) which, moreover varies markedly with time. We have attributed this variation (and, in particular the repeated “quenching” of excess enthalpy generation) to contamination of the D_2O used to replenish the electrolyte by HDO. Moreover, comparisons of the “lower bound” heat transfer coefficient, $(k_R')_{11}$, and of the “true” coefficient $(k_R')_2$ with the predicted variation $\Delta(k_R')$, Figs. 2 and 3 indicate that the quoted power delivered to the resistive calibration heater was in error. In consequence of these deficiencies, the evaluations have had to be restricted to the initial methods used in the ICARUS-systems to assess the presence or absence of excess enthalpy terms (in particular, $(k_R')_1$, $(k_R')_2$, $(k_R')_{11}$, $(\overline{k_R'})_{11}$ and $(\overline{\overline{k_R'}})_{11}$). We have shown that these methods are perfectly adequate to demonstrate that excess enthalpy is indeed generated during the polarisation of the Pd-B electrode in 0.1M LiOD/ D_2O .

Nevertheless, we would stress that the evaluations presented in this paper are incomplete (for example, it would be possible to develop a further set of evaluations based on the changes in current density in the experiments). Extreme examples of the effects of such changes are illustrated in Fig. 9 (which is an expansion of a section of Fig. 4). It can be seen that the level of excess enthalpy generation reached at the higher current density on Day 25 persists for an extended period following the application of the lower current density on Day 26. Such effects have been classified as Case I of the general phenomenon of “Heat-after-Death” (16) (see also (6), (7), (10), (11)). The data derived could also be further interpreted. Such extensions will be the basis of further papers on this topic.

The results presented in this and the companion paper, (3), show that it is possible to demonstrate the production of excess enthalpy in Pd based cathodes polarised in D_2O -based electrolytes even when using a very restricted set of data (just one electrode). It is only necessary to assess the performance of the instrumentation (i.e. the “instrument

function”) by carrying out one (or a set) of “blank” experiments coupled to a complete evaluation of the data sets obtained as has been done in Part I of this series of papers (3). If this is not done, we can be easily led to make incorrect statements about the precision and accuracy of the instrumentation! Once the instrument function has been precisely and accurately established, it is then possible to analyse in detail one (or a set) of experiments using Pd-based cathodes as has been done (in part I) in the present paper. It can be seen that this subsequent investigation leads rapidly to the conclusion that there is excess enthalpy generation when these Pd-based electrodes are cathodically polarised in D₂O - based electrolytes. We can reach this conclusion even when there are evident shortcomings in the experiments, here the use of a calorimeter in which the vacuum in the Dewar jacket had evidently softened (the value of $(k_R')_{12}$ predicted from the Stefan-Boltzmann coefficient and the radiant surface area is $\sim 0.76 \times 10^9 \text{ WK}^{-4}$), the contamination of the D₂O by HDO coupled to a non-standard schedule of the “make-up” of the electrolyte, the use of a very restricted range of current densities compared to that originally employed (5) and the citation of an incorrect value of the power delivered to the Joule heater used to calibrate the instrumentation (possibly coupled to errors in the wiring of the calorimeter to the instrumentation). We note that the isotopic purity of the D₂O can only be established by making appropriate analyses (N.M.R. is a suitable technique). The other errors were to be avoided by using the “switching boxes” supplied with the ICARUS -2 instrumentation, see Fig. 10B, but it appears that these switching boxes were never put into use in the recommended manner. Furthermore, level controllers for the water in the thermostat tanks surrounding the cells were not added to the instrumentation.

Appendix Part II

It has been established that at low to intermediate cell temperatures (say $30^\circ < \theta < 80^\circ$) the behaviour of the calorimeters is modelled adequately by the differential equation

$$C_p M (d\Delta\theta/dt) = [E_{\text{cell}}(t) - E_{\text{thermoneutral, bath}}]I + Q_f(t)$$

change in the	enthalpy input	rate of excess
enthalpy content	due to	enthalpy
of the calorimeter	electrolysis	generation

$$+ \Delta Q_H(t-t_1) - \Delta Q_H(t-t_2) - (3I/4F[P/\{P^*-P\}])[C_{p,D_2O,g} - C_{p,D_2O,l}]\Delta\theta + L]$$

calibration pulse	rate of enthalpy removal by the gas stream with
	$E_{\text{thermoneutral}}$ referred to the bath temperature

$$- (k_R^o)\theta_{\text{bath}}^3[1-\gamma t] \{f_1(\theta)/\theta_{\text{bath}}^3 + 4\phi\Delta\theta\} \quad (\text{A.1})$$

time dependent	effect of	effect of
heat transfer	radiation	conduction
coefficient		

With the calorimeters supplied with the ICARUS Systems, the conductive contribution to heat transfer is very small. This term could therefore be “lumped” into the radiative term by allowing for a small increase in the radiative heat transfer coefficient:

$$\text{Radiative heat transfer} = (k_R')^o[1-\gamma t][(\theta_{\text{bath}} + \Delta\theta)^4 - \theta_{\text{bath}}^4] \quad (\text{A.2})$$

The values of the pseudoradiative “heat transfer coefficient, $(k_R')^o[1-\gamma t]$, derived are close to those calculated from the Stefan-Boltzmann coefficient and the radiative surface area. If

the time dependence of the heat transfer coefficient is not included explicitly in equation (A.2) then

$$\text{Radiative heat transfer} = (k_R') [(\theta_{\text{bath}} + \Delta\theta)^4 - \theta_{\text{bath}}^4] \quad (\text{A.3})$$

where the pseudoradiative heat transfer coefficient, (k_R') , now shows a weak time-dependence.

The simplest starting point is to assume that there is no excess enthalpy generation in the calorimeter (i.e. $Q_{\text{excess}} = 0$) and to evaluate a corresponding “differential lower bound heat transfer coefficient” at a time just before the end of the calibration pulse, $t = t_2$:

$$(k_R')_1 = \{[(E_{\text{cell}}(t) - E_{\text{thermoneutral, bath}})I - \Delta H_{\text{evap}}(t) - C_p M(d\Delta\theta/dt) + \Delta QH(t - t_1) + Q_{\text{excess}}]/f_1(\theta)\} \quad (\text{A.4})$$

This was the first heat transfer coefficient used in our investigations, hence the designation $(k_R')_1$. It will be apparent that the differential lower bound heat transfer coefficient $(k_R')_{11}$, may be evaluated at other points of the measurement cycle, by changing the enthalpy input due to the calibration pulse to

$$\Delta QH(t - t_1) - \Delta QH(t - t_2) \quad (\text{A.5})$$

It is next necessary to evaluate a “true heat transfer coefficient”. The simplest procedure giving $(k_R')_2$ near the end of the calibration period at $t = t_2$ is obtained by including the calibration pulse

$$\begin{aligned} (k_R')_2 = \{ & \Delta QH(t - t_1) + [E_{\text{cell}}(\Delta\theta_2, t_2) - E_{\text{cell}}(\Delta\theta_1, t_2)]I - \Delta H_{\text{evap}}(\Delta\theta_2, t_2) \\ & + \Delta H_{\text{evap}}(\Delta\theta_1, t_2) - C_p M[(d\Delta\theta/dt)_{\Delta\theta_2, t_2} - (d\Delta\theta/dt)_{\Delta\theta_1, t_2}] \} / f_2(\theta) \end{aligned} \quad (\text{A.6})$$

where we now have

$$f_2(\theta) = [\theta_{\text{bath}} + (\Delta\theta_2, t_2)]^4 - [\theta_{\text{bath}} + (\Delta\theta_1, t_2)]^4 \quad (\text{A.7})$$

and where we now assume that Q_{excess} is independent of time

It can be seen that we need to estimate the cell potential, the cell temperature and the differential of this temperature at the time $t=t_2$ which would have been reached in the absence of the calibration pulse [see footnote (A.1)]

Footnote (A.1) This evaluation was carried out in a somewhat different manner in the initial studies (5), (17) (18) in an attempt to avoid the disadvantages of such interpolation procedures. The values of $(k_R')_{11}$ and $(k_R')_{2}$ obtained were used as starting values for the non-linear regression procedure used at that time (5). As we could not make this procedure “user friendly” with the computing power then available to us and as, more especially, the methodology which we adopted was evidently not understood (19). (for a further example of such misunderstanding see (20)) we adopted the methodology described in the present paper. This methodology was also the basis of the ICARUS Systems.

As there is a large number of methods of analysing the experimental time-series characterised by their respective heat transfer coefficients, we have designated these coefficients by $(k_R')_{i,j,k}$ where

$i = 1$ denotes differential

$i = 2$ denotes integral with backward integration of the data sets

$i = 3$ denotes integral with forward integration of the data sets

$j = 0$ denotes the whole data set i.e. $0 < t < T$

$j = 5$ denotes the region adjacent to $t = 0$

$j = 6$ denotes the region adjacent to $t = t_1$

$j = 7$ denotes the region adjacent to $t = t_2$

$j = 8$ denotes a combination of $j = 6$ and $j = 7$

$k = 1$ denotes “lower bound”

$k = 2$ denotes “true”

The coefficient $(k_R')_{1,0,1}$ has usually been written as $(k_R')_{11}$

The present paper has been restricted to the use of the differential heat transfer coefficients.

References Part II

- 1) The ICARUS Systems : Isoperibolic Calorimetry Research and Utilities System, Version 1 (December 1993), Low Power Measuring System for Three Cells, TECHNOVA INC., 13th Floor, Fukoku Seimei Building, 2-2-2 Uchaisaiwai-cho, Chiyuda-Ku, Tokyo 100 Japan.
- 2) ICARUS-2 : : Isoperibolic Calorimetry Research and Utilities System, Version 2.0 (February 1995), TECHNOVA INC., 13th Floor, Fukoku Seimei Building, 2-2-2 Uchaisaiwai-cho, Chiyuda-Ku, Tokyo 100 Japan.
- 3) Our Penultimate Paper on the Calorimetry of the Pt/D₂O and Pd/ D₂O Systems. Part 1 : the Pt/D₂O Blank System ; submitted for publication.
- 4) Report on the First Set of Experiments carried out under the NEDO/NHE Project at the Sapporo Laboratories, June 1994,
- 5) M. Fleischmann, S. Pons, M. V. Anderson, L.J. Li and M. Hawkins, J. Electroanal. Chem., 287 (1990) 293.
- 6) Martin Fleischmann and Stanley Pons, Proceedings of the Third International Conference on Cold Fusion, Universal Academy Press, Frontiers of Science Series N° 4, (FSS-4) ISSN 0915-8502, ISBN 4-946443-12-6 (1993) p47.
- 7) Martin Fleischmann and Stanley Pons, Phys Lett., A, 176 (1993) 118.
- 8) M. Fleischmann, S. Pons, Monique Le Roux and Jeanne Roulette, Trans. Fusion Technol, 26 (1994) 323.
- 9) M.H. Miles, M.A. Imam and M. Fleischmann in Proceedings of the Eighth International Conference on Cold Fusion, Editor F. Scaramuzzi, The Italian Physical Society 70 (2000), 105 ISBN 88-7794-256-8.
- 10) M.H. Miles, M. Fleischmann and M.A. Imam, Report NRL/MR/6320-01-8526 Naval Research Laboratory, Washington, D.C., 20375-5320, March (2001).
- 11) S. Szpak and P.A. Mosier-Boss, Technical Report 1862, Volume 2, SPAWAR Systems Centre, San Diego, February (2002)
- 12) P.A. Mosier-Boss and S. Szpak, Nuovo Cimento, 112A (1999) 577.
- 13) B. Dandapani and M. Fleischmann, J. Electroanal Chem., 39 (1972) 323

- 14) M. Fleischmann, Proceedings of the Fifth International Conference on Cold Fusion (1995) 140.
- 15) Toshiya Saito, Masao Sumi, Naoto Asami and Hideo Ikegami, Proceedings of the Fifth International Conference on Cold Fusion (1995) page 105.
- 16) S. Pons and M. Fleischmann, Trans. Fusion Technol., 26 (1994) 87.
- 17) M. Fleischmann, S. Pons, and M. Hawkins, J. Electroanal. Chem., 261 (1989) 301; 263 (1989) 187.
- 18) M. Fleischmann and S. Pons, J. Electroanal. Chem., 332 (1992) 33.
- 19) R.A. Wilson, J.W. Bray, P.G. Kosky, H.B. Vakil and F.G. Will, J. Electroanal. Chem., 332 (1992) 1.
- 20) Frederick T. Wagner, Thomas E. Moylan, Michael E. Hayden, Ulrike Narger and James L. Booth, J. Electroanal. Chem., 295 (1990) 393.

Table 1 The values of $10^9(k_R')_{11}$ (at $t=t_2$), $10^9(k_R')_1$, $10^9(k_R')_2$ and $10^9\Delta(k_R')$ for the whole of the experiment with the Pd-B cathode

Time Day	s	cell current/A	$10^9(k_R')_{11}$ /WK ⁻⁴	$10^9(k_R')_1$ /WK ⁻⁴	$10^9(k_R')_2$ /WK ⁻⁴	$10^9\Delta(k_R')$ /WK ⁻⁴	$10^9(k_R')_2$ with Q= 0.2720W	$10^9\Delta(k_R')$ /WK ⁻⁴
1	45000	0.15036	0.79622	no calibration		-0.00075		-0.00075
2	129600	0.15036	0.84165	no calibration		-0.00225		-0.00225
3	214200	0.15036	0.80416	fails	fails	-0.00376		-0.00376
4	298800	0.15036	0.76718	fails	fails	-0.00525		-0.00525
5	383400	0.15036	0.7712	0.7734	0.7578	-0.00187	0.8397	-0.00187
6	468000	0.15036	0.76435	0.7616	0.7417	-0.00337	0.8229	-0.00337
7	552600	0.15036	0.75697	0.758	0.747	-0.00488	0.8282	-0.00488
8	637200	0.15036	0.79614	fails	fails	-0.00638	fails	-0.00638
9	721800	0.15036	0.78931	0.7902	0.75	-0.00049	0.8319	-0.00049
10	806400	0.15036	0.79155	0.7896	0.7465	-0.00199	0.8288	-0.00199
11	891000	0.30155	0.79848	0.7985	0.7449	-0.00395	0.8334	-0.00395
12	975600	0.40171	0.80423	0.8029	0.7368	-0.0023	0.8279	-0.0023
13	1060200	0.50234	0.80154	0.8082	0.7408	-0.0032	0.8358	-0.0032
14	1144800	0.60377	0.77575	0.7765	0.7609	-0.00874	0.859	-0.00874
15	1229400	0.60375	0.82144	0.8172	0.769	-0.00113	0.8666	-0.00113
16	1314000	0.50231	0.77693	0.7764	0.7564	-0.00303	0.8512	-0.00303
17	1398600	0.5023	0.7703	0.7847	0.7528	-0.00313	0.8485	-0.00313
18	1483200	0.5023	0.77711	0.7778	0.7724	-0.00816	0.8677	-0.00816
19	1567800	0.5023	0.77055	0.7697	0.738	-0.00332	0.8323	-0.00332
20	1652400	0.5023	0.7783	0.7758	0.7372	-0.00834	0.8325	-0.00834
21	1737000	0.5023	0.77273	0.7716	0.7425	-0.00351	0.8367	-0.00351
22	1821600	0.40173	0.77621	0.7765	0.7476	-0.00803	0.8401	-0.00803
23	1906200	0.40173	0.7728	0.7742	0.7598	-0.00095	0.853	-0.00095
24	1990800	0.40173	0.76989	0.7737	0.7463	-0.00497	0.8377	-0.00497
25	2075400	0.65383	0.81459	0.8144	0.7563	-0.01024	0.8545	-0.01024
26	2160000	0.20088	0.77757	0.7855	0.764	-0.00219	0.8514	-0.00219
27	2244600	0.2009	0.78213	0.7812	0.7559	0.00566	0.8415	0.00566
28	2329200	0.20088	0.78021	0.7799	0.7543	0.00366	0.8394	0.00366
29	2413800	0.20088	0.77721	0.7768	0.7496	0.00165	0.8344	0.00165
30	2498400	0.20088	0.77446	0.7735	0.7415	-0.00037	0.8254	-0.00037
31	2583000	0.20088	0.77725	0.7713	0.7406	-0.00237	0.8244	-0.00237
32	2667600	0.50111	0.81366	0.8139	0.7593	-0.00588	0.8547	-0.00588
33	2752200	0.50112	0.81912	0.8176	0.7438	-0.00473	0.8424	-0.00473
34	2836800	0.50114	0.81192	0.8115	fails	0.00012	fails	0.00012
35	2921400	0.55046	0.82697	0.8234	fails	-0.00489	fails	-0.00489
36	3006000	0.40005	0.79962	0.7999	0.7835	-0.00496	0.8793	-0.00496
37	3090600	0.40005	0.79487	0.7938	0.7518	0.00214	0.8467	0.00214
38	3175200	0.40005	0.79132	0.7906	0.7493	0.008	0.8435	0.008
39	3259800	0.55049	0.80868	0.8089	0.7589	0.00325	0.8593	0.00325
40	3344400	0.45015	0.7942	0.794	0.7587	0.00934	0.8556	0.00934
41	3429000	0.50057	0.80445	0.8043	0.7588	0.00459	0.8576	0.00459
42	3513600	0.50055	0.79951	0.7993	0.7595	0.01437	0.8583	0.01437
43	3598200	0.50055	0.82979	0.8312	fails	0.00937	fails	0.00937
44	3682800	0.50056	0.81167	0.812	0.7592	0.00436	0.8573	0.00436
45	3767400	0.50055	0.81322	0.8201	fails	0.01045	fails	0.01045
46	3852000	0.60144	0.77963	0.7782	0.7771	0.00495	0.8813	0.00495

47	3936600	0.60143	0.77198	0.773	0.7732	0.01126	0.8792
48	4021200	0.55084	0.77895	0.779	0.7818	0.0055	0.889
49	4105800	0.55083	0.77153	0.7219	fails	0.01602	fails
50	4190400	0.50046	0.78316	0.7811	fails	0.01076	fails
51	4275000	0.50045	0.77309	fails	fails	0.00576	fails
52	4359600	0.50045	0.76773	fails	fails	0.01185	fails
53	4444200	0.6002	0.78085	fails	fails	0.00634	fails
54	4528800	0.60021	0.77342	0.7756	0.7443	0.01267	0.8446
55	4613400	0.79985	0.78743	0.7869	0.7591	0.00567	0.8629
56	4698000	0.69954	0.78118	0.7803	0.7561	0.00534	0.8547
57	4782600	0.50103	0.7846	0.784	0.7609	0.01313	0.8562
58	4867200	0.50104	0.77796	0.7777	0.7546	0.00812	0.8499
59	4951800	0.50104	0.77343	0.7729	0.7516	0.01298	0.8458
60	5036400	0.8995	0.82477	0.8355	fails	0.018	fails
61	5121000	1.0008	0.85333	0.8514	fails	0.01743	fails
62	5205600	1.0005	0.82455	0.7826	fails	0.01726	fails
63	5290200	1.0006	0.80043	0.7991	fails	0.02577	fails
64	5374800	1.0005-0.8	0.80805	fails	fails	0.01676	fails
65	5459400	0.80446	0.8011	0.8	0.7342	0.0087	0.8381
66	5544000	0.80444	0.79225	0.7508	0.7707	0.01668	0.875
67	5628600	1.0045	0.80181	fails	fails	0.00709	fails
68	5713200	0.9989	cell boils dry				

Table 2 Extract from the $(k_R)_{11}$ -spreadsheets for experiments FP2-97120402-M7c2 (Pd-B cathode) as produced in the evaluation of this experiment provided by N.H.E.
Region of start of calibration pulse; Day 29 of the experiment.

Time/s	θ cell short thermistor	θ cell long thermistor	Ecell/V	Icell/A	θ bath	d θ cell/dt short thermistor	Rate of enthalpy input/W	Rate of enthalpy removal by evaporation /W	Rate of enthalpy input by calibration heater/W	$10^{-9}(\theta_{\text{cell}}^4)$ θ_{bath}^4 short thermistor	Rate of excess enthalpy generation /W	$10^{-9}(k_R)_{11}$ /WK ⁻¹ short thermistor	Water equivalent /JK ⁻¹ (see text)	d θ cell/dt long thermistor	Rate of enthalpy removal by evaporation /W	$10^{-9}(\theta_{\text{cell}}^4)$ θ_{bath}^4 long thermistor	Rate of excess enthalpy generation /W long thermistor	$10^{-9}(k_R)_{11}$ /WK ⁻¹ long thermistor	Water equivalent /JK ⁻¹ (see text)
94156375	304.078	304.081	5.2873	0.20089	295.199	8.33E-06	0.7528	-3.04E-03	0	0.955679	0.0127	0.780256	-1029.5	6.67E-06	-3.04E-03	0.956017	0.0121	0.780835	-1327.12
94156675	304.084	304.075	5.2768	0.20089	295.185	8.33E-06	0.7507	-3.04E-03	0	0.957795	0.0164	0.776329	-1483.99	-1.33E-05	-3.04E-03	0.956783	0.005	0.788248	867.139
94156975	304.083	304.073	5.2934	0.20089	295.184	3.33E-06	0.754	-3.04E-03	0	0.957785	0.0107	0.782377	-2707.2	5.00E-06	-3.04E-03	0.95666	0.0106	0.782445	-1625.98
94157275	304.086	304.078	5.2888	0.20089	295.188	1.00E-05	0.7531	-3.04E-03	0	0.957711	0.0148	0.77806	-988.815	1.17E-05	-3.04E-03	0.956811	0.0149	0.777794	-786.254
94157575	304.089	304.08	5.2842	0.20089	295.185	-1.50E-05	0.7521	-3.04E-03	0	0.958357	0.004	0.789317	757.497	8.33E-06	-3.04E-03	0.957345	0.0146	0.778208	-1266.94
94157875	304.077	304.083	5.2872	0.20089	295.196	-1.00E-05	0.7528	-3.04E-03	0	0.955876	0.0039	0.789473	875.337	-1.67E-06	-3.04E-03	0.95655	0.0085	0.784646	5573.908
94158175	304.083	304.079	5.3085	0.20089	295.193	1.67E-05	0.7571	-3.04E-03	0	0.956859	0.0134	0.779478	-315.402	-1.50E-05	-3.04E-03	0.956409	-0.0025	0.796066	326.599
94158475	304.087	304.074	5.2992	0.20089	295.189	-1.17E-05	0.7552	-3.04E-03	0	0.957721	0.0021	0.791319	669.396	0.00E+00	-3.04E-03	0.956259	0.0066	0.786554	0
94158775	304.076	304.079	5.2772	0.20089	295.199	-2.00E-05	0.7508	-3.04E-03	0	0.955455	0.0006	0.792847	521.396	-3.33E-06	-3.04E-03	0.955792	0.0091	0.784022	3208.848
94159075	304.075	304.072	5.2785	0.20089	295.186	1.67E-06	0.751	-3.04E-03	0	0.95668	0.012	0.781007	-6683.22	0.00E+00	-3.04E-03	0.956342	0.0109	0.782137	0
94159375	304.077	304.079	5.2879	0.20089	295.193	6.67E-06	0.7529	-3.04E-03	0	0.956184	0.0121	0.780824	-1328.65	5.00E-06	-3.04E-03	0.956409	0.0115	0.781494	-1807.3
94159675	304.079	304.075	5.2834	0.20089	295.184	0.00E+00	0.752	-3.04E-03	0	0.957335	0.0107	0.782314	0	-1.83E-05	-3.04E-03	0.956885	0.0014	0.792071	564.812
94159975	304.077	304.068	5.2857	0.20089	295.192	-5.00E-06	0.7525	-3.04E-03	0	0.956287	0.0069	0.786256	1875.943	-1.67E-06	-3.04E-03	0.955275	0.0078	0.785381	5145.12
94160275	304.076	304.074	5.2874	0.20089	295.191	-1.33E-05	0.7528	-3.04E-03	0	0.956278	0.0025	0.790891	677.4	6.67E-06	-3.04E-03	0.956053	0.0121	0.780827	-1327.98
94160575	304.069	304.072	5.2787	0.20089	295.192	8.33E-06	0.7511	-3.04E-03	0	0.955388	0.0142	0.778688	-1208.87	-6.67E-06	-3.04E-03	0.955725	0.0071	0.786102	1551.329
94160875	304.081	304.07	5.2796	0.20089	295.192	5.00E-06	0.7512	-3.04E-03	0	0.956737	0.0134	0.779483	-2192.87	1.00E-05	-3.04E-03	0.9555	0.0149	0.777793	-998.086
94161175	304.072	304.078	5.2853	0.2009	295.195	-2.00E-05	0.7524	-3.04E-03	0	0.955416	-0.0011	0.794623	436.546	3.83E-05	-3.04E-03	0.956091	0.0281	0.76416	-241.755
94161475	304.069	304.093	5.2807	0.20089	295.176	3.33E-06	0.7515	-3.04E-03	0	0.957034	0.0126	0.780328	-3292.44	-1.00E-05	-3.04E-03	0.959733	0.0082	0.784937	1312.035
94161775	304.074	304.072	5.2782	0.20089	295.186	1.17E-05	0.751	-3.04E-03	0	0.956567	0.0168	0.775915	-952.407	-3.50E-05	-3.04E-03	0.956342	-0.0062	0.800004	312.359
94162075	304.076	304.072	5.2846	0.20089	295.191	6.67E-06	0.7523	-3.04E-03	0	0.956278	0.0129	0.780055	-1439.41	0.00E+00	-3.04E-03	0.955828	0.0092	0.78384	0
94162375	304.078	304.072	5.2864	0.20089	295.182	-3.33E-06	0.7526	-3.04E-03	0	0.957429	0.0085	0.784612	3043.93	2.00E-05	-3.04E-03	0.956754	0.0194	0.773217	-480.499
94162675	304.074	304.084	5.294	0.20089	295.181	-3.33E-06	0.7541	-3.04E-03	0	0.957082	0.0067	0.786493	2502.683	1.50E-05	-3.04E-03	0.958206	0.0166	0.776191	-615.749

94162975	304.076	304.081	5.2928	0.20089	295.188	-1.00E-05	0.7539	-3.04E-03	0	0.956586	0.0033	0.790063	819.211	-1.33E-05	-3.04E-03	0.957149	0.0021	0.791304	647.937
94163275	304.068	304.076	5.289	0.20089	295.19	5.00E-05	0.7531	-3.04E-03	0	0.955481	0.0105	0.782489	-1615.39	-2.67E-05	-3.04E-03	0.956381	-0.0043	0.797973	329.708
94163575	304.079	304.065	5.2837	0.2009	295.202	1.50E-05	0.7521	-3.04E-03	0	0.955483	0.0165	0.776279	-607.21	-5.00E-06	-3.04E-03	0.953909	0.0054	0.787836	1571.295
94163875	304.077	304.073	5.2851	0.20089	295.193	-1.00E-05	0.7524	-3.04E-03	0	0.956184	0.0045	0.788777	942.017	0.0000+00	-3.04E-03	0.955734	0.0091	0.784022	0
94164175	304.073	304.065	5.2833	0.20089	295.19	-1.67E-06	0.752	-3.04E-03	0	0.956043	0.0089	0.784245	5800.472	-1.00E-05	-3.04E-03	0.955144	0.0041	0.789261	895.235
94164475	304.076	304.067	5.2884	0.20089	295.189	3.33E-06	0.753	-3.04E-03	0	0.956483	0.0106	0.782393	-2698.77	8.33E-06	-3.04E-03	0.955471	0.0123	0.780666	-982.933
94164775	304.075	304.07	5.2966	0.20089	295.185	-1.67E-06	0.7547	-3.04E-03	0	0.956783	0.0068	0.786431	4550.536	-6.67E-06	-3.04E-03	0.95622	0.0039	0.789456	1070.58
94165075	304.075	304.063	5.2911	0.20089	295.189	-6.67E-06	0.7536	-3.04E-03	0	0.956371	0.0051	0.788176	1254.177	6.67E-06	-3.04E-03	0.955022	0.0106	0.78245	-1093.28
94165375	304.071	304.074	5.2971	0.20089	295.202	6.67E-06	0.7548	-3.04E-03	0	0.954584	0.009	0.784071	-860.88	8.33E-06	-3.04E-03	0.954921	0.0101	0.782939	-720.895
94165675	304.079	304.068	5.2773	0.20089	295.2	5.00E-06	0.7508	-3.04E-03	0	0.955689	0.013	0.779855	-2118.89	-6.67E-06	-3.04E-03	0.954452	0.0063	0.786857	1441.643
94165975	304.074	304.07	5.2881	0.2009	295.188	-1.00E-05	0.753	-3.04E-03	0	0.956361	0.004	0.7893	892.015	1.67E-06	-3.04E-03	0.955912	0.0094	0.783692	-5137.52
94166275	304.073	304.069	5.2773	0.20089	295.188	-5.00E-06	0.7508	-3.04E-03	0	0.956249	0.0086	0.784523	2207.904	-3.33E-06	-3.04E-03	0.955799	0.009	0.784039	3204.553
94166575	304.071	304.068	5.2787	0.2009	295.189	3.33E-06	0.7511	-3.04E-03	0	0.955921	0.0121	0.780854	-3137.63	5.00E-06	-3.04E-03	0.955584	0.0126	0.780276	-2038.11
94166875	304.075	304.072	5.29	0.20089	295.196	1.17E-05	0.7533	-3.04E-03	0	0.955651	0.0137	0.779138	-686.748	3.33E-06	-3.04E-03	0.955313	0.0094	0.783688	-2323.15
94167175	304.078	304.07	5.2929	0.2009	295.183	-5.00E-06	0.754	-3.04E-03	0	0.957326	0.0063	0.786953	1744.037	5.00E-06	-3.04E-03	0.956426	0.0105	0.782571	-1601.01
94167475	304.072	304.075	5.2837	0.20089	295.183	-1.33E-05	0.7521	-3.04E-03	0	0.956651	0.0035	0.789806	755.307	1.67E-06	-3.04E-03	0.956988	0.0112	0.781847	-6203.39
94167775	304.07	304.071	5.2785	0.20089	295.195	1.17E-05	0.751	-3.04E-03	0	0.955191	0.0157	0.777096	-853.592	-1.33E-05	-3.04E-03	0.955304	0.0035	0.789826	753.6
94168075	304.079	304.067	5.2915	0.2009	295.198	3.50E-05	0.7537	-3.04E-03	0	0.955895	0.025	0.767332	-224.792	3.00E-05	-3.04E-03	0.954545	0.0215	0.770986	-226.495
94168375	304.091	304.089	5.2877	0.20089	295.187	2.80E-04	0.7529	-3.04E-03	0	0.958376	0.1478	0.639244	-37.998	3.12E-04	-3.04E-03	0.958151	0.1632	0.6232	-33.564
94168675	304.247	304.254	5.279	0.20089	295.196	5.07E-04	0.7511	-3.07E-03	0	0.97501	0.2739	0.512605	-50.552	5.03E-04	-3.07E-03	0.975799	0.2729	0.513863	-52.133
94168975	304.395	304.391	5.2649	0.20089	295.189	4.78E-04	0.7483	-3.09E-03	0	0.992415	0.2767	0.514724	-88.394	4.58E-04	-3.12E-03	1.007234	0.2665	0.524839	-91.469
94169275	304.534	304.529	5.2654	0.2009	295.192	4.45E-04	0.7484	-3.12E-03	0	1.007799	0.2724	0.523187	-122.192	4.43E-04	-3.12E-03	1.007234	0.2712	0.524292	-121.638
94169575	304.662	304.657	5.2446	0.2009	295.194	3.93E-04	0.7443	-3.14E-03	0	1.022063	0.2626	0.536545	-177.698	4.08E-04	-3.14E-03	1.021497	0.2695	0.529648	-170.069
94169875	304.77	304.774	5.2492	0.2009	295.195	3.77E-04	0.7452	-3.16E-03	0	1.034182	0.2632	0.539	-208.655	3.78E-04	-3.16E-03	1.034635	0.2644	0.537974	-208.688
94170175	304.888	304.884	5.2371	0.20089	295.183	3.78E-04	0.7427	-3.18E-03	0	1.048786	0.2781	0.528343	-244.937	3.65E-04	-3.18E-03	1.048333	0.2712	0.534805	-252.897
94170475	304.997	304.993	5.2378	0.20089	295.192	3.48E-04	0.7429	-3.20E-03	0	1.060224	0.2723	0.536652	-291.783	3.45E-04	-3.20E-03	1.05977	0.2703	0.538423	-293.556
94170775	305.097	305.091	5.2436	0.2009	295.186	3.25E-04	0.7441	-3.22E-03	0	1.072196	0.2692	0.542452	-338.374	3.22E-04	-3.21E-03	1.071514	0.267	0.544322	-340.195
94171075	305.192	305.186	5.2243	0.20089	295.196	3.02E-04	0.7401	-3.23E-03	0	1.081964	0.2695	0.544464	-403.21	2.98E-04	-3.23E-03	1.081281	0.2673	0.546319	-405.897
94171375	305.278	305.27	5.2203	0.2009	295.195	2.80E-04	0.7394	-3.25E-03	0	1.091849	0.2675	0.548542	-465.221	2.83E-04	-3.25E-03	1.090939	0.2684	0.547504	-457.193
94171675	305.36	305.356	5.2249	0.20089	295.194	2.63E-04	0.7403	-3.26E-03	0	1.101288	0.2659	0.552068	-519.879	2.72E-04	-3.26E-03	1.100832	0.2696	0.548589	-502.598
94171975	305.436	305.433	5.2139	0.2009	295.184	2.38E-04	0.7381	-3.28E-03	0	1.110976	0.2635	0.556292	-615.747	2.72E-04	-3.28E-03	1.110634	0.2796	0.541758	-539.194
94172275	305.503	305.519	5.2065	0.2009	295.196	2.45E-04	0.7366	-3.29E-03	0	1.11738	0.2734	0.548839	-625.852	2.53E-04	-3.29E-02	1.119205	0.2789	0.544293	-610.993
94172575	305.583	305.585	5.2147	0.2009	295.189	2.37E-04	0.7382	-3.30E-03	0	1.127228	0.2755	0.549115	-674.009	1.98E-04	-3.30E-03	1.127456	0.2569	0.565663	-805.195
94172875	305.645	305.638	5.2124	0.20089	295.196	1.77E-04	0.7377	-3.31E-03	0	1.133587	0.2517	0.571508	-934.209	2.13E-04	-3.31E-03	1.132787	0.269	0.556049	-770.663
94173175	305.689	305.713	5.2049	0.20089	295.191	2.00E-04	0.7362	-3.32E-03	0	1.139128	0.269	0.557359	-854.771	2.10E-04	-3.33E-03	1.14187	0.2761	0.551725	-824.45
94173475	305.765	305.764	5.1958	0.2009	295.204	2.05E-04	0.7345	-3.34E-03	0	1.146477	0.2791	0.550089	-871.318	1.77E-04	-3.34E-03	1.146363	0.2651	0.562254	-1010.54
94173775	305.812	305.819	5.1963	0.2009	295.188	1.55E-04	0.7346	-3.35E-03	0	1.153499	0.26	0.56807	-1187.94	1.73E-04	-3.35E-03	1.1543	0.2697	0.559894	-1065.97
94174075	305.858	305.868	5.192	0.2009	295.202	1.77E-04	0.7337	-3.35E-03	0	1.157322	0.2746	0.556255	-1064.19	1.48E-04	-3.36E-03	1.158467	0.2616	0.567688	-1273.59
94174375	305.918	305.908	5.1955	0.20089	295.19	1.68E-04	0.7344	-3.37E-03	0	1.165426	0.2763	0.556454	-1151.18	1.65E-04	-3.36E-03	1.164281	0.2737	0.558406	-1168.91
94174675	305.959	305.967	5.1885	0.20089	295.187	1.37E-04	0.7329	-3.37E-03	0	1.170431	0.2661	0.566133	-1457.56	1.55E-04	-3.37E-03	1.171347	0.275	0.558718	-1303.88
94174975	306	306	5.1866	0.2009	295.185	1.47E-04	0.7326	-3.38E-03	0	1.175334	0.2753	0.559282	-1386.66	1.25E-04	-3.38E-03	1.175334	0.2647	0.568316	-1627.01
94175275	306.047	306.042	5.1814	0.2009	295.198	1.35E-04	0.7316	-3.39E-03	0	1.179385	0.2738	0.561316	-1538.1	1.38E-04	-3.39E-03	1.178812	0.275	0.560204	-1497.74
94175575	306.081	306.083	5.1779	0.20089	295.195	1.23E-04	0.7308	-3.40E-03	0	1.183593	0.2722	0.563538	-1717.28	1.43E-04	-3.40E-03	1.183822	0.2822	0.555152	-1478.93
94175875	306.121	306.128	5.1876	0.2009	295.188	1.12E-04	0.7328	-3.40E-03	0	1.188902	0.2687	0.567492	-1916.72	1.23E-04	-3.40E-03	1.189705	0.2751	0.562304	-1740.59

Table 3 Extract from the $(k_R')_{11}$ - spreadsheets for experiment FP2-97120402-M7c2 (Pd-B cathode) as produced by the ICARUS-2 evaluation of this experiment

Region of start of calibration pulse; Day 29 of the experiment

1	2	3	4	5	6	7	8	9	10	11	12	13	14	15	16
Time/s	θ cell	E cell/V	$10^{-9}(\theta_{\text{cell}}^4)$	CpM d0	Rate of	Rate of	$[(6)-(7)]$	(5)	$[(6)-(7)+(10)]$	$10^{-9}(k_R')_{11}$	$10^9(k_R')_{11}$	mean (8)	mean (10)	mean (11)	mean (12)
	short		θ_{bath}^4	cell/dt	enthalpy	enthalpy	4	4	4	/WK ⁻⁴	/WK ⁻⁴	sd (8)	sd (10)	sd (11)	sd (12)
	thermistor		short		input/W	removal	/WK ⁻⁴	/WK ⁻⁴	/WK ⁻⁴			rsd (8)	rsd (10)%	rsd (11)%	rsd (12)%
			thermistor			by									
						evaporation									
						/W									
94147975														0.78378	1.0449
														0.00295	0.00397
														0.377	0.38
94151275														0.78434	1.04551
														0.00469	0.00479
														0.78434	0.38
94154575														0.78495	1.04618
														0.00371	0.00373
														0.473	0.357
94156075														0.78419	1.04541
94156375	304.078	5.2873	0.955679	0.00408	0.7528	-3.04E-03	0.78453	0.00427	1.04612	0.780256	1.04185			0.00051	0.00063
94156675	304.084	5.2768	0.957795	0.00408	0.7507	-3.04E-03	0.78061	0.00426	1.04163	0.776329	1.03735			0.066	0.06
94156975	304.083	5.2934	0.957785	0.00163	0.754	-3.04E-03	0.78406	0.0017	1.04508	0.782377	1.0434				
94157275	304.086	5.2888	0.957711	0.0049	0.7531	-3.04E-03	0.78318	0.00512	1.04422	0.77806	1.0341				
94157575	304.089	5.2842	0.958357	-0.00735	0.7521	-3.04E-03	0.78161	-0.00767	1.04247	0.789317	1.05018				
94157875	304.077	5.2872	0.955876	-0.0049	0.7528	-3.04E-03	0.78437	-0.00513	1.04591	0.789473	1.05101	0.78368	1.04416	0.78375	1.04463

94158175	304.083	5.3085	0.956859	0.00818	0.7571	-3.04E-03	0.78806	0.00855	1.04933	0.779478	1.04102	0.00196	0.00292	0.00556	0.00617
94158475	304.087	5.2992	0.957721	-0.00573	0.7552	-3.04E-03	0.78536	-0.00598	1.0464	0.791319	1.05236	0.25	0.279	0.709	0.591
94158775	304.076	5.2772	0.955455	-0.0098	0.7508	-3.04E-03	0.78262	-0.01026	1.04428	0.792847	1.0545				
94159075	304.075	5.2785	0.95668	0.00082	0.751	-3.04E-03	0.78183	0.00086	1.04315	0.781007	1.04233				
94159375	304.077	5.2879	0.956184	0.00327	0.7529	-3.04E-03	0.78422	0.00342	1.04568	0.780824	1.04228				
94159675	304.079	5.2834	0.957335	0	0.752	-3.04E-03	0.78234	0	1.04348	0.782314	1.04346				
94159975	304.077	5.2857	0.956287	-0.00345	0.7525	-3.04E-03	0.78372	-0.00256	1.04515	0.786256	1.04768				
94160275	304.076	5.2874	0.956278	-0.00652	0.7528	-3.04E-03	0.78404	-0.00682	1.04547	0.790891	1.05232				
94160575	304.069	5.2787	0.955388	0.00408	0.7511	-3.04E-03	0.78299	0.00427	1.04466	0.778688	1.04036				
94160875	304.081	5.2796	0.956737	0.00245	0.7512	-3.04E-03	0.78199	0.00256	1.04329	0.779483	1.04079				
94161175	304.072	5.2853	0.955416	-0.0098	0.7524	-3.04E-03	0.78433	-0.01026	1.046	0.794623	1.05629	0.78322	1.04484	0.78361	1.04497
94161475	304.069	5.2807	0.957034	0.00163	0.7515	-3.04E-03	0.78299	0.0017	1.04421	0.780328	1.04155	0.00089	0.00101	0.00536	0.00541
94161775	304.074	5.2782	0.956567	0.00573	0.751	-3.04E-03	0.78192	0.006	1.04327	0.775915	1.03727	0.114	0.096	0.684	0.517
94162075	304.076	5.2846	0.956278	0.00327	0.7523	-3.04E-03	0.78352	0.00342	1.04495	0.780055	1.04149				
94162375	304.078	5.2864	0.957429	-0.00163	0.7526	-3.04E-03	0.78289	-0.0017	1.04401	0.784612	1.04573				
94162675	304.074	5.294	0.957082	-0.00163	0.7541	-3.04E-03	0.78474	-0.0017	1.04595	0.786493	1.0477				
94162975	304.076	5.2928	0.956586	-0.0049	0.7539	-3.04E-03	0.78494	-0.00512	1.04629	0.790063	1.05141				
94163275	304.068	5.289	0.955481	0.00245	0.7531	-3.04E-03	0.78501	0.00256	1.04666	0.782487	1.04413				
94163575	304.079	5.2837	0.955483	0.00735	0.7521	-3.04E-03	0.78346	0.00769	1.04561	0.776279	1.03793				
94163875	304.077	5.2851	0.956184	-0.0049	0.7524	-3.04E-03	0.7837	-0.00512	1.04516	0.788777	1.05023				
94164175	304.073	5.2833	0.956043	-0.00082	0.752	-3.04E-03	0.7834	-0.00086	1.04489	0.784245	1.04574				
94164475	304.076	5.2884	0.956483	0.00163	0.753	-3.04E-03	0.78408	0.0017	1.04545	0.782393	1.04877	0.78451	1.04602	0.78473	1.04624
94164775	304.075	5.2966	0.956783	-0.00082	0.7547	-3.04E-03	0.78561	-0.00086	1.0469	0.786431	1.04772	0.00127	0.00133	0.00412	0.00403
94165075	304.075	5.2911	0.956371	-0.00327	0.7536	-3.04E-03	0.7848	-0.00342	1.0462	0.788176	1.04958	0.162	0.127	0.525	0.385
94165375	304.071	5.2971	0.954584	0.00327	0.7548	-3.04E-03	0.78753	0.00343	1.04942	0.784071	1.04597				
94165675	304.079	5.2773	0.955689	0.00245	0.7508	-3.04E-03	0.78243	0.00256	1.04402	0.779855	1.04145				
94165975	304.074	5.2881	0.956361	-0.0049	0.753	-3.04E-03	0.78418	-0.00512	1.04554	0.7893	1.05071				
94166275	304.073	5.2773	0.956249	-0.00245	0.7508	-3.04E-03	0.78197	-0.00256	1.04341	0.784523	1.04596				
94166575	304.071	5.2787	0.955921	0.00163	0.7511	-3.04E-03	0.78255	0.00171	1.04408	0.780854	1.04238				
94166875	304.073	5.29	0.955651	0.00513	0.7533	-3.04E-03	0.78508	0.006	1.04668	0.779138					
94167175	304.078	5.2929	0.957326	-0.00245	0.754	-3.04E-03	0.78444	-0.00256	1.04558	0.786953					
94167475	304.072	5.2837	0.956651	-0.00652	0.7521	-3.04E-03	0.783	-0.00682	1.04433	0.789806					
94167775	304.07	5.2785	0.955191	0.00573	0.751	-3.04E-03	0.78305	0.006	1.04478	0.777096		0.77504	1.03377	0.69595	0.95482
94168075	304.079	5.2915	0.955895	0.01715	0.7537	-3.04E-03	0.7853	0.01794	1.04684	0.767332		0.01503	0.0196	0.11688	0.12079
94168375	304.091	5.2877	0.958376	0.1372	0.7529	-3.04E-03	0.78243	0.14316	1.04329	0.639244	0.9001	1.94	1.9	16.8	12.7
94168675	304.247	5.279	0.97501	0.24893	0.7511	-3.07E-03	0.7672	0.2548	1.022	0.512605	0.76901				
94168975	304.395	5.2649	0.992415	0.23422	0.7483	-3.09E-03	0.75091	0.23601	1.00282	0.514724	0.76663				
94169275	304.534	5.2654	1.007799	0.21805	0.7484	-3.12E-03	0.73954	0.21636	0.98761	0.523187	0.77125				
94169575	304.662	5.2446	1.022063	0.19257	0.7443	-3.14E-03	0.72515	0.18841	0.96972	0.536545	0.78115				

94169875	304.77	5.2492	1.034182	0.18473	0.7452	-3.16E-03	0.71751	0.17862	0.95925	0.539	0.78074						
94170175	304.888	5.2371	1.048786	0.18522	0.7427	-3.18E-03	0.70512	0.1766	0.94349	0.528343	0.76671						
94170475	304.997	5.2378	1.060224	0.17052	0.7429	-3.20E-03	0.69768	0.16083	0.93348	0.536652	0.77245						
94170775	305.097	5.2436	1.072196	0.15925	0.7441	-3.22E-03	0.691	0.14853	0.92417	0.542452	0.77562						
94171075	305.192	5.2243	1.081964	0.14798	0.7401	-3.23E-03	0.68105	0.13677	0.91211	0.544464	0.77553	0.6846	0.91654	0.54385	0.77578		
94171375	305.278	5.2203	1.091849	0.1372	0.7394	-3.25E-03	0.67422	0.12566	0.90319	0.548542	0.77751	0.02359	0.03076	0.0078	0.00453		
94171675	305.36	5.2249	1.101288	0.12887	0.7403	-3.26E-03	0.66925	0.11702	0.89626	0.552068	0.77908	3.45	3.36	1.43	0.584		
94171975	305.436	5.2139	1.110976	0.11662	0.7381	-3.28E-03	0.66142	0.10497	0.88645	0.556292	0.78132						
94172275	305.503	5.2065	1.11738	0.12005	0.7366	-3.29E-03	0.65628	0.10744	0.88001	0.548839	0.77258						
94172575	305.583	5.2147	1.127228	0.11613	0.7382	-3.30E-03	0.65195	0.10302	0.87374	0.549115	0.7709						
94172875	305.645	5.2124	1.133587	0.08673	0.7377	-3.31E-03	0.64785	0.07651	0.86839	0.571508	0.79205						
94173175	305.689	5.2049	1.139128	0.098	0.7362	-3.32E-03	0.64337	0.08603	0.86284	0.557359	0.77683						
94173475	305.765	5.1958	1.146477	0.10045	0.7345	-3.34E-03	0.63775	0.08762	0.8558	0.550089	0.76815						
94173775	305.812	5.1963	1.153499	0.07595	0.7346	-3.35E-03	0.63394	0.06584	0.85067	0.56807	0.7848						
94174075	305.858	5.192	1.157322	0.08673	7337	-3.35E-03	0.63107	0.07494	0.84708	0.556255	0.77227						
94174375	305.918	5.1955	1.165426	0.08232	0.7344	-3.37E-03	0.62726	0.07064	0.84178	0.556454	0.77097	0.62823	0.84324	0.56159	0.7766		
94174675	305.959	5.1885	1.170431	0.06713	0.7329	-3.37E-03	0.6233	0.05735	0.8369	0.566133	0.77973	0.01108	0.01434	0.00611	0.00657		
94174975	306	5.1866	1.175334	0.07203	0.7326	-3.38E-03	0.62044	0.06128	0.83314	0.559282	0.77199	1.76	1.7	1.09	0.846		
94175275	306.047	5.1814	1.179385	0.06615	0.7316	-3.39E-03	0.61746	0.05609	0.82943	0.561316	0.77329						
94175575	306.081	5.1779	1.183593	0.06027	0.7308	-3.40E-03	0.61458	0.05092	0.8258	0.563538	0.77476						
94175875	306.121	5.1876	1.188902	0.05488	0.7328	-3.40E-03	0.61351	0.04616	0.82379	0.567492	0.77777						
94177675														0.56961	0.77669		
														0.00452	0.0042		
														0.794	0.541		
94179175														0.56612	0.77596		
														0.01931	0.00054		
94180975														0.57184	0.7751		
														0.00297	0.003		
														0.52	0.387		
94184275														0.57441	0.77577		

0.00556	0.00556
0.969	0.966

94187575

0.57544	0.77583
0.01086	0.0109
1.89	1.41

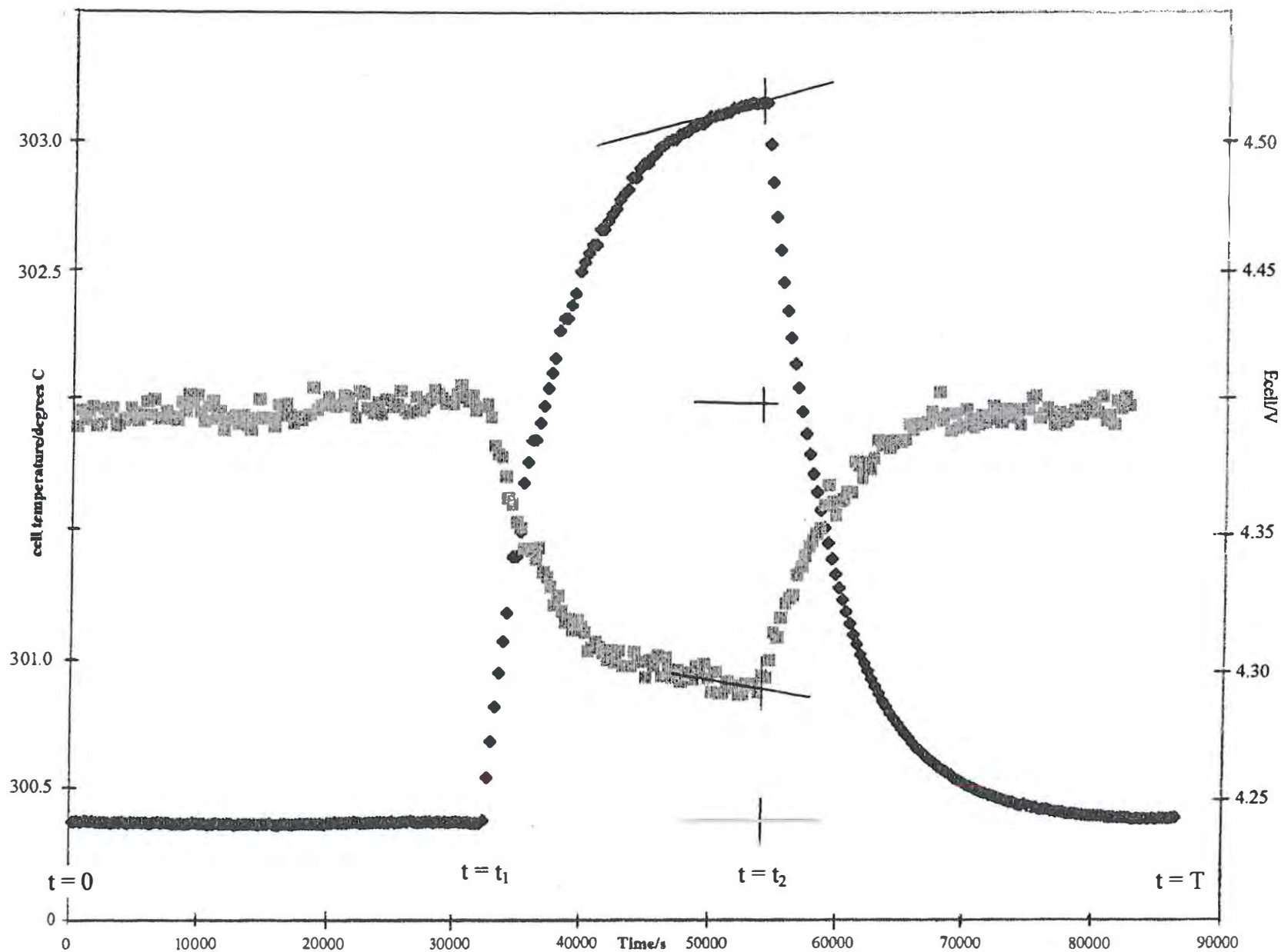


Fig. 1 An example of the “raw data”. The temperature-time and cell potential-time series for the measurement cycle on the fifth day, Cell current 0.15034A. The constructions show the values of the temperatures and cell potentials required for the calculation of $(k_R')_1$ and $(k_R')_2$.

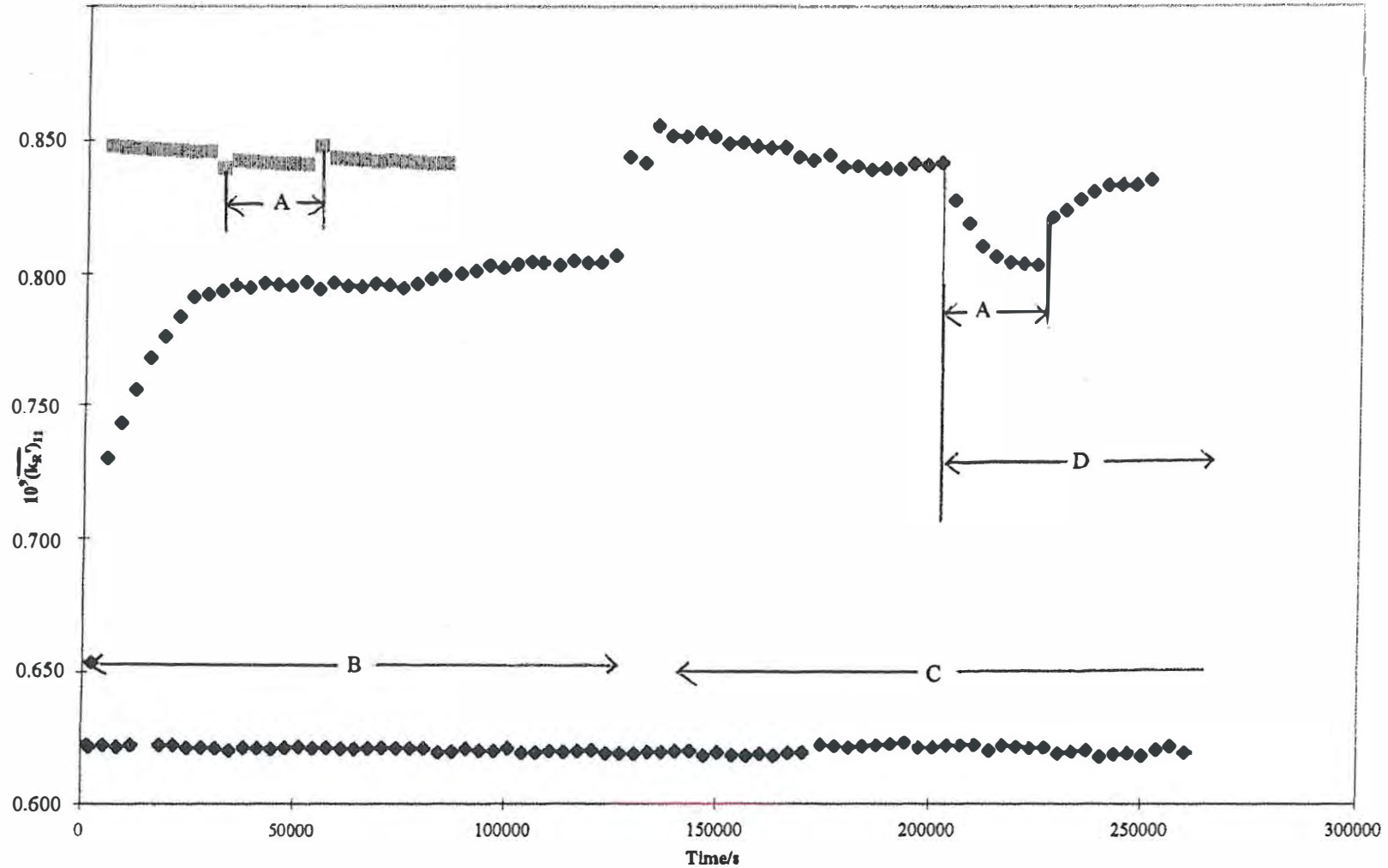


Fig. 2 Comparison of the variation of $10^9(k_R')_{II}$ with time for the polarisation of the Pd-B electrode with the behaviour of the Pt electrode (see(3)) in the initial stages of the experiments, \diamond . Respective cell currents 0.15034 and 0.2000 A. The figure also shows $10^9(k_R')_{II}$ for the Pd-B-Ce electrode at a median cell current of 0.42A. The slope of this plot must be multiplied by 0.357 to give the variation predicted for the Pd-B electrode. Note the changes in $10^9(k_R')_{II}$ induced by the calibration pulses indicate incorrect wiring of this experiment (9).

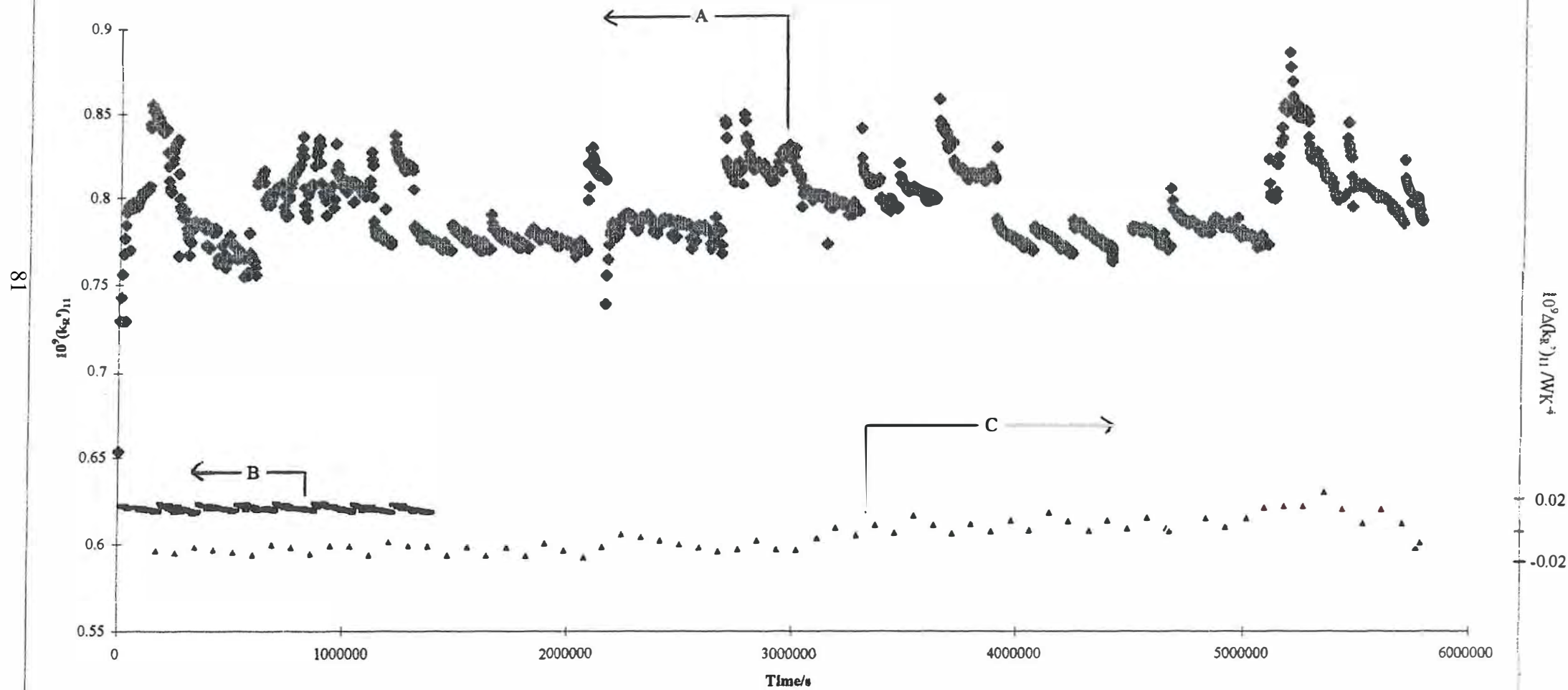
A : Heater pulse

B : excess enthalpy generation due to absorption of D in lattice

C : onset of excess enthalpy generation

D : effects of positive feedback

Fig. 3 the variation of $10^9(k_R')_{11}$ with time for Days 1-67 of the experiment using the Pd-B cathode



A $10^9(k_R')_{11}$ for the Pd-B electrode

B $10^9(k_R')_{11}$ for the Pt "blank" system using an ICARUS -2 calorimeter

C $\Delta 10^9(k_R')_{11}$ for the Pd-B electrode predicted from the changes due to the cell currents and the schedule of additions of D_2O to the cell

Fig. 4A The variation of the rate of specific excess enthalpy generation/ Wcm^{-3} between the start of the experiment and Day 33

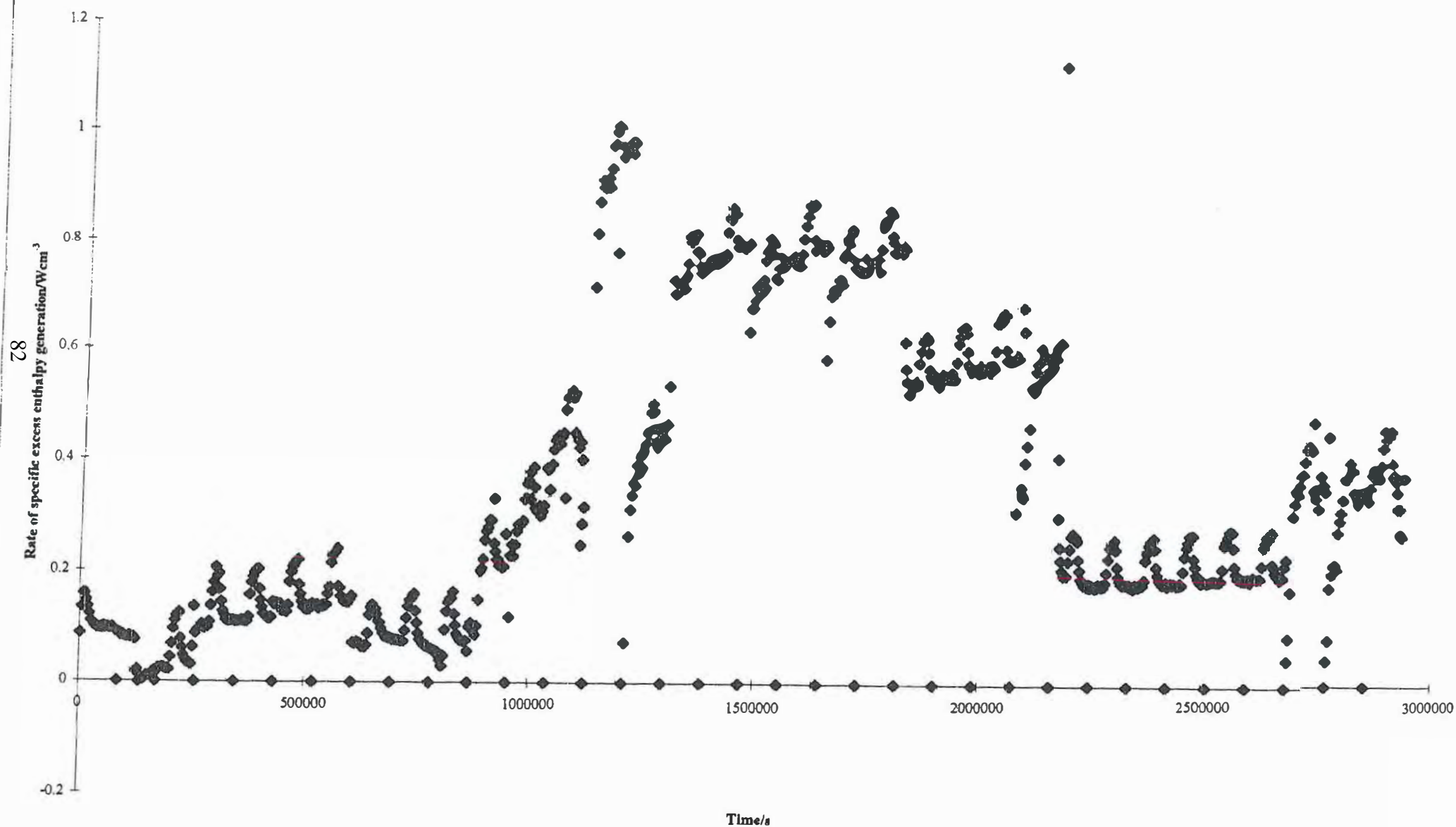


Fig.4B The variation of the rate of specific excess enthalpy generation/ W cm^{-3} between Days 33 and 67

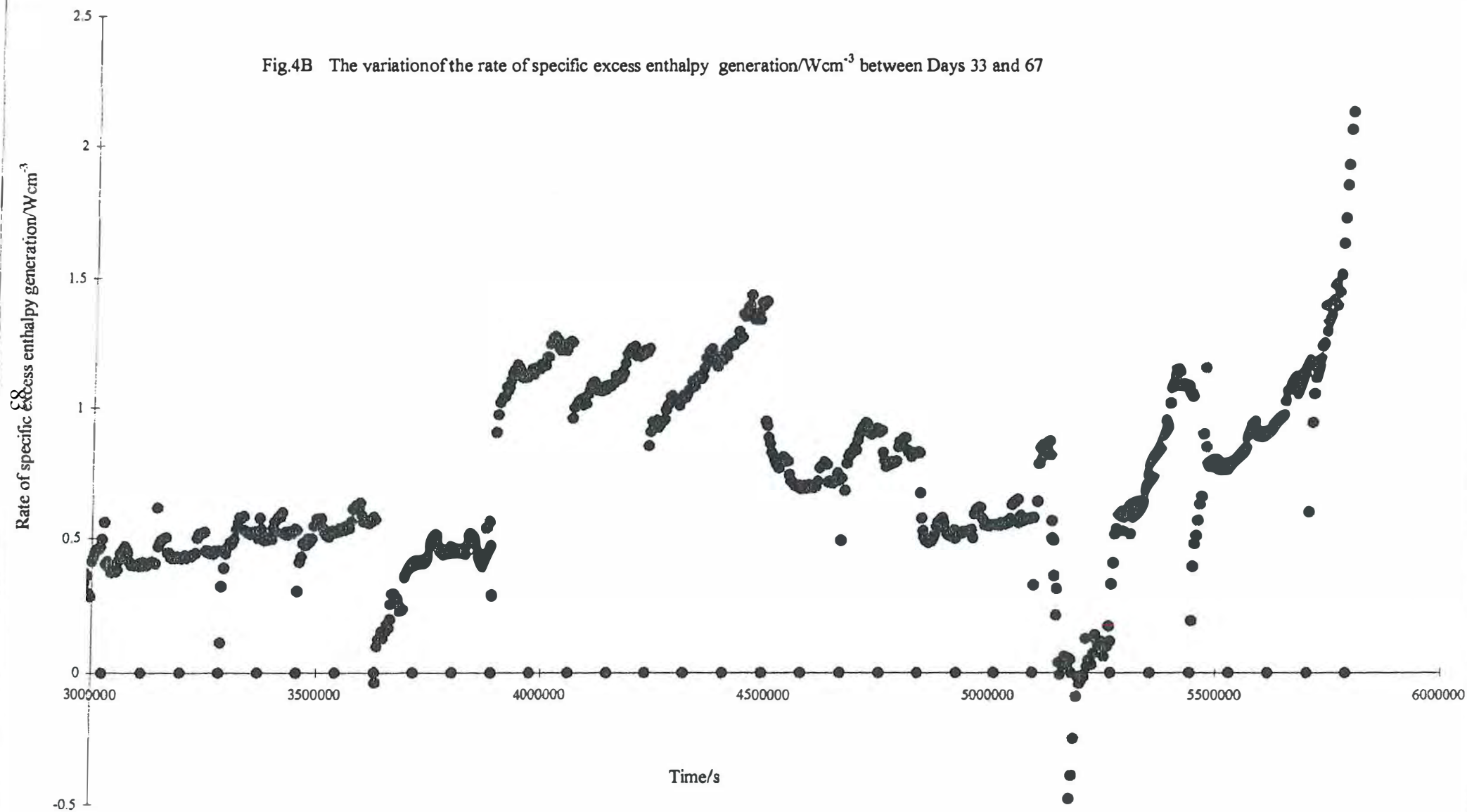


Fig.4C The variation of the rate of specific excess enthalpy generation/ Wcm^{-3} on Day 68 of the experiment

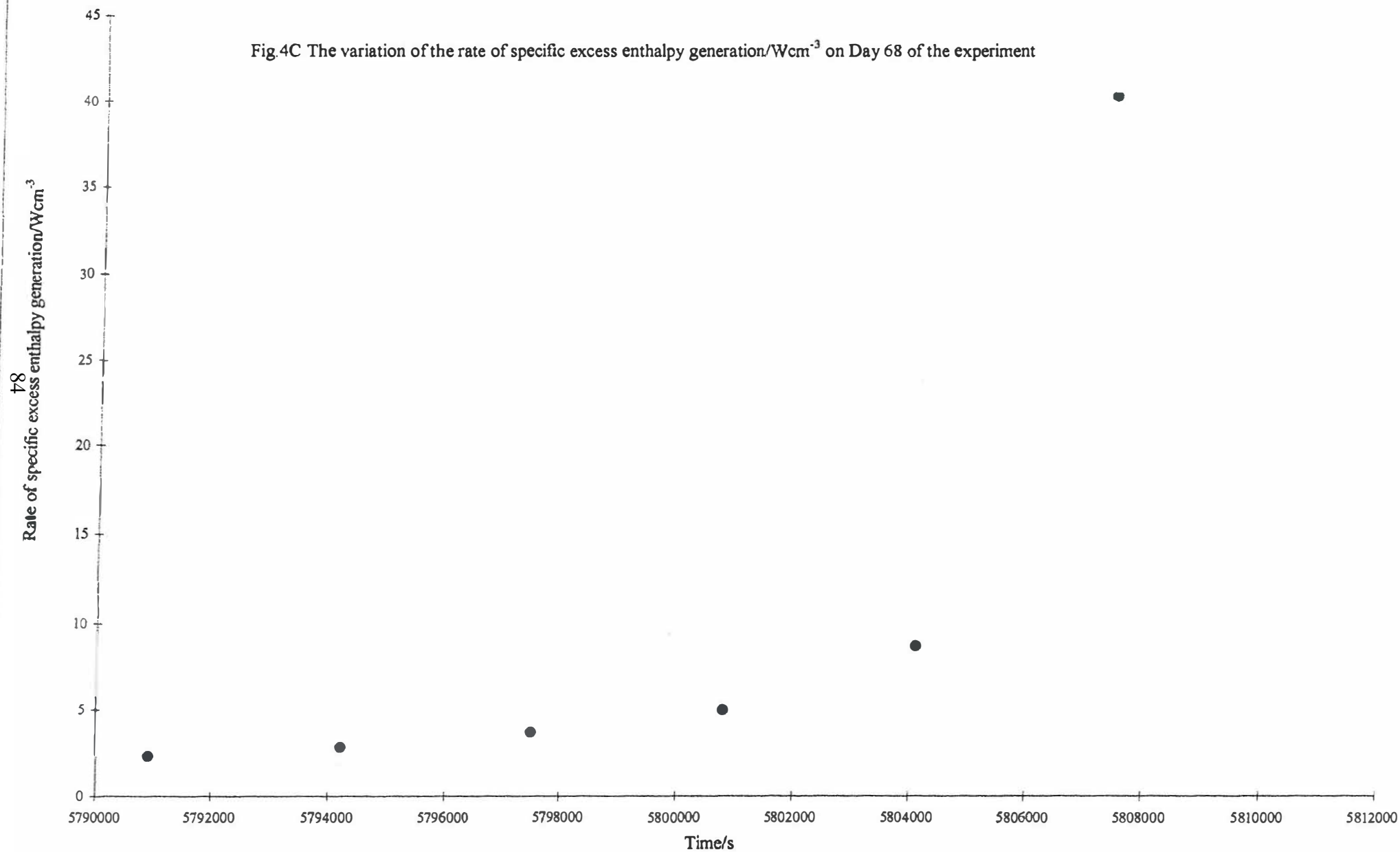
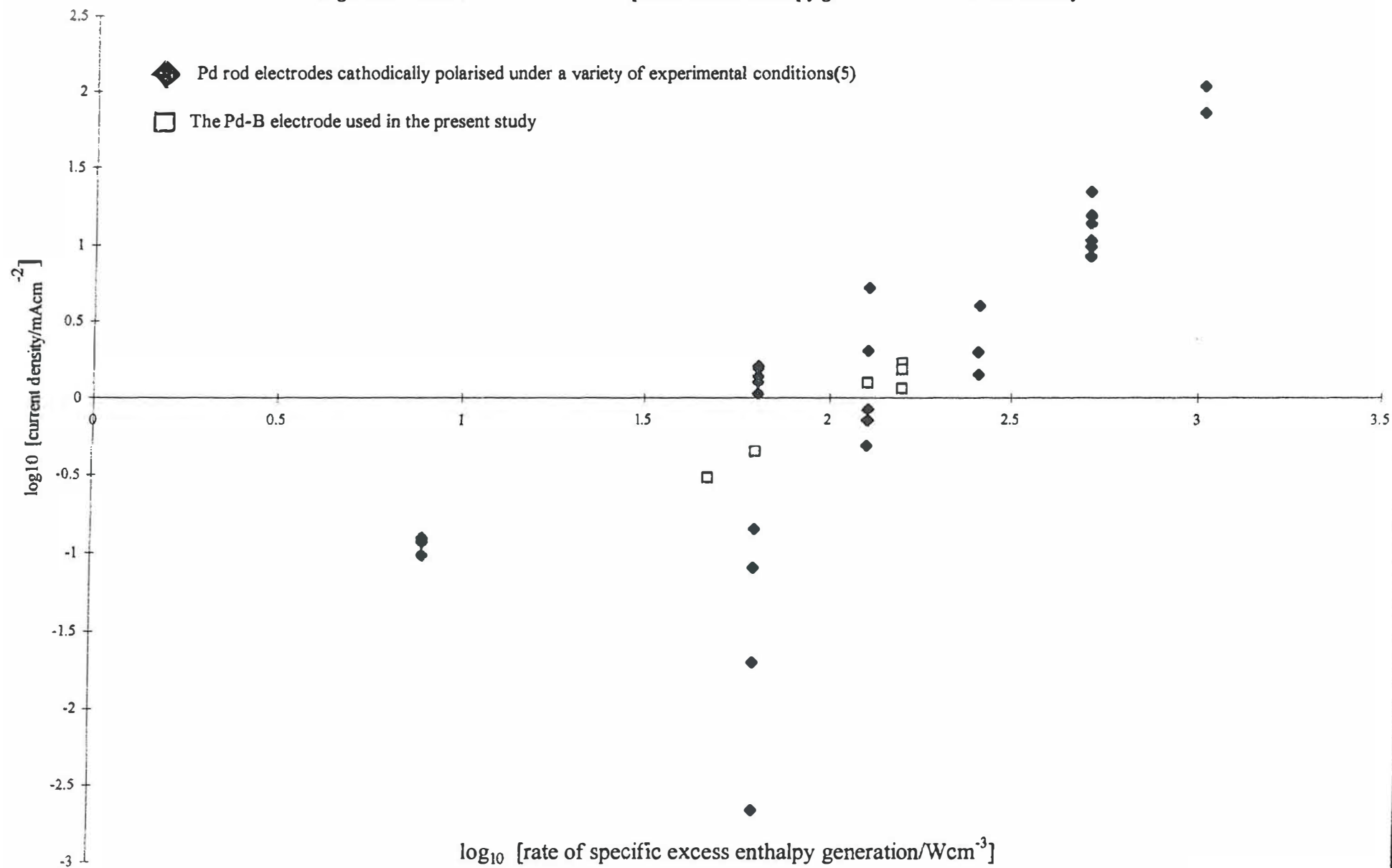


Fig.5 The variation of the rate of the specific excess enthalpy generation with current density



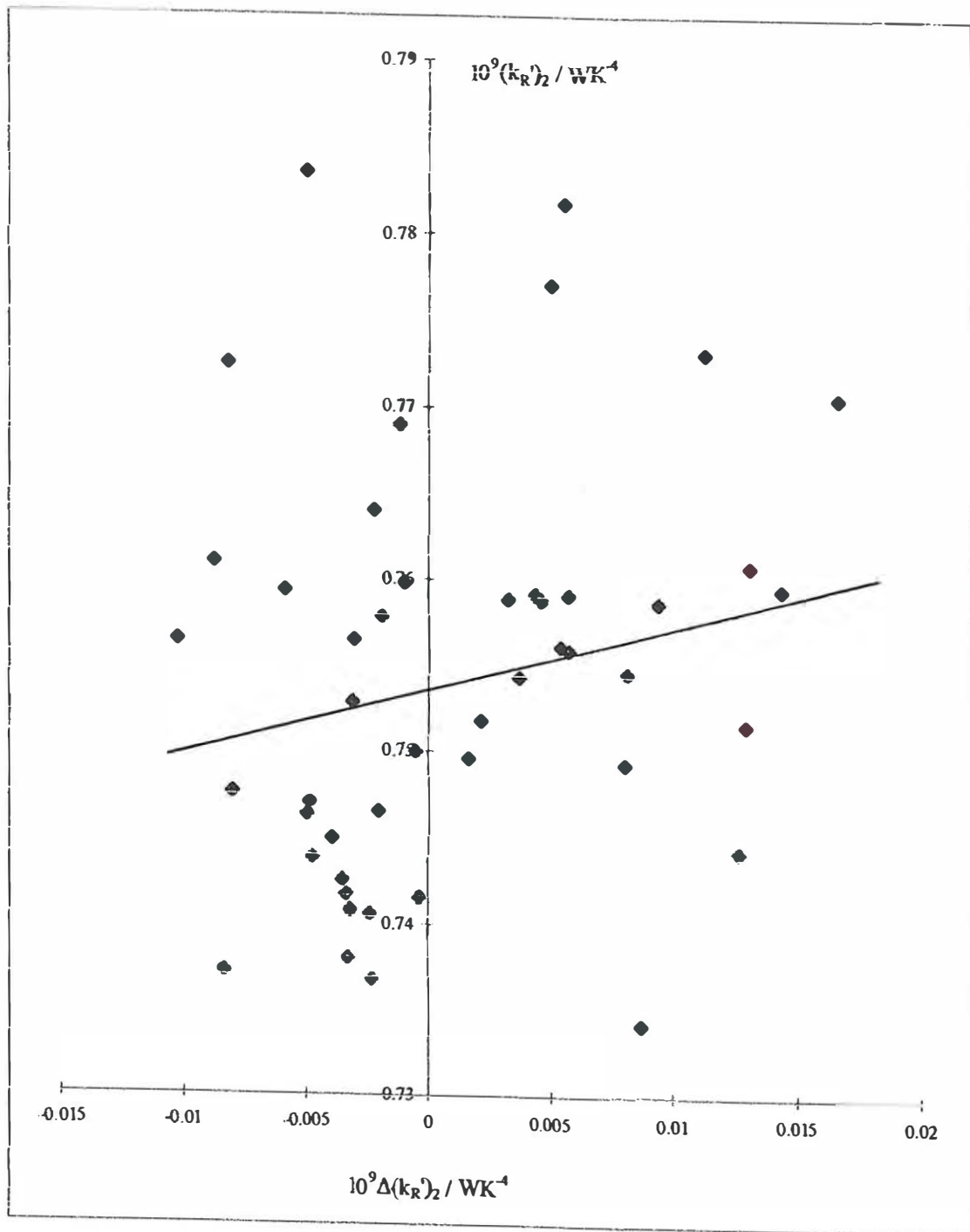


Fig. 6 Plot of the observed variation of the "true" heat transfer coefficient $10^9 (k_R')_2 / \text{WK}^{-4}$ versus the predicted variation $10^9 \Delta(k_R)_2 / \text{WK}^{-4}$. The plot also shows the regression line through the points, $r = 0.345$.

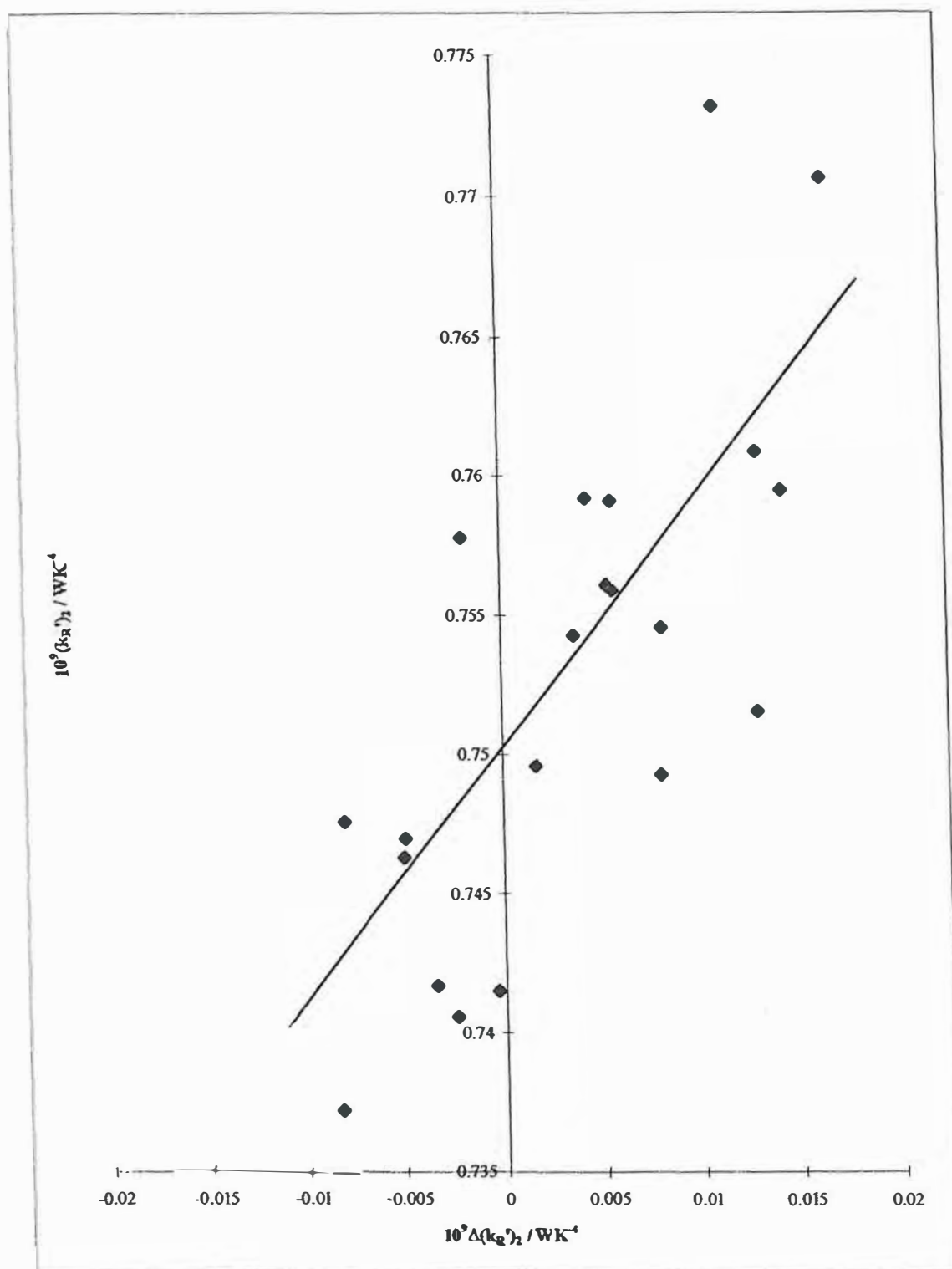


Fig. 7 The plot shown in Fig. 6 but with elimination of invalid data points.

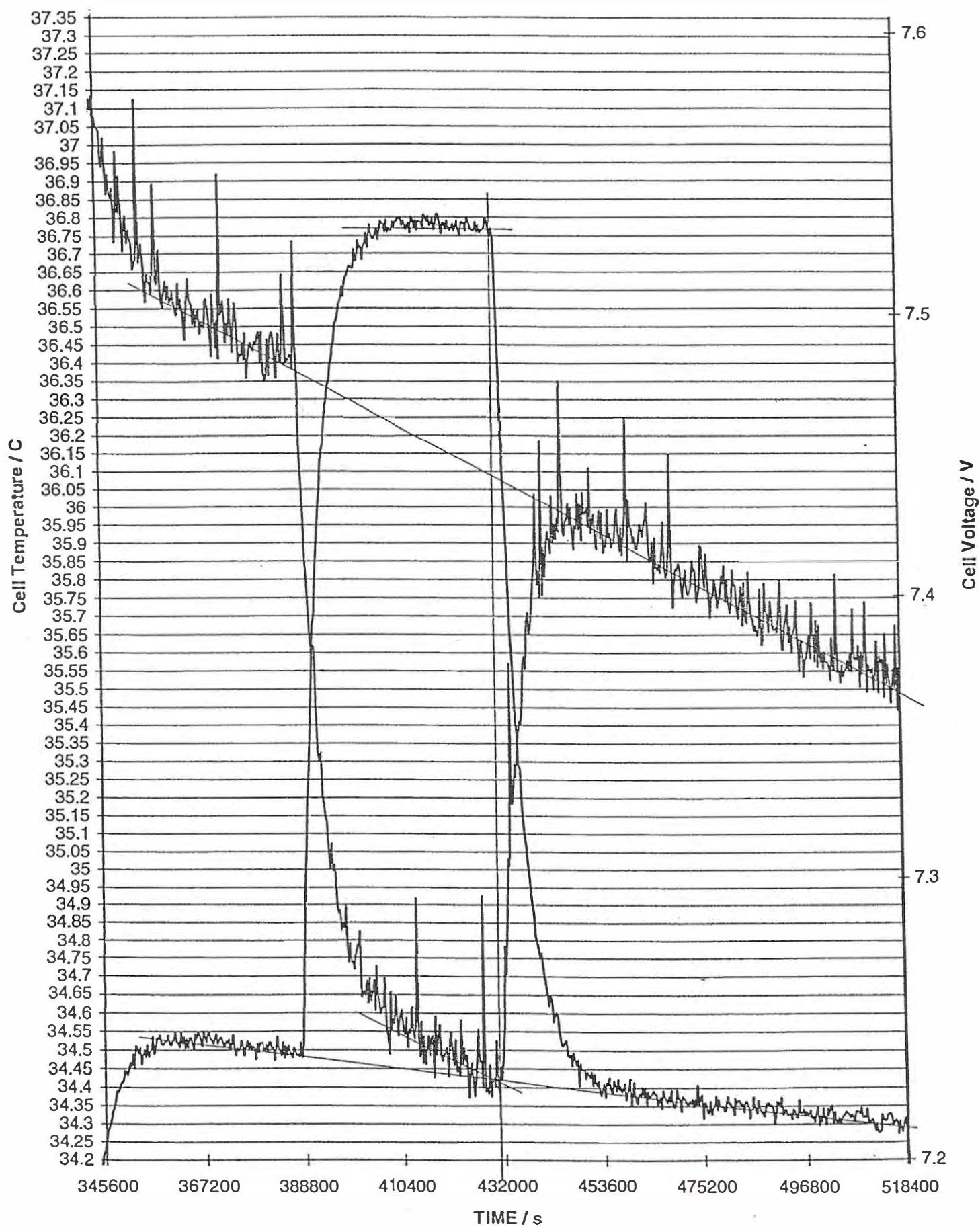
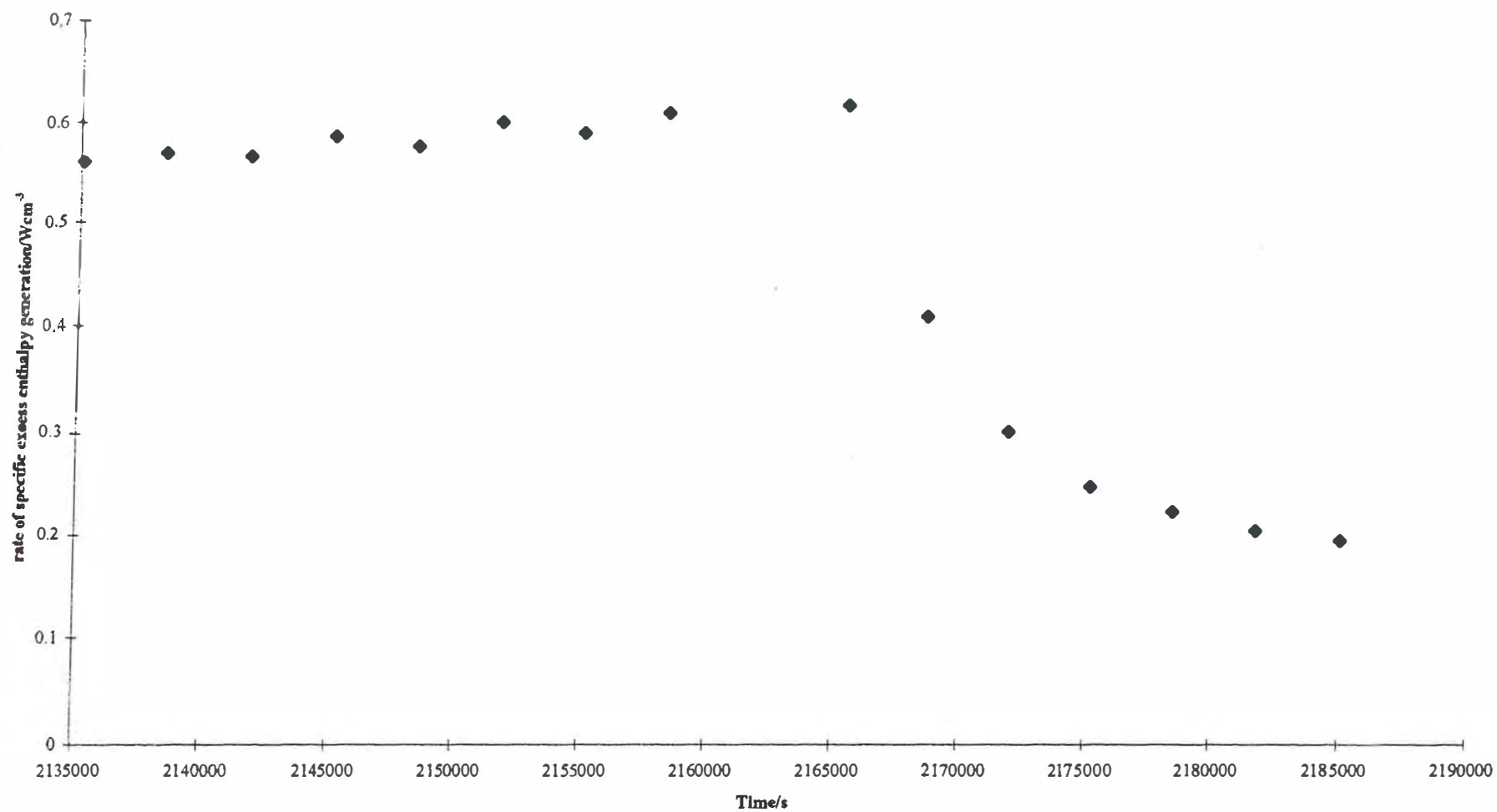


Fig. 8 The operation of cell 4141 on Days 5 and 6 [Pt electrode diameter 1.5mm, length 12.5mm] in 0.1M LiOD in D₂O ; cell current 0.2000A, $\Delta Q = 0.25063$ W

Fig.9 The rate of specific excess enthalpy generation in the region of the start of Day 26. cell current changed from ~ 0.65 to ~ 0.20 A



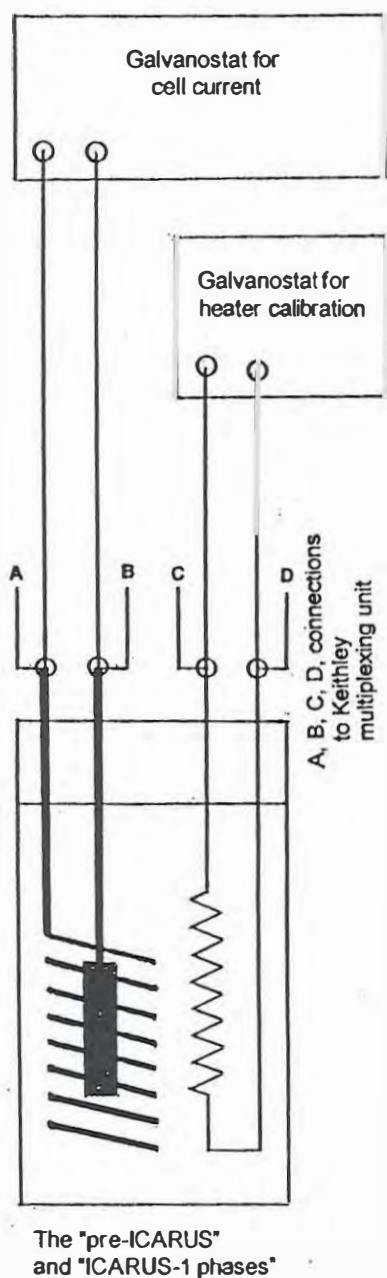


Fig. 10A Schematic of the polarising circuit used with the ICARUS -1 System.

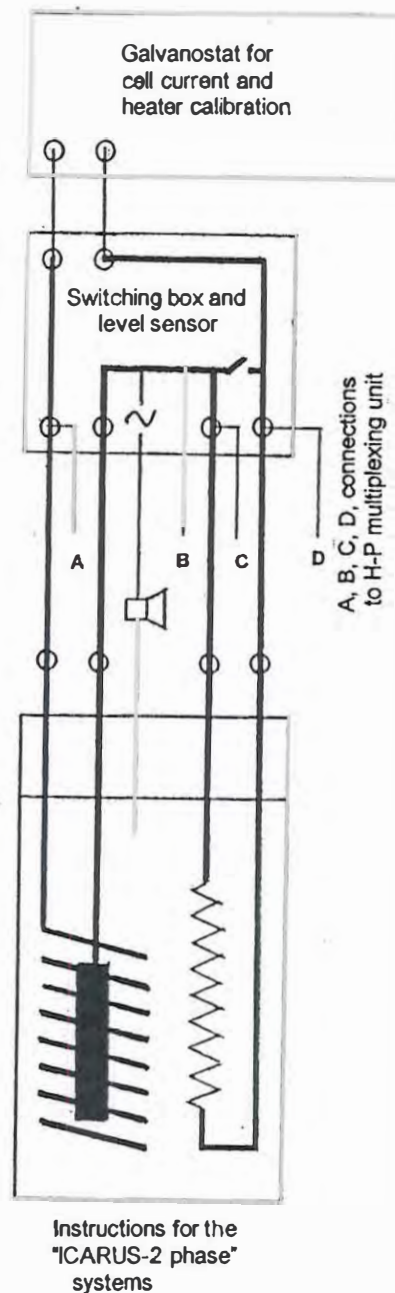


Fig. 10B Schematic of the polarising circuit used with the ICARUS -2 System. The figure shows the provision of the means of . using the cell current to calibrate the system as well as the means for testing the level of the electrolyte in the cell.

OUR PENULTIMATE PAPERS ON THE ISOPERIBOLIC CALORIMETRY OF THE
Pt-D₂O AND Pd-D₂O SYSTEMS. Part III : THE Pd-D CODEPOSITION SYSTEM

M.Fleischmann, Bury Lodge, Duck Street, Tisbury, Salisbury, Wilts., SP3 6LJ, U.K.

M.H. Miles, Department of Chemistry, University of La Verne, La Verne, CA91750, U.S.A.

S. Szpak, SSC San Diego, San Diego, CA 92152-5001, U.S.A.

P.A. Mosier-Boss, SSC San Diego, San Diego, CA 92152-5001, U.S.A.

ABSTRACT

The Pd-D codeposition system (1) has been investigated by means of isoperibolic calorimetry. It is shown that high rates of excess enthalpy generation are achieved at relatively short times by using this methodology (as compared to the rates achieved when using “massive” electrodes (2), (3), (4), (5), (6), (7), (8)) and the system also shows the early effects of the development of “positive feedback”. In view of the marked variation of the rate of excess enthalpy generation with time, the data analysis must be restricted to the evaluation and use of the differential heat transfer coefficients.

It is shown that the heat transfer coefficient given for this system by the group at the New Hydrogen Energy Laboratories, Sapporo, Japan had to be incorrect as it was less than the value calculated from the Stefan-Boltzmann coefficient and the radiant surface area. Furthermore, the value differed from that evaluated for experiments when using Pd-B alloy electrodes in the same cell. These disparities are attributed to the inappropriate evaluation of the integral heat transfer coefficients. Nevertheless, positive rates of excess enthalpy generation are derived even when using the impossibly low value of the heat transfer coefficient. It is also shown that the recombination of the gases evolved in the cell (which is

frequently invoked to explain excess enthalpy generation) leads to the impossible conclusion that the “lower bound” heat transfer coefficient exceeds the “true” value.

INTRODUCTION

The Pd-D electrochemical codeposition system (1) provides an interesting example of excess enthalpy generation in Pd-based systems (see e.g. (2), (3), (4), (5), (6), (7)) because the codeposition of the Pd and D avoids many of the difficulties associated with the use of massive electrodes. For example, we can observe an early generation of marked levels of excess enthalpy throughout the body of the electrode (see further below). These features make the codeposition system a particularly interesting example for the test of the calorimetric methods used in these investigations.

The measurements analysed in this paper were carried out by one of us (M.H.M.) during his stay at the New Hydrogen Energy Laboratories, Sapporo, Japan using an ICARUS-1 Calorimeter in an ICARUS-2 Data Acquisition and Measurement System (Isoperibolic Calorimetric Research and Utilities System), (9). Full details of the investigation may become available in due course (10).

EXPERIMENTAL

The codeposition of Pd and D was carried out in the calorimetric ICARUS-1 Dewar-type cell from a solution 0.025 MPdCl₂, 0.15 M ND₄Cl and 0.15 M ND₄OD in D₂O (Isotec 99.9 atom %D) onto a Cu-rod electrode, substrate area ~4 cm². If all the Pd contained in the solution was deposited onto the surface, we obtain a volume of the deposit ~ 0.0225 cm³. The use of this volume therefore gives a lower bound for the specific rate of excess enthalpy generation.

The polarisation of the cell and the data acquisition were carried out using an ICARUS -2 system which produced the $(k_R')_{11}$ - spreadsheets used by the group in Sapporo (for comments on this spreadsheet and the original spreadsheet supplied with the ICARUS -2 system, see (10)). The definition of the heat transfer coefficients which control the behaviour of the cell and which are used in this paper is given in Appendix A. (see also (11), (12)). The experiment was carried out using the same cell, thermostat tank and associated equipment as had been used for the measurements on the Pd-B electrode which have been reported previously (4), (5), (6), (7).

DATA EVALUATION

The rate of the specific excess enthalpy generation in the Pd-D codeposition system is compared in Fig. 1 with the rates previously observed for “massive” Pd electrodes under a variety of conditions (2), and with those which can be derived from the measurements with the Pd-B electrodes, (3). The basis of the evaluation for the Pd-D codeposition system is discussed below. It can be seen that the rates for the codeposition system are much higher than those for the “massive” electrodes and these high rates are also established at relatively short times. Furthermore, the effects of “positive feedback”, (13), (14), (15), are also established at short times (see Fig. 3 below). In consequence, the “lower bound” heat transfer coefficient, $(k_R')_{11}$, shows a marked time dependence, Fig. 2. This coefficient is based on the assumption of a zero rate of excess enthalpy generation in the system (e.g. see (11), (12)) and is the simplest result which we can derive from the experiments (note, for example, that it is independent of any method of calibration). Under the conditions of the experiment, the maximum change in $(k_R')_{11}$ which we could attribute to the effects of the progressive electrolysis is $0.01 \times 10^{-9} \text{ WK}^{-4}$ (e.g. see (3), (8)). It follows, therefore, that the assumption of a zero rate of excess enthalpy generation is incorrect ; indeed, the results given in Fig. 3 demonstrate the presence of a marked and variable rate of excess enthalpy generation. In turn, this shows that the evaluation of the data must rely in the main on the preliminary methods of analysis which are based on the interpretations of $(k_R')_{11}$ and $(k_R')_{12}$ coupled to the possible extension of the interpretation to the differential heat transfer coefficients such as $(k_R')_{161}^0$ and $(k_R')_{162}^0$ evaluated over restricted ranges of time.

Fig. 4 illustrates the determination of $(k_R')_{161}^0$ for the initial stages of the application of the calibration pulse on Day 6 (calibration pulses were applied on Days 6, 7 and 8 of this experiment). We obtain $10^9(k_R')_{161}^0 = 0.73099 \text{ WK}^{-4}$, $\text{CpM} = 456.9 \text{ JK}^{-1}$ while the regression coefficient is $r = 0.9922$. The use of such plots was specified for the initial stages of the application of the ICARUS-1 methodology (16) (although the interpretation of the integral heat transfer coefficients such as $(k_R')_{261}^0$ was to be preferred compared to that of the differential coefficients). The determination of the corresponding “differential true heat transfer coefficient, $(k_R')_{162}^0$ is illustrated in Fig. 5 (again for the calibration on Day 6). We obtain $10^9(k_R')_{162}^0 = 0.82474 \text{ WK}^{-4}$, $\text{CpM} = 475.1 \text{ JK}^{-1}$, $r = 0.9993$. However, as we have noted on other occasions, this determination is unreliable especially as regards the derived value of CpM ; note the large values of the abscissae especially for the points which have the highest statistical weight. If we therefore restrict attention to the points nearest the origin we obtain $10^9(k_R')_{162}^0 = 0.85573 \text{ WK}^{-4}$. The derived values of $(k_R')_{162}^0$ therefore straddle the value $0.85065 \times 10^9 \text{ WK}^{-4}$ which was found in the investigation of the Pd-B electrode, (3), (4), (5).

This degree of agreement must be regarded as being satisfactory bearing in mind that $(k_R')_{162}$ is the least accurate value of the “true” heat transfer coefficient which may be determined by this methodology. We have therefore taken the value $10^9(k_R')_{162}^0 = 0.85065 \text{ WK}^{-4}$ for the further assessment of parts of the experiment outlined below.

The degree of agreement between the experiments using the Pd-B cathodes and the Pd-D codeposition methodology derived here may be contrasted with the values of the “true” heat transfer coefficients derived by the evaluations given by N.H.E. viz 0.7935 WK^{-4} and 0.69986 WK^{-4} respectively. We do not know the nature of the evaluations carried out by N.H.E. but we believe that these must have been based on the forward integration of the data sets leading to the evaluation of $(k_R')_{362}^0$. We note that we advised against the use of this methodology in the Handbooks accompanying the ICARUS instrumentation (9), (16) and pointed out that it was especially prone to error in the presence of the effects of “positive feedback” unless these effects were expressly allowed for (e.g. see (5), (6)). A further surprising feature of the value of the heat transfer coefficient given for the Pd-D codeposition experiment is that the value $10^9(k_R')_{362}^0 = 0.69986 \text{ WK}^{-4}$ is actually less than the minimum value $0.72 < 10^9(k_R')_{362}^0 < 0.76 \text{ WK}^{-4}$ which applies to cells of the type used for heat transfer by radiation alone (i.e. the Stefan - Boltzmann value), an evident impossibility because heat transfer must also include a contribution due to conductivity. Thus, as we have noted previously the value $10^9(k_R')_{262}^0 = 0.85065 \text{ WK}^{-4}$ for the cell used in this codeposition experiment and the earlier study of Pd-B

electrodes implies a “softening” of the vacuum in the Dewar Cell. A value of the heat transfer coefficient smaller than the Stefan - Boltzmann value could only be observed if the cell was behaving as a spontaneous refrigerator i.e. if we had a contravention of the Second Law of Thermodynamics. The most likely reason for the low values of the heat transfer coefficients given by the analyses due to the group at N.H.E. for the experiments on the Pd-B and Pd-D codeposition experiments is the neglect of the effects of variable rates of excess enthalpy generation and of “positive feedback”. The presence of these effects can be demonstrated directly from the consideration of the time-dependence of the “lower bound” heat transfer coefficient e.g. for the measurement cycle on Day 6 of the experiment, Fig. 3. For example, we can see immediately that the application of the heater calibration pulse leads to an increase of the rate of excess enthalpy generation. These data have been illustrated for Day 6 of the experiment as this is the most likely date for the evaluations carried out by N.H.E. As has been pointed out above, the presence of rates of excess enthalpy generation showing a marked time-variation force us to restrict the evaluations to those of the differential “lower bound” and “true” heat transfer coefficients, $(k_R')^0_{161}$ and $(k_R')^0_{162}$ of the preliminary methods of data analysis of the ICARUS systems.

Fig. 3 also shows some of the key values of the “true” heat transfer coefficient discussed in this paper. We consider next the time-dependence of the “lower bound” heat transfer coefficient for the whole experiment, Fig. 2, and the corresponding rates of excess enthalpy generation, Fig. 6, where we have used the value $10^9(k_R')^0_{12} = 0.85065 \text{ WK}^{-4}$ in the calculation. This is the value of $10^9(k_R')^0_{262}$ for the experiment with the Pd-B electrode but allowing for the effects of “positive feedback” (5), (6), (7). Fig. 2 also shows in succession the values of $10^9(k_R')^0_{362}$ for that experiment as well as the value of this heat transfer coefficient for the Pd-D codeposition experiment. Table 1 lists the values of the 11-point means of the “lower bound” heat transfer coefficient, $10^9(k_R')_{11}$, and Table 2 lists the corresponding rates of excess enthalpy generation given in Fig. 6 as well as the rates calculated using the value of the “true” heat transfer coefficient given by the evaluation due to N.H.E. In view of the high rates of excess enthalpy generation in this system, we can see that we obtain positive rates for most of the experimental time range and, even, for most of day 6 when using the impossibly low value of the heat transfer coefficient given by N.H.E. The use of the maximum value of $(k_R')_{11}$ shown in Fig. 3 will give higher rates of excess enthalpy generation and these will naturally remain positive throughout the time range of the experiment. We note that this strategy was proposed (13) to allow the evaluation of the minimum rates of excess enthalpy generation.

The reduction of electrogenerated oxygen has frequently been proposed as an explanation of excess enthalpy production (e.g. recently the correspondence following (17)). These proposals have been made in the absence of any attempt to measure and interpret the magnitude of any such term and, even though, this had already been shown to be negligibly small in the first full publication on this topic (see Table 4 of (2)); for more recent determinations see (11), (18)). Moreover, the consequences of making such an assumption have not been examined. In Fig. 7 we illustrate one such consequence ; the “lower bound” heat transfer coefficient is now larger than the “true” values over most of the time range of the experiment (the whole time range if the value $10^9(k_R)'_{362} = 0.69986 \text{ WK}^{-4}$ given by N.H.E. is accepted). This is again an evident impossibility unless the cell is generating as a spontaneous refrigerator over the whole of this time range.

Fig. 8 gives the schedule of the cell currents used in the experiment. As this figure and fig. 2 show, a steady-state operation of the cell is most likely to have been achieved in the time ranges 200,000-300,000 s and 500,000-600,000 s. The values of the specific rates of excess enthalpy generation in these time slots have been shown on Fig. 1 in comparison with those for the initial study (2) and with those for the Pd-B electrodes, (3), (4), (5), (6), (7), (10). The advantages of using the co-deposition methodology, (1), will be self evident.

Fig. 8 also shows that the phenomenon of “Heat -after-Death” is most likely to have been established during the last period of operation on Day 2 and the first period on Day 3 following the stepwise reduction of the current (this has been classified as Case 1 of the phenomenon (19)). The results are shown in Fig. 9. In constructing this figure it has been assumed that the upper bound of any excess enthalpy generation due to the reduction of oxygen is given by the last values of, $Q_{\text{excess}} = 0.009 \text{ W}$, on Day 1 i.e. the values of Q_{excess} shown in Fig. 9 are a “lower bound”.

DISCUSSION

The results presented in this paper show that the Pd-D codeposition system (1) has many advantages compared to the use of “massive, solid” electrodes (2), (3), (4), (5), (6), (7), (8). The use of the codeposition system leads to the early generation of high rates of the specific

excess enthalpy generation coupled to the early onset of the effects of “positive feedback”. It is these factors which can lead to the erroneous calibration of the cells which is a feature of the evaluations provided by the group at the New Hydrogen Energies Laboratories in Sapporo, Japan. The accurate calibration of the cells (the integral heat transfer coefficients produced by backward integration of the time series) require at the least a constancy of the rates of excess enthalpy generation (better, a zero rate of excess enthalpy generation). It follows that such accurate calibrations can only be derived in appropriate “blank” systems or, else, in systems where the rate of excess enthalpy generation is constant in time. If these required conditions are not met, one needs to rely on the less precise evaluations of the differential lower bound and the less accurate differential true heat transfer coefficient as has been done in the present paper. However, the precision and accuracy of these coefficients is perfectly adequate for the semi-quantitative evaluation of the data sets.

We have noted also that the measurements show all the other features of the investigations with “massive” electrodes to which we have previously drawn attention such as the phenomenon of “Heat -after-Death” (13). It is the existence of this phenomenon which prompts us to believe that energy efficient enthalpy generating systems could be devised based on the development of the electrochemical methodology.

It is appropriate here to comment also on criticisms which have been made recently, (17), on the evaluation of the data sets for experiments on “Cold Fusion”. It is asserted that such evaluations are based on calibrations derived by the statistical methods of regression analysis : such evaluations are deemed to be unsatisfactory in the absence of a proof that changes in the global heat transfer coefficient do not take place. We observe that this criticism does not apply to the observation of the phenomenon of excess enthalpy generation as we do not need to rely on evaluations using regression analysis when making semi-quantitative estimates when these rates are adequately high (as is the case for the Pd-D codeposition system investigated in the present paper). In this case we can simply use the maximum value of the “lower bound” heat transfer coefficient as an estimate of the “true” value and thereby evaluate minimum values of the rates of excess enthalpy generation (e.g. see (13)). It should be noted also that this procedure is quite independent of any method of calibration.

We also make two further observations on these recent criticisms. In the first place, we have never observed changes in the global heat transfer coefficients in experiments on appropriate “blank” systems (2), (11), (18). Secondly, the assertion that excess enthalpy generation can be explained by such changes develops a scenario which cannot be investigated by any simple methodology (the heat transfer coefficients and rates of excess enthalpy generation are parallel

in the parameter space of the instruments)¹ We believe that the onus of proof of invoking changes in the global heat transfer coefficients as explanations of the observation of excess enthalpy generation rests on the authors making suggestions of this kind rather than advancing the hypothesis that the detection of excess enthalpy generation cannot be believed unless it can be proved that there are no changes in these global coefficients.

¹ A separation can be achieved by carrying out calorimetric measurements in the frequency domain which should certainly be part-and-parcel of any future investigative methodology. Such measurements have the additional advantage of giving access to the cross-coupling terms which are undoubtedly present in these systems (c.g. see the effects of “positive feedback”).

Appendix Part III

It has been established that at low to intermediate cell temperatures (say $30^\circ < \theta < 80^\circ$) the behaviour of the calorimeters is modelled adequately by the differential equation

$$\begin{aligned}
 C_p M (d\Delta\theta/dt) &= [E_{\text{cell}}(t) - E_{\text{thermoneutral, bath}}] I & + & Q_f(t) \\
 \text{change in the} & \text{enthalpy input} & & \text{rate of excess} \\
 \text{enthalpy content} & \text{due to} & & \text{enthalpy} \\
 \text{of the calorimeter} & \text{electrolysis} & & \text{generation} \\
 & + \Delta QH(t-t_1) - \Delta QH(t-t_2) - (3I/4F[P/\{P^*-P\}])[C_{p,D_2O,g} - C_{p,D_2O,l}]\Delta\theta + L] \\
 & \text{calibration pulse} & \text{rate of enthalpy removal by the gas stream with} \\
 & & E_{\text{thermoneutral}} \text{ referred to the bath temperature} \\
 & - (k_R^\circ)\theta_{\text{bath}}^3[1-\gamma t] \{f_1(\theta)/\theta_{\text{bath}}^3 + 4\phi\Delta\theta\} & \text{A.1} \\
 \text{time dependent} & \text{effect of} & \text{effect of} \\
 \text{heat transfer} & \text{radiation} & \text{conduction} \\
 \text{coefficient} & &
 \end{aligned}$$

With the calorimeters supplied with the ICARUS Systems, the conductive contribution to heat transfer is very small. This term could therefore be “lumped” into the radiative term by allowing for a small increase in the radiative heat transfer coefficient:

$$\text{Radiative heat transfer} = (k_R')^\circ [1-\gamma t] [(\theta_{\text{bath}} + \Delta\theta)^4 - \theta_{\text{bath}}^4] \quad \text{A.2}$$

The values of the pseudoradiative “heat transfer coefficient, $(k_R')^\circ [1-\gamma t]$, derived are close to those calculated from the Stefan-Boltzmann coefficient and the radiative surface area. If the time dependence of the heat transfer coefficient is not included explicitly in equation (A.2) then

$$\text{Radiative heat transfer} = (k_R') [(\theta_{\text{bath}} + \Delta\theta)^4 - \theta_{\text{bath}}^4] \quad \text{A.3}$$

where the pseudoradiative heat transfer coefficient, (k_R') , now shows a weak time-dependence.

The simplest starting point is to assume that there is no excess enthalpy generation in the calorimeter and to evaluate a corresponding “differential lower bound heat transfer coefficient” at a time just before the end of the calibration pulse, $t = t_2$:

$$(k_R')_1 = [(E_{\text{cell}}(t) - E_{\text{thermoneutral, bath}})I - \Delta H_{\text{evap}}(t) - C_p M (d\Delta\theta/dt) + \Delta QH(t-t_1)]/f_1(\theta) \quad \text{A.4}$$

This was the first heat transfer coefficient used in our investigations, hence the designation $(k_R')_1$. It will be apparent that the differential lower bound heat transfer coefficient $(k_R')_{11}$, may be evaluated at other points of the measurement cycle, by changing the enthalpy input due to the calibration pulse to

$$\Delta QH(t-t_1) - \Delta QH(t-t_2) \quad \text{A.5}$$

It is next necessary to evaluate a “true heat transfer coefficient”. The simplest procedure giving $(k_R')_2$ near the end of the calibration period at $t=t_2$ is obtained by including the calibration pulse

$$(k_R')_2 = \{ \Delta Q + [E_{\text{cell}}(\Delta\theta_2, t_2) - E_{\text{cell}}(\Delta\theta_1, t_2)]I - \Delta H_{\text{evap}}(\Delta\theta_2, t_2) + \Delta H_{\text{evap}}(\Delta\theta_1, t_2) - C_p M [(d\Delta\theta/dt)_{\Delta\theta_2, t_2} - (d\Delta\theta/dt)_{\Delta\theta_1, t_2}] \} / f_2(\theta) \quad \text{A.6}$$

where we now have

$$f_2(\theta) = [\theta_{\text{bath}} + (\Delta\theta_2, t_2)]^4 - [\theta_{\text{bath}} + (\Delta\theta_1, t_2)]^4 \quad \text{A.7}$$

It can be seen that we need to estimate the cell potential, the cell temperature and the differential of this temperature at the time $t=t_2$ which would have been reached in the absence of the calibration pulse [see footnote (A.1)]

Footnote (A.1) This evaluation was carried out in a somewhat different manner in the initial studies (2), (19) (20) in an attempt to avoid the disadvantages of such interpolation procedures. The values of $(k_R')_{11}$ and $(k_R')_2$ obtained were used as starting values for the non-linear regression procedure used at that time (2). As we could not make this procedure “user friendly” with the computing power then available to us and as, more especially, the methodology which we adopted was evidently not understood (21). (for a further example of such misunderstanding see (22)) we adopted the

methodology described in the present paper. This methodology was also the basis of the ICARUS Systems.

As there is a large number of methods of analysing the experimental time-series characterised by their respective heat transfer coefficients, we have designated these coefficients by $(k_R')_{i,j,k}$ where

$i = 1$ denotes differential

$i = 2$ denotes integral with backward integration of the data sets

$i = 3$ denotes integral with forward integration of the data sets

$j = 0$ denotes the whole data set i.e. $0 < t < T$

$j = 5$ denotes the region adjacent to $t = 0$

$j = 6$ denotes the region adjacent to $t = t_1$

$j = 7$ denotes the region adjacent to $t = t_2$

$j = 8$ denotes a combination of $j = 6$ and $j = 7$

$k = 1$ denotes “lower bound”

$k = 2$ denotes “true”

The coefficient $(k_R')_{1,0,1}$ has usually been written as $(k_R')_{11}$

The present paper has been restricted to the use of the differential heat transfer coefficients.

When considering the application of equations A.4 and A.6 to any position in the measurement cycles, it is also convenient to rewrite these equations in the “straight line” forms applicable to the time region $t_1 < t < t_2$

$$\{[E_{\text{cell}}(t) - E_{\text{thermo neutral, bath}}] I - \Delta H_{\text{evap}}(t) + \Delta QH(t-t_1) + Q_{\text{excess}}\} f_1(\theta)$$

$$= (k_R')_{161}^0 \sim [C_p M \frac{d(\Delta\theta)}{dt}] f_1(\theta) \quad \text{A.8}$$

$$\{[E_{\text{cell}}(\Delta\theta_2, t) - E_{\text{cell}}(\Delta\theta_1, t)] I - \Delta H_{\text{evap}}(\Delta\theta_2, t) + \Delta H_{\text{evap}}(\Delta\theta_1, t) + \Delta QH(t-t_1)\} / f_2(\theta)$$

$$= (k_R')^o_{162} + C_p M \left[\left(\frac{d(\Delta\theta_2)}{dt} \right)_t - \left(\frac{d(\Delta\theta_1)}{dt} \right)_t \right] / f_2(\theta) \quad A.9$$

where $\Delta\theta_2$ specifies the observed time series and $\Delta\theta_1$, is the interpolation between the time regions $0 < t < t_1$ and $t_2 < t < \Gamma$. $(k_R')^o_{161}$ and $(k_R')^o_{162}$ are now the intercepts of the plots such as these shown in Figs. 4 and 5 which will be the values of the differential “lower bound” and “true” heat transfer coefficients in the region close to $t = t_2$

REFERENCES

- 1) P.A. Mosier-Boss and S. Szpak, *Nuovo Cimento*, 112A (1999) 577.
- 2) M. Fleischmann, S. Pons M.W. Anderson, L.J. Li and M. Hawkins, *J. Electroanal. Chem.*, 287 (1990) 293
- 3) M.H. Miles, M.A. Imam and M. Fleischmann, "A CALORIMETRIC INVESTIGATION OF THE Pd-B SYSTEM" Paper presented to the Tenth International Conference on Cold Fusion, August 24th-29th, 2003, Cambridge, Massachusetts, U.S.A.
- 4) M.H. Miles, Proceedings of the 8th International Conference on Cold Fusion, Lerici (La Spezia), Italy, May 2000, Conference Proceedings of the Italian Physical Society, Editor: F. Scaramuzzi, 70 (2000) 97, ISBN 88-7794-256-8.
- 5) M.H. Miles, M.A. Imam and M. Fleischmann, Proceedings of the 8th International Conference on Cold Fusion, Lerici (La Spezia), Italy, May 2000, Conference Proceedings of the Italian Physical Society, Editor: F. Scaramuzzi, 70 (2000) 97, ISBN 88-7794-256-8.
- 6) M.H. Miles, M. Fleischmann and M.A. Imam, Report NRL/MR/6320-01-8526 Naval Research Laboratory, Washington, D.C. 20375-5320, U.S.A. (2001).
- 7) S. Szpak and P.A. Mosier-Boss, Editors, Technical Report 1862, SSC San Diego, San Diego, CA 92152-5001, U.S.A. (2002).
- 8) M.H. Miles and M. Fleischmann : "Our Penultimate Paper on the Calorimetry of the Pt-D₂O and Pd-D₂O Systems. Part II : the Pd-B and Pd-B-Ce Systems", submitted for publication.
- 9) ICARUS -2 Isoperibolic Calorimetry Research and Utilities System, Version 2.0 (February 1995), Tehnova Inc., 13th Floor, Fukoku Seimei Building, 2-2-2 Uckaisaiwai-cho, Tokyo 100, Japan.
- 10) M.H. Miles, S. Szpak, P.A. Mosier-Boss and M. Fleischmann, paper submitted for publication.
- 11) M. Fleischmann and M.H. Miles : "THE INSTRUMENT FUNCTION" OF ISOPERIBOLIC CALORIMETERS ; EXCESS ENTHALPY GENERATION DUE TO THE PARASITIC REDUCTION OF OXYGEN. Paper presented to the Tenth International Conference on Cold Fusion, August 24th-29th, 2003, Cambridge, Massachusetts, U.S.A.
- 12) M. Fleischmann, S. Pons, Monique Le Roux and Jeanne Roulette, *Trans. Fusion Technol.*, 26 (1994) 323.
- 13) M. Fleischmann and S. Pons, Proceedings of the 3rd International Conference on Cold Fusion, Nagoya, Japan; Editor : H.I. Ikegami. *Frontiers of Science Series No 4*, Universal Academy Press, Tokyo, (1993) page 47; ISSN 0915-8502.
- 14) M. Fleischmann and S. Pons, *Phys. Lett. A* 176 (1993) 118.

- 15) M. Fleischmann, Proceedings of the 5th International Conference on Cold Fusion, Monte Carlo (1995) page 140.
- 16) The ICARUS Systems : Isoperibolic Calorimetry Research and Utilities System, Version 1 (December 1993), Low Power Measuring System for three Cells, TECHNOVA INC., 13th Floor, Fukoku Seimei Building, 2-2-2 Uchaisaiwai-cho, Chiyoda-Ku, Tokyo 100, Japan.
- 17) K. Shanahan, *Thermochimica Acta*, 387 (2002) 95.
- 18) M.H. Miles and M. Fleischmann, "Our Penultimate Papers on the Isoperibolic Calorimetry of the . . . Pt-D₂O and Pd-D₂O Systems. Part 1 : the Pt-D₂O Blank system". Submitted for publication.
- 19) M. Fleischmann, S. Pons and M. Hawkins, *J. Electroanal. Chem.*, 261 (1989) 301; 263 (1989) 187.
- 20) M. Fleischmann and S. Pons, *J. Electroanal. Chem.*, 332 (1992) 33.
- 21) R.A. Wilson, J.W. Bray, P.G. Kosky, H.B. Vakil and F.G. Will, *J. Electroanal. Chem.*, 332 (1992) 1
- 22) Frederick T. Wagner, Thomas E. Moylen, Michael E. Hayden, Ulrike Narger and James L. Booth, *J. Electroanal. Chem.*, 295 (1990) 393.

Table 1. The lower bound heat transfer coefficient $10^9 (k_R')_{11} / \text{WK}^{-4}$

Time Day elapsed time s	Day 1	Day 2	Day 3	Day 4	Day 5	Day 6	Day 7	Day 8
	$10^9 (k_R')_{11}$ $/\text{WK}^{-4}$	$10^9 (k_R')_{11}$ $/\text{WK}^{-4}$	$10^9 (k_R')_{11}$ $/\text{WK}^{-4}$	$10^9 (k_R')_{11}$ $/\text{WK}^{-4}$	$10^9 (k_R')_{11}$ $/\text{WK}^{-4}$	$10^9 (k_R')_{11}$ $/\text{WK}^{-4}$	$10^9 (k_R')_{11}$ $/\text{WK}^{-4}$	$10^9 (k_R')_{11}$ $/\text{WK}^{-4}$
1800	-1.49344	-0.0858	0.48749	0.3779	0.47856	0.48795	0.47908	0.64577
5100	-0.70979	0.34444	0.51924	0.3769	0.48069	0.66113	0.54971	0.62039
8400	-0.1475	0.42665	0.56842	0.3857	0.47658	0.68499	0.56902	0.59728
11700	0.10495	0.45697	0.60763	0.38513	0.49595	0.69593	0.57723	0.59217
15000	0.7183	0.4719	0.6177	0.40059	0.50665	0.70689	0.58014	0.60469
18300	0.36411	0.4878	0.59164	0.397	0.50006	0.71081	0.58526	0.60626
21600	0.28528	0.48922	0.5781	0.40712	0.50202	0.7105	0.59038	0.61095
24900	0.30856	0.48677	0.55356	0.40022	0.50282	0.71544	0.59203	0.61694
28200	0.26101	0.48041	0.51248	0.39695	0.51479	0.70512	0.59315	0.62725
31500	0.24967	0.50864	0.47774	0.41212	0.50517	0.72403	0.59709	0.63011
34800	0.2712	0.50441	0.43012	0.41215	0.51357	0.74247	0.61318	0.6435
38100	0.26742	0.49508	0.41646	0.41505	0.51741	0.7326	0.62329	0.64007
41400	0.26761	0.50243	0.39305	0.40257	0.49585	0.72861	0.62832	0.61976
44700	0.247	0.46767	0.38561	0.41191	0.53356	0.70235	0.63007	0.61181
48000	0.26664	0.46198	0.38465	0.40935	0.51358	0.67093	0.63268	0.61681
51300	0.26633	0.44048	0.37473	0.43111	0.5147	0.66371	0.63223	0.60868
54600	0.2753	0.42352	0.3573	0.46939	0.51523	0.63598	0.62664	0.60996
57900	0.27652	0.413	0.3722	0.44984	0.5181	0.57951	0.61373	0.60061
61200	0.26939	0.40534	0.37129	0.44095	0.51988	0.56039	0.60734	0.5925
64500	0.26886	0.42088	0.37269	0.45733	0.53518	0.54096	0.59936	0.59693
67800	0.25866	0.39459	0.38083	0.47008	0.52991	0.54166	0.59795	0.60128
71100	0.26025	0.39528	0.37277	0.45343	0.53734	0.53409	0.59504	0.60751
74400	0.2728	0.38396	0.37248	0.46642	0.54202	0.5271	0.596	0.61177
77700	0.2796	0.39671	0.36822	0.48096	0.52483	0.53565	0.59509	0.61503
81000	0.28216	0.45576	0.37228	0.46812	0.53008	0.51625	0.59824	0.61224
84300	0.27082	0.54783	0.37474	0.47155	0.51503	0.52769	0.59676	0.60391

Table 2

	day 1					day 2					day 3					day 4			
Time day	I/Amp	$10^9(k_R')_{12}$	Q excess	Q excess	I/Amp	$10^9(k_R')_{12}$	Q excess	Q excess	I/Amp	$10^9(k_R')_{12}$	Q excess	Q excess	I/Amp	$10^9(k_R')_{12}$	Q excess	Q excess	I/Amp	$10^9(k_R')_{12}$	
elapsed		/WK ⁻⁴	$10^9(k_R')_{12}$	$10^9(k_R')_{12}$		/WK ⁻⁴	$10^9(k_R')_{12}$	$10^9(k_R')_{12}$		/WK ⁻⁴	$10^9(k_R')_{12}$	$10^9(k_R')_{12}$		/WK ⁻⁴	$10^9(k_R')_{12}$	$10^9(k_R')_{12}$		/WK ⁻⁴	
time/sec		recomb	0.69986	0.85065		recomb	0.69986	0.85065		recomb	0.69986	0.85065		recomb	0.69986	0.85065		recomb	
day 1																			
1800	↑ 0.00632	1.86993	0.01074	0.01149	↑ 0.1	1.33311	0.0863	0.1055	↑ 0.201 ↓ 0.05 ↓ 0.02	1.45751	0.06863	0.11746	↑ 0.02	0.93537					
5100		0.1141	0.01663	0.0185		0.9527	0.08956	0.12762		1.22418	0.07987	0.14797		0.92426					
8400		0.35531	0.01631	0.01923		0.88615	0.0915	0.1416		1.1297	0.07191	0.15503		0.94446					
10800										1.09292	0.066	0.15864							
11700		0.55773	0.01366	0.01713		0.86181	0.09219	0.14945						0.93926					
12900										0.76982	0.03566	0.12366							
15000		1.20315	0.00065	0.00372		0.85094	0.09222	0.1533		0.78795	0.03703	0.10555		0.95505					
18300		0.99111	0.00486	0.00704		0.8548	0.08862	0.15165		0.83058	0.03455	0.08296		0.95202					
21600		0.9512	0.00597	0.00813		0.85044	0.08946	0.15351		0.79961	0.02499	0.06095		0.96339					
24900		0.99413	0.00552	0.00767		0.84515	0.09121	0.15575		0.73352	0.02422	0.04917		0.95457					
28200	0.9359	0.00635	0.00854	0.83319	0.09182	0.15739	0.76005	0.02217	0.04025	0.94964									
31500	0.91152	0.00662	0.00883	0.8533	0.08337	0.14911	0.79574	0.02059	0.03462	0.96275									
34800	0.92503	0.00632	0.00862	0.8635	0.08487	0.15031	0.80718	0.02113	0.03248	0.96444									
38100	0.91559	0.0063	0.00857	0.84726	0.08866	0.15394	0.84704	0.01942	0.02975	0.9678									
41400	0.90316	0.00649	0.00877	0.86424	0.08458	0.14852	0.86655	0.01947	0.02887	0.95281									
44700	0.87782	0.00697	0.00929	0.8539	0.09202	0.15194	0.88806	0.01844	0.02729	0.95688									
48000	0.88766	0.00675	0.0091	0.88205	0.08682	0.1419	0.91102	0.01766	0.0261	0.94973									
51300	0.8934	0.00672	0.00899	0.89031	0.08486	0.13628	0.91647	0.0177	0.0259	0.97419									
54600	0.89035	0.00657	0.00896	0.89654	0.08996	0.13846	0.90987	0.01834	0.02639	0.99735									
57900	0.88824	0.00674	0.00913	0.90443	0.0895	0.13656	0.92378	0.01751	0.02557	1.00285									
61200	0.88534	0.00691	0.00929	0.91171	0.08918	0.13482	0.92976	0.01734	0.02529	0.99615									
64500	0.90073	0.00646	0.00885	0.94415	0.08173	0.12592	0.93355	0.0172	0.02512	1.01491									
67800	0.86425	0.00715	0.00957	0.9287	0.08764	0.13092	0.94378	0.01664	0.0245	1.03273									
71100	0.87189	0.00691	0.00927	0.93581	0.0864	0.12917	0.9385	0.01704	0.02489	1.02014									
74400	0.87246	0.00693	0.00937	0.92988	0.09055	0.13305	0.93728	0.01696	0.02487	1.03398									
77700	0.88269	0.00674	0.00918	0.94329	0.08642	0.1287	0.92898	0.01742	0.02534	1.05093									
81000	0.89624	0.00661	0.009	1.01495	0.06713	0.10848	0.93572	0.0172	0.02512	1.04204									
84300	0.87444	0.00691	0.00934	1.15002	0.03793	0.0764	0.93039	0.01724	0.02523	1.04129									

day 5			day 6			day 7			day 8		
Q excess $10^9(k_R')_{12}$	Q excess $10^9(k_R')_{12}$	I/Amp	$10^9(k_R')_{12}$ / WK ⁻⁴	Q excess $10^9(k_R')_{12}$	Q excess $10^9(k_R')_{12}$	I/Amp	Q excess $10^9(k_R')_{12}$	Q excess $10^9(k_R')_{12}$	I/Amp	Q excess $10^9(k_R')_{12}$	Q excess $10^9(k_R')_{12}$
0.69986	0.85065		recomb	0.69986	0.85065		0.69986	0.85065		0.69986	0.85065
0.01721	0.02519	↑	1.03015	0.01153	0.01939	↑	0.04165	0.04552	↑	0.12251	0.20892
0.01715	0.02514		1.05208	0.01106	0.01891		0.01939	0.04651		0.1187	0.2387
0.01673	0.02476		1.04119	0.01169	0.01958		0.01051	0.05062		0.11751	0.25376
0.01675	0.02477	↑	1.05911	0.01062	0.01848	↑	0.00483	0.05116	↑	0.11752	0.26196
0.0159	0.02392		1.07303	0.01001	0.01732		-0.00227	0.04665		0.11974	0.27053
0.01618	0.02419		1.0809	0.0104	0.0182		-0.00159	0.04797		0.11751	0.27213
0.01559	0.02357	↑	1.0759	0.01016	0.01791	↑	-0.00472	0.04643	↑	0.1131	0.26888
0.01593	0.02396		1.06786	0.01029	0.01816		-0.00462	0.04417		0.11123	0.26676
0.01617	0.02421		1.079	0.00972	0.01763		-0.0011	0.04637		0.1095	0.26423
0.01542	0.02349	↑	1.07202	0.01013	0.01797	↑	-0.00181	0.04042	↑	0.10684	0.26194
0.01533	0.02338		1.08265	0.00966	0.01747		-0.00316	0.04714		0.0971	0.26913
0.01519	0.02323		1.08446	0.00949	0.01733		-0.00782	0.05977		0.09247	0.27674
0.01594	0.02402	↑	1.06653	0.01058	0.01839	↑	-0.01095	0.06732	↑	0.09037	0.28131
0.01557	0.02373		1.10138	0.00864	0.01647		0.00295	0.08619		0.08975	0.28369
0.01585	0.02408		1.08704	0.00959	0.01734		0.02258	0.10967		0.08701	0.28233
0.01459	0.02278	↑	1.08913	0.00951	0.01725	↑	0.02688	0.11907	↑	0.08745	0.28324
0.01342	0.02156		1.08864	0.0095	0.01725		0.02742	0.12875		0.09149	0.28013
0.01336	0.0214		1.09814	0.00925	0.01691		0.05282	0.13647		0.09713	0.26179
0.01421	0.02222	↑	1.0962	0.00921	0.01693	↑	0.05937	0.13059	↑	0.09805	0.25513
0.01283	0.0208		1.11369	0.00843	0.01615		0.06574	0.13095		0.10368	0.25827
0.01204	0.01994		1.10959	0.00865	0.01632		0.06974	0.12444		0.10402	0.25607
0.01289	0.02076	↑	1.11949	0.00821	0.01583	↑	0.0739	0.12682	↑	0.10483	0.25565
0.01213	0.01996		1.13364	0.00787	0.01538		0.068	0.12741		0.10333	0.24425
0.01132	0.01913		1.10956	0.00871	0.01631		0.06519	0.12351		0.10493	0.25465
0.01202	0.01984	↑	1.11469	0.00862	0.01624	↑	0.07105	0.13027	↑	0.10041	0.24927
0.01182	0.01962		1.10928	0.01068	0.01828		0.065	0.12151		0.10205	0.2513

Fig.1 The variation of the rate of the specific excess enthalpy generation with current density

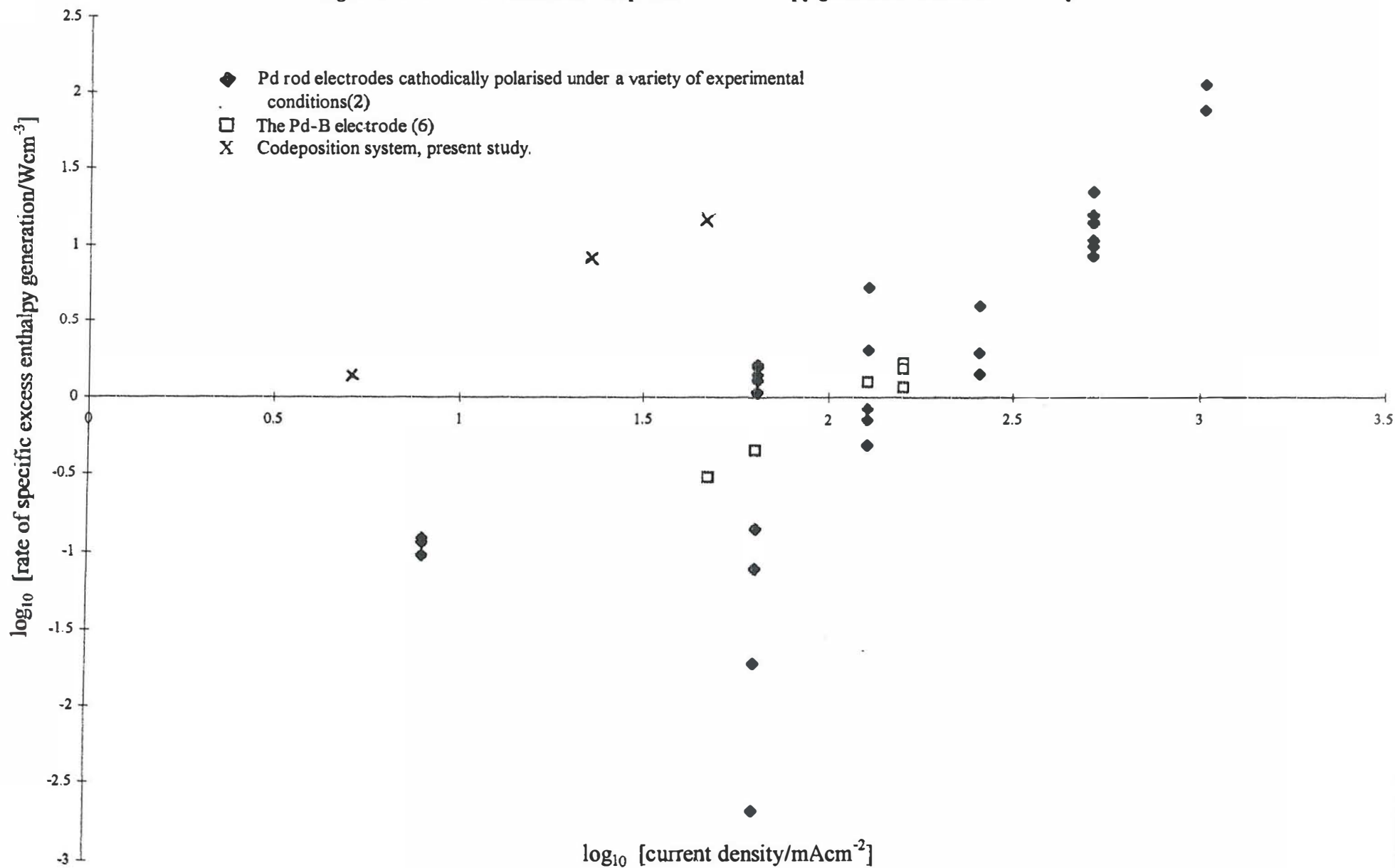


Fig.2 The lower bound heat transfer coefficient $10^9(k_R')_{11} / \text{WK}^{-4}$

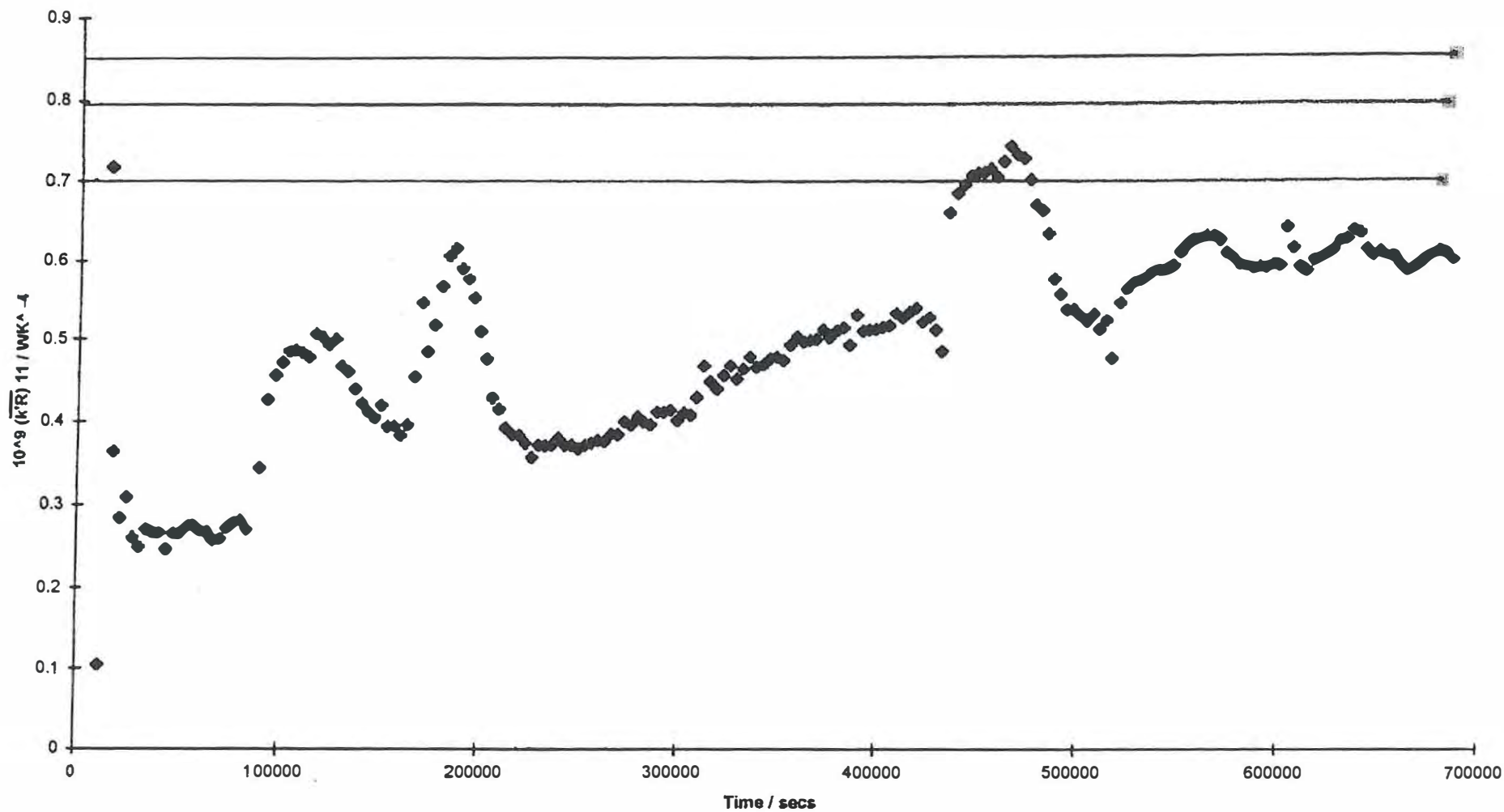


Fig.3 The lower bound heat transfer coefficient $10^9(k_R')_{11} / WK^{-4}$ for Day 6 of the experiment.

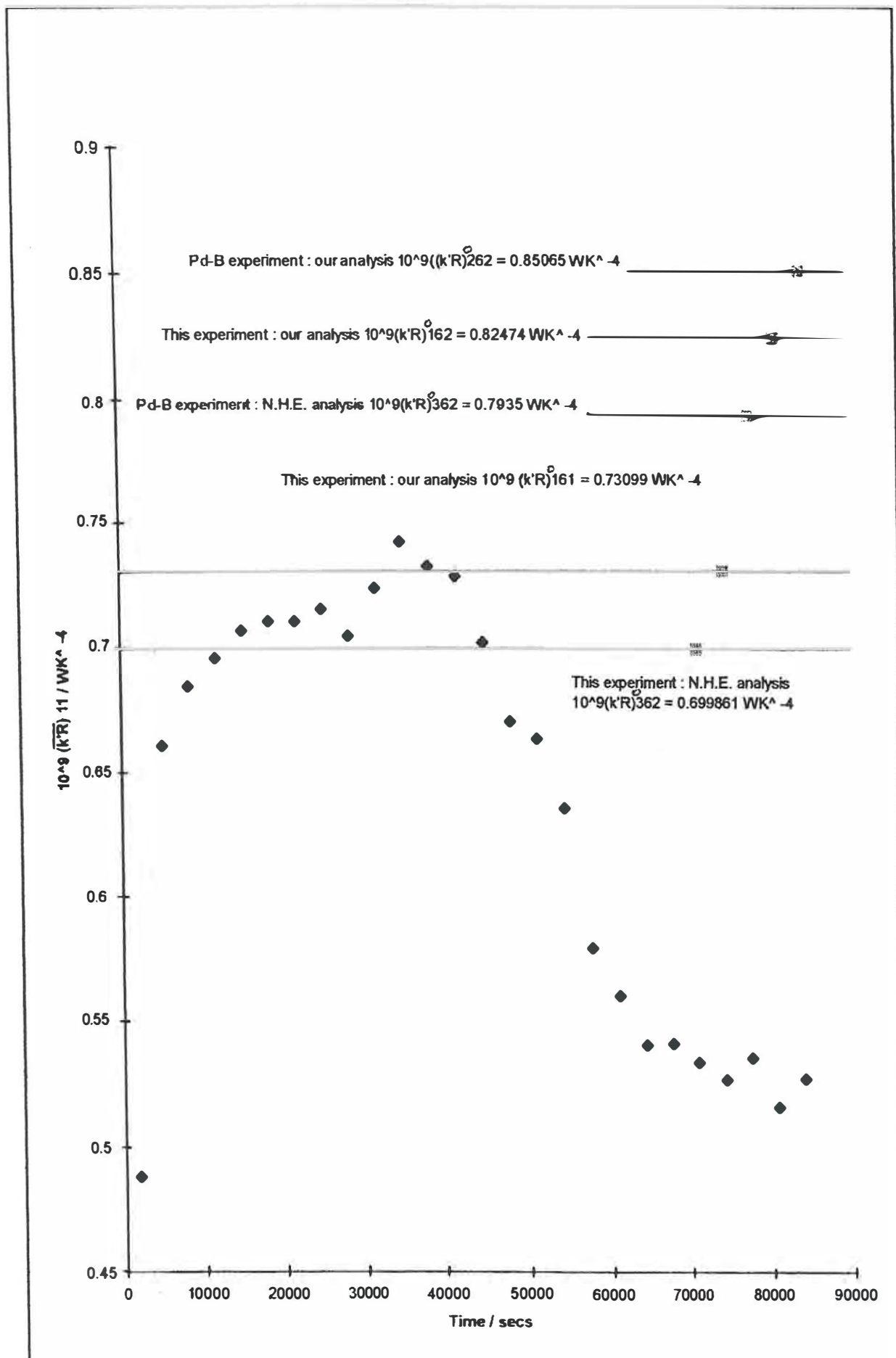


Fig.4 The determination of $10^9(k_R')^0_{161}$ on Day 6.

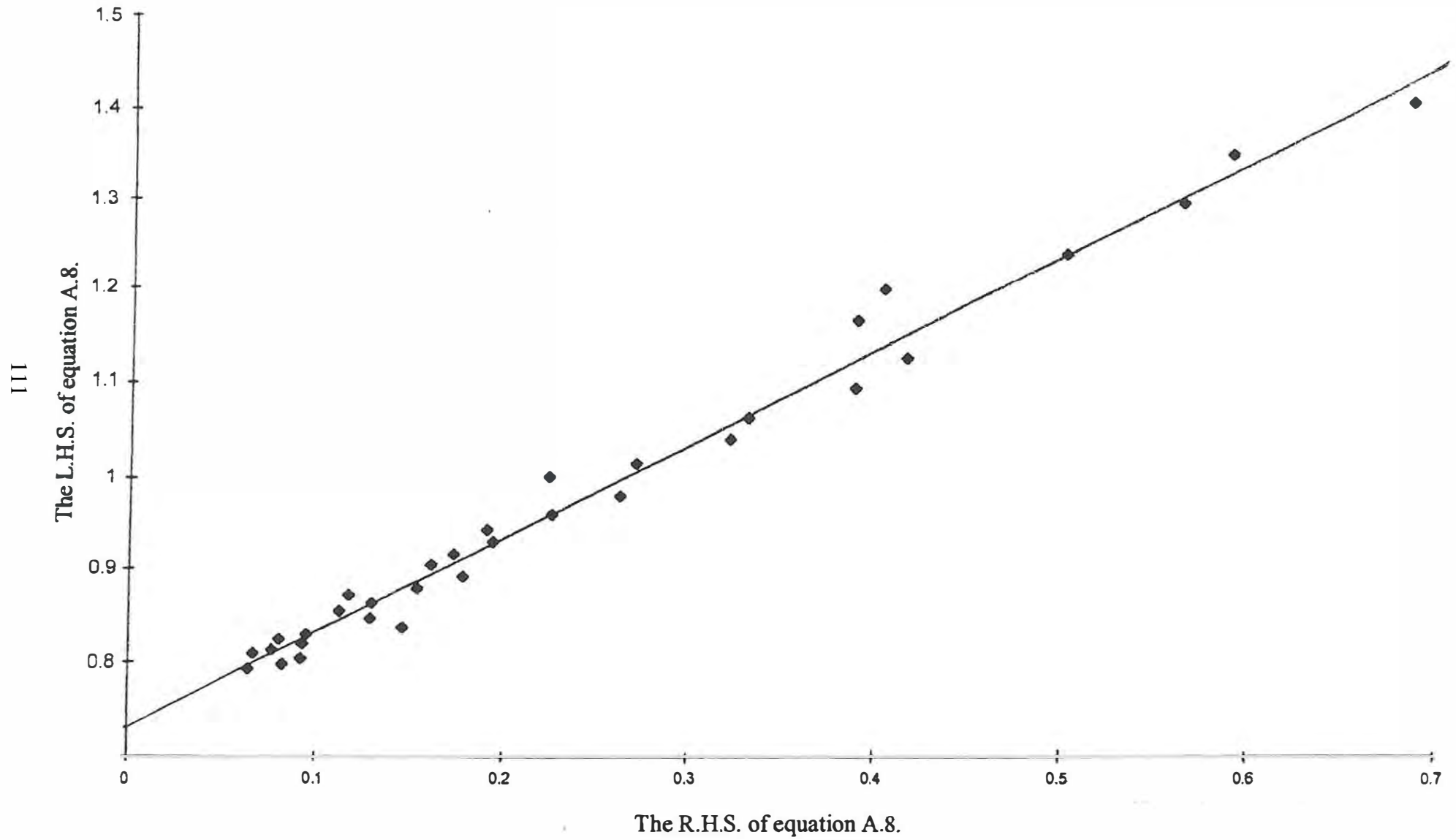


Fig.5 The determination of $10^9(k_R')_{162}^\circ$ on Day 6.

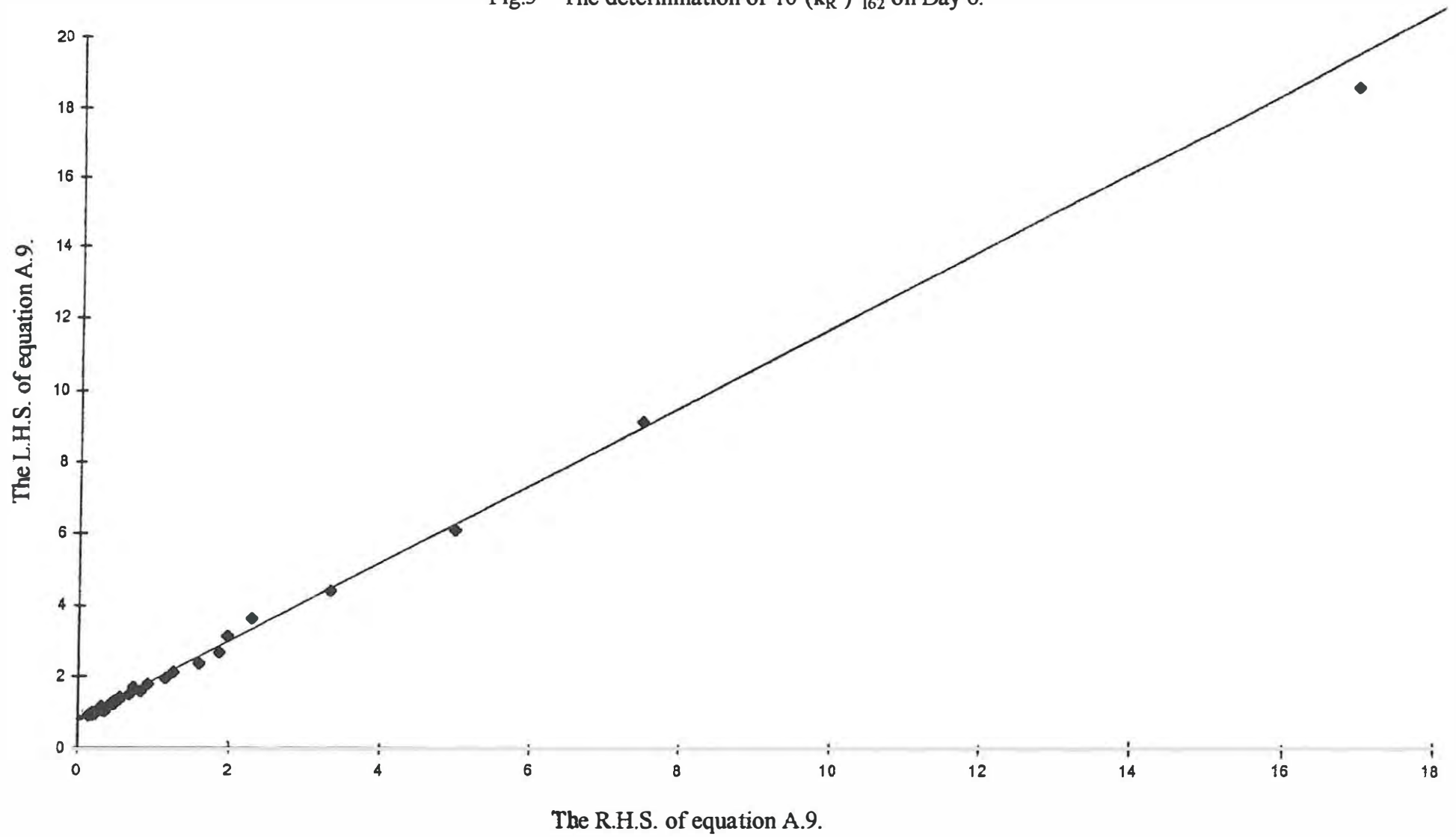


Fig.6 The rates of excess enthalpy generation

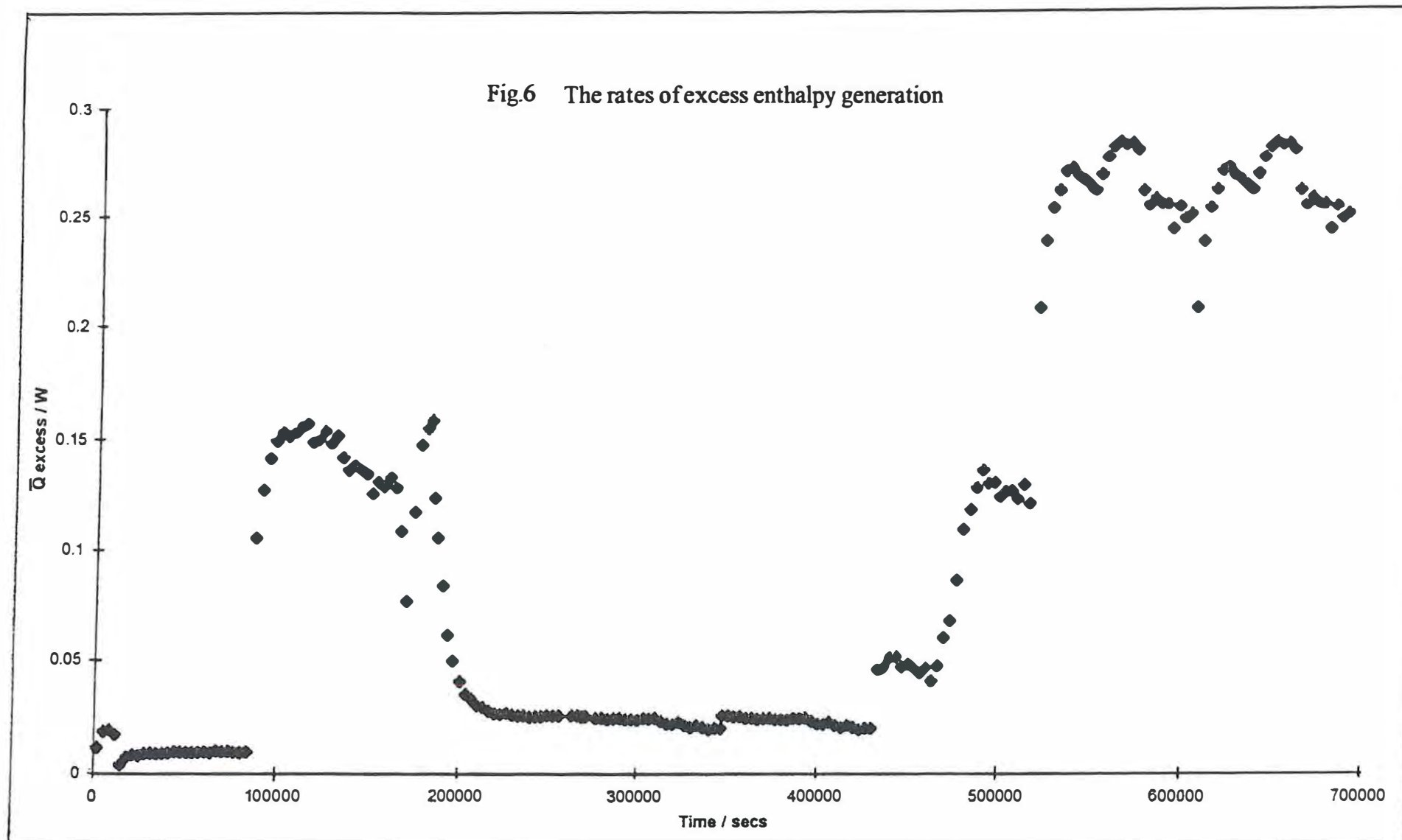


Fig.7 The effect of the complete reduction of electrogenerated oxygen on the lower bound heat transfer coefficient.

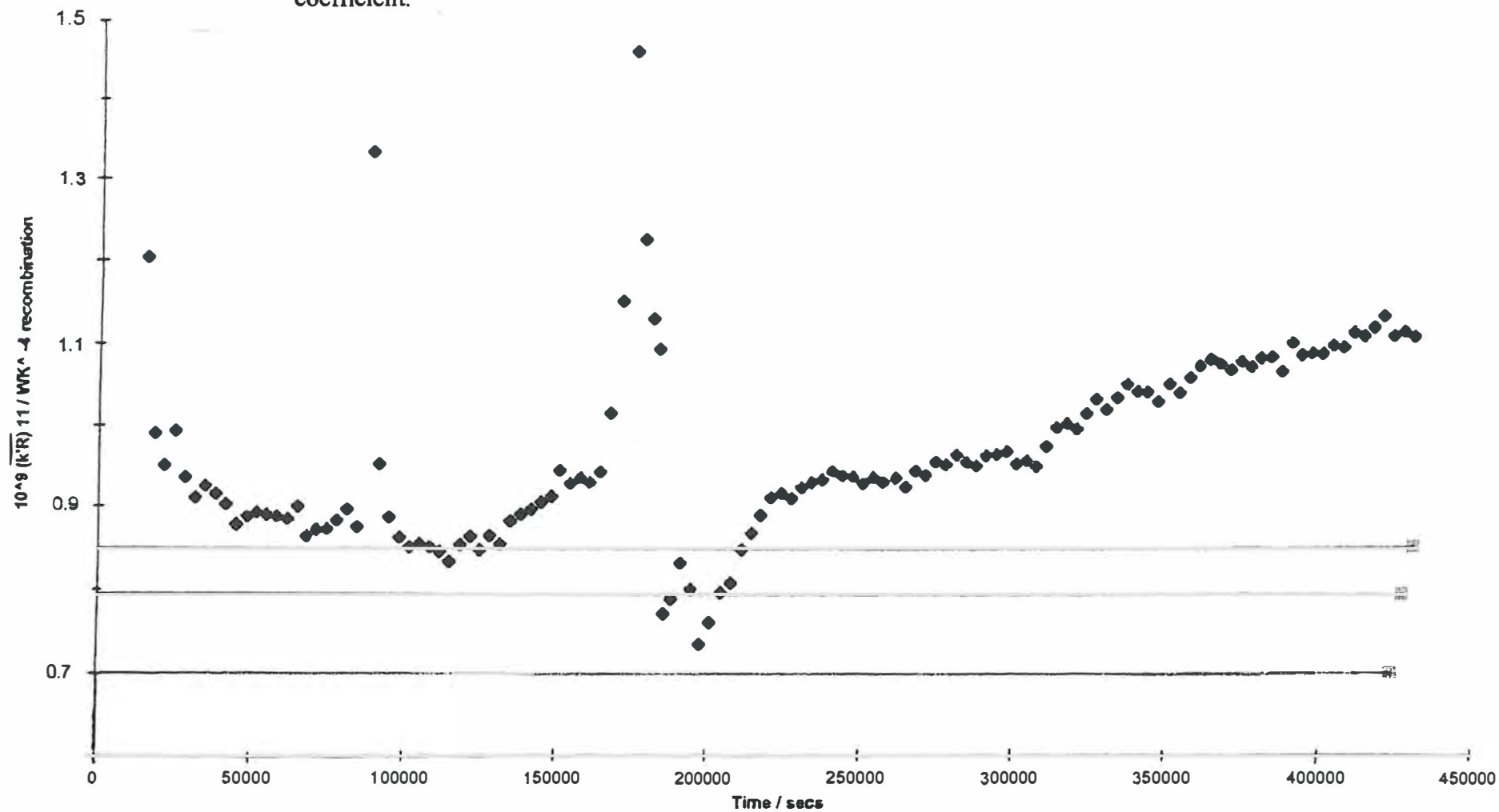


Fig.8 The schedule of cell currents used in the experiment.

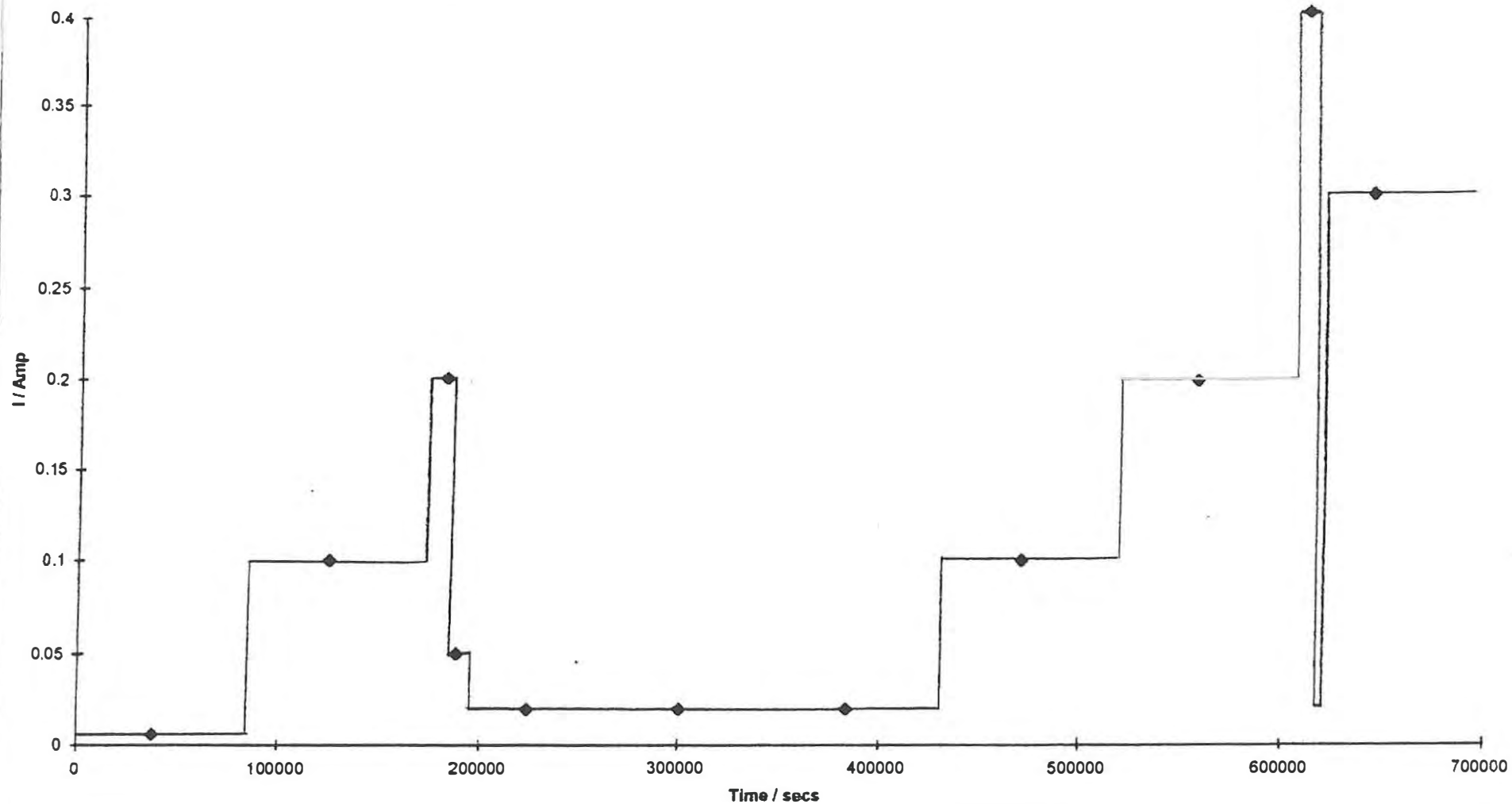
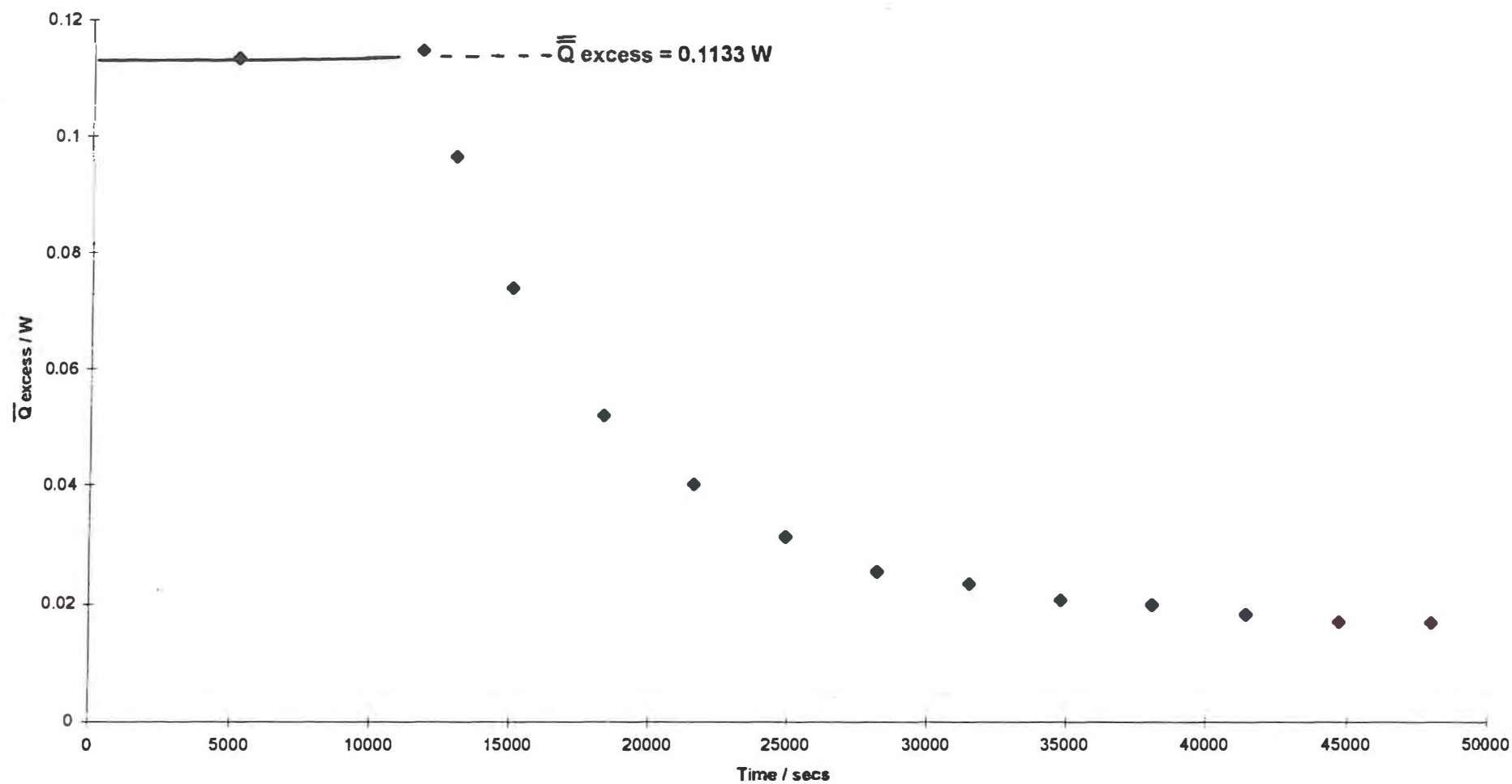


Fig.9 The rate of excess enthalpy generation in the region of the transition from Day 2 to Day 3.



Our Penultimate Papers on the Isoperibolic Calorimetry of the Pt/D₂O and Pd/ D₂O Systems.

Part IV: An Experiment with a Pd-Cathode in 0.1M LiOD/ D₂O carried out in 1989.

M. Fleischmann, Bury Lodge, Duck Street, Tisbury, Salisbury, Wilts., SP3 6LJ, U.K.

M.H. Miles, Department of Chemistry, University of La Verne, La Verne, CA 91750, U.S.A.

Abstract

Using the preliminary methods of data analysis later incorporated into the ICARUS -1 and ICARUS -2 Systems (1), (2), we show that the rate of excess enthalpy production achieved with a 0.1 cm diameter x 10cm length cathode reached a specific generation of at least 9.5 Wcm^{-3} for a polarisation at a current density of 0.253 Acm^{-2} carried out in 0.1M LiOD/D₂O. The experiment with this electrode had a special importance in the lack of development of the topic known as “Cold Fusion”.

Introduction

The results obtained in 1989 for electrodes such as the 0.1 cm diameter x 10 cm length electrode used in this study (which have been previously briefly discussed in the literature (3)) are presented as a further illustration of the answer to the question : “why were we so certain that there is excess enthalpy generation during the cathodic polarisation of Pd -based electrodes as compared to the lack of any such excess enthalpy generation for the Pt -blank system ? ” (see also (4), (5), (6)).

Experimental

The polarisations were carried out in a Dewar-type single compartment cell of the type illustrated in Fig. 1 A. The characteristics of this cell are discussed in this paper. The other experimental details were identical to those described in the first full report (3).

The polarisations fell into two parts : an initial sequence of measurements using a cell current of 0.2 A in the time interval $117,154 < t < 1,587,319$ s followed by a period $1,587,319 < t < 1,718,846$ s on open circuit. This was followed in turn by a second short polarisation $1,718,846 < t < 1,949,250$ s again at a cell current of 0.2 A succeeded by a sequence of measurement cycles during $1,949,250 < t < 3,156,970$ s carried out at a cell current of 0.4 A. The cell current was again reduced to 0.2 A during $3,156,970 < t < 3,162,369$ s and then increased to 0.8 A during $3,162,369 < t < 4,999,795$ s at which time the experiment was terminated (this second period included a short section during $4,012,195 < t < 4,029,337$ s when the cell was again on open circuit).

Results and Data Evaluation.

The Initial Consideration of the Data.

We quote first of all from a preceding paper (7):

“In the development of any new area of research (and especially in one likely to arouse controversy !) it is desirable to achieve first of all a qualitative demonstration of the phenomena involved in the explanation of the observations. It is the qualitative demonstrations which are unambiguous: the quantitative analysis of the experimental results can be the subject of debate but, if these quantitative analyses stand in opposition to the qualitative demonstration, then these methods of analysis must be judged to be incorrect.”

Fig. 2 is an illustration of this approach (8). We need to ask; how can we explain an increase of cell temperature with a decrease of the input enthalpy without invoking the presence of excess enthalpy generation ? A further illustration of this behaviour has been given in (7) and, indeed, the first full publication on this topic (3) also contained related illustrations¹

¹ These publications did not lead to any discussion of this aspect and none of the many critics of “Cold Fusion” could be drawn into any attempt to explain the behaviour of increases of cell temperature with decreases of enthalpy input in the absence of excess enthalpy generation. We therefore ask interested readers (and especially the many critics of “Cold Fusion”) to send us descriptions of their interpretations. Please send any replies to M.H.M.

Figs. 3A and B illustrate related but somewhat more complicated observations based on the present investigation. Thus Fig. 3A gives an extract of the temperature -time series for the polarisations carried out at cell currents of 0.4 and 0.8 A. To start the interpretation, let us assume that there is no generation of excess enthalpy at the lower cell current so that we can derive the mean heat transfer coefficients listed in the figure. The value $10^9(k_R')_{11} = 1.2768 \text{ WK}^{-4}$ based on the interpretation of purely radiative heat transfer is much larger than the value $10^9(k_R')_{11} = 0.57 \text{ WK}^{-4}$ which can be calculated from the Stefan-Boltzmann coefficient and the radiative surface area of the cell used, Fig. 1A, (for definitions of the heat transfer coefficients, see Appendix A). It follows that there is an appreciable conductive contribution which we attributed principally to conduction across the nominal vacuum gap (due to inadequate evacuation / baking out of the Dewar cell). Interpretation of the temperature-time series in terms of a purely conductive heat transfer gives $(k_C')_{11} = 0.14727 \text{ WK}^{-1}$. These two values of the heat transfer coefficient give the extrema of the possible behaviour. Interpretation in terms of a combination of radiative and conductive heat transfer gives the thermal output as $(0.57 \times 10^{-9} f_1(\theta) + 0.08989 \Delta\theta)W$ where we assume that the radiative component is given by the Stefan-Boltzmann value (compare (9), (10))². If we now assume that the same values of the heat transfer coefficient apply to the measurements carried out at the cell current of 0.8 A, we obtain the behaviour shown in Fig. 3B. Alternatively, we can assume that there is again no generation of excess enthalpy at this higher cell current which gives the lower bound heat transfer coefficients listed in the lower part of Fig. 3A. We can see a marked reduction in the values of the coefficients as compared to the values observed at a cell current of 0.4 A which we attributed to an increase in the rate of excess enthalpy generation.³

It has frequently been asserted that the observation of excess enthalpy generation is some artefact of the methods of calibration of the calorimeters, especially of the regression procedures which we have used in some parts of our investigations (e.g. see the most recent comments in (11)). It can be seen, however, that the interpretation we have given in this section is simply based on the evaluation of enthalpy balances with the additional supposition that the rate of excess enthalpy generation varies with the cell current. This is equally true for the evaluation of the lower bound, $(k_R')_1$ and true, $(k_R')_2$, heat transfer coefficients described below.

² These calculations have to be carried out iteratively. As the process is poorly convergent (requiring ~60 iterations to ensure convergence in the third decimal place), it is necessary to take special steps to speed the convergence.

³ As for the comments made in Footnote 1, we ask interested readers (and especially the many critics of "Cold Fusion") to send us descriptions of their interpretations which avoid invoking of any excess enthalpy generation. Please send any comments to M.H.M.

The Further Evaluation of the Data.

The first step is to test whether equation (A.1) correctly models the behaviour of the calorimeter. Figs. 4A and B give sections of the “raw data” for the initial stages of the application of the two cell currents, 0.4 and 0.8 A. Figs. 5A and B give tests of equations (A.8) and (A.9) for the initial stages of the application of 0.4 A, Fig. 4A, where heat transfer has been assumed to be given by the purely radiative term, equation (A.2).⁴ It is evident that equation (A.1) does indeed model the calorimeter correctly. However, as we have noted above, the derived heat transfer coefficients exceed the values which one can calculate from the Stefan-Boltzmann coefficient and the radiant surface area ($10^9(k_R')^0_{161} \simeq 0.57 \text{ WK}^{-4}$). The evaluations presented here have, nevertheless, been based on the pseudo-radiative representation of heat transfer as the accuracy of the data is insufficient to allow a reliable separate evaluation of the radiative and conductive contributions to the heat transfer coefficient⁵

It can be seen that the true heat transfer coefficient, $(k_R')^0_{162}$, calculated in this way (see Fig. 5B and the first entry in Table 1) is reasonably close to the value which has been calculated from the experimental $\theta - t$ series assuming zero generation of excess enthalpy (the second entry in Table 1). However, the fact that $(k_R')^0_{162} > (k_R')^0_{161}$ (see Figs 5A and 5B and the first entry in Table 1) shows that there is some generation of excess enthalpy even at the lower cell current (see further below).

The application of the same methodology to the change of cell current 0.2 \rightarrow 0.8 A on Days 36 \rightarrow 37 (see Figs. 6A and 6B and the seventh entry in Table 1) shows that $(k_R')^0_{161}$ is now reduced which we attribute to the onset of more marked excess enthalpy generation at the higher cell current. This is associated with the onset of “positive feedback” (see the discussion of the calibrations on Day 22 below) and it is not surprising, therefore, that the evaluation of $(k_R')^0_{162}$ fails (see the seventh entry on Table 1)⁶ The marked reduction of $(k_R')^0_{162}$ is caused by the anomalously high increase in the cell temperature due to the presence of “positive feedback”.

A more generally useful method of calibrating the calorimeters relies on the injection of Joule heat using the resistive heater, Fig. 1. In this particular experiment, there were five days on which such

⁴ The analyses given in this paper have been confined to evaluations based on the differential heat transfer coefficients as this was the methodology which we used in 1988/89 (together with the fitting of equation (A.1) to the data sets using non-linear regression). However, as we have shown elsewhere (e.g. (4) and references cited therein) an higher precision and accuracy is achieved when the evaluation is based on the integral heat transfer coefficients based on the backward integration of the data sets.

⁵ We note also that evaluations carried out in 1988/89 always either included the relevant calibration in the data sets or were based on calibrations carried out above the temperature at which the data were evaluated. This second procedure leads to an underestimate of any excess enthalpy term.

⁶ It is not possible for the true heat transfer coefficient to be less than the lower bound value because this would require the cell to function as a spontaneous refrigerator i.e. to violate the Second Law of Thermodynamics. The endothermicity of the cell reaction has already been taken into account by the use of the thermoneutral potential.

calibrations were carried out (Days 22 and 35 at the cell current of 0.4A and Days 40, 46 and 55 at 0.8 A; see the entries 3,5,8,9 and 10 in Table 1); Fig. 7 illustrates this particular method of calibration. We can see that this method gives two values of the lower bound heat transfer coefficient, the first using the interpolated values of the cell temperature and potential in the hypothetical absence of the calibration pulse (entries 3B, 5B, 8B, 9B and 10B in Table 1) and the second using the observed values (entries 3A, 5A, 8A, 9A and 10A in the Table). We can see that the values given in the entries 3B and 5B are unchanged from that which applies to the start-up of the experiment (entries 1 and 2). We conclude that the rate of excess enthalpy generation is unchanged throughout the experiment duration at the cell current of 0.4 A. However, a low level of excess enthalpy generation is shown by the reduction of the lower bound heat transfer coefficient compared to the true value (see further below).

The situation is completely different, however, if we consider the cell temperatures and potentials observed for the application of the calibration pulse, entries 3A and 8A, Table 1. We note that in the initial stages of the application of the 0.4 A cell current, i.e. Day 22 entry 3A in Table 1, we observe a marked lowering of the lower bound heat transfer coefficient which must be due to an increase in the rate of excess enthalpy generation induced by the calibration pulse. Observations of this kind were, in fact, the first evidence for the presence of “positive feedback” which was later discussed in e.g. (12), (13), (14). In view of the presence of this phenomenon, we can also observe marked reductions in the calculated values of the true heat transfer coefficient - an entirely spurious effect.

Further Evaluations

The evaluation of the specific rate of excess enthalpy generation e.g. using

$$\text{specific rate} = [(k_R')_{12} - (k_R')_{11}] \frac{f_1(\theta)}{V} \quad (1)$$

(where V is the volume of the electrode) requires us to be certain as to the correct values of the true and lower bound heat transfer coefficients. This question of the correct value of $(k_R')_{12}$ was addressed in the first phase of our investigations by carrying out extensive series of calibrations at low cell currents illustrated in Fig. 8 by a calibration carried out after the restart of the experiment at $t = 1,718,846$ s; the values of the heat transfer coefficients are given in Table 2 for Day 20. However, it became apparent that there was a malfunction of the experiment during the initial polarisations in $0 < t < 1,718,846$ s. This is

illustrated in Fig. 9 by the variation of the lower bound heat transfer coefficient during day 1 of the experiment: some of the points shown could be judged to be affected by the malfunction of the instrumentation. Nevertheless, we can see that $(k_R')_{11}$ is initially low (even negative !) due to the excess enthalpy generation caused by the absorption of deuterium. The lower bound heat transfer coefficient then rises at about the diffusional relaxation time reaching a value of $\sim 1.32 \text{ WK}^{-4}$ before showing a slow decrease with time. If we assume that there is only a low level of excess enthalpy generation in the initial stages of the experiment, we can conclude that the maximum value of the lower bound heat transfer coefficient is approximately equal to the true heat transfer coefficient as shown for Day 1 in Table 2⁷

A re-examination of this data set has shown, however, that the malfunction of the instrument was confined to the period $0 < t < 483,329 \text{ s}$. It is therefore possible to evaluate the calibrations carried out between Day 5 $< t < \text{Day 17}$ and the results are given in Table 2. The results given in this Table together with those in Table 1 lead us to conclude that the true heat transfer coefficient is of order 1.32 WK^{-4} .

We can also see from Table 1 that marked excess enthalpy production is confined to the polarisation at a cell current of 0.8 A. (see also Fig. 3B)⁸. The estimation of the specific rates clearly requires the evaluation of $(k_R')_{11}$ for this period of the experiment. Unfortunately, there were only three calibrations in the relevant period (see Table 1). However, the fact that equation (A.1) evidently models the system correctly indicates that we can also use the perturbations due to the additions of D_2O (to make up for losses due to electrolysis and evaporation) to derive values of $(k_R')_{151}^0$. The evaluation is illustrated in Fig. 10 and it can be seen that we can derive satisfactory values of $(k_R')_{151}^0$ as well as of $C_p M$. The values obtained are listed in Table 3 and the mean of these values is given as the eleventh entry in Table 1. We conclude that the lower bound heat transfer coefficient was of the order $10^9 (k_R')_1^0 = 1.1703 \text{ WK}^{-4}$.

Unfortunately, it is not possible to apply the same method to the measurements at 0.4A as the amplitude of the signals is too small to allow separate evaluations following each addition of D_2O . However, signal averaging over all the additions for Days 20 - 36 gives the analysis shown in Fig. 11 and the value of the lower bound heat transfer coefficient given as the sixth entry in Table 1. This value is in line with all the other determinations given in this Table for measurements at the lower cell current and justifies the conclusion that excess enthalpy generation can only be at a very low level under these conditions.

We note again (compare (15)) that is not possible to develop this method to allow the determination of the true heat transfer coefficient.

⁷ This hypothesis was used later as a method of calibrating the calorimeters (12).

⁸ We concluded in 1989 that excess enthalpy production required a threshold current density lying in the range $50 - 100 \text{ mA cm}^{-2}$.

The Rates of Excess Enthalpy Generation.

Substitution of the values of the true and lower bound heat transfer coefficients and of the relevant value of $f_1(\theta)$ in equation (1) gives a specific excess rate of $\sim 9.5 \text{ Wcm}^{-3}$ which corresponds to $\sim 22\%$ of the enthalpy input under these conditions. The specific excess rate is compared in Fig. 12 with the values which have been previously reported for measurements under comparable conditions (3). The degree of agreement is perhaps not surprising although we note that the evaluations in the earlier study were carried out by non-linear regression fitting for complete measurement cycles.⁹

Inclusion of the enthalpy content of the evolved gases (which could be recovered by combustion) gives an energy efficiency of $\sim 85\%$ which approaches the breakeven value. It became evident that it would be possible to exceed this value by suitable redesign of the cells (the original design was not energy efficient) coupled to an increase of the electrolyte concentration and the use of larger diameter electrodes.

We also note that the mean heat transfer coefficients listed in Table 2 show that the generation of excess enthalpy was $\approx 16 \text{ mJ}$ at the cell current of 0.2 A . We believe that excess enthalpies of this order are due to the reduction of electrogenerated oxygen on the surface area of the cathode. The predicted value of this term for a 4 - electron reduction of O_2 is $\approx 24 \text{ mJ}$. The more exact evaluation of this term (for the use of a Pt-cathode) is discussed in (4).

Discussion

The work carried out in the summer of 1989 led to a reassessment of the experiment design and of the experimental protocols. The points covered included those listed in Appendix B. Notwithstanding the need to make these changes, it can be seen that the experiment discussed in this paper showed most of the effects which have been illustrated subsequently.

The simplicity of the qualitative (or, at any rate semi-quantitative) results given in Fig. 2, 3A and 3B may be contrasted with the more complicated procedures required for the quantitative evaluations (Figs. 4A - 11) leading to the estimate of the specific rate of excess enthalpy generation, Fig.12. It became clear that the quantitative evaluations required the execution of comprehensive series of experiments, including experiments on suitable "blank" systems (see Appendix B (6)). Failure to carry out such comprehensive evaluations (and failure to validate the performance of the instrumentation using "blank"

⁹ The present experiment was not included in the previous publication, (3), in view of the difference in the methods of data evaluation. However, it became apparent that the application of non-linear regression was not understood by the scientific public and we therefore switched attention to the use of linear regression. For further comments see (13).

systems, see e.g. (4)) was expected to lead to the inevitable conclusion that the measurements were subject to large errors. However, the main aim of the present investigation was to serve as a response to the request that we could demonstrate the generation of excess enthalpy at specific rates of at least 5 Wcm⁻³. Although we demonstrated that this target value could be achieved, the results obtained did not lead to the hoped for discussions of the topic nor to the hoped for support for the further development of the work. Instead, the discussion became focused on trivial side issues which were frequently based on misrepresentations of the work which we had carried out.

Appendix A

It has been established that at low to intermediate cell temperatures (say $30^\circ < \theta < 80^\circ$) the behaviour of the calorimeters is modelled adequately by the differential equation

$$\begin{aligned}
 C_p M (d\Delta\theta/dt) &= [E_{\text{cell}}(t) - E_{\text{thermonutral, bath}}] I & + & Q_r(t) \\
 \text{change in the} & \text{enthalpy input} & & \text{rate of excess} \\
 \text{enthalpy content} & \text{due to} & & \text{enthalpy} \\
 \text{of the calorimeter} & \text{electrolysis} & & \text{generation} \\
 & + \Delta QH(t-t_1) - \Delta QH(t-t_2) - (3I/4F[P/\{P^*-P\}])[C_{p,D_2O,g} - C_{p,D_2O,l}]\Delta\theta + L] \\
 \text{calibration pulse} & \text{rate of enthalpy removal by the gas stream with} \\
 & E_{\text{thermonutral}} \text{ referred to the bath temperature} \\
 & - (k_R^0)\theta_{\text{bath}}^3[1-\gamma t] \{f_1(\theta)/\theta_{\text{bath}}^3 + 4\phi\Delta\theta\}
 \end{aligned} \tag{A.1}$$

time dependent heat transfer coefficient effect of radiation effect of conduction

With the calorimeters supplied with the ICARUS Systems, the conductive contribution to heat transfer is very small. This term could therefore be “lumped” into the radiative term by allowing for a small increase in the radiative heat transfer coefficient:

$$\text{Radiative heat transfer} = (k_R')^0 [1-\gamma t] [(\theta_{\text{bath}} + \Delta\theta)^4 - \theta_{\text{bath}}^4] \tag{A.2}$$

The values of the pseudoradiative “heat transfer coefficient, $(k_R')^0 [1-\gamma t]$, derived are close to those calculated from the Stefan-Boltzmann coefficient and the radiative surface area. If the time dependence of the heat transfer coefficient is not included explicitly in equation (A.2) then

$$\text{Radiative heat transfer} = (k_R') [(\theta_{\text{bath}} + \Delta\theta)^4 - \theta_{\text{bath}}^4] \tag{A.3}$$

where the pseudoradiative heat transfer coefficient, (k_R') , now shows a weak time-dependence.

The simplest starting point is to assume that there is no excess enthalpy generation in the calorimeter and to evaluate a corresponding “differential lower bound heat transfer coefficient” at a time just before the end of the calibration pulse, $t = t_2$:

$$(k_R')_1 = [(E_{\text{cell}}(t) - E_{\text{thermoneutral, bath}})I - \Delta H_{\text{evap}}(t) - C_p M (d\Delta\theta/dt) + \Delta QH(t - t_1)] / f_1(\theta) \quad \text{A.4}$$

This was the first heat transfer coefficient used in our investigations, hence the designation $(k_R')_1$. It will be apparent that the differential lower bound heat transfer coefficient $(k_R')_{11}$, may be evaluated at other points of the measurement cycle, by changing the enthalpy input due to the calibration pulse to

$$\Delta QH(t - t_1) - \Delta QH(t - t_2) \quad \text{A.5}$$

It is next necessary to evaluate a “true heat transfer coefficient”. The simplest procedure giving $(k_R')_2$ near the end of the calibration period at $t = t_2$ is obtained by including the calibration pulse

$$(k_R')_2 = \{ \Delta Q + [E_{\text{cell}}(\Delta\theta_2, t_2) - E_{\text{cell}}(\Delta\theta_1, t_2)]I - \Delta H_{\text{evap}}(\Delta\theta_2, t_2) + \Delta H_{\text{evap}}(\Delta\theta_1, t_2) - C_p M [(d\Delta\theta/dt)_{\Delta\theta_2, t_2} - (d\Delta\theta/dt)_{\Delta\theta_1, t_2}] \} / f_2(\theta) \quad \text{A.6}$$

where we now have

$$f_2(\theta) = [\theta_{\text{bath}} + (\Delta\theta_2, t_2)]^4 - [\theta_{\text{bath}} + (\Delta\theta_1, t_2)]^4 \quad \text{A.7}$$

It can be seen that we need to estimate the cell potential, the cell temperature and the differential of this temperature at the time $t = t_2$ which would have been reached in the absence of the calibration pulse [see footnote (A.1)]

Footnote (A.1) This evaluation was carried out in a somewhat different manner in the initial studies (3), (16) (17) in an attempt to avoid the disadvantages of such interpolation procedures. The values of $(k_R')_{11}$ and $(k_R')_2$ obtained were used as starting values for the non-linear regression procedure used at that time (3). As we could not make this procedure “user friendly” with the computing power then available to us and as, more especially, the methodology which we adopted was evidently not understood (18). (for a further example of such misunderstanding see (19)) we adopted the

methodology described in the present paper. This methodology was also the basis of the ICARUS Systems.

As there is a large number of methods of analysing the experimental time-series characterised by their respective heat transfer coefficients, we have designated these coefficients by $(k_R')_{i,j,k}$ where

$i = 1$ denotes differential

$i = 2$ denotes integral with backward integration of the data sets

$i = 3$ denotes integral with forward integration of the data sets

$j = 0$ denotes the whole data set i.e. $0 < t < T$

$j = 5$ denotes the region adjacent to $t = 0$

$j = 6$ denotes the region adjacent to $t = t_1$

$j = 7$ denotes the region adjacent to $t = t_2$

$j = 8$ denotes a combination of $j = 6$ and $j = 7$

$k = 1$ denotes “lower bound”

$k = 2$ denotes “true”

The coefficient $(k_R')_{1,0,1}$ has usually been written as $(k_R')_{11}$

The present paper has been restricted to the use of the differential heat transfer coefficients.

When considering the application of equations A.4 and A.6 to any position in the measurement cycles, it is also convenient to rewrite these equations in the “straight line” forms applicable to the time region $t_1 < t < t_2$

$$\begin{aligned} & \{ [E_{\text{cell}}(t) - E_{\text{thermo neutral, bath}}] I - \Delta H_{\text{cvap}}(t) + \Delta QH(t-t_1) + Q_{\text{excess}} \} f_1(\theta) \\ & = (k_R')_{161}^0 \sim [C_p M \frac{d(\Delta\theta)}{dt}] f_1(\theta) \end{aligned} \quad \text{A.8}$$

$$\{ [E_{\text{cell}}(\Delta\theta_2, t) - E_{\text{cell}}(\Delta\theta_1, t)] I - \Delta H_{\text{cvap}}(\Delta\theta_2, t) + \Delta H_{\text{cvap}}(\Delta\theta_1, t) + \Delta QH(t-t_1) \} / f_2(\theta)$$

$$= (k_R')^0_{162} + C_p M \left[\left(\frac{d(\Delta\theta_2)}{dt} \right)_t - \left(\frac{d(\Delta\theta_1)}{dt} \right)_t \right] [(f_2(\theta))]^{-1} \quad \text{A.9}$$

where $\Delta\theta_2$ specifies the observed time series and $\Delta\theta_1$ is the interpolation between the time regions $0 < t < t_1$ and $t_2 < t < T$. $(k_R')^0_{161}$ and $(k_R')^0_{162}$ are now the intercepts of the plots such as these shown in Figs. 5A-6B, 10, 11 which will be the values of the differential “lower bound” and “true” heat transfer coefficients in the region close to $t = t_2$

Appendix B

The redesign of the experiments covered inter-alia the following points;

- 1) the substitution of the cell design illustrated in Fig. 1A by that shown in Fig. 1B so as to reduce the changes in cell temperature due to the progressive electrolysis of the cell contents. These modified cells were also to be evacuated to an “hard vacuum” so that heat transfer would be controlled by radiation across the lower, unsilvered, parts of the cells;
- 2) the further stabilisation of the room temperature using two controllers working in parallel. As heat rejection from the water baths surrounding the cells was to the ambient atmosphere (using stirrer-regulators) this ensured that a large number of experiments could be carried out with systems each having two thermal impedances operating in series;
- 3) the use of just three cells in each water thermostat;
- 4) the adoption of 48-hour measurement cycles (the periods following each addition of D₂O); addition of D₂O was to be restricted to the times following the start of each measurement cycle (contrast Fig. 5); calibration pulses (each lasting 12 hours) were to be applied 12 hours after the start of each measurement cycle followed by 24 hours after the cessation of each calibration pulse; calibration pulses were to be applied during each measurement cycle;
- 5) the main purpose of the calibration pulses was to be an aid for the detection of positive feedback; use of the pulses to calibrate the calorimeters was to be subject to many restrictions;
- 6) the execution of several series of “blank” experiments (the polarisation of Pt-cathodes in 0.1M LiOD/D₂O) to allow the characterisation of the calorimeters;
- 7) the raising of the cell current following the detection of the effects of positive feedback so as to drive the systems through the transitional regime

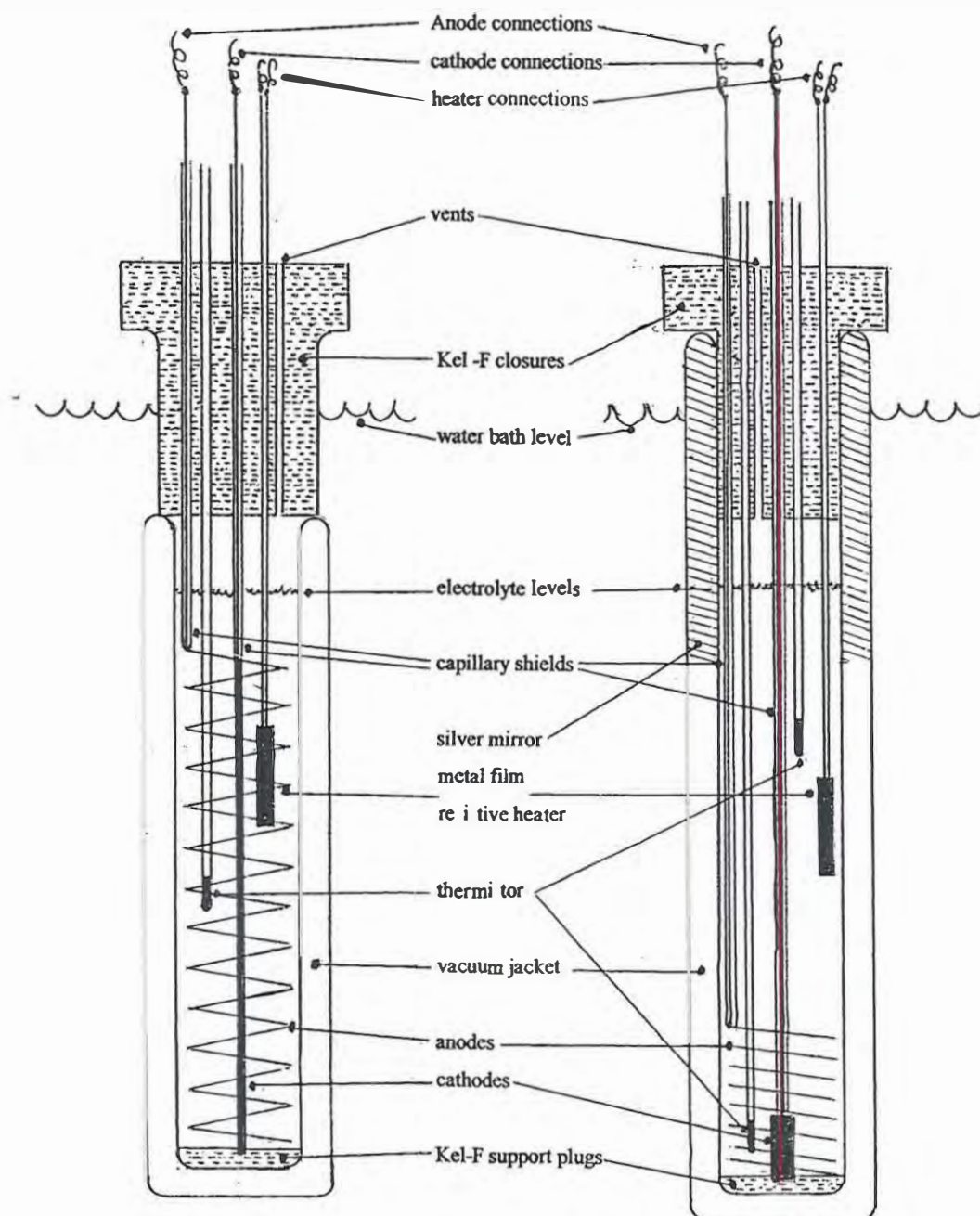
- 8) examination of the responses for the effects of “Heat-After-Death” (15, (16), the persistence of excess enthalpy generation following the termination of polarisation or the reduction of the cell current¹⁰
- 9) use of larger diameter electrodes so as to improve the energy efficiency and to avoid the distortion of the electrodes observed with those of 0.1cm diameter.

¹⁰ the experiment discussed in this paper showed some evidence for the presence of this phenomenon as the cooling curves following the termination of polarisation were retarded compared to those predicted from the water equivalent of the cell and the true heat transfer coefficient. However, experiments with 0.1cm diameter electrodes were judged to be unsuitable for the investigation of the phenomenon.

References

- 1) The ICARUS -1 System: Isoperibolic Calorimetry : Acquisition, Research and Utilities System, Version 1.0 (December 1993), Low Power Measuring System for Three Cells, TECHNOVA INC., 13th Floor, Fukoku Seimei Building, 2-2-2 Uchisaiwai-cho, Chiyoda-Ku, Tokyo 100, Japan.
- 2) The ICARUS -2 System: Isoperibolic Calorimetry : Acquisition, Research and Utilities System, Version 2.0 (February 1995), TECHNOVA INC., 13th Floor, Fukoku Seimei Building, 2-2-2 Uchisaiwai-cho, Chiyoda-Ku, Tokyo 100, Japan.
- 3) M. Fleischmann, S. Pons, M.W. Anderson, L.J. Li and M. Hawkins, J. Electroanal. Chem., 287 (1990) 293.
- 4) M. Fleischmann and M.H. Miles, "Our Penultimate Papers on the Isoperibolic calorimetry of the Pt/D₂O and Pd/D₂O systems. Part I: the Pt/D₂O blank system" submitted for publication.
- 5) M. Fleischmann and M.H. Miles and M.A. Imam "Our Penultimate Papers on the Isoperibolic calorimetry of the Pt/D₂O and Pd/D₂O systems. Part II: the Pd/B and Pd-B-Ce Systems." submitted for publication.
- 6) M.H. Miles, S. Szpak, P.A. Mosier-Boss and M. Fleischmann: "Our Penultimate Papers on the Isoperibolic calorimetry of the Pt/D₂O and Pd/D₂O systems. Part III: the Pd-D Codeposition System." submitted for publication.
- 7) M. Fleischmann in Eds. T. Bressani, E. Del Giudice and G. Preparata, "The Science of Cold Fusion; Proceedings of the 2nd Annual Conference on Cold Fusion", Conference Proceedings of the Italian Physical Society, Bologna, Italy, 33 (1991) 475, ISBN 88-7794-045-X.
- 8) M.H. Miles, J. Electroanal. Chem., 482 (2000) 56.
- 9) Wilford N. Hansen in Eds. T. Bressani, E. Del Giudice and G. Preparata, "The Science of Cold Fusion; Proceedings of the 2nd Annual Conference on Cold Fusion", Conference Proceedings of the Italian Physical Society, Bologna, Italy, 33 (1991) 491, ISBN 88-7794-045-X.
- 10) Wilford N. Hansen and Michael E. Melich, Trans. Fusion Technol., 26 (1994) 355.
- 11) Kirk L. Shanahan, Thermochimica Acta, 387, (2002), 95.
- 12) Martin Fleischmann and Stanley Pons in "Frontiers of Cold Fusion" Ed. H. Ikegami, Frontiers of Science Series No 4, Universal Academy Press Inc., Tokyo, (1993), ISBN 4-946443-12-6.
- 13) M. Fleischmann, S. Pons, Monique Le Roux and Jeanne Roulette, Trans. Fusion Technol., 26 (1994) 323.
- 14) M. Fleischmann, Proceedings of the 5th International Conference on Cold Fusion, Monte Carlo, (1995) 140.
- 15) S. Szpak and P.A. Mosier-Boss, Technical Report 1862, Volume I, SPAWAR Systems Centre, San Diego, February (2002).

- 16) M. Fleischmann, S. Pons and M. Hawkins, *J. Electroanal. Chem.*, 261 (1989) 301.
- 17) M. Fleischmann and S. Pons, *J. Electroanal. Chem.*, 332 (1992) 33.
- 18) R.A. Wilson, J. W. Bray, P.G. Kosky, H.B. Vakil and F.G. Will, *J. Electroanal. Chem.*, 332(1992) 1.
- 19) Frederick T. Wagner, Thomas E. Moylen, Michael E. Hayden, Ulrike Narger and James L. Booth, *J. Electroanal. Chem.*, 295 (1990) 393.

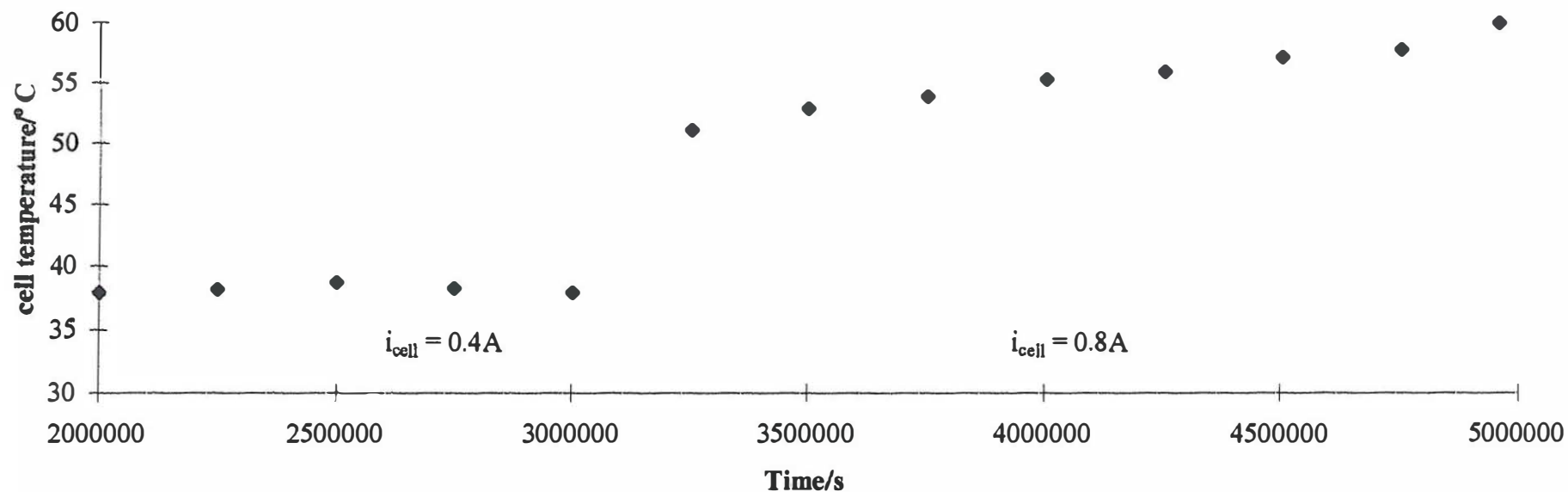


Glass rod framing
not shown

Fig. 1A Dewar-type cell used in the initial experiments and for the experiment discussed in the present paper.

Fig. 1B Modification of the Dewar-type cell taking account of the points listed in Appendix B. Cells of this type were used in all subsequent experiments (e.g. see (4), (5), (6)).

Fig.3A Extract from the temperature-time series for the polarisation of a 0.1cm diameter x 10cm length Pd electrode in 0.1MLiOD/D O at the cell currents shown.



The derived values of the lower bound heat transfer coefficient (see text)

$$10^9(k_R')_{11} = 1.2768 \text{WK}^{-4}$$

$$\text{output} = 0.57f_1(\theta) + 0.08989\Delta\theta\text{W}$$

$$10^9(k_R')_{11} = 1.1316 \text{WK}^{-4}$$

$$\text{output} = 0.57f_1(\theta) + 0.06756\Delta\theta\text{W}$$

Fig. 3B Prediction of the cell temperature using the mean pseudo-radiative lower bound heat transfer coefficient, $(k_R')_{ll}$, and the optimal representation of the mean lower bound heat transfer coefficient $(0.57+(k_i)\Delta\theta)$

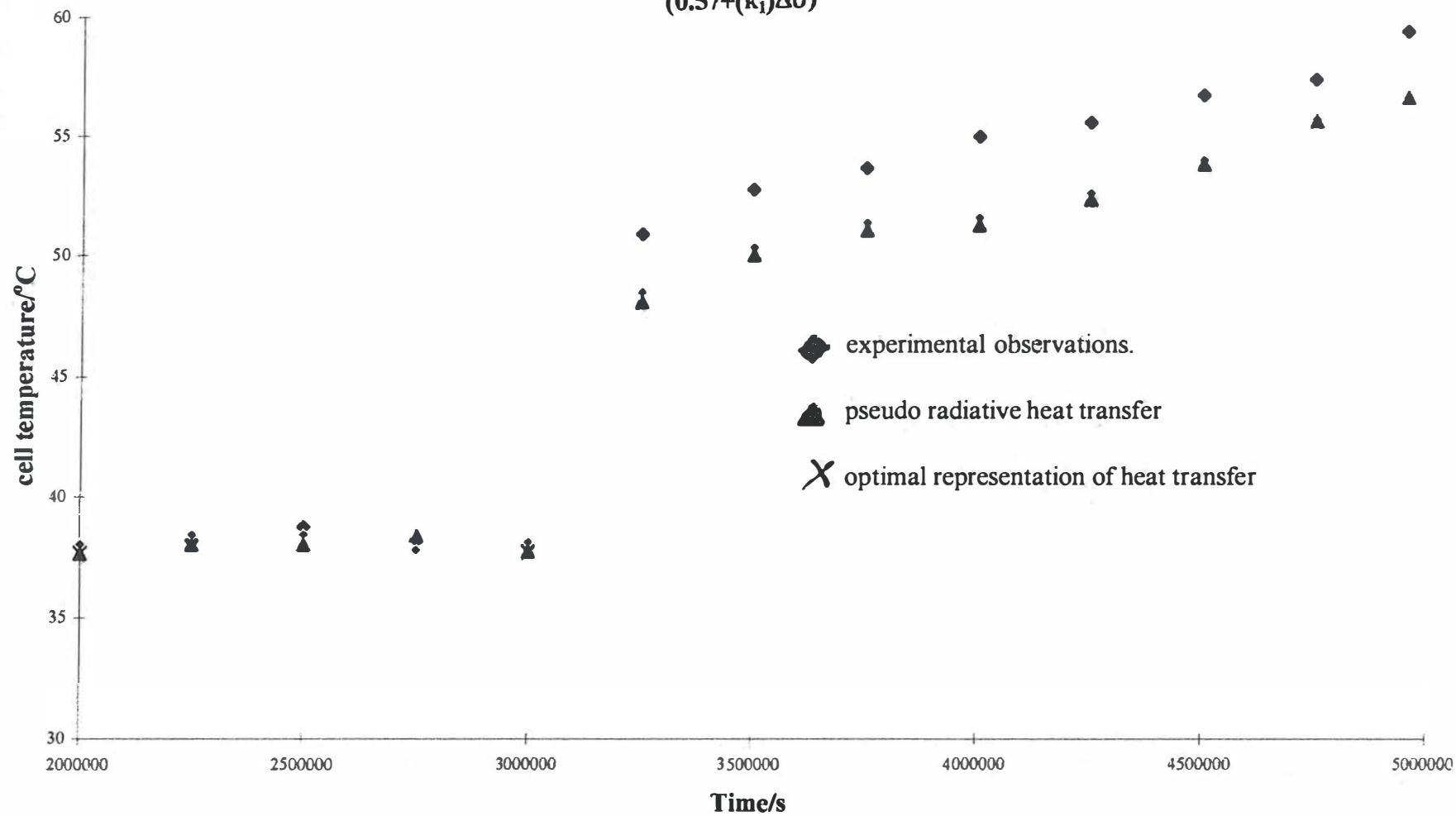


Fig. 4A Extract of the raw data for day 20 of the experiment.

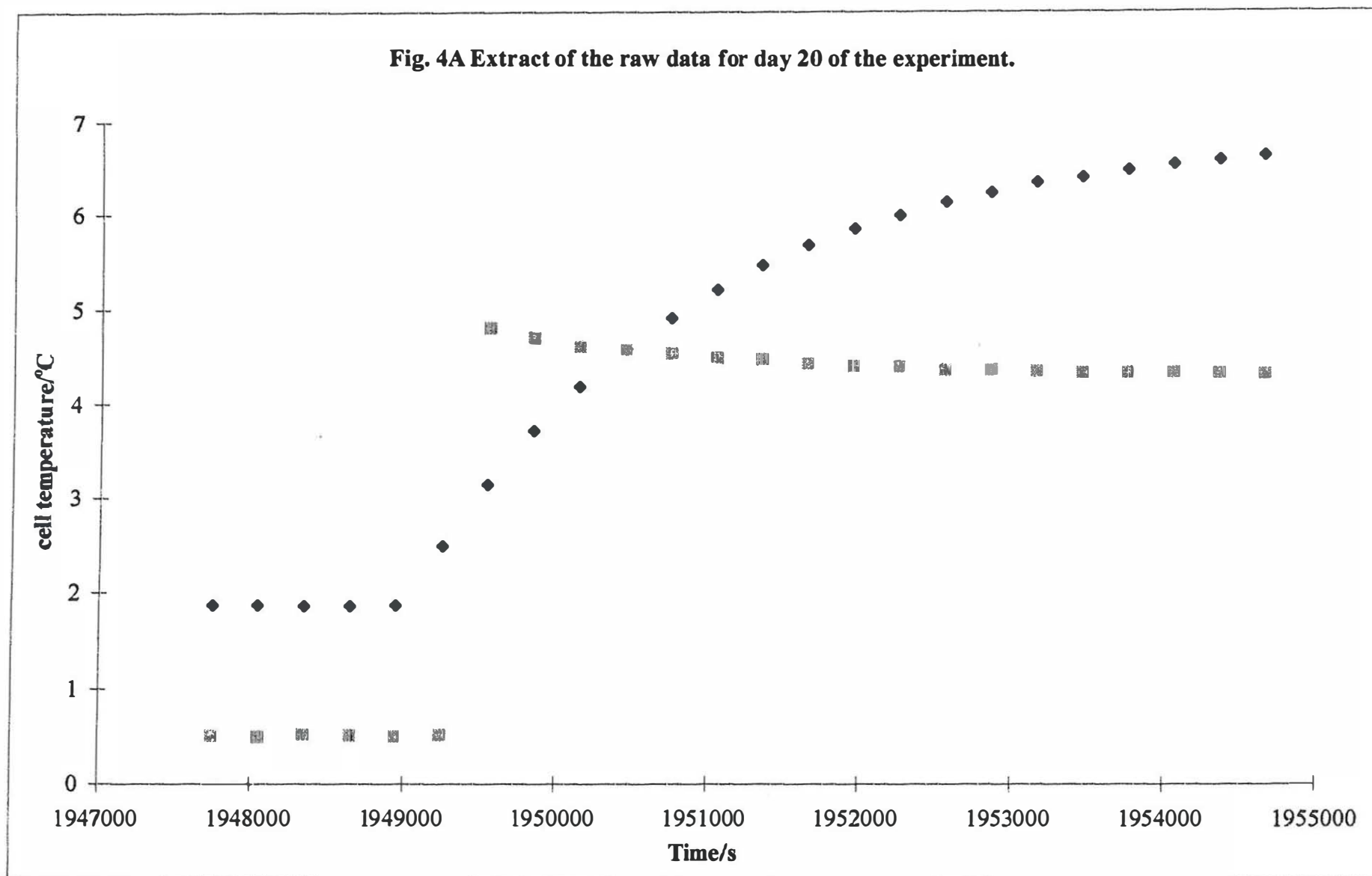
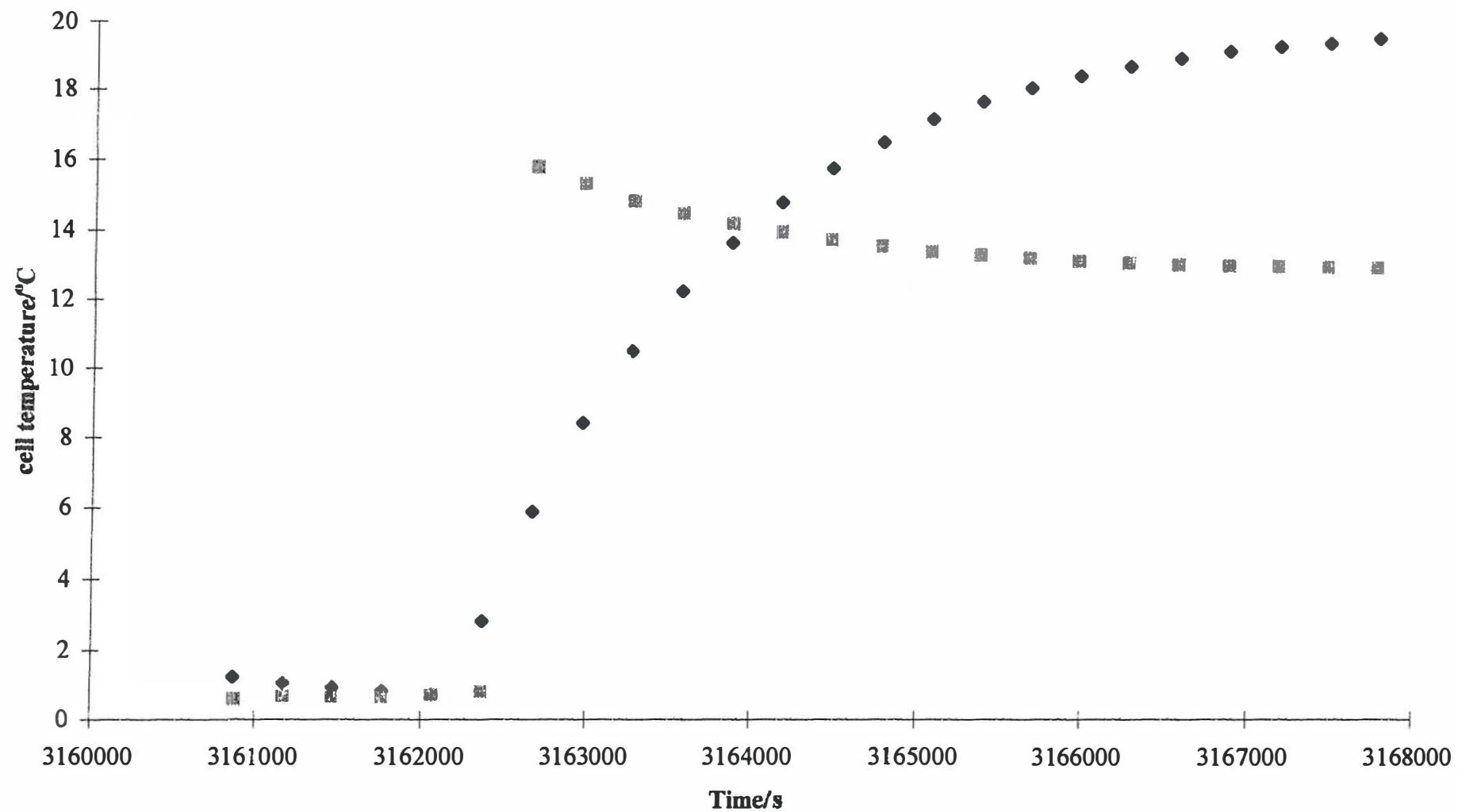
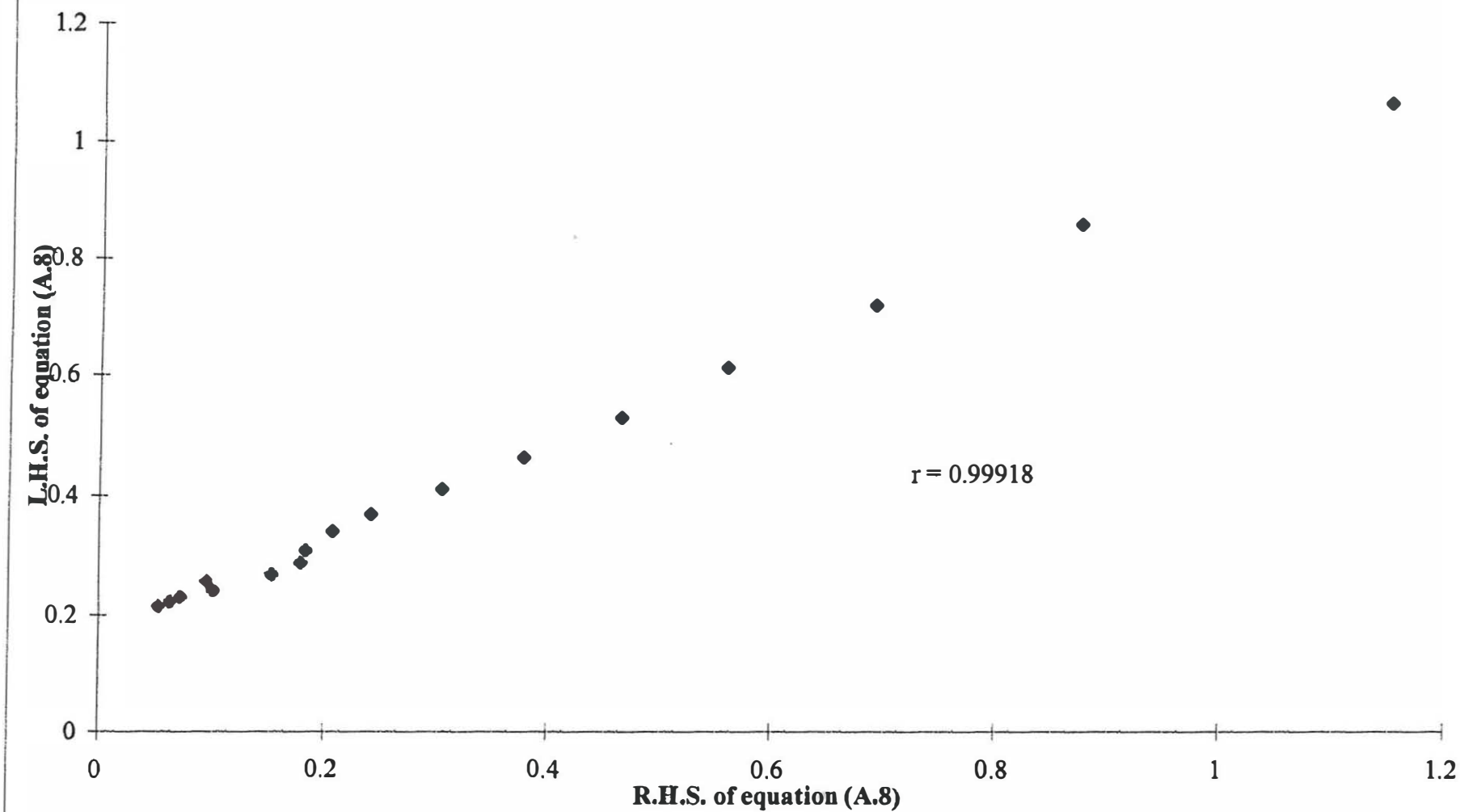


Fig. 4B Extract of the raw data for day 36 of the experiment.



**Fig. 5A Test of the application of equation (A.8) to the raw data for day21 of the experiment
(see Fig. 4A)**



**Fig.5 B Test of the application of equation (A.9) to the raw data for Day 21 of the experiment
(see Fig. 4A)**

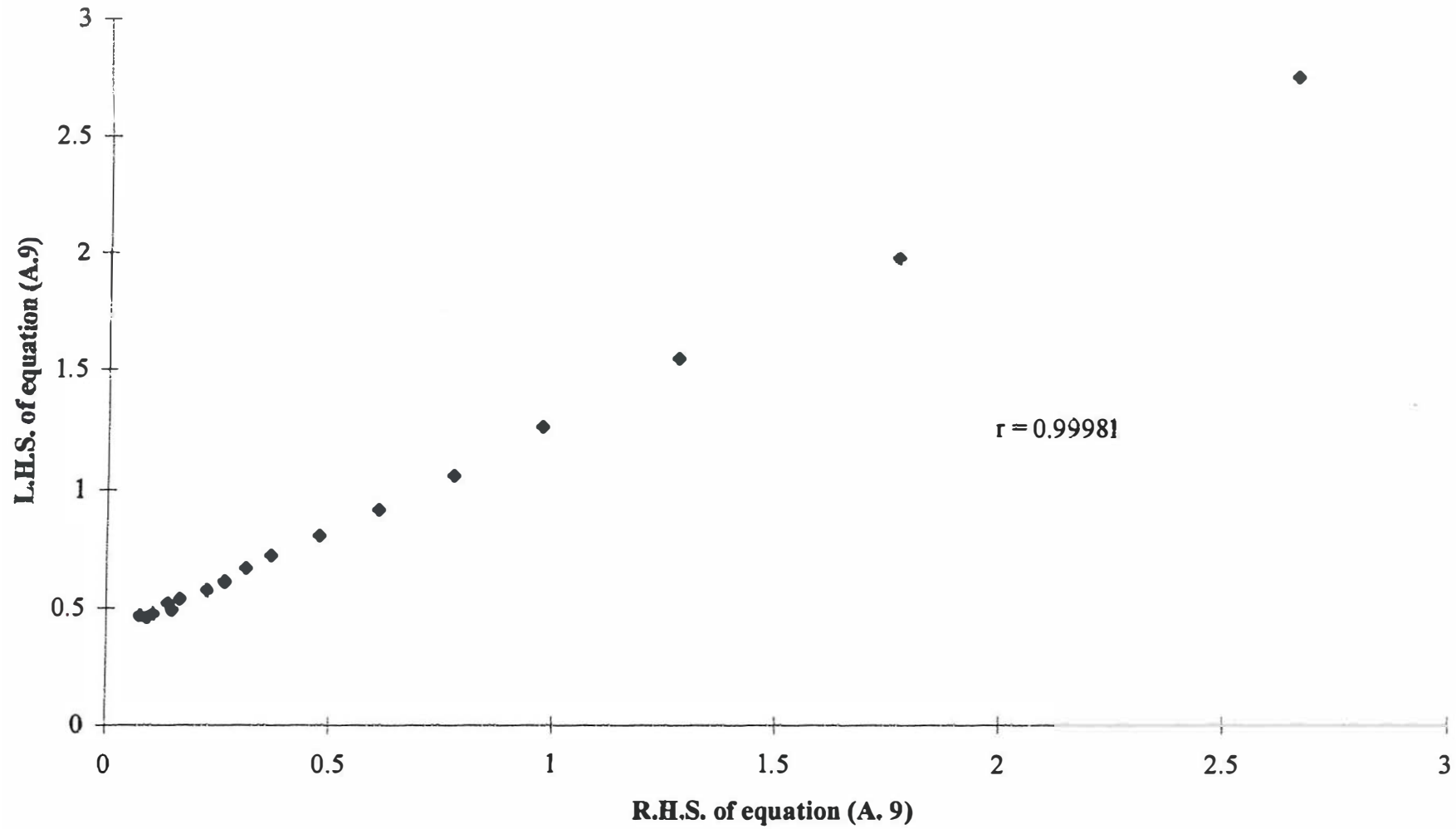


**Fig. 6A Test of the application of equation (A.8) to the raw data for day 36 of the experiment
(se Fig. 4B)**

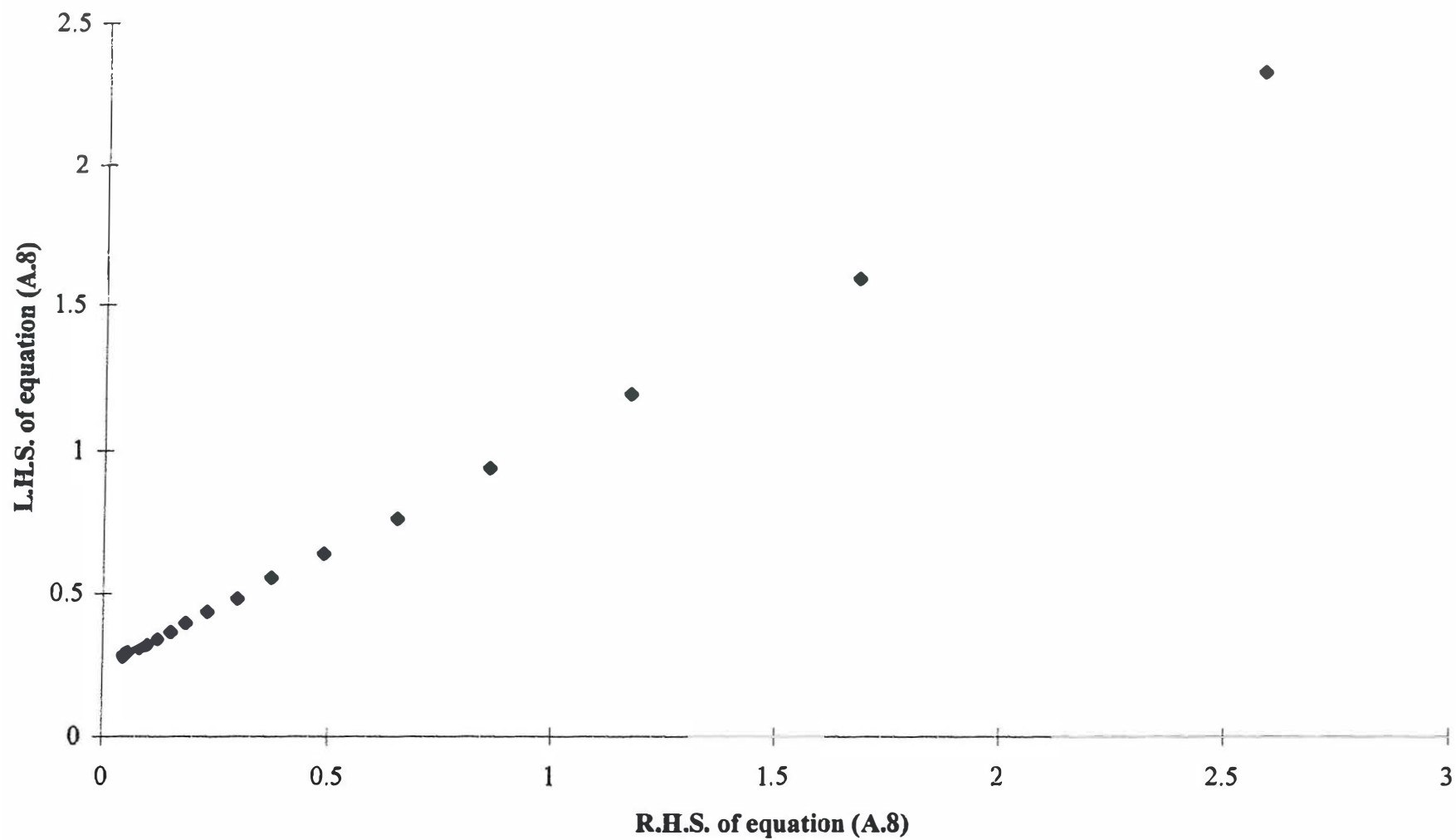


**Fig. 6B Test of the application of equation (A.9) to the raw data for Day 36 of the experiment
(see Fig. 4B)**

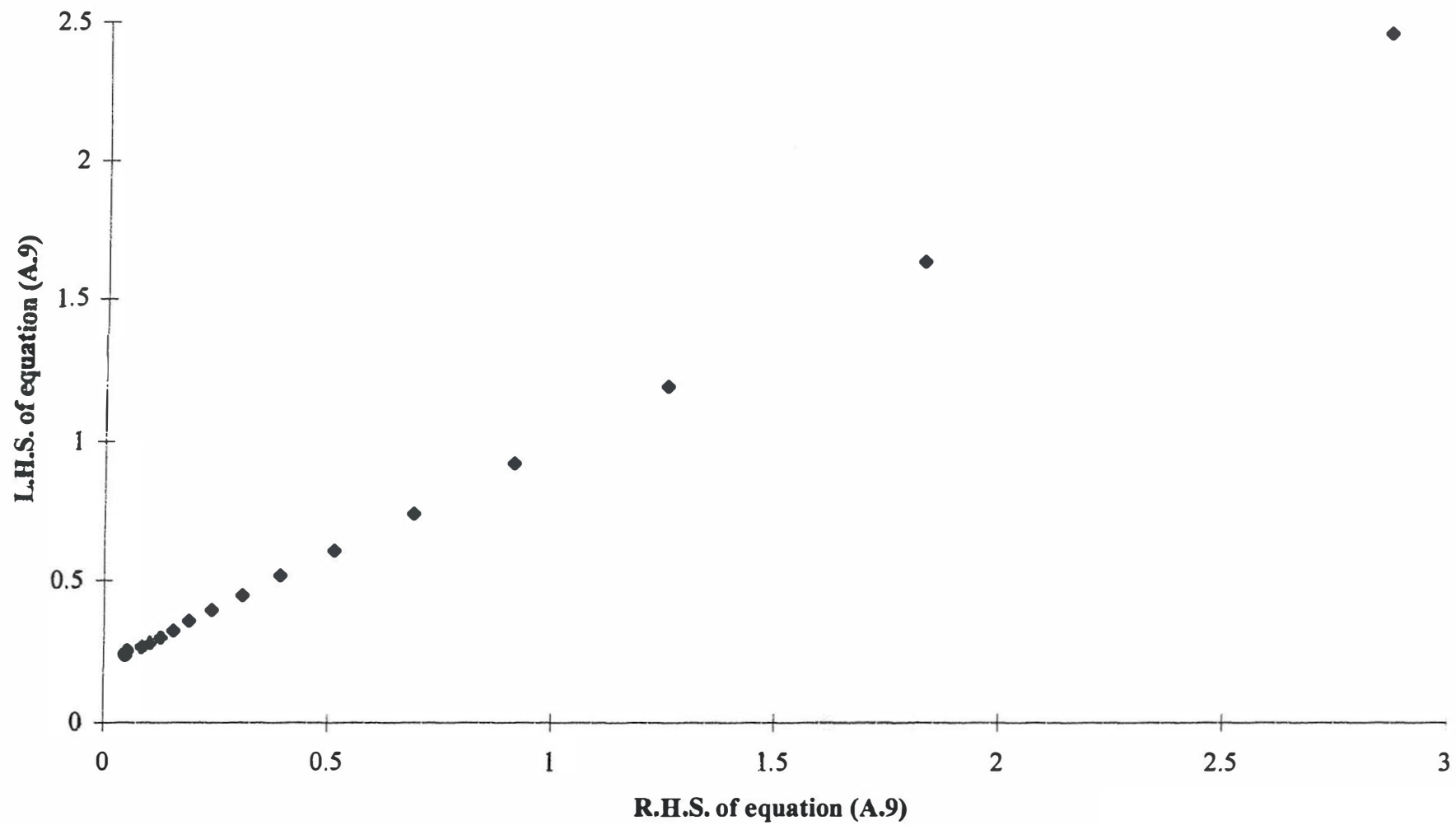


Fig. 7 The calibration of the cell on Day 55 of the experiment; cell current = 0.8A; the constructions on the figure show the information required for calculation of $(k_R')_1$ and $(k_R')_2$

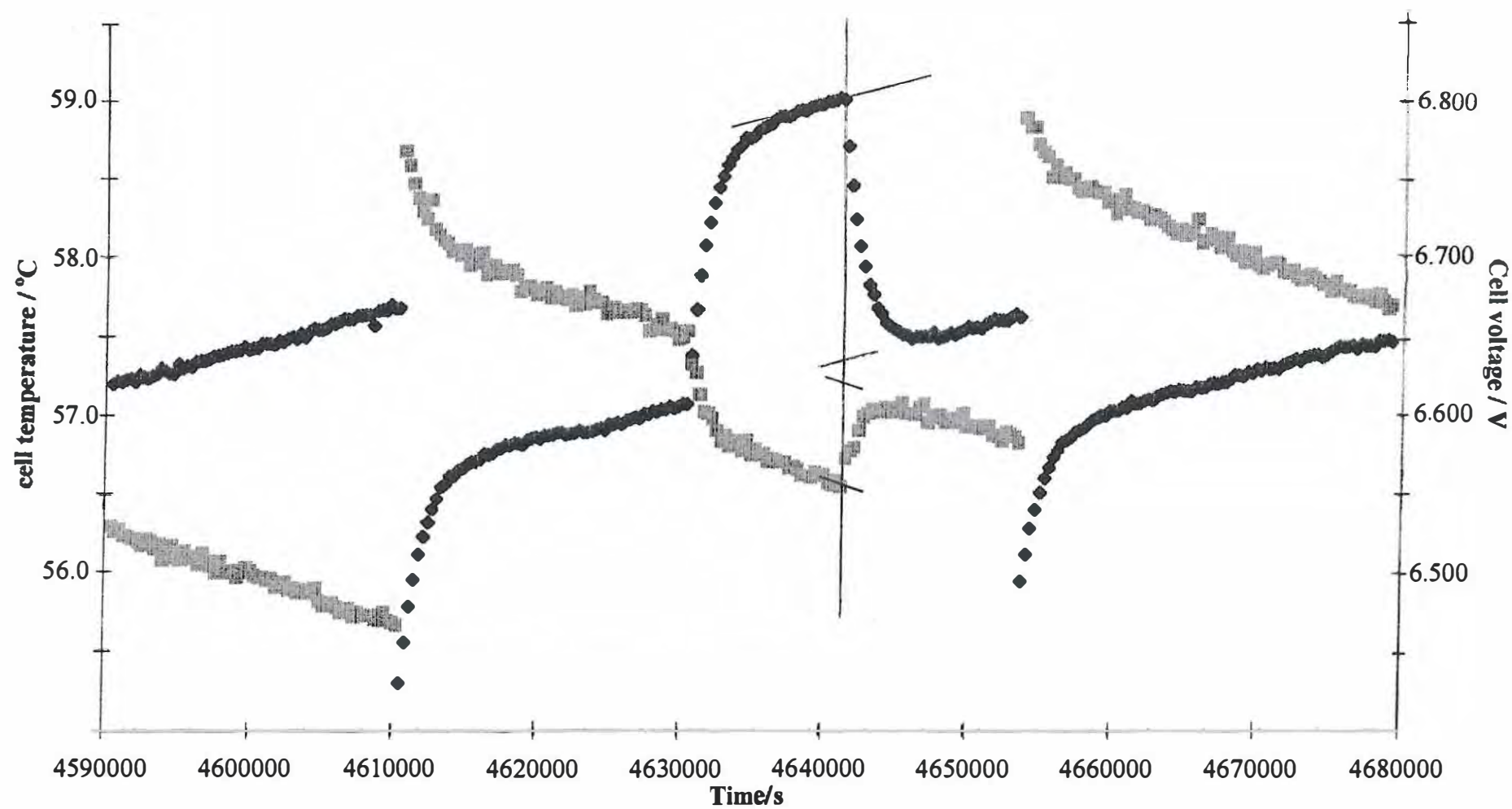


Fig. 8 the calibration of the cell on Day 20 of the experiment

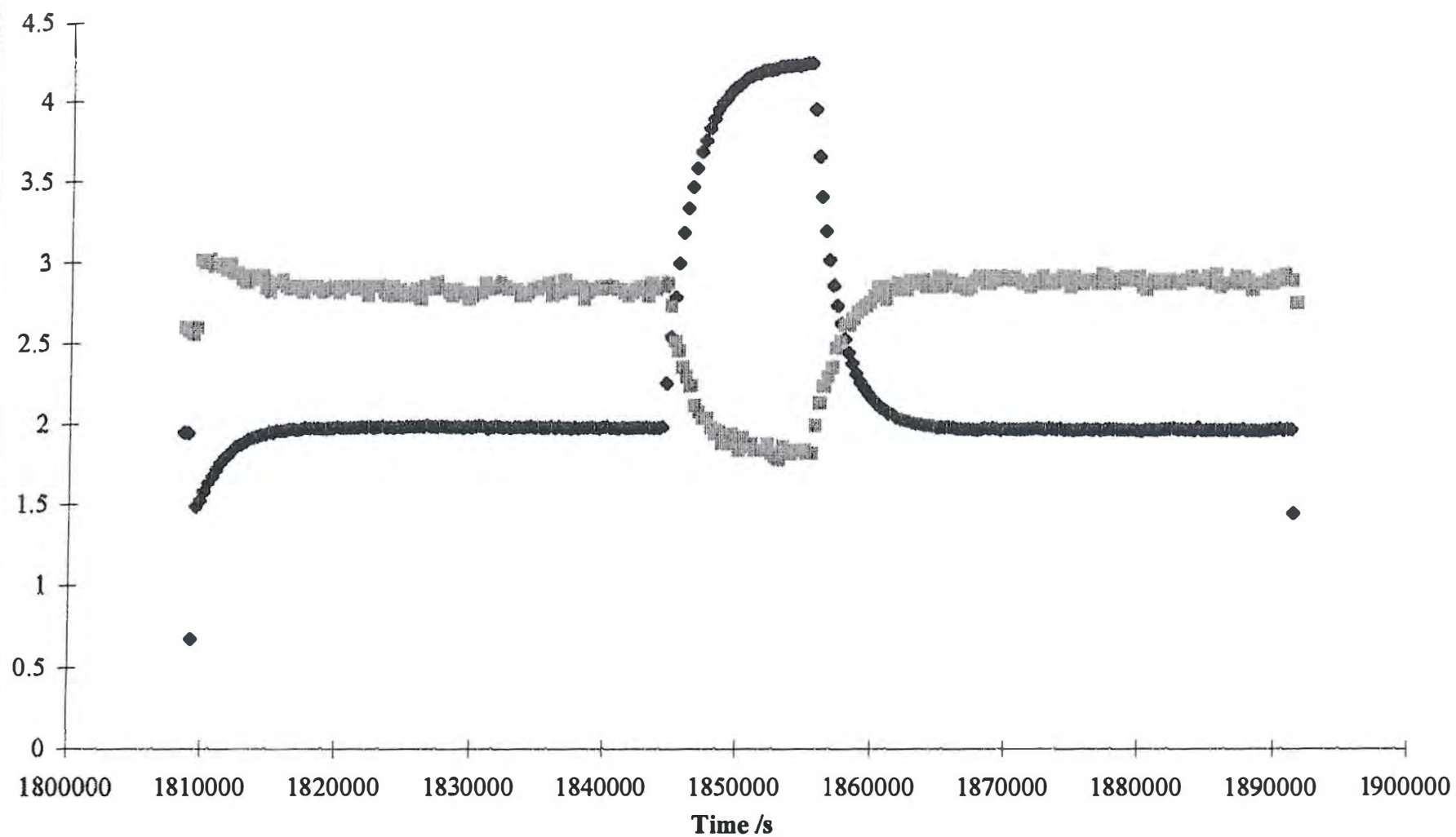


Fig. 9 Day 1 of preliminary polarisation at 0.2A $C_p M = 380 JK^{-1}$

cell current = 0.2A

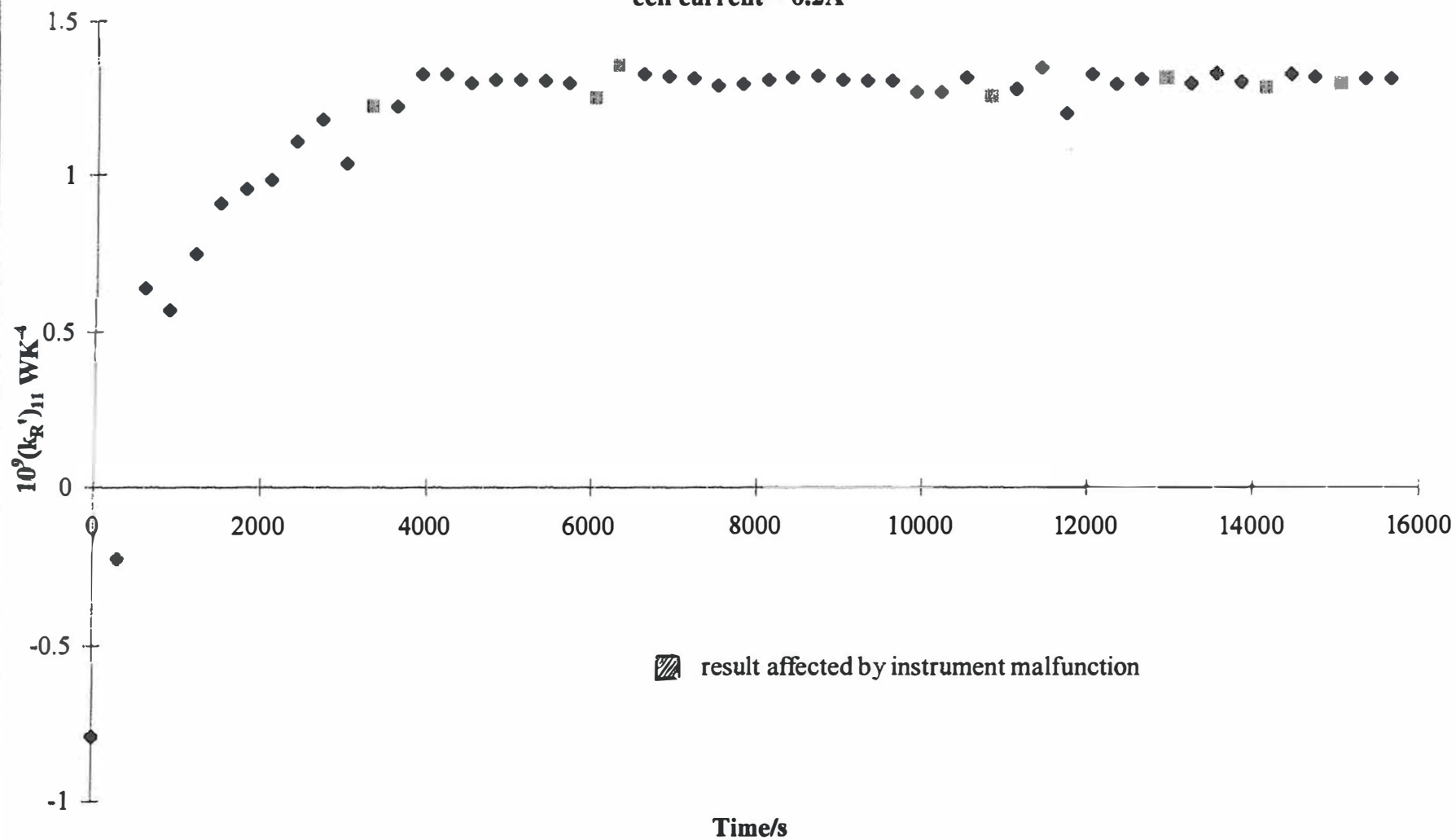


Fig. 10 Test of the application of equation (A.8) to the relaxation of the temperature-time series following the addition of D_2O to the cell; Day 39 of the experiment.

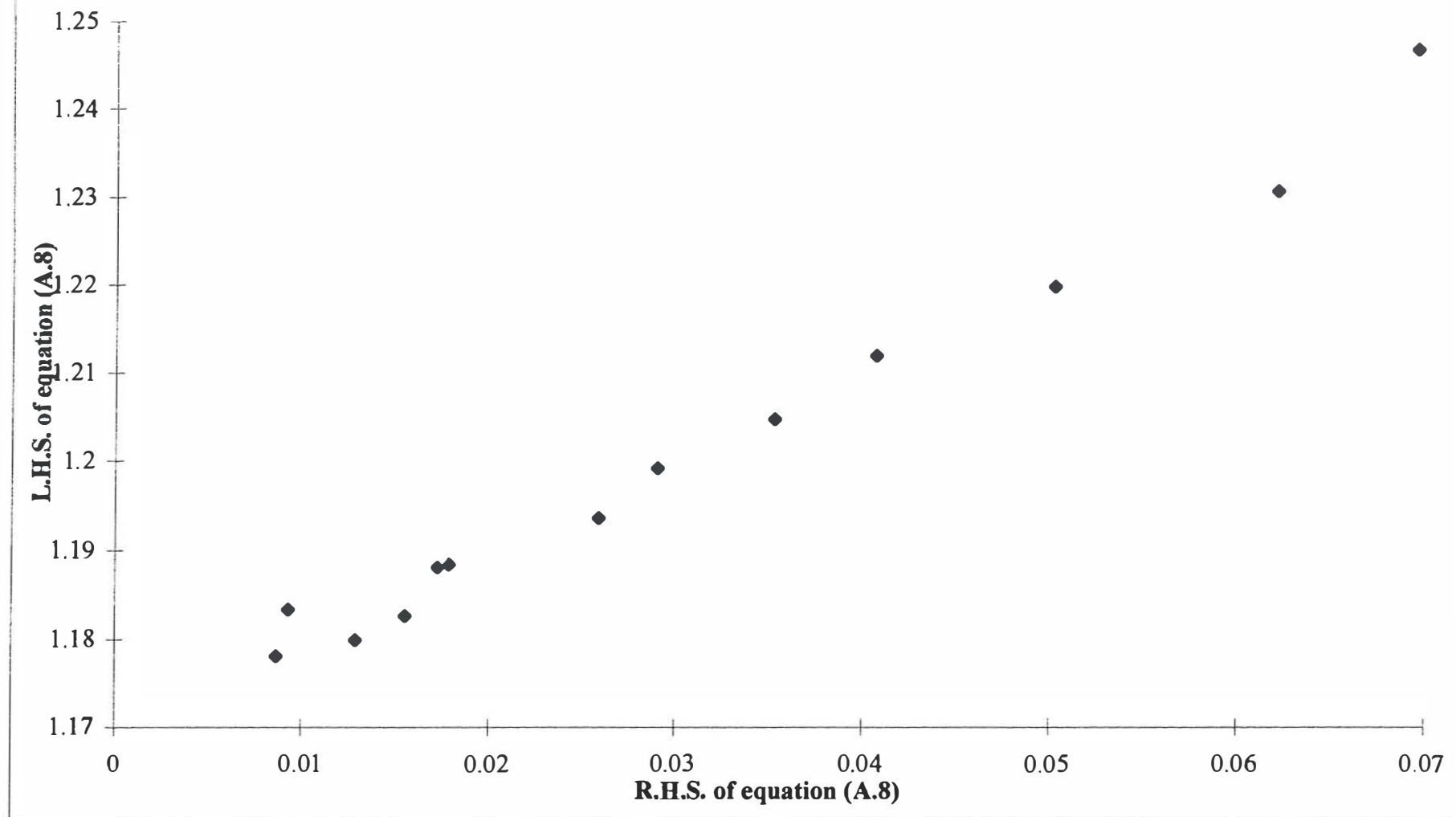


Fig. 11 Test of the application of equation (A.8) to the mean of the raw data (Days 20-36) of the experiment; cell current = 0.4000A.

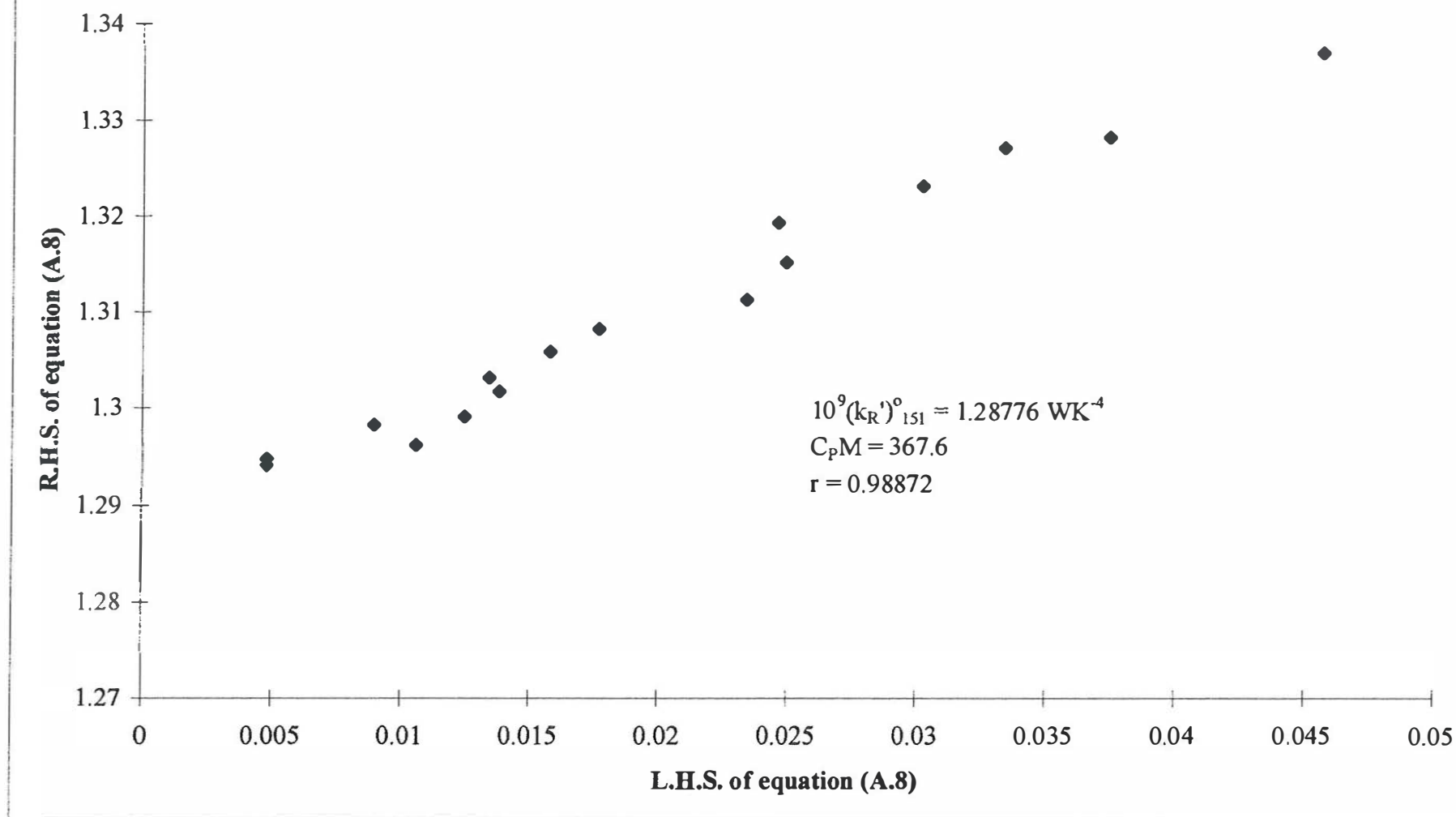


Fig. 12 Comparison of the specific rate of excess enthalpy production observed in the present experiment with values determined in 1989 (3)

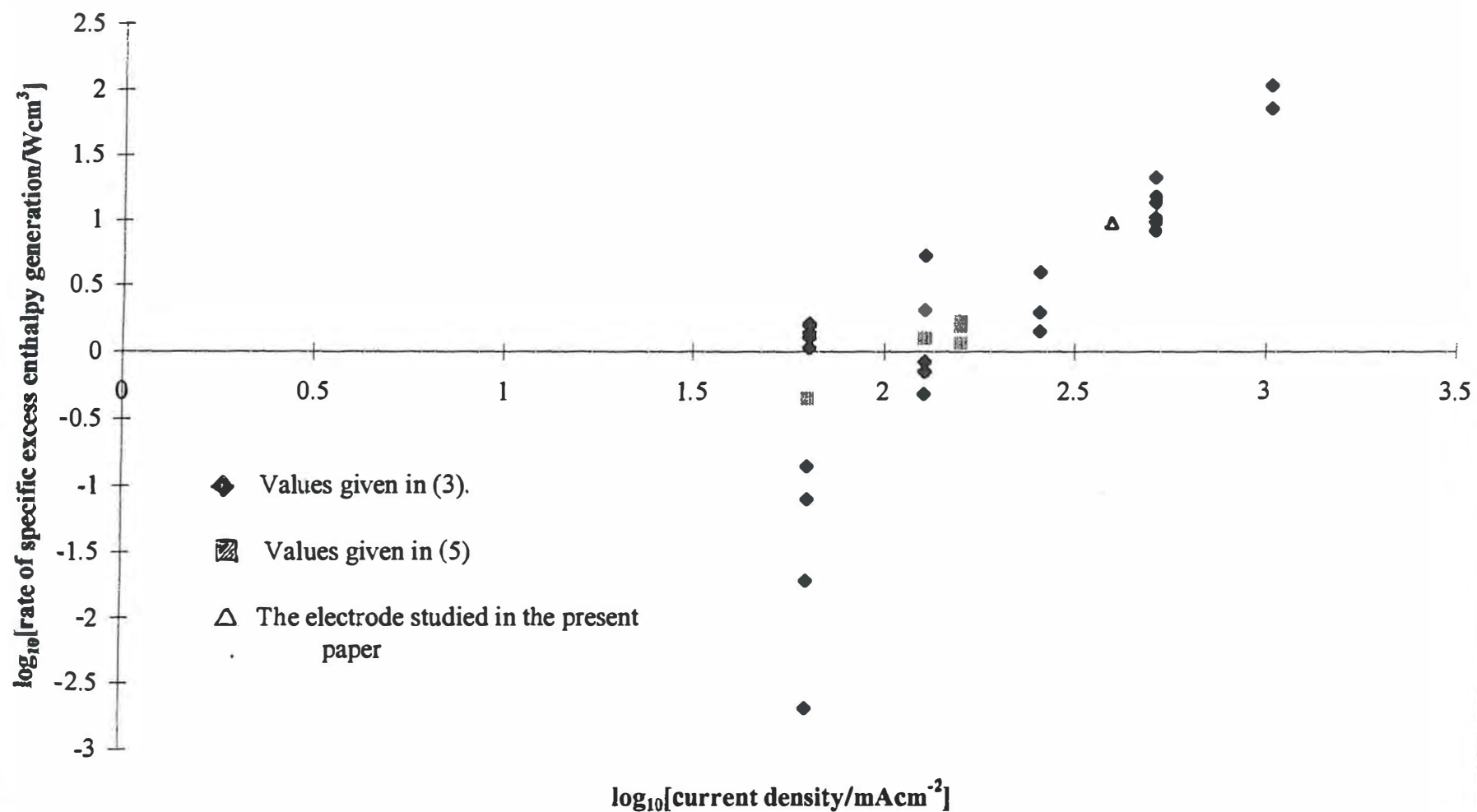


Table 1 Calibration of the Calorimeter.

Identification of the calibration	Time /Day	Cell current / A	10^9 (pseudo-radiative lower bound heat transfer coefficient) / WK^{-4}	10^9 (pseudo-radiative true heat transfer coefficient) / WK^{-4}	Method of Calibration
1	21	0.2→0.4	1.2683	1.2820	change of cell current giving $(k_R')^{o_{161}}$ and $(k_R')^{o_{162}}$
2	21→22	0.4	1.2768	1.2768	Experimental θ -t plots and assuming no generation of excess enthalpy.
3A	22	0.4	1.1929	1.2388	Injection of Joule heat giving $(k_R')_1$ and $(k_R')_2$
3B	22	0.4	1.2561		Interpolation to give $(k_R')_1$ for base line only.
4	34→35	0.4	1.2768	1.2768	Experimental θ -t plots and assuming no generation of excess enthalpy.
5A	35	0.4	1.2433	1.2388	Injection of Joule heat giving $(k_R')_1$ and $(k_R')_2$.
5B	35	0.4	1.2446		Interpolation to give $(k_R')_1$ for base line only.
6	20→36	0.4	1.2878		Addition of D_2O : evaluation of $(k_R')^{o_{161}}$
7	36→37	0.2→0.8	1.1450	1.1042 (method fails)	Change of cell current giving $(k_R')^{o_{161}}$ and $(k_R')^{o_{162}}$ (method fails).
8A	40	0.8	1.1088	1.3550	Injection of Joule heat giving $(k_R')_1$ and $(k_R')_2$.
8B	40	0.8	1.0818		Interpolation to give $(k_R')_1$ for base line only.
9A	46	0.8	1.1358	1.2928	Injection of Joule heat giving $(k_R')_1$ and $(k_R')_2$.
9B	46	0.8	1.1092		Interpolation to give $(k_R')_1$ for base line only.
10A	55	0.8	1.1710	1.2638	Injection of Joule heat giving $(k_R')_1$ and $(k_R')_2$.
10B	55	0.8	1.1472		Interpolation to give $(k_R')_1$ for base line only.
11	37→57	0.8	1.0818		Addition of D_2O : evaluation of $(k_R')^{o_{161}}$ from Table 3

Table 2 Measurement of the lower bound, $(k_R')_1$, and true $(k_R')_2$, pseudo-radiative heat transfer coefficients at the cell current 0.2000A

Time / Day	$10^9(k_R')_1$, / WK ⁻⁴	$10^9(k_R')_2$, / WK ⁻⁴	Comments
1	1.32	1.32	Assuming no generation of excess enthalpy and equating $(k_R')_2$ to the maximum value of $(k_R')_1$ (see Fig. 9 and Fig. 12))
5	1.3133	1.3054	
5	1.2910	1.2884	
5→6	1.2865	1.2894	
14	1.2695	1.3075	Preliminary polarisation.
14	1.2501	1.2935	$10^9(\overline{k_R'})_1 = 1.2629 \text{ WK}^{-4}$
14→15	1.2208	1.2584	$10^9(\overline{k_R'})_2 = 1.2895 \text{ WK}^{-4}$
15	1.2025	1.2578	
15	1.2212	1.2464	
17	1.2961	1.3268	
17	1.2783	1.3214	
20	1.2807	1.3314	Renewed experiment.

Table 3 Values of the heat transfer coefficient $10^9(k_R')^o_{151}$ for the period $3,100,945 < t < 4,999,795s$.

Time / Day	$10^9(k_R')^o_{151} / WK^{-4}$	Time / Day	$10^9(k_R')^o_{151} / WK^{-4}$	Time / Day	$10^9(k_R')^o_{151} / WK^{-4}$
36→37	1.1681	45	1.1494	53→54	1.1946
37→38	1.1752	45	1.1660	54	1.1754
38	1.1782	46	1.1587	54→55	1.2007
39	1.1686	47	1.1651	55	1.21691
39	1.1772	47	1.1496	55→56	1.2128
39→40	1.1685	47→48	1.1571	56	1.2395
40	1.1483	48→49	1.1524	56→57	1.2147
40→41	1.1559	49	1.1563	57	1.1857
41	1.1646	50	1.1609	end of experiment	mean of 38 measurements $10^9(k_R')^o_{151} = 1.1703$
41→42	1.1563	50→51	1.1631		
42	1.1547	51	1.1614		
42→43	1.1651	51→52	1.1534		
43	1.1495	52	1.1679		
43→44	1.1264	52→53	1.1668		
44	1.1472	53	1.1973		

The “Instrument Function” of Isoperibolic Calorimeters : Excess Enthalpy Generation due to the Parasitic Reduction of Oxygen.

M. Fleischmann

Bury lodge, Duck Street, Tisbury, Salisbury, Wilts., SP3 6LJ, U.K.

M.H. Miles

Department of Chemistry, University of La Verne, CA 91750, U.S.A.

Two criticisms which are frequently advanced to counter observations of the generation of excess enthalpy in the cathodic polarisations of Pd-based electrodes in D₂O-based electrolytes (e.g. see (1), (2)) are usually based on the assertion that the isoperibolic calorimeters used in these studies are imprecise and inaccurate. Furthermore, any excess enthalpy generation is then attributed to the reduction of electrogenerated oxygen although such assertions have not been accompanied by appropriate measurements. There is naturally a link between these two assertions.

The first step in the development of any investigative methodology should be the determination of the relevant “instrument functions” of the instrumentation used, here the isoperibolic calorimeter illustrated in Fig. 1. We note the following key features of this design:

- (i) heat transfer is controlled by radiation across the vacuum gap, this heat transfer being predominantly due to the lower, unsilvered parts of the cells. The heat transfer is therefore given by the product of the Stefan-Boltzmann coefficient and the radiant surface area as has been confirmed in numerous studies. Increases from the predicted value must therefore indicate malfunctions of the cells (e.g. “softening” of the vacuum) and/or mistakes in the data analyses.
- (ii) as heat transfer is due to radiation across the gap, the thermal impedance has no “memory”. It is therefore possible to examine the non-steady state behaviour of the systems especially the response to calibration pulses supplied by the Joule resistive heaters. It is evident that this crucially important design criterion has not been understood by the many critics of “Cold Fusion” (e.g. see (3)).
- (iii) the long and narrow design of the calorimeters ensures that the contents are well mixed by the gas sparging induced by gas evolution at the anodes and cathodes. The radial and axial mixing times of the system (as revealed by tracer experiments) are ~3 s and ~20 s whereas the thermal relaxation time of the ICARUS-2 cell investigated in the present paper is ~5000 s^{1,2}.
- (iv) in view of (iii) the contents of the calorimeter have always been at a uniform temperature.
- (v) equally, the heat sinks (water baths) surrounding the calorimeters have always been at a uniform temperature. This has been ensured by using a combined rejection of heat to the surrounding ambient room temperature coupled to thermostatic control of the water baths. The room temperature has been itself controlled using two independent temperature controllers operated in parallel. The overall system therefore used two thermal impedances operated in series.

¹ The differential equation representing the model of the calorimeter is non-linear and inhomogeneous (see equations A.1 and A.2 of the Appendix). The estimate of a “thermal relaxation time” is therefore approximate.

² The calorimeters used in the initial studies (1), (2) had heat transfer coefficients which exceeded the product of the Stefan-Boltzmann coefficient and the radiant surface area and this was attributed to conduction across the vacuum gap due to inadequate evacuation of the cells. It was not clear therefore whether the system should have been modelled as being “pseudo-radiative” or “pseudo-conductive” (depending on whether the conductive or radiative contribution was neglected ; for an alternative strategy see (4), (5)). The thermal relaxation time of these cells was ~3000 s.

- (vi) the cells have always been operated in the “open mode” i.e. the products of electrolysis have been vented to the ambient³ N.M.R. measurements confirmed that this strategy (imposing continuous isotopic separation of H) ensured the maintenance of the initial isotopic composition of the electrolyte.
- (vii) the use of 0.1M LiOD/D₂O ensured that there were no parasitic reactions (other than the reduction of electrogenerated oxygen) which could affect the thermal balances of the system.
- (viii) the volumes of the gases evolved agreed to within ~1% of those calculated assuming 100% Faradaic efficiency of the electrolytic reactions provided we neglected the initial parts of the measurement sequences during which there is charging of Pd-based electrodes by hydrogen isotopes. The volume of D₂O required to maintain the levels of electrolyte in the cells also agreed with those calculated by Faraday’s Laws. There is therefore no possibility of invoking the large-scale recombination of the evolved gases to explain excess enthalpy generation.
- (ix) measurements of the cell and calibration currents, of the cell and bath temperatures and of the cell potentials and potentials across the resistive calibration heaters were made every 300 s⁴
- (x) three calorimetric cells were maintained in each thermostat tank.
- (xi) in view of the small extent of the head spaces (which contained no exposed bare metal parts), the systems could be operated in absolute safety.

Measurements and Interpretation.

Fig. 2 gives a plot of the “raw data” (the cell temperature and input enthalpy for days 9 and 10 of the measurement cycles) carried out on a Pt cathode ($\phi = 1$ mm, $\ell = 2$ cm). These time series show small decreases with time following each perturbation due to the increase of the electrolyte concentration caused by the progressive electrolysis. In turn, this leads to a decrease in the enthalpy input and hence the cell temperature.

Two times are of special interest; $t = t_1$ the start of the calibration period and $t = t_2$ the end of this period. The times $t = 0$ following the “topping up” of the cell after the previous measurement cycle and $t = T$ the end of this cycle are of lesser interest (see further below). Estimates of the pseudo-radiative lower bound heat transfer coefficient, $(k_R')_1$, and of the pseudo-radiative true heat transfer coefficient, $(k_R')_2$, can be made near $t = t_2$, equations A.4 and A.6 in the Appendix. In the first of these estimates, we assume that there is no generation of excess enthalpy, hence the designation “lower bound”; the presence of any *known* source of excess enthalpy would increase the enthalpy input and hence increase the heat transfer coefficient. In the evaluation of $(k_R')_2$ we also have to estimate the input power and cell temperature which would have been reached in the absence of the heater calibration. This can be done by interpolating the time series for the regions $t < t_1$ and $t_2 < t < T$. The reason for stipulating $t_1 = 12$ hours, $t_2 = 24$ hours and $T = 48$ hours will be self-evident. Contraction of these times to say $t_1 = 6$ hours, $t_2 = 12$ hours and $T = 24$ hours inevitably lowers the precision of $(k_R')_1$ and accuracy of $(k_R')_2$ but, unfortunately such contractions have been the norm in most investigations carried out by other research groups.

The values of these “robust” estimates (made from A3 sized plots of the “raw data”) are shown in Columns 2 and 3 of Table 1 for a series of 7 measurement cycles. These were the first

³ It should be noted that this strategy avoids the introduction of large localised and fluctuating sources of heat in the gas spaces (which is a characteristic of cells fitted with catalytic recombiners).

⁴ A limit on the rate of data acquisition is set by the time lags induced by the thin glass shields surrounding the thermistors, ~10 s. (see also further below). Furthermore, it would be possible to exceed this rate of data acquisition if the time lags in the glass shields were taken into account.

estimates which were made (hence their designation) and were used as starting values for more precise and accurate evaluations using non-linear regression⁵. It is important that $(k_R')_1$ and $(k_R')_2$ are respectively the least precise and accurate estimates of the heat transfer coefficient which we can make from the data. They are also subject to errors due to the refilling of the cells to make up for losses in D₂O due to electrolysis (see further below).

The next stage of the analysis is the evaluation of the differential lower bound heat transfer coefficient, $(k_R')_{11}$, throughout the time range of the measurement cycle. The subscript 11 here denotes that we are evaluating a differential coefficient and that we are considering a lower bound value. We have always used a second order central difference in the differentials of the temperature-time series. Fig. 3 shows the 11-point means, $(\overline{k_R'})_{11}$ of $(k_R')_{11}$ and the further 6-point means, $(\overline{\overline{k_R'}})_{11}$, of $(\overline{k_R'})_{11}$ for days 1 and 2 of the measurement cycles (there was no calibration of the system during this time).

We can use these coefficients in several ways to assess the performance of the instrumentation. Thus we can estimate a value of the true heat transfer coefficient from the mean of the values in Column 3, Table 1, or else, we can assume that this coefficient varies in the same way with time as does the lower bound value, Fig. 3⁶. We can then evaluate the differential rates of excess enthalpy generation using

$$\text{differential rate of excess enthalpy generation} = [(k_R')_2 - (k_R')_{11}] f_1(\theta) \quad (1)$$

$$\text{where } f_1(\theta) = (\text{cell temperature})^4 - (\text{bath temperature})^4 \quad (2)$$

(see also Appendix A). Fig. 4 gives the upper and lower tail distributions for Days 3-16 of the data sets (~4000 measurements) using the second set of assumptions i.e. allowing for the variation of $(k_R')_2$ with time. We can see that the data are consistent with a normal distribution of errors (due principally to errors in the temperature measurements) on which is superimposed a small steady state rate of excess enthalpy production (due to the reduction of electrogenerated oxygen and which accounts for the positive deviations of the plots from those for a purely normal distribution of errors especially in the region of the upper tail distribution).

We can also evaluate the corresponding rates of excess enthalpy production in a variety of ways. The methodology which we adopted in 1991-93 (and which we have also used here) is to evaluate the total excess enthalpy as a function of time and then to divide the relevant excess enthalpy by the time elapsed since the start of the measurement cycles (here $t = 0$ at the start of Day 3). The results for the two limiting sets of assumptions (i.e. allowing for the variation of $(k_R')_2$ with time or else using the single value of $(k_R')_2$ at $t = 86,400$ s) are given in Figs. 5A and B. We can see that the effects of the random variations in the differential lower bound heat transfer coefficient, Fig. 3, are gradually suppressed with increasing time, the rate approaching ~ 1.1 mW. The significance of this value is discussed below. At the same time, we can see that the magnitudes of the excess rates given in Figs. 5A and B are affected by the assumptions made about the time dependence of the

⁵ In the original investigation (1), (2), $(k_R')_2$ was estimated near $t = t_1$, in an attempt to eliminate one of the required interpolations. Although this procedure was explained in (2) (as was the subsequent application of non-linear regression, further explained in (6)), the basis of our estimates was clearly not understood e.g. see (7).

As we could not make the non-linear regression procedure "user friendly" with the computing power available to us in 1992, we based all further analyses on the application of linear regression (further explained in (8)). This was also the basis of the statistical treatments incorporated into the ICARUS-1 and ICARUS-2 packages (9) and is the methodology which we have adopted in all our investigations since October 1989.

⁶ A better assumption is to base this variation on the integral heat transfer coefficient, $(k_R')_{21}$, Fig. 6; see further below.

true heat transfer coefficient and that the evaluation requires very long integration intervals in order to reduce the effects of random errors to acceptable levels.⁷

The difficulties with the use of the differential heat transfer coefficient are avoided by using appropriate integral coefficients. We can distinguish two principal types denoted by the symbols $(k_R')_{i,j,l}$ where $i = 2$ signifies backward integration (i.e. typically starting from $t = T$, $t = t_2$ or $t = t_1$), $i = 3$ signifies forward integration (starting typically from $t = 0$, $t = t_1$ or $t = t_2$), $j = 5, 6, 7$ or 8 denotes the regions adjacent to $t = 0$, $t = t_1$ or $t = t_2$ or a combination of the regions adjacent to $t = t_1$ and $t = t_2$ and $l = 1$ signifies “lower bound” while $l = 2$ signifies “true”. In this scheme of description $i = 1$ stands for “differential” while omission of the central subscript, j , denotes that we are considering the whole measurement cycle $0 < t < T$. We can evidently base the evaluations on many versions of the heat transfer coefficient (which are all, of course, related to each other) so that it is necessary to standardise on the usage of a sensible subset of these coefficients.

Fig. 6 gives a comparison of the integral coefficients $(k_R')_{2l}$ (see equation A.8) and $(k_R')_{3l}$ (see equation A.9) with $(k_R')_{1l}$. It can be seen that if we exclude the first ~100 data points adjacent to $t = T$ in the evaluation of $(k_R')_{2l}$ and the first ~100 data points adjacent to $t = 0$ in the evaluation of $(k_R')_{3l}$ (time zones in which the benefits of the integral procedure are established), the variability of $(k_R')_{2l}$ and $(k_R')_{3l}$ is actually much smaller than that of $(k_R')_{1l}$.

The interrelation of these coefficients can be understood as follows:

the variation of $(k_R')_{1l}$ with time can be represented to the first order by

$$(k_R')_{1l} = (k_R')_{1l}^0 (1 - \gamma t) \quad (3)$$

where $(k_R')_{1l}^0$ is the value of $(k_R')_{1l}$ at $t = 0$. If the time dependence of the heat transfer coefficients is included in the differential equation (A.1) representing the calorimeter, we obtain for example, equation (A.13). If we now regard $f_l(\theta)$ as being constant throughout a measurement cycle (which is a rough approximation for the case of the “lower bound heat transfer coefficients” in the absence of a calibration pulse) we obtain

$$(k_R')_{2l} = (k_R')_{2l}^0 \left[1 + \frac{\gamma(T - t)}{2} \right] \quad (A.14)$$

and

$$(k_R')_{3l} = (k_R')_{3l}^0 \left[1 - \frac{\gamma t}{2} \right] \quad (A.15)$$

where $(k_R')_{2l}^0$ and $(k_R')_{3l}^0$ are respectively the values of $(k_R')_{2l}$ and $(k_R')_{3l}$ at $t = T$ and $t = 0$. It follows that the slopes of the plots of $(k_R')_{2l}$ and $(k_R')_{3l}$ versus time are roughly one half of the corresponding plot of $(k_R')_{1l}$ and hence those for $(k_R')_{2l}$ and $(k_R')_{3l}$ as is shown by Fig. 6.

An alternative approach towards the evaluation of accurate values of the heat transfer coefficients can be based on the application of equations such as (A.8), (A.9), (A.11) and (A.12). Such evaluations give $(k_R')_{i,j,l}^0$, which are the intercepts at the chosen origins of the abscissae of $C_p M d(\Delta\theta)/dt$, (note that these intercepts are independent of the value of $C_p M$); the water equivalents are derived from the slopes of the plots.

⁷ The evaluations carried out in 1991-93 were restricted to the first measurement cycle (with allowance for the variation of the true heat transfer coefficient with time as in Fig. 5A). This led to the erroneous conclusions that the accuracy of $(k_R')_2$ was about one order of magnitude below the precision of $(k_R')_1$ and that the rates of excess enthalpy production were about one tenth of the rate which could be attributed to the reduction of electrogenerated oxygen (in turn attributed to a degassing of this species from the solution adjacent to the cathode by the electrogenerated bubbles of deuterium). In fact, the accuracy of $(k_R')_2$ must be comparable to the precision of $(k_R')_1$.

Figs. 7A, 7B and 8 illustrate the determination of $(k_R')_{261}^0$ and $(k_R')_{262}^0$ with the start and end of the integration procedures being set at $t = t_2$ and $t = t_1$, (for Figs. 7A and 8) and $t = T$ and $t = t_1$, for Fig. 7B. It should be noted that the origin for the plots in Figs. 7A and 8 is well-defined near $t = t_2$ (where $d\Delta\theta/dt \sim 0$) which is the point in time at which we require the heat transfer coefficients. The small values of the abscissae should be especially noted as should the degradation of the performance when setting the origin at $t = T$ (Fig. 7B) compared to $t = t_2$ (Fig. 7A). The evaluation of these heat transfer coefficients became one of the targets of the ICARUS procedures; the values determined for these sets of measurements are listed in Columns 4-7 of Table 1. The values of $(k_R')_{261}^0$ determined in this way, Column 4 of Table 1, are somewhat larger than the values of $(k_R')_{21}$ determined at the same point in time listed in Column 8. This is expected as the extrapolations determine $(k_R')_{11}$ at $t = t_2$ (rather than $(k_R')_{21}$). We would expect that the means of $(k_R')_{261}^0$ and $(k_R')_{262}^0$ (Columns 4 and 6 of Table 1) to be close to the means of $(k_R')_1$ and $(k_R')_2$ (Columns 2 and 3 of Table 1). Table 1 shows that this is indeed the case.

Columns 9-12 list the values of $(k_R')_{361}^0$ and $(k_R')_{362}^0$ (and the associated values of the water equivalents and statistics) based on the forward integration of the data from $t = t_1$. Such evaluations are unsatisfactory from several points of view. In the first place, the origin of the plots required for the derivation of these coefficients is not well defined ($d\Delta\theta/dt \neq 0$ as $t \rightarrow t_1$); secondly, the range of the extrapolations is too long; thirdly, the values of the abscissae are large and comparable to the ordinates. It is not surprising therefore that the determination of the heat transfer coefficients using these particular procedures fails (see Columns 9-12 of Table 1). It was pointed out that evaluations near the end of the calibration pulse would be more satisfactory than those close to the start of this pulse, $t = t_1$, as can be seen from a comparison of Columns 13-16 with 9-12 of Table 1. As the time at which the derived heat transfer coefficients might apply was uncertain, the procedures based on the forward integration of the data sets was excluded from the ICARUS Systems⁸. However, the evaluation of $(k_R')_{31}$ near $t = t_2$, Column 17 of Table 1, was included to serve as a check on the procedures.

It is important to point out a major limitation of these analyses. It can be seen that the time-dependence of the evaluated coefficients (e.g. see Figs. 3 and 6) is entirely in accord with the expected behaviour, equations (A.1) and (A.2). It was therefore hoped that the derived values of C_pM could be used to provide the minor corrections to the level of the electrolyte to allow the presentation of the derived heat transfer coefficients on a single plot versus the electrolyte content of the cells. However, this objective could never be realised. The water equivalents are derived from the slopes of the plots such as those in Figs. 7A-8. Inevitably, this introduces errors into the estimates of C_pM and the accuracy of the heat transfer coefficients is insufficient to allow the correction of the heat transfer coefficients for changes in the electrolyte level between successive measurement cycles.⁹

In the full text of the paper dealing with this subject (10) we have covered additionally;

- (i) the response of the system following the “topping up” of the cells to make up for losses of D_2O due to electrolysis in the previous measurement cycle (rather than the responses due to the calibration pulse). We have shown that the heat transfer coefficients $(k_R')_{251}^0$ and $(k_R')_{252}^0$ have

⁸ However, we believe that the evaluations carried out by the group at the New Hydrogen Energy Laboratories have been based on such forward integrations.

⁹ A level controller was added to the ICARUS-2 instrumentation and it was estimated that this would reduce the errors in the heat transfer coefficients to $\pm 0.04\%$. However, these level controllers were never used. Level controllers for the water baths surrounding the calorimeters were also never constructed. The ICARUS-2 system was also designed to use the cell currents to drive the calibration heaters (so as to remove all possibility of errors introduced by differences in the power outputs delivered to the cell and calibration heaters). However, this modification of the experiment was never used.

- only limited accuracy using the methodology as currently developed; however, this approach requires further investigation;
- (ii) the evaluation of $(k_R')_{271}^0$; however, the determination of the heat transfer coefficient at $t = T$ was not of any particular significance and this particular evaluation was not included in the data evaluation package (9);
 - (iii) assessments of the errors in the various evaluations of the heat transfer coefficients. It was shown that the assessment of errors in the integral heat transfer coefficients can become limited by the cut-off limit of the interpretation i.e. if the errors are less than $\pm 0.00001 \times 10^9 (k_R')$.¹⁰

In common with other investigations (e.g. see (2), (8)) it was observed that the relevant standard deviations are so small that it should be possible to make thermal balances to within 0.1 mW for a typical input of 1 W. The analysis presented here shows that such balances should be made using the integral heat transfer coefficients $(k_R')_{22}$ estimated at $t = 0$. Table 2 illustrates such a calculation made using the seven applicable measurement cycles. The rate of excess enthalpy generation shown in Column 8 is 0.0011 W and these rates are also shown in Figs. 5A and B in comparison with those calculated using the differential heat transfer coefficients $(k_R')_{12}$. These rates, are approximately equal to the rates which may be calculated for the reduction of electrogenerated oxygen present in the cell (compare (12)). It will be clear that we must regard these rates as being constant during each measurement cycle, an assumption which is evidently justified. The data shown in Column 8 of Table 2 confirm that such rates can be estimated to within ± 0.0001 W which requires that the accuracy of the true integral heat transfer coefficient must be nearly equal to the precision of the lower bound values i.e. that the errors are $\pm 0.01\%$.

Discussion

The material presented in this paper shows that exact data analyses should be based on the evaluation of the true integral heat transfer coefficient, $(k_R')_{22}$ coupled to the integral lower bound heat transfer coefficient, $(k_R')_{21}$. Accurate and precise estimates of these coefficients can be obtained from $(k_R')_{262}^0$ and $(k_R')_{261}^0$, the values which apply to the calibration period $t_1 < t < t_2$. The procedure which has been illustrated here was part of that incorporated into the ICARUS-System methodology (9).

The accuracy of $(k_R')_{22}$ and the precision of $(k_R')_{21}$ are very nearly equal with errors of $\sim \pm 0.01\%$. Such errors can in fact be estimated from the errors in the temperature measurements coupled to the averaging procedures described in this paper. The precision and accuracy which can be achieved should be compared to the rather wild statements which have been made in the literature about the accuracy of this type of instrumentation. Such statements can be seen to be the outcome of inadequate experiments coupled to inadequate and incomplete interpretations.

It will be seen that the application of the integral heat transfer coefficients requires that the rates of any excess enthalpy generation be constant in time. In turn, this requires that the experiments be carried out using suitable "blank systems". If the rates of excess enthalpy generation vary with time, we will inevitably conclude that the instrumentation has enhanced errors. Moreover, such a conclusion will apply to any calorimetric system which we might propose. The lack of execution of "blank experiments" is undoubtedly a contributory factor to the confusing statements which have been made in the literature.

The wild statements which have been made in the literature extend also to the effects of the reduction of electrogenerated oxygen. These rates can be estimated perfectly adequately by carrying

¹⁰ It was noted that the individual values of the integral heat transfer coefficients are not statistically independent as the process of integration uses all the preceding values of the raw data. A method of avoiding this difficulty by sectioning the data sets was illustrated (10).

out suitable “blank experiments”. We note that if the precision and accuracy of the instrumentation is lowered to say $\pm 1\%$, it will then be impossible to measure such rates; equally, it will be impossible to monitor the build-up of excess enthalpy generation until this has reached specific rates in the range $0.1\text{--}1\text{ Wcm}^{-3}$. Such deficiencies are no doubt at the root of many of the further confusing results and statements which have been made in the literature. In this connection we note that correctly designed isoperibolic calorimeters should be classified as “ideal reactors” using the nomenclature of Chemical Reaction Engineering (13). While it would be possible to design other types of reactor (such as flow reactors) to satisfy the criteria of “ideal plug flow”, such research has only recently been initiated (14). Existing designs fall under the heading of “dispersive plug flow” and such designs are undoubtedly non-ideal.

We observe also that the calibration of the cells could be based equally well on the determination of the lower bound heat transfer coefficients for suitable “blank experiments”. The use of such coefficients in the data analysis for Pd-based cathodes in D_2O -based electrolytes would then automatically discriminate against the contribution of the reduction of electrogenerated oxygen to the total rates of excess enthalpy generation.

Appendix

It has been established that at low to intermediate cell temperatures (say $30^\circ < \theta < 80^\circ$) the behaviour of the calorimeters is modelled adequately by the differential equation

$$C_p M (d\Delta\theta/dt) = [E_{\text{cell}}(t) - E_{\text{thermoneutral, bath}}] I + Q_R(t) + \Delta QH(t-t_1) - \Delta QH(t-t_2) - (3I/4F[P/\{P^*-P\}])[C_{p,D_2O,g} - C_{p,D_2O,l})\Delta\theta + L] - (k_R')\theta_{\text{bath}}^3[1-\gamma t] \{f_1(\theta)/\theta_{\text{bath}}^3 + 4\phi\Delta\theta\}$$

change in the enthalpy content of the calorimeter
enthalpy input due to electrolysis
rate of excess enthalpy generation

calibration pulse
rate of enthalpy removal by the gas stream with $E_{\text{thermoneutral}}$ referred to the bath temperature

time dependent heat transfer coefficient
effect of radiation
effect of conduction

(A.1)

With the calorimeters supplied with the ICARUS Systems, the conductive contribution to heat transfer is very small. This term could therefore be “lumped” into the radiative term by allowing for a small increase in the radiative heat transfer coefficient:

$$\text{Radiative heat transfer} = (k_R')^0 [1-\gamma t] [(\theta_{\text{bath}} + \Delta\theta)^4 - \theta_{\text{bath}}^4] \quad (\text{A.2})$$

The values of the pseudoradiative “heat transfer coefficient, $(k_R')^0 [1-\gamma t]$, derived are close to those calculated from the Stefan-Boltzmann coefficient and the radiative surface area. If the time dependence of the heat transfer coefficient is not included explicitly in equation (A.2) then

$$\text{Radiative heat transfer} = (k_R') [(\theta_{\text{bath}} + \Delta\theta)^4 - \theta_{\text{bath}}^4] \quad (\text{A.3})$$

where the pseudoradiative heat transfer coefficient, (k_R') , now shows a weak time-dependence.

The simplest starting point is to assume that there is no excess enthalpy generation in the calorimeter and to evaluate a corresponding “differential lower bound heat transfer coefficient” at a time just before the end of the calibration pulse, $t = t_2$:

$$(k_R')_1 = [(E_{\text{cell}}(t) - E_{\text{thermoneutral, bath}})I - \Delta H_{\text{evap}}(t) - C_p M (d\Delta\theta/dt) + \Delta QH(t-t_1)] / f_1(\theta) \quad (\text{A.4})$$

This was the first heat transfer coefficient used in our investigations, hence the designation $(k_R')_1$. It will be apparent that the differential lower bound heat transfer coefficient $(k_R')_{11}$, may be evaluated at other points of the measurement cycle, by changing the enthalpy input due to the calibration pulse to

$$\Delta QH(t-t_1) - \Delta QH(t-t_2) \quad (\text{A.5})$$

It is next necessary to evaluate a “true heat transfer coefficient”. The simplest procedure giving $(k_R')_2$ near the end of the calibration period at $t=t_2$ is obtained by including the calibration pulse

$$(k_R')_2 = \{ \Delta Q + [E_{\text{cell}}(\Delta\theta_2, t_2) - E_{\text{cell}}(\Delta\theta_1, t_2)]I - \Delta H_{\text{evap}}(\Delta\theta_2, t_2) + \Delta H_{\text{evap}}(\Delta\theta_1, t_2) - C_p M [(d\Delta\theta/dt)_{\Delta\theta_2, t_2} - (d\Delta\theta/dt)_{\Delta\theta_1, t_2}] \} / f_2(\theta) \quad (\text{A.6})$$

where we now have

$$f_2(\theta) = [\theta_{\text{bath}} + (\Delta\theta_2, t_2)]^4 - [\theta_{\text{bath}} + (\Delta\theta_1, t_2)]^4 \quad (\text{A.7})$$

It can be seen that we need to estimate the cell potential, the cell temperature and the differential of this temperature at the time $t=t_2$ which would have been reached in the absence of the calibration pulse [see footnote (A.1)]

Footnote (A.1) This evaluation was carried out in a somewhat different manner in the initial studies (1), (2) (10) in an attempt to avoid the disadvantages of such interpolation procedures. The values of $(k_R')_{11}$ and $(k_R')_2$ obtained were used as starting values for the non-linear regression procedure used at that time (2). As we could not make this procedure “user friendly” with the computing power then available to us and as, more especially, the methodology which we adopted was evidently not understood (7). (for a further example of such misunderstanding see (3)) we adopted the methodology described in the present paper. This methodology was also the basis of the ICARUS Systems (9).

As is explained in the main text, it is preferable to base the evaluation of the “raw data” on the integrals of the enthalpy input and of the temperature functions rather than to lower the precision and accuracy of the evaluations by using the differentials of the inherently noisy temperature-time series.

For the backward integrals starting from $t \simeq T$ we obtain

$$(k_R')_{21} = \frac{\int_T^t \text{net enthalpy input } (\tau) d\tau}{\int_T^t f_1(\theta) d\tau} - \frac{C_p M [\Delta\theta(t) - \Delta\theta(T)]}{\int_T^t f_1(\theta) d\tau} - \frac{Q_f [t - T]}{\int_T^t f_1(\theta) d\tau} \quad (\text{A.8})$$

while forward integration from the start of the measurement cycle

$$(k_R')_{31} = \frac{\int_0^t \text{net enthalpy input } (\tau) d\tau}{\int_0^t f_1(\theta) d\tau} - \frac{C_p M [\Delta\theta(t) - \Delta\theta(0)]}{\int_0^t f_1(\theta) d\tau} - \frac{Q_f [t]}{\int_0^t f_1(\theta) d\tau} \quad (\text{A.9})$$

The evaluation of the heat transfer coefficients applicable to particular time regions ($j = 5, 6, 7, 8$) simply requires changes in the lower limits of the relevant integrals.

The evaluation of the “true heat transfer coefficients” requires the combination of the enthalpy inputs in equations (A.8) and (A.9) with the thermal inputs made at one or a series of points. This can be carried out in a number of ways; we confine attention here to the procedure originally suggested in the Handbook for the ICARUS - 1 System (9). If we consider $(k_R')_{362}$ and if we make a thermal balance just before the application of the calibration pulse, then if the system has relaxed adequately so that we can set $d\Delta\theta/\approx 0$

$$0 = [\text{Net enthalpy input } (t_1)][t - t_1] + Q_d[t - t_1] - (k_R')_{362} \{[(\theta_{\text{bath}} + \Delta\theta(t_1))^4 - \theta_{\text{bath}}^4]\}[t - t_1] \quad (\text{A.10})$$

Combination with equation (A.9) (with the appropriate change in the lower limit of the integration) gives

$$(k_R')_{362} = \frac{\int_{t_1}^t \text{net enthalpy input } (\tau) d\tau - [\text{net enthalpy input } (t_1)][t - t_1]}{\int_{t_1}^t f_1(\theta) d\tau} - \frac{C_p M [\Delta\theta(t) - \Delta\theta(t_1)]}{\int_{t_1}^t f_1(\theta) d\tau} \quad (\text{A.11})$$

The corresponding equation for $(k_R')_{262}$ follows from (A.11) on replacing t_1 by t_2 . It is convenient to write all the equations for the determination of the relevant heat transfer coefficients in the “straight line form” e.g.

$$\begin{aligned} & \frac{\int_{t_2}^t \text{net enthalpy input } (\tau) d\tau - [\text{net enthalpy input } (t_1)][t - t_2]}{\int_{t_2}^t f_1(\theta) d\tau} \\ &= \frac{C_p M [\Delta\theta(t) - \Delta\theta(t_2)]}{\int_{t_2}^t f_1(\theta) d\tau} + (k_R')_{262}^0 \end{aligned} \quad (\text{A.12})$$

where $(k_R')_{262}^0$ can be seen to be the value of the integral heat transfer coefficient at $t = t_2$. The value of t_2 should be chosen to be the mid-point of the measurement cycle as $(k_R')_{262}^0$ is the most useful (and well defined) value of the true heat transfer coefficient. It should be noted that extrapolations such as (A.12) automatically remove the effects of $C_p M$ on the value of the derived heat transfer coefficient (a desirable feature because the water equivalents of the cells have the highest errors).

The integral lower bound heat transfer coefficient, $(k_R')^0_{261}$ (equation (A.8) with T replaced by t_2) and the integral true heat transfer coefficient, $(k_R')^0_{262}$, (equation (A.12)) were the “target procedures” for the ICARUS -style evaluations of the experimental data (9).

It should be noted that the definitions of the integral heat transfer coefficients given in this Appendix have regarded these coefficients as being constant in time whereas we would, in fact, anticipate a weak time dependence e.g. equation (A.2) or Fig.6. This weak time-dependence causes an equally weak time-dependence of the derived heat transfer coefficients. Use of the more exact equation (A.2) gives for example for the derived values of $(k_R')_{21}$ in (A.8)

$$(k_R')_{21} = (k_R')^0_{21} [1 - \gamma(t-T) + \gamma \int_T^t \int_T^t f_1(\theta) d\tau d\tau / \int_T^t f_1(\theta) d\tau] \quad (A.13)$$

where $(k_R')^0_{21}$ is the value of $(k_R')_{21}$ at $t = T$. An ultimate test of the validity of the representation of the calorimeters by the differential equation (A.1) is therefore the question of whether the heat transfer can be represented by a single time-dependence coefficient, here $(k_R')^0_{21}$. This question is discussed further in the main text.

We also note that if we regard $f_1(\theta)$ as being constant throughout the measurement cycle (which is a rough approximation for the case of the “lower bound heat transfer coefficients”) then (A.13) becomes

$$(k_R')_{21} = (k_R')^0_{21} [1 + \gamma(T - t)/2] \quad (A.14)$$

Similarly, we obtain

$$(k_R')_{31} = (k_R')^0_{31} [1 - \gamma/2] \quad (A.15)$$

where $(k_R')^0_{31}$ is now the value of $(k_R')_{31}$ at $t = 0$. It follows that the slopes of the plots of $(k_R')_{21}$ and $(k_R')_{31}$ versus time are roughly one half of the plot of $(k_R')_{11}$ versus time (cf. Fig. 6)

For a more complete discussion see (15), (16).

References

- 1) M. Fleischmann, S. Pons and M. Hawkins, J. Electroanal. Chem., 261 (1989) 301; 263 (1989) 187.
- 2) M. Fleischmann, S. Pons, M.W. Anderson, L. J. Li and M. Hawkins, J. Electroanal. Chem., 287 (1990) 293
- 3) Frederick T. Wagner, Thomas E. Moylan, Michael E. Hayden, Ulrike Narger and James L. Booth, J. Electroanal. Chem., 295 (1990) 393.
- 4) Wilford N. Hansen, Proceedings of the Second Conference on "Cold Fusion", Conference Proceedings of the Italian Physical Society, Bologna; Editors: Tullio Bressani, Emilio Del Giudice and Giuliano Preparata, 33 (1991) 491 ; ISBN 88-7794-045-X.
See also Michael E. Melich and Wilford N. Hansen, Proceedings of the Third International Conference on "Cold Fusion, Universal Academy Press, Frontiers of Science Series No 4 Tokyo ; Editor H. Ikegami (1993) 397 ; ISBN 4-946493-12-6.
- 5) Wilford N. Hansen, see this Meeting.
- 6) M. Fleischmann and S. Pons, J. Electroanal. Chem., 332 (1992) 33.
- 7) R. H. Wilson, J. W. Bray, P. G. Kosky, H. B. Valil and F. G. Will, J. Electroanal. Chem., 332 (1992) 1.
- 8) M. Fleischmann, S. Pons, Monique Le Roux and Jeanne Roulette, Trans. Fusion Technol., 26 (1994) 323.
- 9) The ICARUS Systems; Isoperibolic Calorimetry: Acquisition, Research and Utilities System, Version 1 (December 1993), Low Power Measuring System for Three Cells, Technova Inc., 13th Floor, Fukoku Seimei Building, 2-2-2 Uchisaiwai-cho, Chiyoda-Ku, Tokyo 100, Japan.

ICARUS -2 ; Isoperibolic Calorimetry : Acquisition, Research and Utilities System. Document Version 2.0 (February 1995). Technova Inc., 13th Floor, Fukoku Seimei Building, 2-2-2 Uchisaiwai-cho, Chiyoda-Ku, Tokyo 100, Japan.
- 10) M. Fleischmann and M. H. Miles, "Our Penultimate Papers on the Isoperibolic Calorimetry of the Pt/D₂O Systems ; Part I : the Pt/D₂O Blank System", submitted for publication.
- 11) Martin Fleischmann and Stanley Pons in Editor H. Ikegami, "Frontiers of Cold Fusion" Proceedings of the Third International Conference on Cold Fusion, Universal Academy Press, Tokyo, 100-91, Japan, Frontiers of Science Series No 4 ISSN 0915-8502, ISBN 4-946443-12-6 (1993), 47.
- 12) Fritz G. Will, J. Electroanal. Chem., 426 (1997) 177.
- 13) O. Levenspiel, "Chemical Reaction Engineering" (1972) John Wiley, London.
- 14) M.H. Miles, see this Meeting.

- 15) M.H. Miles, M. Fleischmann and M.A. Imam, Report NRL/MR/6320-01-8526, Naval Research Laboratory, Washington, DC 20375-5320, March 2001.
- 16) S. Szpak and P.A. Mosier-Boss, Technical Report, Volume 2, SPAWAR Systems Center, San Diego, February 2002.

TABLE I Summary of some important values of the heat transfer coefficients.

[illegible]

Table 2								
Thermal balances using the integral heat transfer coefficient based on backward integration of the data sets.								
1	2	3	4	5	6	7	8	
Days	input $d\tau$	$10^{-9} \int_1(\theta)dt$	$10^9(k_R')_{262}$	$10^9(k_R')_{262}$	thermal	output	equivalent	
	/J	K ⁴ s	/WK ⁻⁴	/WK ⁻⁴	output	input $d\tau$	excess rate	
			near $t \approx t_2$	near $t \approx 0$	/J	/J	/W	
3 and 4	140501.1	226640.2	0.6187	0.6195	140403.6	181.313	0.00109	
5 and 6	141849	228529.4	0.62034	0.62114	141948.8	182.824	0.00110	
7 and 8	141774.4	228484.3	0.62021	0.62101	141891	182.788	0.00110	
9 and 10	143166.6	230672.1	0.61995	0.62075	143189.7	184.538	0.00111	
11 and 12	143956.7	231844.2	0.62043	0.62123	144028.6	185.476	0.00112	
13 and 14	145003.8	233772.4	0.62011	0.62091	145151.6	187.018	0.00113	
15 and 16	144858	233584.8	0.61974	0.62054	144948.7	186.868	0.00113	

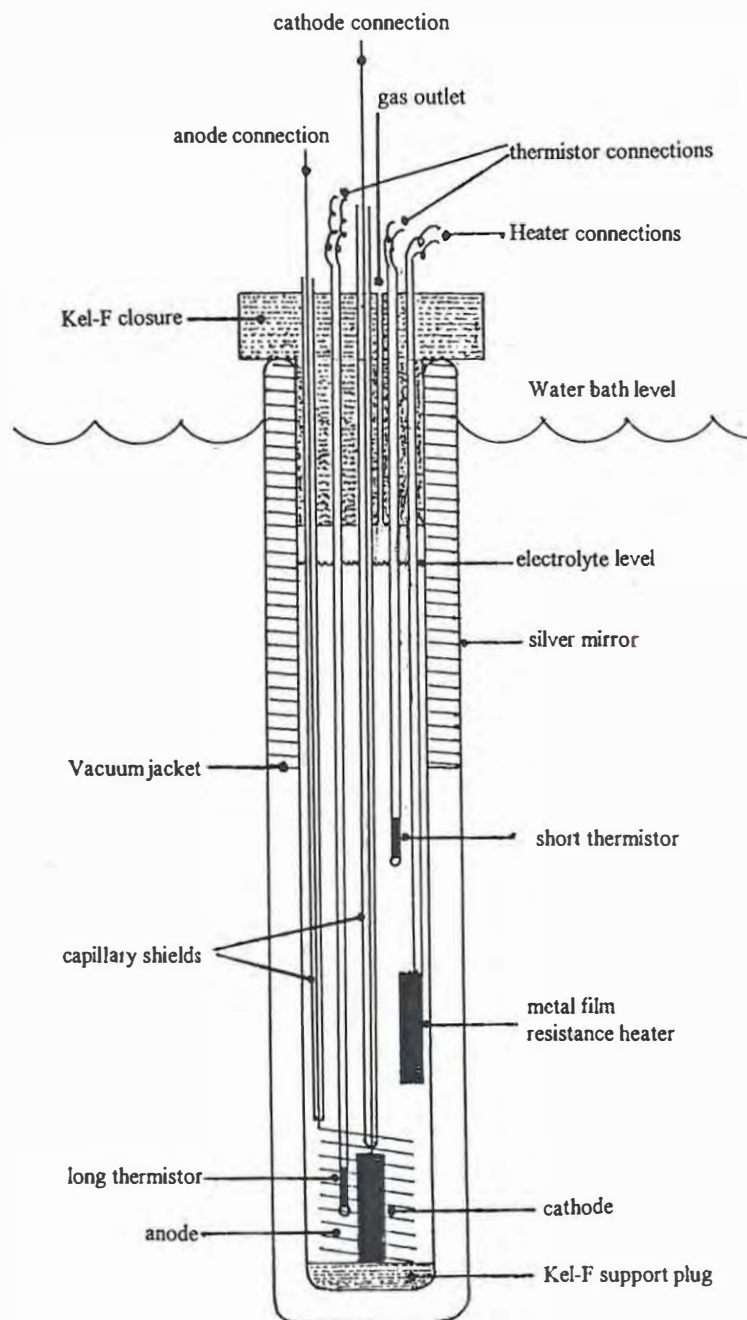


Fig. 1 The Isoperibolic Calorimetric Cell.

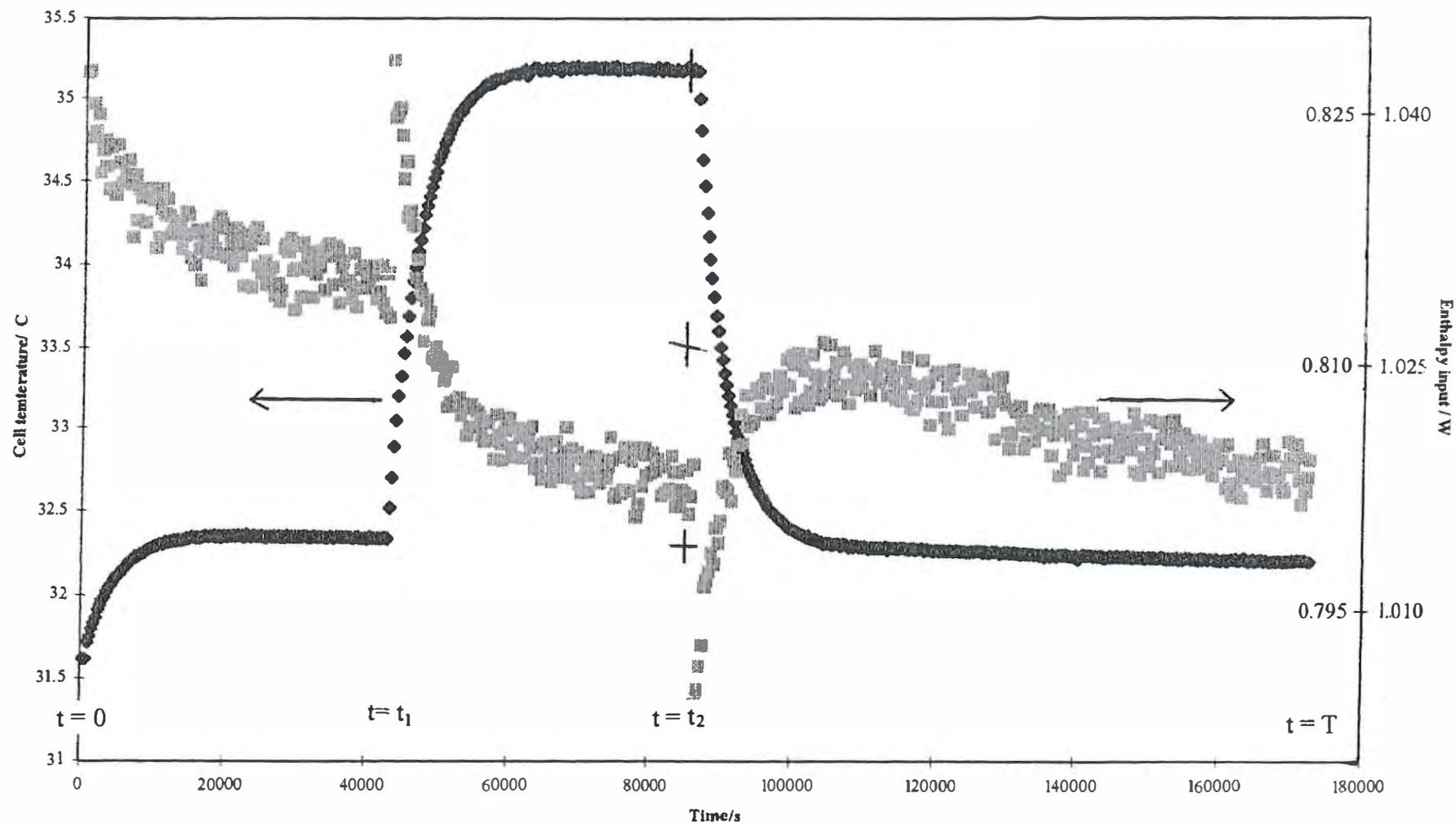


Fig. 2 Plot of the "raw data" for days 9 and 10 of the "blank experiment".

Pt cathode ($\phi = 1\text{mm}$, $\ell = 2\text{cm}$) polarised at 0.2A in $0.1\text{ M LiOD}/\text{D}_2\text{O}$.

Estimates of the pseudo-radiative lower bound heat transfer coefficient, $(k_R')_1$, and of the pseudo-radiative true heat transfer coefficient, $(k_R')_2$, can be made near the end of the calibration period at $t = t_2$.

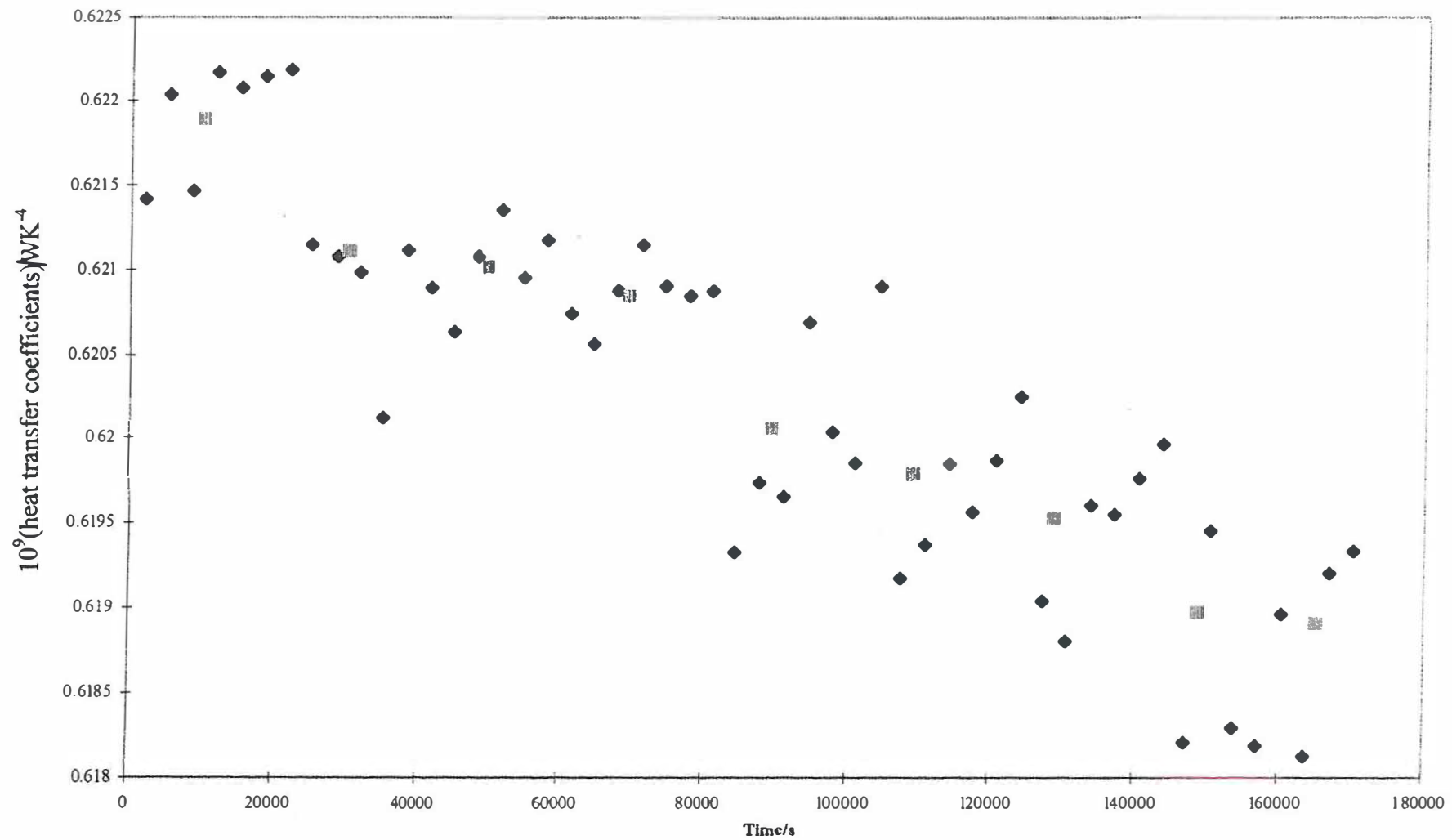


Fig. 3 The values of $(\overline{k_R})_{11}$ \diamond , and of $(\overline{k_R}')_{11}$ \square , for days 1 and 2 of the measurement cycles.

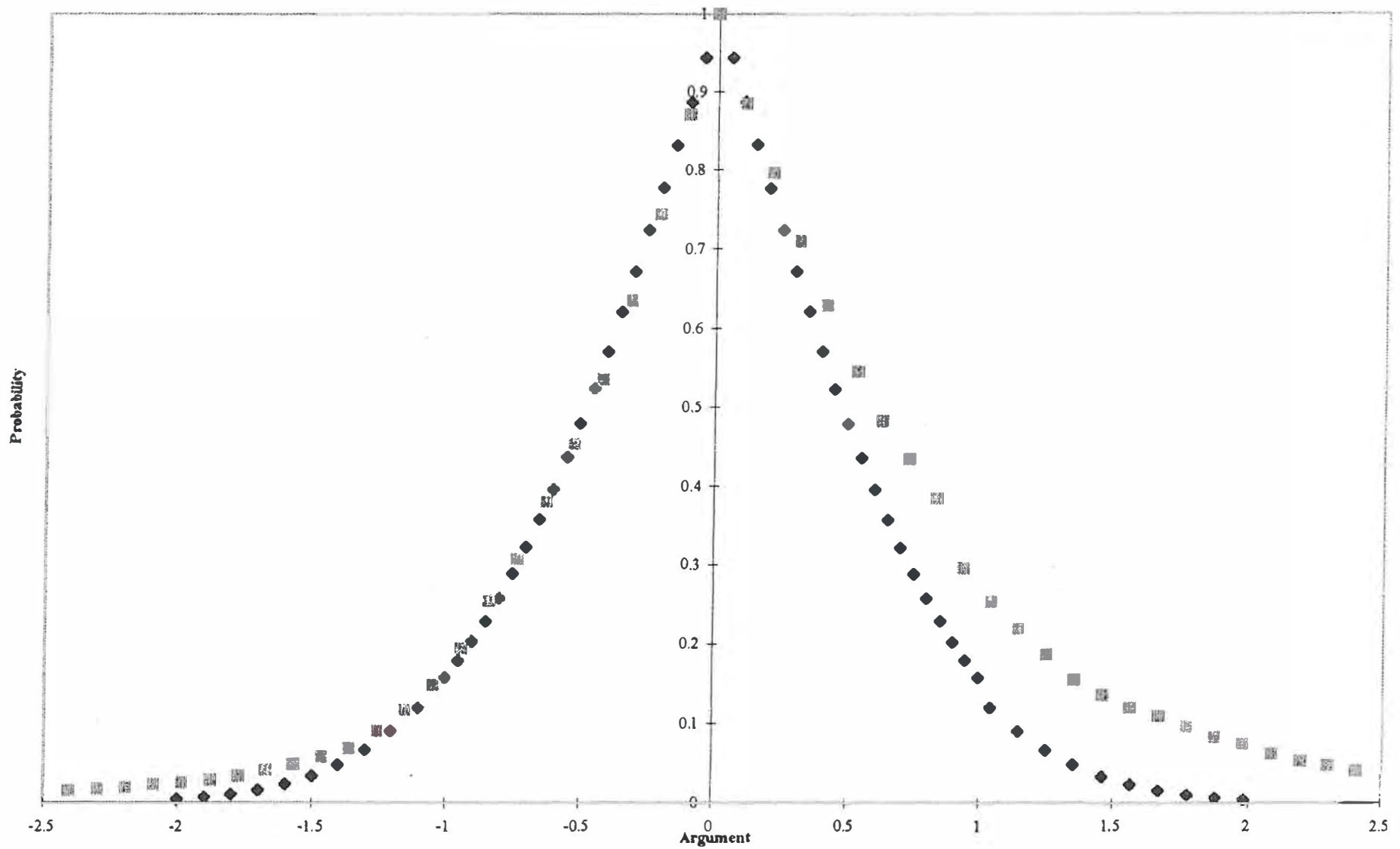


Fig. 4 The upper and lower tail distributions of the differential rates of excess enthalpy generation for days 3-16 of the measurement cycles, ▣; comparison with a normal distribution of errors, ◆.

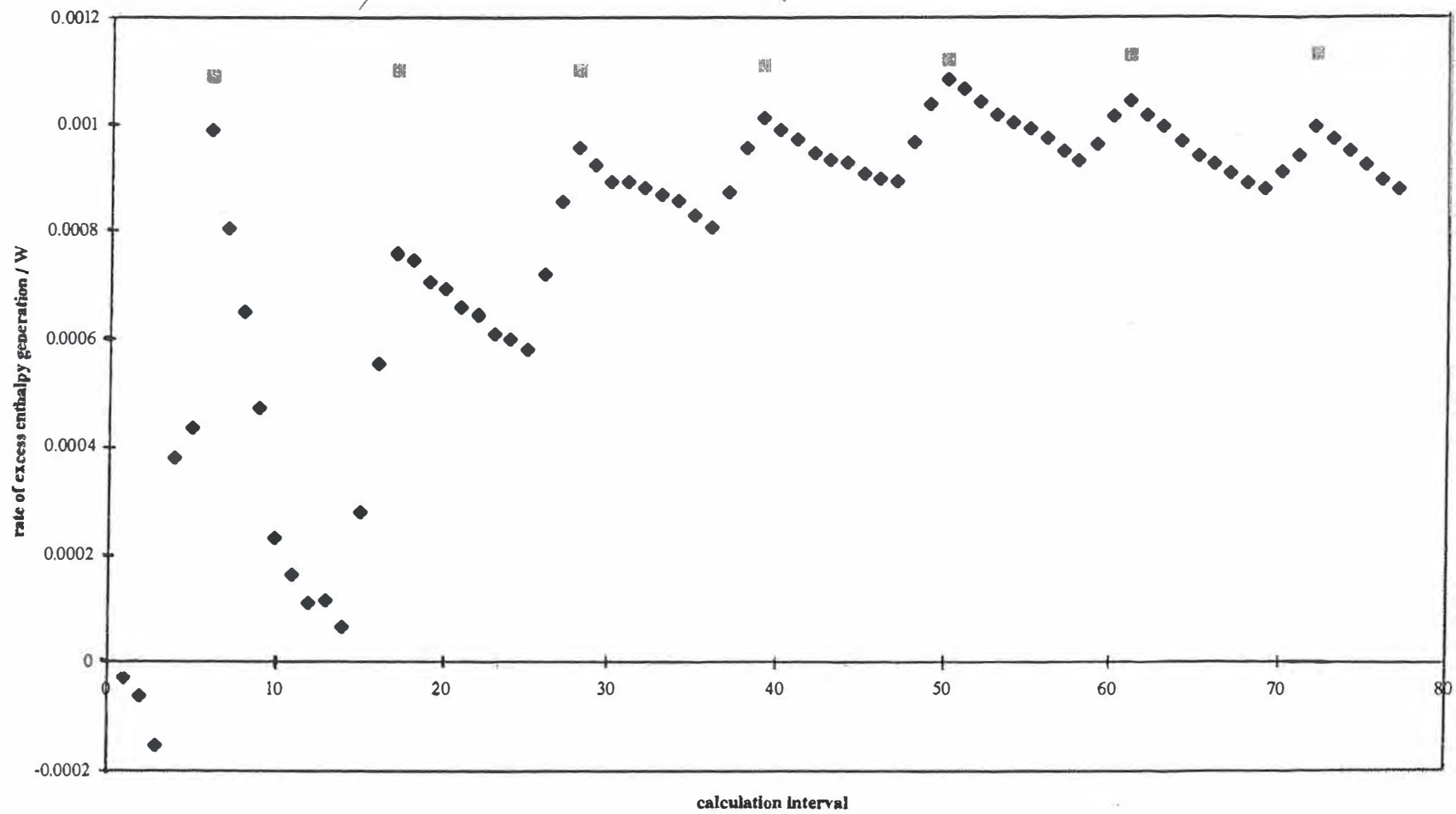


Fig. 5A The differential rates of excess enthalpy generation calculated with a true heat transfer coefficient varying with time, ◆. The figure also shows rates calculated using the integral value of the heat transfer coefficient ◻, see table 2 below.

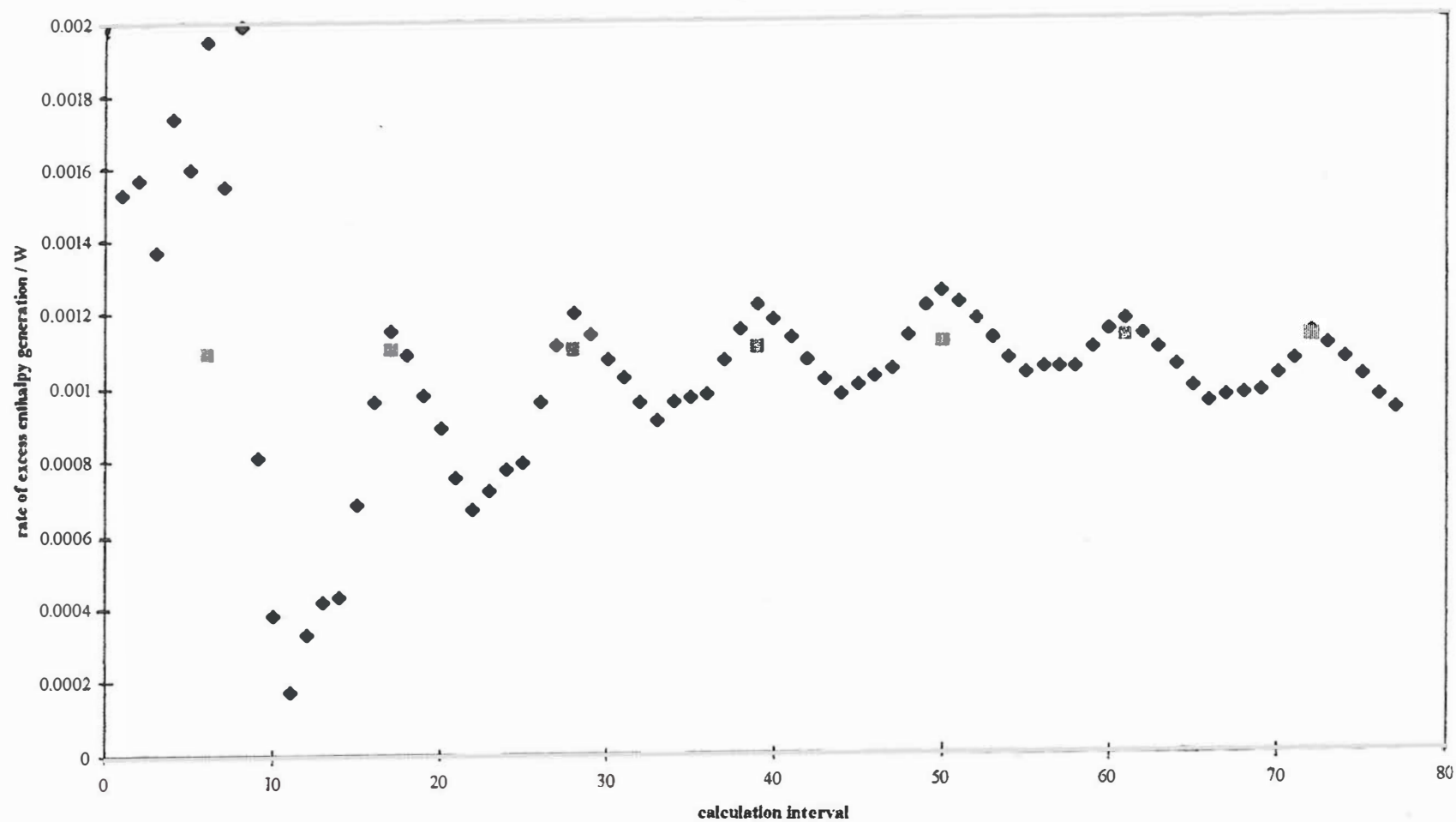


Fig. 5B The differential rates of excess enthalpy generation calculated using a single value of the true heat transfer coefficient at $t = 86,400\text{s}$, \blacklozenge . The figure also shows rates calculated using the integral value of the heat transfer coefficients, \blacksquare , see Table 2 below.

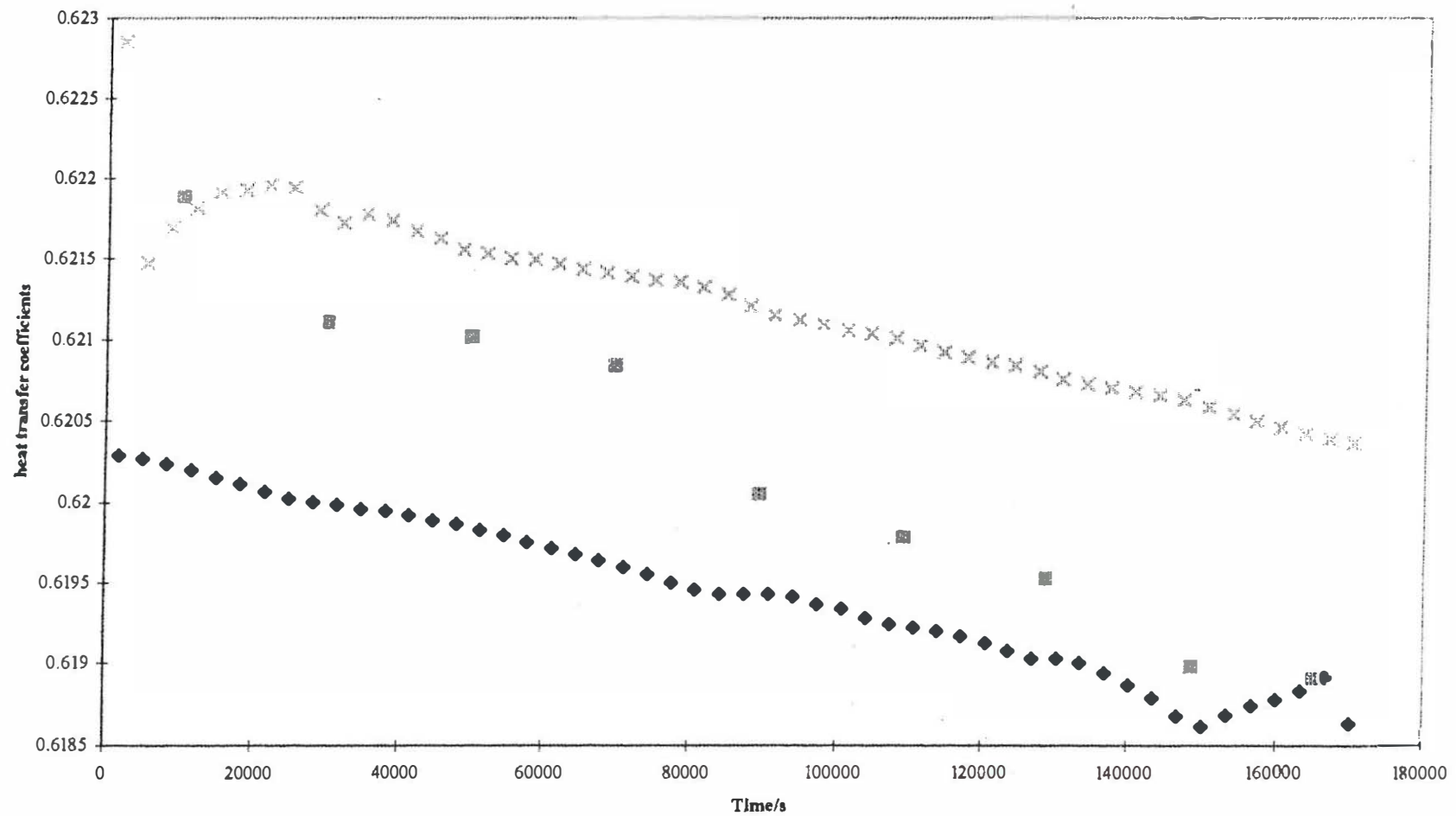


Fig. 6 Comparison of the variation with time of the integral heat transfer coefficients, $(k_R')_{31}$ and $(k_R')_{21}$ x, ♦, with the differential lower bound heat transfer coefficient, $(\overline{k_R'})_{11}$ ■ Days 1 and 2 of the measurement cycles.

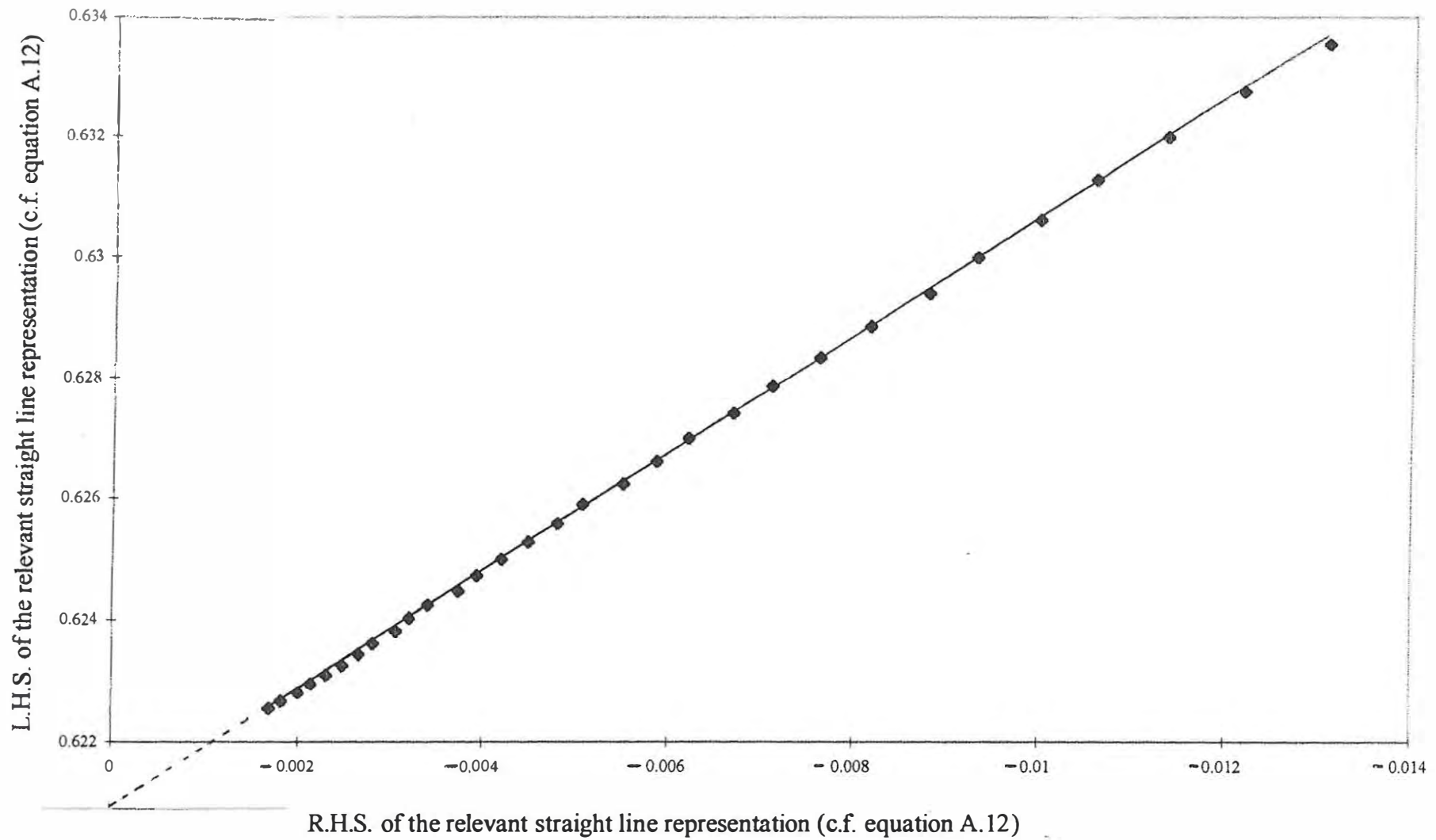
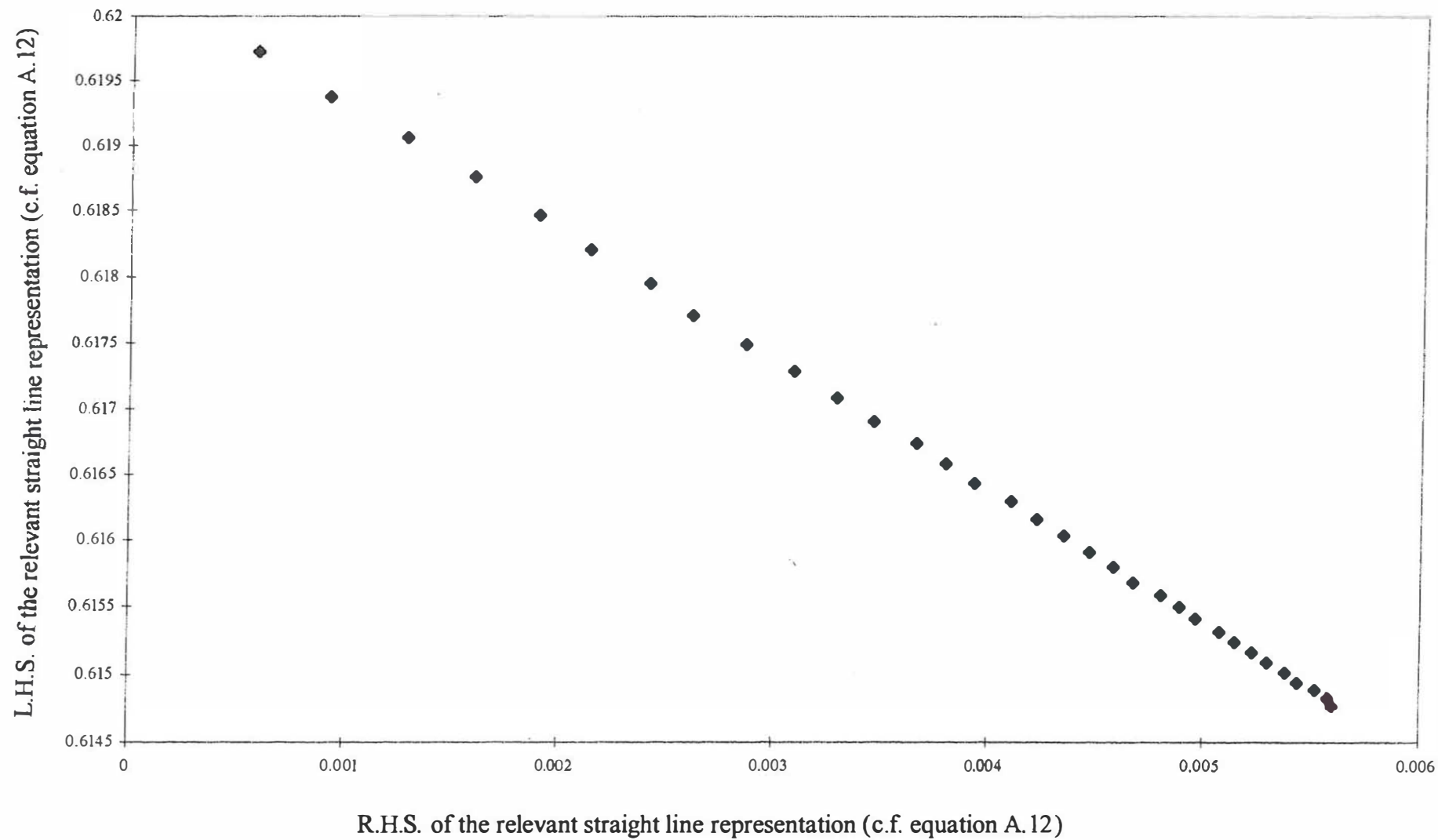


Fig. 7A Evaluation of $(k_R')_{261}^0$ and C_{pM} for Days 9 and 10 of the measurement cycles. Origin for the integrations set at $t = t_2$.



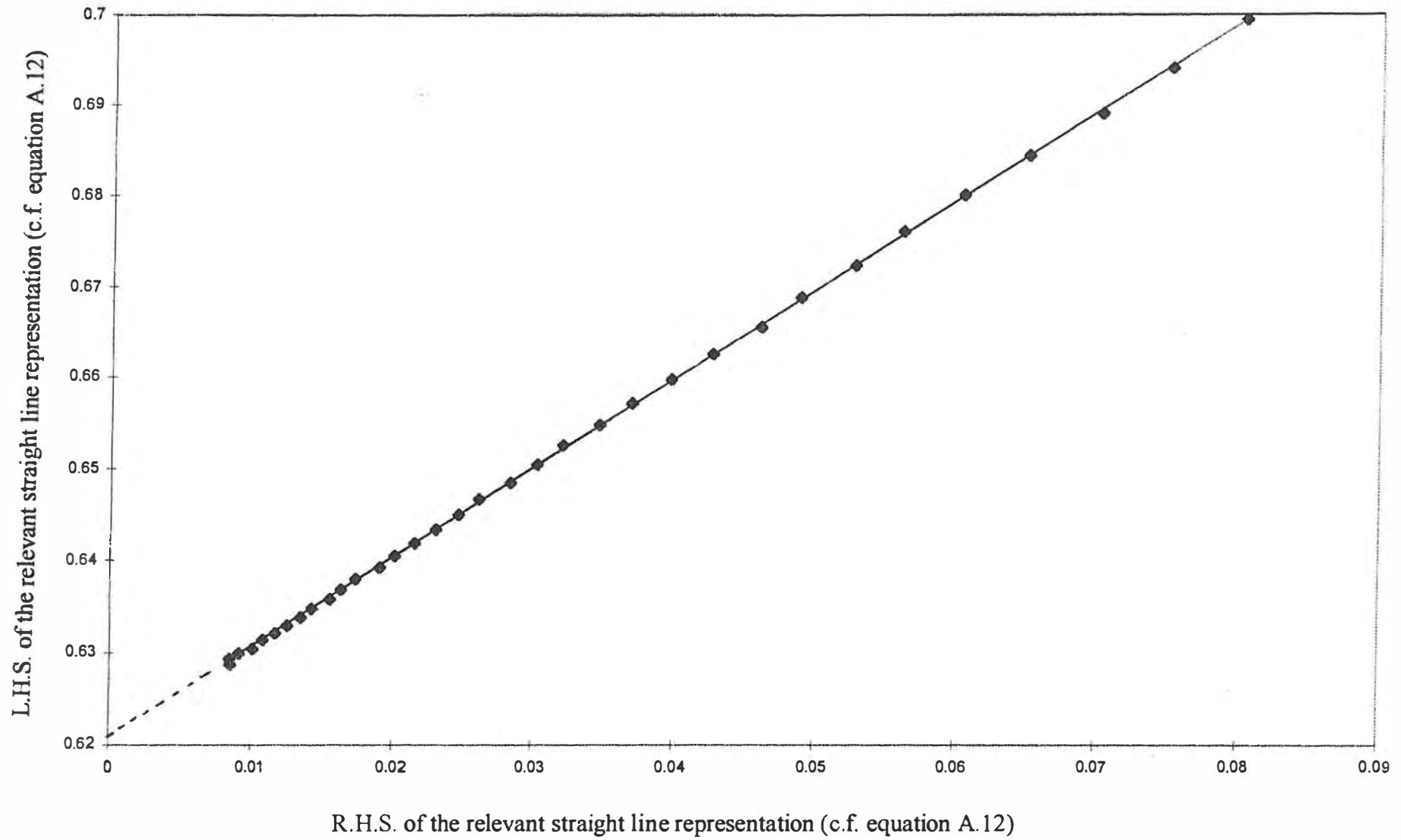


Fig. 8 Evaluation of $(k_R')_{262}^{\circ}$ and CpM for Days 9 and 10 of the measurement cycles. Origin for the integrations set at $t = t_2$.

More about Positive Feedback; more about Boiling

M. FLEISCHMANN

IMRA S.A., Science Center, 220 Rue Albert Caquot, Sophia Antipolis, 06560
Valbonne, France.

Introduction

We have already described elsewhere (1,2) some of the principles which have guided our search for the generation of high rates of excess enthalpy generation at elevated temperatures, say, up to the boiling points of the electrolytes (3,4). One of these principles has been the prediction that the partial molar enthalpy of absorption of hydrogen (or deuterium) in palladium (5) will become positive at the high charging ratios ($X = D/Pd$) required for excess enthalpy generation (6,7), see Fig 1.

Although a transition from exothermic to endothermic absorption is probably not a necessary condition for achieving excess enthalpy generation at elevated temperatures¹, such a transition will certainly facilitate the achievement of high charging ratios. For example, increases of temperature will then themselves lead to increases in X and thereby in the rates of excess enthalpy generation. These are the conditions required for the development of "positive feedback" and, in this paper, we report on two lines of investigation which have indicated the presence of these effects². We then outline the way in which our understanding of this phenomenon has guided our investigation of excess enthalpy generation at elevated temperatures.

"Positive Feedback"

The most direct and systematic evidence for the presence of "positive feedback" can be obtained from the routine calibrations at long experiment times of the Pd/D_2O system in the isoperibolic calorimeters which we use in parts of our investigations (for an illustration see Fig 4A (8)). As we have described elsewhere (1,2,3,4), we have laid considerable stress on the "lower bound heat transfer coefficient $(k_R')_{ll}$ ", obtained from the experimental data by assuming that there is no source of excess enthalpy in the cell, $Q_R(t) = 0$. Rearrangement of the differential equation governing the behaviour of the cell gives

¹Thus the application of a sufficiently large difference in Galvani potential (either between a Pd-cathode and the electrolyte or within the metal phase itself) will always be able to counteract the effects of the heat of absorption if this remains exothermic.

²We obtained the first evidence for the presence of "positive feedback" during 1986, a phenomenon which we later described under the euphemistic heading "uncontrolled releases of thermal energy". Our subsequent work has been carried out under narrowly and tightly controlled conditions to limit the consequences of these effects.

$$(k'_R)_{11} = \frac{\left[\begin{aligned} & [E_{cell}(t) - E_{thermoneutral,bath}] I \\ & + \Delta QH(t - t_1) - \Delta QH(t - t_2) \\ & - \frac{3I}{4F} \left[\frac{P(t)}{P^* - P(t)} \right] [(C_{P,D_2O,g} - C_{P,D_2O,\ell}) \Delta\theta(t) + L_{D_2O}] \\ & - C_{P,D_2O,\ell} M^0 \frac{d\Delta\theta}{dt} \end{aligned} \right]}{[(\theta_{bath} + \Delta\theta(t))^4 - \theta_{bath}^4]} \quad (1)$$

Here we have assumed that any small conductive contribution to heat transfer, $k_c \Delta\theta$, can be lumped into the radiative term by increasing the true radiative heat transfer coefficient from k_R to k'_R . The reason why $(k'_R)_{11}$ is a lower bound is because the inclusion of any excess enthalpy term must inevitably increase the derived heat transfer coefficient. $(k'_R)_{11}$ can be evaluated at any point of the coupled temperature-time and cell potential-time series, such as the points t_1 , just before the application of the heater calibration pulse (with neglect of $\Delta\theta$) or the time t_2 at the completion of this pulse (with inclusion of $\Delta\theta$): see the schematic Fig 2.

For appropriate blank experiments (Pt in H_2O or D_2O), $(k'_R)_{11}$ rapidly approaches a constant value and the standard deviation of these values is 0.1-0.2% of the mean (see also Fig 4B below). We regard this standard deviation as a measure of the precision of the experiments. The reason why it cannot be regarded as a measure of the accuracy (even for blank experiments) is because the possible reduction of electrogenerated oxygen would contribute an extra rate of enthalpy generation (electrogenerated hydrogen or deuterium cannot be re-oxidised at oxide-coated Pt anodes). It is necessary, therefore, to calibrate the system so as to compare the precision of $(k'_R)_{11}$ with the accuracy of (k'_R) . The simplest way of achieving such calibrations is to make a thermal balance at a single point in time, just before the termination of the calibration pulse, $t = t_2$, Fig 2. We have designated the heat transfer coefficient derived in this way as $(k'_R)_2$:

$$(k'_R)_2 = \frac{\left\{ \begin{aligned} & [E_{cell}(\Delta\theta_1, t_2) - E_{cell}(\Delta\theta_2, t_2)] I + \Delta Q \\ & - \frac{3I}{4F} \left[\frac{P(\Delta\theta_2, t_2)}{P^* - P(\Delta\theta_2, t_2)} \right] [(C_{P,D_2O,g} - C_{P,D_2O,\ell})(\Delta\theta_2)_{t_2} + L_{D_2O}] \\ & + \frac{3I}{4F} \left[\frac{P(\Delta\theta_1, t_2)}{P^* - P(\Delta\theta_1, t_2)} \right] [(C_{P,D_2O,g} - C_{P,D_2O,\ell})(\Delta\theta_1)_{t_2} + L_{D_2O}] \\ & - C_{P,D_2O,\ell} M^0 \left(\frac{d\Delta\theta}{dt} \right)_{\Delta\theta_2, t_2} + C_{P,D_2O,\ell} M^0 \left(\frac{d\Delta\theta}{dt} \right)_{\Delta\theta_1, t_2} \end{aligned} \right\}}{[(\theta_{bath} + (\Delta\theta_2)_{t_2})^4 - (\theta_{bath} + (\Delta\theta_1)_{t_2})^4]} \quad (2)$$

The relative standard deviations of $(k'_R)_2$ are in the range 1-2% of the mean and these standard deviations are measures of the accuracy which can be achieved by

making thermal balances at a single point in time. The principal reason for the order of magnitude difference between the precision of $(k_R')_{11}$ and the accuracy of $(k_R')_2$ is the fact that the denominator of (2) is determined by the difference of two comparably large terms, whereas that of (1) is determined by one of the terms alone³.

For the investigation of blank experiments (Pt in H₂O or D₂O), we find that the heat transfer coefficients related to $(k_R')_{11}$ are somewhat smaller than those related to $(k_R')_2$ (we describe these heat transfer coefficients with the generic designations $(k_R')_{i,1}$ and $(k_R')_{i,2}$). We believe that the reason for this small difference is the contribution of a small rate of excess enthalpy generation due to the reduction of electrogenerated oxygen, see above (1,2). By contrast to these blank experiments, $(k_R')_{11}$ for the Pd-H₂O system is initially markedly reduced, so much so that under suitable conditions $(k_R')_{11}$ may be negative at short times. The reason for this reduction in $(k_R')_{11}$ is the exothermic dissolution of H in Pd. However, this phenomenon decays with the diffusional relaxation time and at longer times $(k_R')_{11}$ is again closely similar to the true value of the heat transfer coefficient, $(k_R')_2$.

The condition $(k_R')_{11} < (k_R')_2$ is maintained for prolonged periods of time, typically 2-6 weeks. However, at sufficiently long times we frequently observe a strange reversal of behaviour in that $(k_R')_2$ apparently becomes smaller than $(k_R')_{11}$. Such behaviour must have a quite special explanation because the condition $(k_R')_2 < (k_R')_{11}$ is forbidden by the Second Law of Thermodynamics (taken at its face value, the cell would have to behave as a spontaneous refrigerator to explain the result). The condition $(k_R')_2 < (k_R')_{11}$ is maintained for a limited period of time but eventually the system reverts to the expected behaviour, $(k_R')_{11} < (k_R')_2$.

We illustrate this transition with three calibration cycles taken from the results accumulated under the Japanese New Hydrogen Energy Project⁴, Figs 3A-C. It will be seen that the transition is associated with further peculiarities. The temperature-time series both before and after the transition show the expected approach to a quasi-steady-state following the application of the heater calibration pulse and a relaxation to the base line following the termination of this pulse⁵, Figs 3A and C. By contrast, during the transition, Fig 3B, the temperature does not approach a quasi-steady-state at the end of the calibration pulse, nor does the temperature relax to the base line at

³We have described elsewhere (1,2,3,4) changes in the methods of data processing which allow us to increase the precision of $(k_R')_{11}$ and the accuracy of $(k_R')_2$ by factors of ≈ 10 . These methods rely on the use of the integrals of the experimental quantities rather than on evaluations at single points in time as for $(k_R')_{11}$ and $(k_R')_2$. These enhancements of the precision and accuracy are not required for the discussion of the topics considered in the present paper except for the comparison outlined in the following paragraph.

⁴We are greatly indebted to NHE for permission to use this illustration, as well as that in Fig 4A.

⁵As the temperature-time and cell potential-time series are coupled, see equations (1) and (2), the thermal relaxation times depend on both time series. A rough approximation is (9)

$$\tau = \frac{C_{P,D,O,t} M^0}{\left[4k_R' \theta_{\text{bath}}^3 - \left(\frac{dE_{\text{cell}}}{d\Delta\theta} \right) I \right]} \quad (3)$$

A more exact result based on a series-type solution of the differential equation governing the behaviour of the calorimeters is available as an internal Technova Report. As $(dE_{\text{cell}}/d\Delta\theta)$ is negative (see Figs 3A-C), the temperature dependence of E_{cell} shortens τ from the external value. Indeed, the two terms in the denominator of (3) are of comparable magnitudes and we expect that the cells should show "negative feedback" under normal conditions.

the end of this pulse (compare the behaviour of the cells investigated by the group at Harwell, Figs 2A and B (8)). We have to conclude that the temperature rise induced by the heater calibration pulse itself induces an increase in the rate of generation excess enthalpy both during the application of the calibration pulse as well as after its termination. These are the conditions required for “positive feedback” which is evidently sufficiently marked to outweigh the normal “negative feedback” shown by the cells.

It is a consequence of the “positive feedback” that the temperature at the end of the calibration pulse is higher than it would be in the absence of such feedback. As a result, $(k_R')_2$ is smaller than expected so that we can reach the condition $(k_R')_2 < (k_R')_{11}$.

A possible explanation of the onset of “positive feedback” is a reversal in the heat of absorption at sufficiently high charging ratios, Fig 1. Although other explanations could be invoked (and should be explored), it is natural to search for direct evidence of changes in the heat of absorption - a matter of some difficulty. A possible approach is the detailed examination of the variation of $(k_R')_{11}$ with time in the region of the calibration pulses because transient sources of excess enthalpy in the cell affect $(k_R')_{11}$ directly. Fig 4A shows one such example: we see that the application of the heater pulse leads to a transient increase in $(k_R')_{11}$ which must be interpreted as a transient endothermic process in the cell. We observe this positive excursion in $(k_R')_{11}$, although the longer-term effect of the application of the calibration pulse is a decrease of $(k_R')_{11}$ which must be due to an increase in the rate of excess enthalpy generation. We note also that if the effects of “positive feedback” are not fully established, we would expect to see a transient decrease in $(k_R')_{11}$ at the termination of the heater calibration pulse due to the reversal of endothermic absorption, i.e. the establishment of transient exothermic desorption. Such effects can, indeed, sometimes be observed as in the example shown in Fig 4A.

The behaviour of $(k_R')_{11}$ shown in Fig 4A should be judged in the context of the variability of $(k_R')_{11}$ observed in typical blank experiments, Fig 4B (see also above). In the interpretation of such data it should be borne in mind that about one-third of the standard deviation of the measurements is due to the systematic decrease of $(k_R')_{11}$ with time during any given two-day period⁶.

We note finally that the experiments give other evidence for the presence of a reversal of the heat of absorption. Thus in the region where we observe “positive feedback”, we also observe fluctuations in the cell temperature and cell potential (3,4). These fluctuations may be quite small (as for the Pd-systems) or marked (as, especially, for Pd-Rh alloys), regular or, in the limit, chaotic. We observe that such oscillations would be expected in the region where $\Delta H = 0$ because the fluctuations in entropy will become unbounded. However, it is likely that the reversal in the heat of absorption is itself due to a complex phenomenon such as the formation of the proposed third γ -phase (10). Phase transitions would also lead to oscillatory behaviour.

More about Boiling

The explanation of the effects of “positive feedback” in terms of a reversal of sign of the partial molar enthalpy of absorption with increasing charging ratio, Fig 1,

⁶This period is set by the time interval between the “topping-up” of the cells to make up for losses of D_2O due to electrolysis and, at temperatures approaching the boiling point, due to evaporation.

also provides us with a rationale for other features of the behaviour of the Pd-D₂O system. Thus, it is likely that the achievement of pronounced levels of the rates of excess enthalpy generation requires the attainment of the regime of "positive feedback", which in turn requires the use of prolonged periods of polarisation, a matter to which attention has been drawn repeatedly. However, the attainment of the condition of "positive feedback" is not sufficient to ensure sustained, high, levels of the rates of excess enthalpy generation. Maintenance of the systems in the region giving pronounced oscillations will eventually diminish or even destroy excess enthalpy generation. The explanation of "positive feedback" in terms of the reversal of the sign of the partial molar enthalpy of absorption indicates that the attainment of this regime needs to be coupled to sustained increases in temperature to ensure that the charging ratio will show the necessary increases required to achieve increases in the rates of excess enthalpy generation. It follows that the use of essentially isothermal calorimetry (a strategy which has been followed in most investigations) is ill-advised, indeed self-defeating.

It is desirable therefore to examine the extent to which the reported achievement of boiling conditions (1,2) fits into this overall pattern. The routine calibration of the cells, Figs 5A and B, allows us to monitor the system behaviour and it is certainly true that the rapid increases in temperature towards the boiling point are only achieved following the detection of "positive feedback", as has been indicated in Fig 3B. The rates of excess enthalpy generation can become very high under these conditions, so much so that the cells are "driven to dryness" in relatively short periods of time (the last half of the cell contents (45 ml) may be evaporated in 11-15 min). The particular cells used (see Fig 4A (8)) are not suitable for accurate measurements and we therefore adopt conservative approaches to the interpretation of the experimental data (1,2). The simplest first step is to calculate the amount of energy available for evaporation of D₂O, Fig 6. Here we have used the true value of the heat transfer coefficient to calculate the radiative output. The total energy available is $\cong 70.5$ kJ, sufficient to evaporate $\cong 1.7$ M of D₂O. This leaves a deficit of 127 kJ required for the evaporation of the remaining 3.05 M D₂O.

In the absence of excess enthalpy generation, we reach a further impossible conclusion. As Fig 6 shows, the cumulative energy would then need to be negative for the first $\cong 7.7$ hours of operation of the cell during the last period of operation. This again contravenes the Second Law of Thermodynamics. We conclude, therefore, that we must necessarily invoke excess enthalpy generation to explain the thermal balancing of the cell. However, our explanation of the behaviour must also be extended to give an account of the time dependence of the cell contents. The simplest assumption which we can make is that which has been used as a basis of the construction of Fig 6. This gives us curve A on Fig 7 and is clearly inadmissible. An alternative assumption is that the total cell contents in D₂O (5 M) are evaporated during the last period of operation, i.e. we rule out that the cell has been driven to boiling (1,2). We can derive such a "force fit" by regarding the atmospheric pressure, P*, as an adjustable parameter. We obtain curve C in Fig 7 and need to postulate the variation of the rate of excess enthalpy generation with time shown in Fig 8. However, such an explanation is again in conflict with other aspects of the experimental evidence. In the first place, we need to assume a value of P* which is below that of the recorded atmospheric pressure. Secondly, we conclude that the cell would then have to have been half-empty some 2.5 hours before achieving "boiling to dryness",

whereas video recordings show that this point was reached some 11 minutes before “boiling to dryness”⁷. The third assumption which we can make is that the rate of excess enthalpy generation can be calculated using the actual atmospheric pressure. This gives us the lower curve in Fig 8 for the rate of excess enthalpy generation in Fig 8 and the time course, curve B, for the cell contents in Fig 7. We conclude that we must now assume a period of intense boiling to account for the removal of the last half of the cell contents. This is in line with our visual observations and in turn leads to high final rates of excess enthalpy generation shown in Fig 8. The two plots in Fig 8 give the extrema of the behaviour: the actual behaviour must lie between the two limits but clearly closer to that given by the scenario leading to curve B in Fig 7 than that leading to curve C (1,2).

Conclusion

Prolonged polarization of cells containing Pd-based cathodes leads to “positive feedback”, which can be attributed (at least in part) to a change from exothermic to endothermic absorption with increasing charging ratio. Increase of the cell temperature then leads to marked increases in the rates of excess enthalpy generation and enthalpy generation at the boiling point can be achieved.

References

1. M. Fleischmann and S. Pons in “Frontiers of Cold Fusion: Proceedings of the Third International Conference on Cold Fusion”, Nagoya, Japan (21-25 October 1992) ed. H. Ikegami, Frontiers of Science Series No. 4, Universal Academy Press, Tokyo (1993) page 47; ISSN 0915-8502.
2. Martin Fleischmann and Stanley Pons, Phys. Lett. A, 176, 118 (1993).
3. M. Fleischmann, S. Pons, Monique Le Roux and Jeanne Roulette in: Proceedings of the Fourth International Conference on Cold Fusion, Lahaina, Maui, Hawaii, U.S.A. (6-9 December 1993) T.E. Passell, Editor, Volume 1 page 1-1, EPRI TR-104188-VI.
4. M. Fleischmann, S. Pons, Monique Le Roux and Jeanne Roulette, Trans. Fusion Technology, 26, 323 (1994).
5. T.B. Flanagan and J. F. Lynch, J. Phys. Chem., 79, 444 (1975).
6. M. C. H. McKubre, S. Crouch-Baker, A. M. Riley, S. I. Smedley and F. L. Tanzella, in “Frontiers of Cold Fusion: Proceedings of the 3rd International Conference on Cold Fusion”, Nagoya, Japan, October 21-25 (1992) ed. H. Ikegami, Frontiers of Science Series No. 4, Universal Academy Press, Tokyo (1993) page 5; ISSN 0915-8502.
7. K. Kunitatsu, H. Hasegawa, A. Kubota, N. Imai, M. Ishikawa, H. Akita and Y. Tsuchida, in “Frontiers of Cold Fusion: Proceedings of the 3rd International Conference on Cold Fusion”, Nagoya, Japan, October 21-25 (1992) ed. H. Ikegami, Frontiers of Science Series No. 4, Universal Academy Press, Tokyo (1993) page 31; ISSN 0915-8502.
8. M. Fleischmann, “The Experimenters’ Regress”, see these Proceedings of the Fifth International Conference on Cold Fusion, Monte Carlo (9-13 April 1995).
9. M. Fleischmann, S. Pons, M. W. Anderson, L.J. Li and M. Hawkins, J. Electroanal. Chem., 287, 293 (1990).
10. G. Preparata, “Cold Fusion ‘93: Some Theoretical Ideas”, paper T1.2 presented at the Fourth International Conference on Cold Fusion, Maui, Hawaii, U.S.A. (6-9 December 1993).

⁷Although our use of video recordings to time the cell contents has been criticised, we note that it is hardly possible to confuse 11 minutes with 2.5 hours.

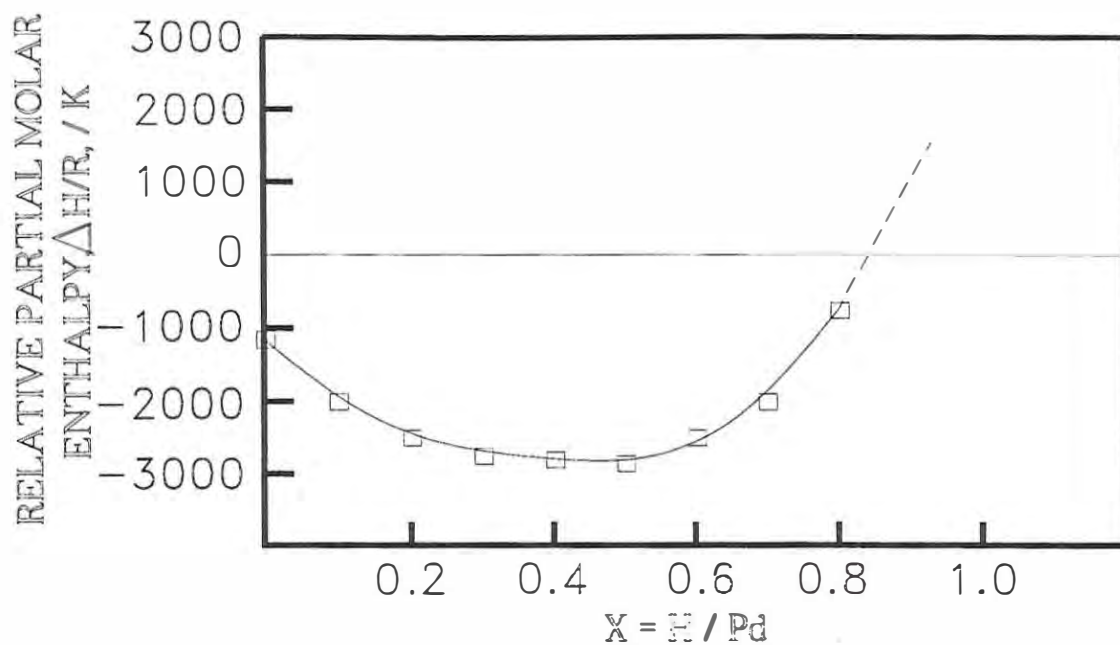


Fig 1. The variation of the relative partial molar enthalpy of hydrogen in palladium as a function of the charging ratio.

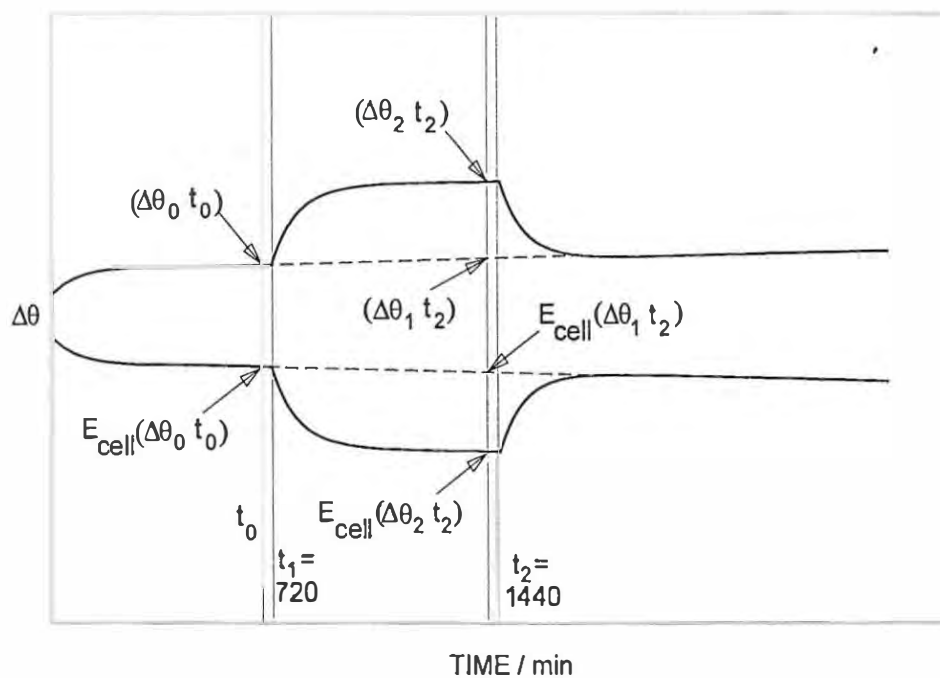


Fig 2. Schematic diagram of the methodology used in the calculations.

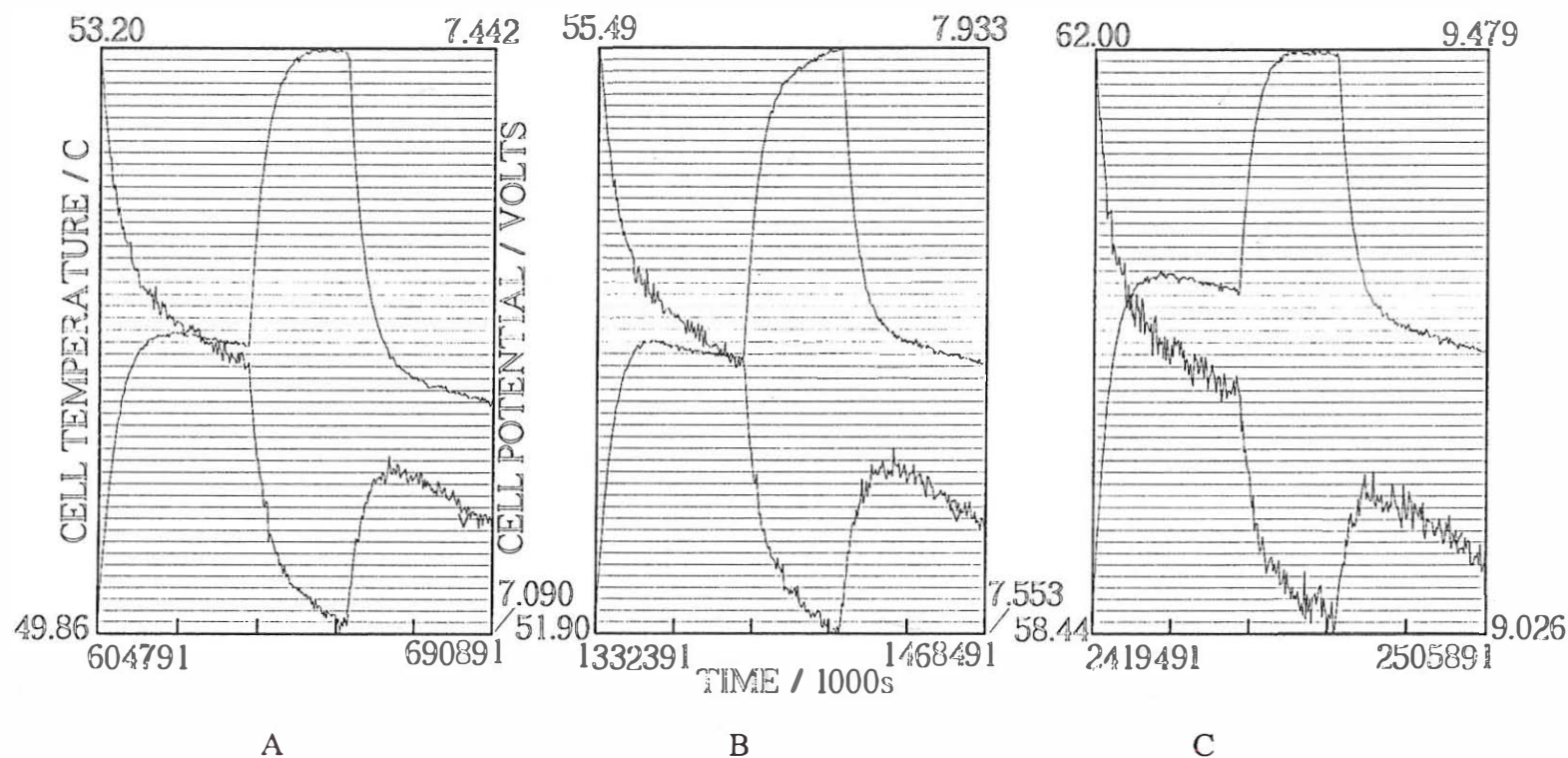


Fig 3. Experiment 4661 of the N.H.E. data sets. Pd 90 Ag10 cathode, 0.4 cm diameter, 1.25 cm length polarized in 0.1 M LiOD in D₂O; cell current = 0.5A, $\Delta Q = 0.2504$ W; the “raw data” of the cell temperature and cell potential as a function of time

A: a calibration before the onset of “positive feedback”

B: a calibration in the region of “positive feedback”

C: a calibration after the region of “positive feedback”.

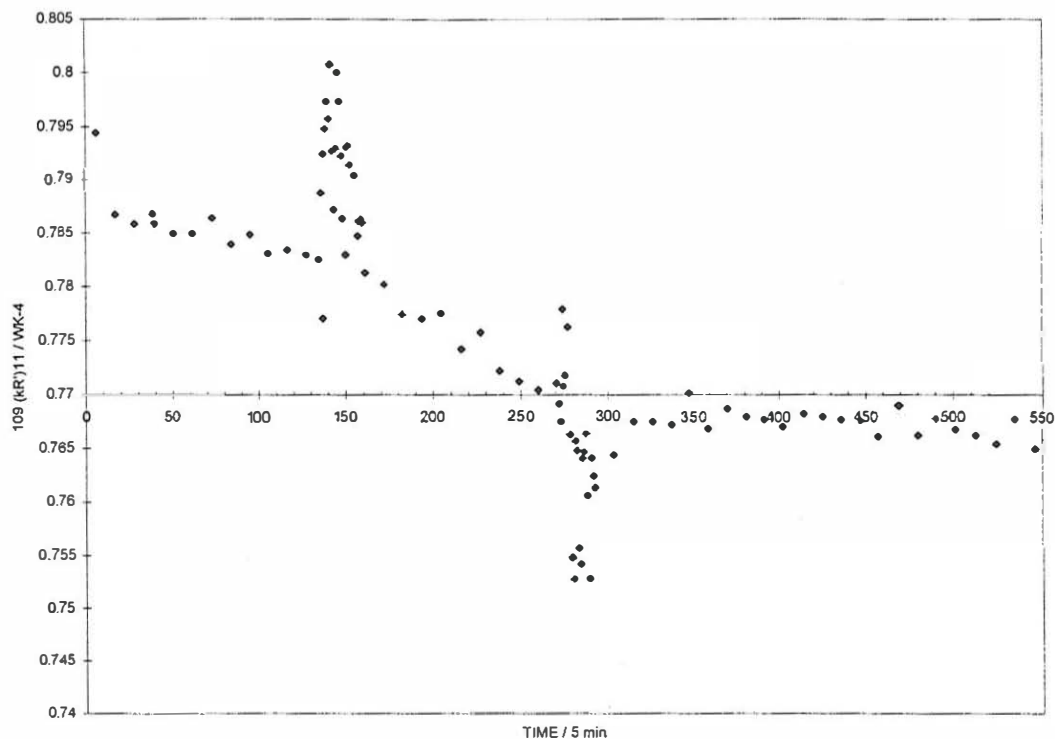


Fig 4A. Experiment 4731 of the N.H.E. data sets. Pd 90 Ag 10 cathode, 0.4 cm diameter, 1.25 cm length polarized in 0.1 M LiOD in D₂O; cell current = 0.2A, $\Delta Q = 0.2504$ W; the variation of $(k_R')_{11}$ with time during days 33 and 34 of polarization. The start and end of the heater calibration pulse are shown by the positive and negative excursions of $(k_R')_{11}$.

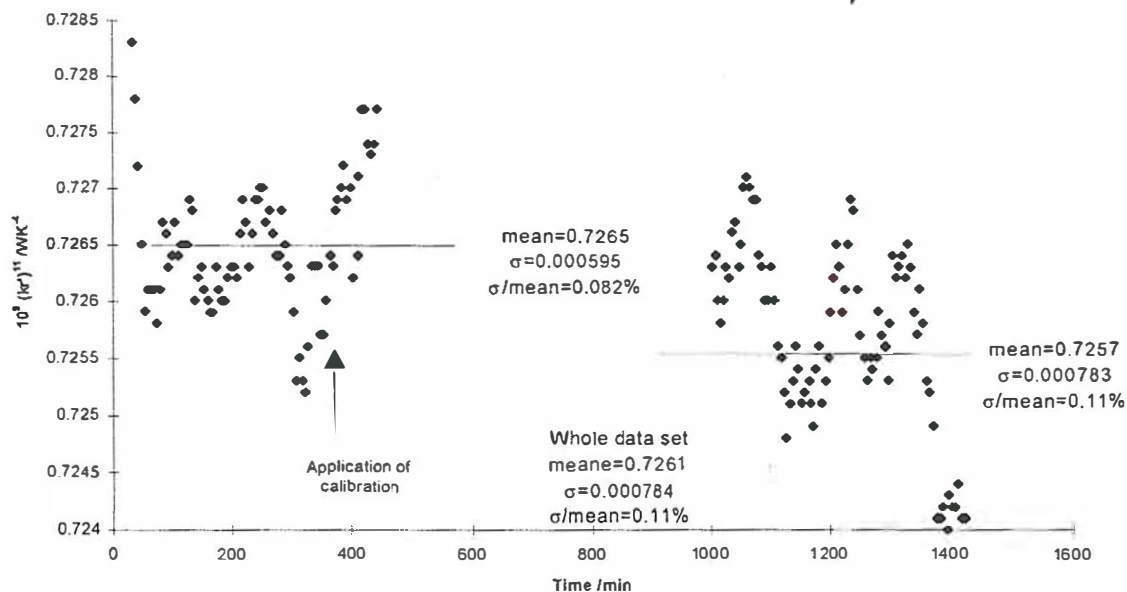


Fig 4B. Variation of $(k_R')_{11}$ with time for a blank experiment. Pt cathode 0.125 cm diameter, 1.25 cm length polarized in 0.1 M LiOD in D₂O; cell current = 0.2A. The region before and after completion of the calibration pulse.

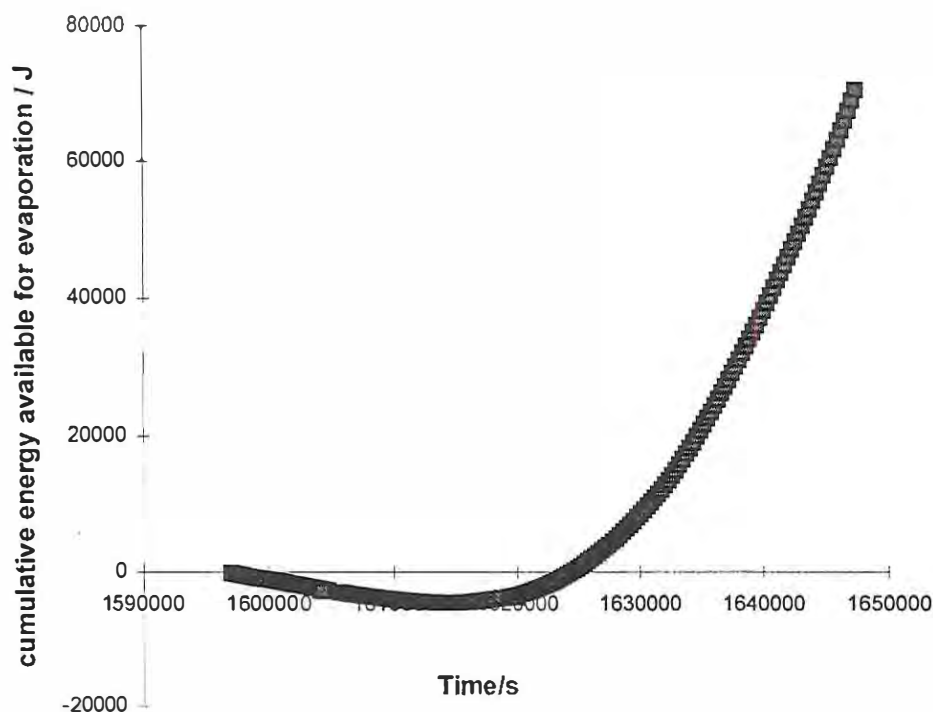


Fig 6. The cumulative energy available for evaporation of D_2O for the last period of operation of the experiment illustrated in Fig. 5A based on the assumption that there is no generation of excess enthalpy.

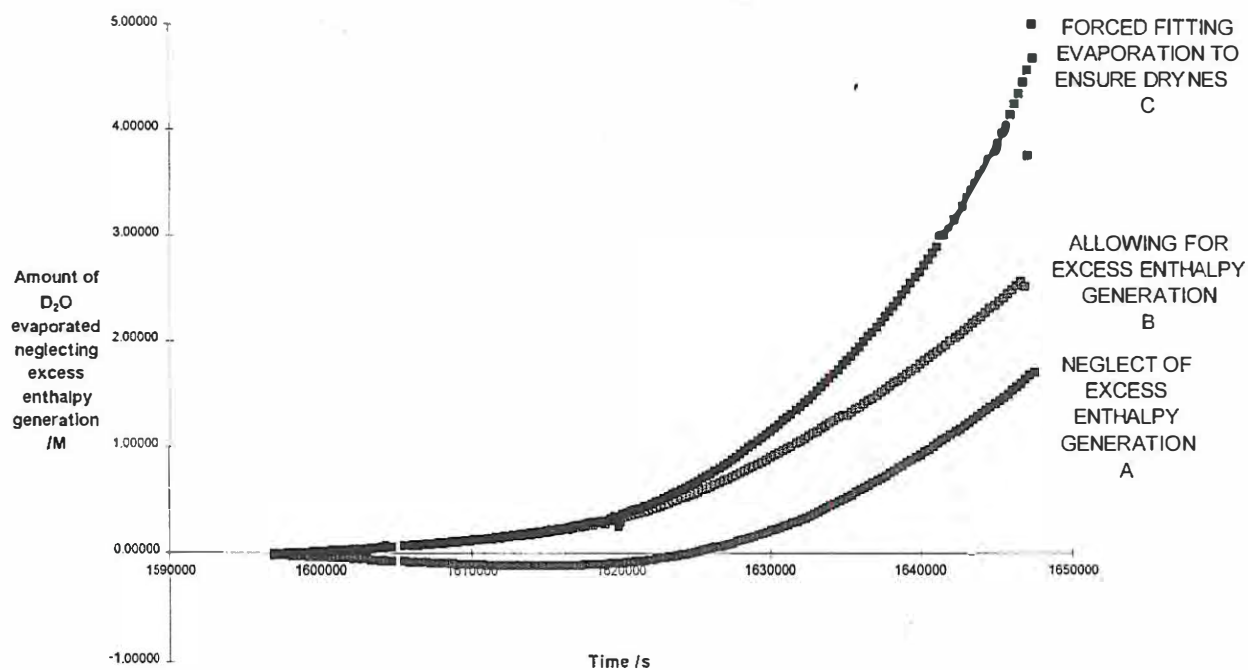


Fig 7. The variation of the evaporated D_2O with time for the last period of operation of the experiment illustrated in Fig 5A.

A: assuming that there is no generation of excess enthalpy

B: including the excess enthalpy calculated from the temperature-time and cell potential-time curves with P^* given by the atmospheric pressure

C: as B but with P^* reduced to 0.953 bar to force fit the evaporation to be completed during the last period of operation of the experiment.

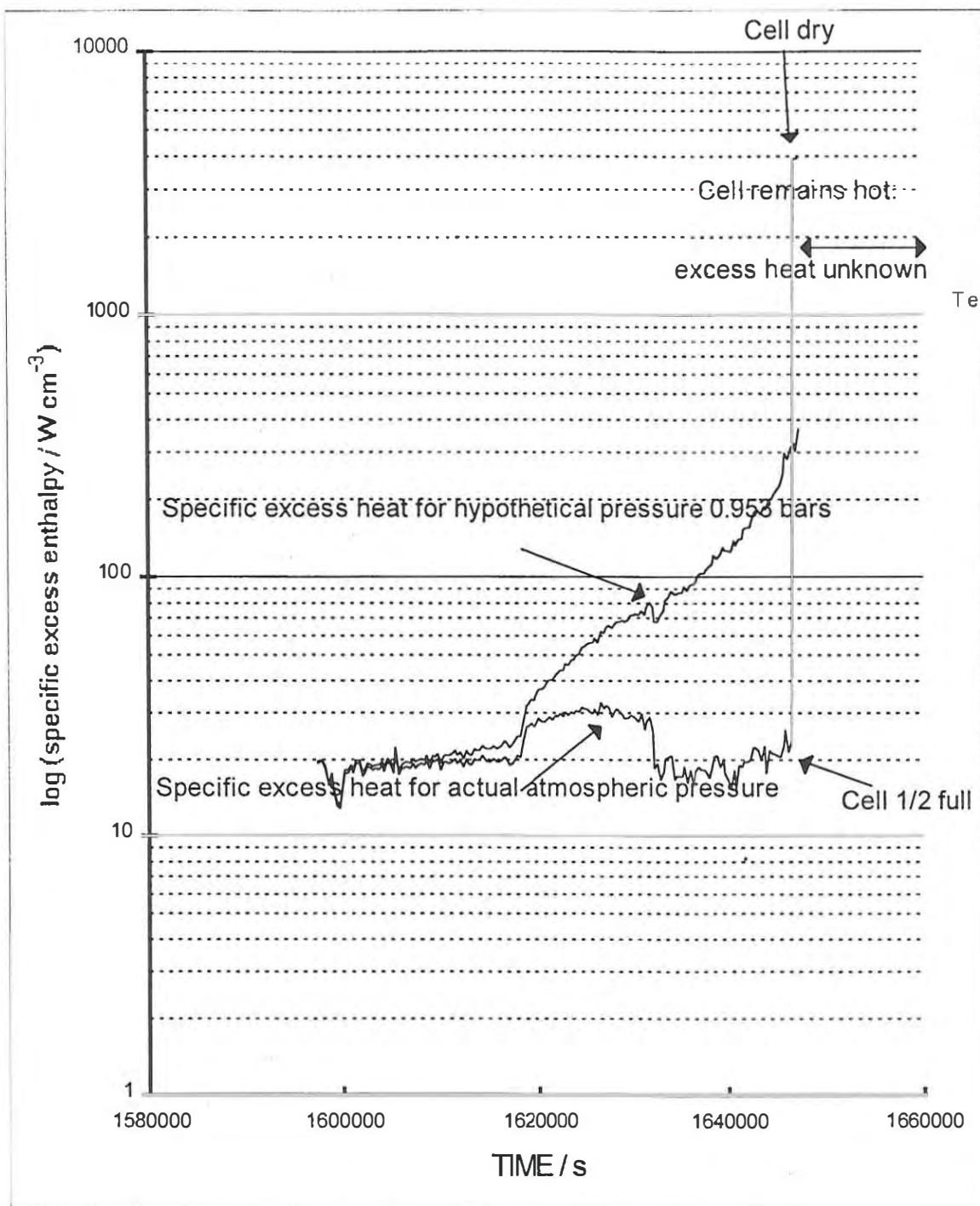
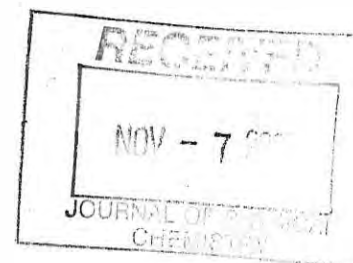


Fig 8. The variation of the rate of excess enthalpy generation with time for the assumptions B and C used in the construction of Fig 7.

Chapter II: An Example of Difficulties in Publishing LENR-Related Results

In 2005, Dr. Melvin Miles, currently a professor at the University of La Verne, submitted a manuscript entitled “The Precision and Accuracy of Isoperibolic Calorimetry as Applied to the Pt/D₂O System” for consideration for publication in the Journal of Physical Chemistry B. The paper was sent out for review. Based upon the reviewer comments, the paper was rejected by the editor. Dr. Miles wrote a letter addressing the reviewer comments. However, this did not convince the editor of the journal to reconsider his decision to not publish the paper. The purpose of this chapter is to demonstrate the difficulties researchers encounter when attempting to publish in this area of research. This chapter includes a copy of the original manuscript that was submitted to the Journal of Physical Chemistry B as well as the exchange of letters between Dr. Miles and the editor of the journal.

The Precision and Accuracy of Isoperibolic Calorimetry
as Applied to the Pt/D₂O System



M. Fleischmann, Bury Lodge, Duck Street, Tisbury, Salisbury, Wilts., SP3 6LJ, U.K.

M.H.Miles, Department of Chemistry, University of La Verne, La Verne, CA 91750
U.S.A.

Abstract

In recent years doubts have often been expressed about the precision and accuracy of isoperibolic calorimeters of the type illustrated in Fig. 1. We assess the validity of such statements by means of experiments on "blank systems", here Pt cathodes polarised in 0.1M LiOD/D₂O. The differential and integral heat transfer coefficients are evaluated and it is shown that the latter based on backward integration of the data sets should be used in accurate evaluations of the experimental data. It is shown that the precision is better than 99.99% while the accuracy is close to this figure.

The high precision and accuracy allow the determination of enthalpy generation due to the reduction of oxygen electrogenerated in the cell. It is shown that this was ~0.0011W for the experiments in question whereas the input enthalpy to the cell was ~0.8W for these particular experiments.

Some preliminary considerations about the design of calorimetric systems.

The experiments reported in this paper are closely related to those which we have reported previously (1), (2). An ICARUS-2 cell has been used and polarisations have been carried out using an ICARUS-2 system (3).

If we consult any of the classical texts of Chemical Engineering (e.g. see (4)) we find that reactors in which there are both chemical and thermal changes should be classified as being "ideal" and "non-ideal". The "well-stirred tank" and "plug flow

reactor" are pre-eminently examples of the "ideal" type whereas "dispersive plug flow" should be regarded as being "non-ideal". It should be evident that "isoperibolic calorimetry" might be classified as being "ideal" (we have to justify some additional criteria to satisfy this description). Although it might well be possible to design calorimetric systems which would satisfy the criteria of a "an ideal plug flow reactor" (e.g. research on fluidised beds of Pd particles) such research has not been carried out hitherto, to the best of our knowledge. Research on the fashionable flow reactors is governed by "dispersive plug flow" and should therefore be classified under the "non-ideal" heading.

Fig. 1 illustrates the type of single compartment isoperibolic calorimeter which we have adopted for most of the research on "Cold Fusion" including the present paper. We make the following additional observations about the operation of this calorimeter:

(i) heat transfer is controlled by radiation across the vacuum gap of the Dewar cells, this heat transfer being predominantly due to the lower, unsilvered parts of the cells. The heat transfer coefficient is therefore given by the product of the Stefan-Boltzmann coefficient and the radiant surface area as has been confirmed in numerous studies. (see Discussion section) Deviation from this predicted value of the heat transfer coefficient indicates malfunctions of the cells and/or mistakes in the data analyses.

(ii) Adjustments of the relative extents of the silvered and unsilvered portions allows the change of the heat transfer coefficient by about one order of magnitude ; larger changes require changes in the dimensions of the cells.

(iii) As heat transfer is controlled by heat transfer across the vacuum gap, the thermal impedance has no "memory". It is therefore possible to examine the non-steady state behaviour of the systems in a straightforward manner which affects especially the response of the systems to calibration pulses supplied by the Joule resistive heaters. It is evident that this crucially important design criterion has not been understood by the many critics of "Cold Fusion" (e.g. see (5)).

(iv) The long and narrow design of the calorimeters ensures that the contents are well-mixed by the gas sparging induced by the gas evolution at the anodes and cathodes. The radial and axial mixing times of the system (as revealed by tracer experiments) are ~ 3 s and ~ 20 s whereas the thermal relaxation time of the ICARUS -2 cell investigated in the present paper is ~ 5000 s (see Footnotes (1) and (2)).

Footnote (1) The differential equation representing the model of the calorimeter is non-linear and inhomogeneous (see equation A.2 of the Appendix) The estimate of a “thermal relaxation time” is therefore approximate.

Footnote (2) The calorimeters used in the initial studies (1), (2) had heat transfer coefficients which exceeded the value given by the product of the Stefan-Boltzmann coefficient and the radiant surface area. We attributed the conductive contribution to conductance across the nominal vacuum gap due to inadequate evacuation of the Dewar cells. It was therefore not clear whether the system should have been modelled as being “pseudoradiative” or “pseudoconductive” (depending on whether the conductive or radiative contribution was neglected; for an alternative strategy see (6)); the thermal relaxation time of these cells was ~ 3000 s.

(v) in view of (iv) the contents of the calorimeter have always been at a uniform temperature.

(vi) equally, the temperature of the heat sinks (water baths) surrounding the calorimeters have always been at a uniform temperature. This has been ensured by using a combined rejection of heat to the surrounding ambient room temperature coupled to thermostatic control of the water baths. The room temperature has always been itself controlled using two independent temperature controllers operated in parallel i.e. the overall system used two thermal impedances operated in series.

(vii) the cells have always been operated in the “open mode” i.e. the products of electrolysis have been vented to the ambient [see Footnote (3)]. N.M.R. measurements

Footnote (3) It should be noted that this strategy avoids the introduction of large localised and fluctuating sources of enthalpy in the gas spaces (which is a characteristic of the use of cells fitted with catalytic recombiners).

confirmed that this strategy (imposing continuous isotopic separation of H) ensured the maintenance of the initial isotopic composition of the electrolyte.

(viii) measurements have usually been made using 0.1 M LiOD/D₂O. The use of this electrolyte ensured that there were no parasitic reactions which could affect the thermal balances of the system.

(ix) it was confirmed that the volumes of the gases evolved agreed to within ~ 1% of those calculated assuming 100% Faradaic efficiency of the electrolytic reactions (neglecting the initial part of the measurement sequences during which there is charging of the Pd-based systems by hydrogen isotopes). The volumes of D₂O required to maintain the levels of electrolyte in the cells also agreed with those calculated by Faraday's Laws i.e. there is no possibility of involving large-scale recombination of the electrolytically formed gases to explain excess enthalpy production.

(x) measurements of cell and calibration currents of cell and bath temperatures and of the cell potentials and potentials across the resistive calibration heaters were made every 300s [see Footnote (4)]

Footnote (4) A limit on the rate of data acquisition is set by the time lags induced by the thin glass shields surrounding the thermistors, ~ 10s (see also further below). Furthermore, it would be possible to exceed this rate of acquisition if the time lags in the glass shields were taken into account.

(xi) three calorimetric cells were maintained in each thermostat tank.

(xii) in view of the small extent of the head spaces (which contained no exposed bare metal parts), the systems could be operated in absolute safety.

Measurements and Interpretation.

Fig. 2 gives a plot of the "raw data" (the cell temperature and input enthalpy for days 9 and 10 of the measurement cycles) carried out on a Pt cathode ($\phi = 1\text{ mm}$, $l = 2\text{ cm}$). It can be seen that with increasing time following each perturbation of the system, both these time series show a small progressive decrease with time. This decrease of temperature with time is due to the progressive increase of the electrolyte concentration due to electrolysis; this in turn causes an increase of the conductance and hence a fall in the input power. The fall in the input power leads to a decrease of the cell temperature with time.

Four times are of special interest; $t = 0$ following the "topping-up" of the cell after the previous measurement cycle; $t = t_1$, the start of the calibration period; $t = t_2$, the cessation of the calibration period and $t = T$, the end of the measurement cycle. Estimates of the pseudo-radiative lower bound heat transfer coefficient, $(k_R')_1$, and of the pseudo-radiative true heat transfer coefficient, $(k_R')_2$, can be conveniently made near $t = t_2$, equations A.4 and A.6 in Appendix A. In the first of these estimates we assume that there is no generation of any excess enthalpy, hence the designation of "lower bound"; the presence of any known source of excess enthalpy would increase the enthalpy input and, hence, decrease the heat transfer coefficient. In the second estimate of the pseudo-radiative true heat transfer coefficient, $(k_R')_2$, we also have to estimate the input power and cell temperature which would have been reached in the absence of the heater calibration. We can do this conveniently by interpolating the time series for the regions $t < t_1$ and $t_2 < t < T$: the reason for stipulating $t_1 = 12$ hours, $t_2 = 24$ hours and $T = 48$ hours will be all too self-

evident. Contraction of these times say to $t_1 = 6$ hours, $t_2 = 12$ hours and $T = 24$ hours leads to an inevitable lowering of the precision of $(k_R')_1$ and accuracy of $(k_R')_2$. Unfortunately, such a contraction of the measurement cycles has been the norm in most of the investigations carried out by other research groups.

The values of these "robust" estimates of $(k_R')_1$ and $(k_R')_2$ (made from A-3 sized plots of the "raw data") are shown in Columns 2 and 3 of Table 1 for a series of 7 measurement cycles. The values of $(k_R')_1$ and $(k_R')_2$ were the first estimates of the heat transfer coefficients which we made from the "raw data" (hence their designation) and were used as starting values for more precise and accurate evaluations using non-linear regression [see Footnote(5)]

Footnote (5) In the original investigation (2), $(k_R')_2$ was estimated near $t = t_1$ in an attempt to eliminate one of the required interpolations. Although this procedure was explained in (2) (as was the subsequent application of non-linear regression; for further explanation see (7)) the basis of our estimates was clearly not understood e.g. see (8). As we could not make the non-linear regression methodology "user friendly" with the computing power available to us in 1992, we based all further analyses on the application of linear regression (for further explanation, see (9)) Linear regression was also the basis of the statistical treatments incorporated in the ICARUS -1 and ICARUS -2 packages (3) and is the methodology which we have adopted in all investigations after October 1989.

It is important that $(k_R')_1$ and $(k_R')_2$ are respectively the least precise and least accurate estimates of the heat transfer coefficient which we can make from the data. Furthermore, they are subject to errors due to the refilling of the cells to make up for losses in D_2O due to electrolysis (see further below). The means of the values derived are also shown in Columns 2 and 3 of Table 1. (see also further below).

The next stage of the analysis is the evaluation of the differential lower bound heat transfer coefficients $(k_R')_{11}$, throughout the time range of the measurement cycle. Here the

subscript 11 denotes that we are evaluating a differential coefficient and that we are also considering a lower bound value. We have always used a second order central difference in the estimates of the differentials of the temperature-time series. Fig. 3 shows the 11-point means, $(\overline{k_R'})_{11}$, of $(k_R')_{11}$ and the further 6-point means, $(\overline{\overline{k_R'}})_{11}$, of $(\overline{k_R'})_{11}$ for days 1 and 2 of the measurement cycles; (there was no calibration of the system during this particular cycle).

We can use the differential lower bound heat transfer coefficients in several ways to assess the performance of the instrumentation. Thus, we can estimate the true heat transfer coefficient from the mean of the values in Column 3, Table 1 or else, we can assume that the true heat transfer coefficient varies in the same way with time as does the lower bound value $(k_R')_{11}$, Fig. 3 (a better assumption is to base this variation on the integral heat transfer coefficient, $(k_R')_{21}$, Fig. 6 and see further below). We can then evaluate the differential rates of excess enthalpy generation using

$$\text{differential rate of excess enthalpy generation} = [(k_R')_2 - (k_R')_{11}] f_1(\theta) \quad (1)$$

$$\text{where } f_1(\theta) = (\text{cell temperature})^4 - (\text{bath temperature})^4 \quad (2)$$

(see also Appendix A)

Fig. 4 gives the upper and lower tail distributions for Day 3- 16 of the data sets (c.a. 4000 measurements) using the second set of assumptions (i.e. allowing for the variation of $(k_R')_2$ with time). We can see that the data are consistent with a normal distribution of errors (due principally to errors in the temperature measurements) on which is superimposed a small steady state of excess enthalpy production (which accounts for the positive deviations of the plots from those for purely normal distribution of errors especially in the region of the upper tail distribution).

We can also evaluate the corresponding rates of excess enthalpy generation in a variety of ways. The methodology which we adopted in 1991-1993 (and which we have also used here) is to evaluate the total excess enthalpy as a function of time and then to divide the relevant excess enthalpy by the time elapsed since the start of the measurement cycles (here $t = 0$ on Day 3). The results for the two limiting sets of assumptions (allowing

for the variation of $(k_R')_2$ with time or using a single value of $(k_R')_2$ at $t = 86,400\text{s}$) are given in Figs. 5A and 5B. We can see that the effects of the random variations in the differential lower bound heat transfer coefficient, Fig. 3, are gradually suppressed with increasing time, the rate approaching $\sim 1.3\text{mW}$. The significance of this value will be discussed below. At the same time, we can see that the magnitudes of the excess rates given in Figs. 5A and 5B are affected by the assumptions made about the time dependence of the true heat transfer coefficients and that the evaluation requires very long integration intervals in order to reduce the effects of random errors to acceptable levels. [see Footnote (6)].

Footnote (6) The evaluations carried out in 1991-93 were restricted to the first measurement cycle calculated with allowance of the variation of the true heat transfer coefficient with time, as in Fig. 5A. This led in turn to the erroneous conclusions that the accuracy of $(k_R')_2$ was about one order of magnitude below the precision of $(k_R')_1$ and that the rates of excess enthalpy production were about one tenth of the rate which could be attributed to the reduction of electrogenerated oxygen (in turn attributed to a degassing of this species from the solution adjacent to the cathode by the electrogenerated bubbles of deuterium). It can be seen that these conclusions were incorrect: the accuracy of $(k_R')_2$ must be comparable to the precision of $(k_R')_1$; the question of the reduction of electrogenerated oxygen is discussed further below.

These difficulties are avoided by basing the evaluation on the integral rather than the differential heat transfer coefficients. We can distinguish two types of heat transfer coefficient denoted by the symbols $(k_R')_{i,j,l}$ where $i = 2$ signifies backward integration (i.e. typically starting from $t = T$, $t = t_2$ or $t = t_1$), $i = 3$ signifies forward integration (starting typically from $t = 0$, $t = t_1$ or $t = t_2$), $j = 5, 6, 7$ or 8 denotes the region adjacent to $t = 0$, $t = t_1$, $t = t_2$ or a combination of the regions adjacent to $t = t_1$ and $t = t_2$, $l = 1$ signifies "lower bound" and $l = 2$ signifies "true". In this scheme of description $i = 1$ stands for "differential"; omission of the central subscript, j , denotes that we are considering the whole measurement cycle $0 < t < T$.

It can be seen that we can base the evaluation on many versions of the heat transfer coefficients (which of course, are all related to each other) so that it is necessary to standardise on the usage of a sensible subset of these coefficients.

Fig. 6 gives a comparison of the integral coefficients $(k_R')_{21}$ (see equation A. 8) and $(k_R')_{31}$ (see equation A. 9) with the differential coefficient $(k_R')_{11}$. It can be seen that if we exclude the first ~ 100 data points adjacent to $t = T$ in the evaluation of $(k_R')_{21}$ and the first ~ 100 data points adjacent to $t = 0$ in the evaluation of $(k_R')_{31}$ (time zones in which the benefits of using the integral procedure are established) the variability of $(k_R')_{21}$ and $(k_R')_{31}$ is actually much smaller than the variability of the double mean of the differential lower bound coefficient, $(k_R')_{11}$. The interrelation of these coefficients can be understood as follows :

the variation of $(k_R')_{11}$ with time can be represented to the first order by

$$(k_R')_{11} = (k_R')^0 (1 - \gamma t) \quad (3)$$

where $(k_R')^0_{11}$ is the value of $(k_R')_{11}$ at $t = 0$. On the other hand, in the evaluation of the integral heat transfer coefficients, these coefficients are initially regarded as being constant in time, so that we obtain equations (A.8), (A.9), (A.11) and (A.12) (and similar expressions for other heat transfer coefficients which may be used in the interpretation). If, instead, the time dependence of the heat transfer coefficients is included in the differential equation (A.1) representing the calorimeter, we obtain, for example, equation (A. 13). If we now regard $f_1(\theta)$ as being constant throughout a measurement cycle (which is a rough approximation for the case of the "lower bound heat transfer coefficients" as there is no calibration pulse) we obtain

$$(k_R')_{21} = (k_R')^0_{21} \left[1 + \frac{\gamma(T-t)}{2} \right] \quad (A. 14)$$

and

$$(k_R')_{31} = (k_R')_{31}^0 \left[1 - \frac{t}{T} \right] \quad (A. 15)$$

where $(k_R')_{21}^0$ and $(k_R')_{31}^0$ are respectively the values of $(k_R')_{21}$ and $(k_R')_{31}$ at $t = T$ and $t = 0$. It follows that the slopes of the plots of $(k_R')_{21}$ and $(k_R')_{31}$ versus time are roughly one half of the corresponding plot for $(k_R')_{11}$ and hence of those for $(k_R')_{11}$ and $(k_R')_{11}$ as is shown by Fig. 6.

An alternative approach towards the evaluation of accurate values of the heat transfer coefficients can be based on the application of equations such as (A.8), (A.9), (A.11) and (A.12). Such evaluations give $(k_R')_{ij,l}^0$ which are the intercepts at the chosen origins of the abscissae of $CpM \, d\Delta\theta / dt$ (note that the values of the intercepts are independent of the value of CpM); the water equivalents, CpM , are derived from the slopes of the plots.

Figs. 7A and 7B are anomalous in this sequence because they are based on the responses of the systems to the “topping up” of the cells to make up for losses of D_2O due to electrolysis in the previous measurement cycles (rather than the response due to the calibration pulse). Fig. 7A illustrates the determination of $(k_R')_{251}^0$ where the origin has been set at $t = 14,000s$ whereas this origin is at $t = T$ for the evaluation illustrated in Fig. 7B. It was found that the values of $(k_R')_{251}^0$ determined in this way agreed with the value of $(k_R')_{11}$ evaluated at $t = 14,000s$ (e.g. see Fig. 6) and these values are listed for this series of measurement cycles in Column 4 of Table1. However, although the values of $(k_R')_{251}^0$ determined with the time origin set at $t = T$ were smaller than those determined with the origin set at $t = 14,000$, (e.g. compare Figs. 7A and B), this decrease was, in general, too small. We therefore concluded that it would not be possible to use this methodology to determine $(k_R')_{251}^0$ with the time origin set to t_2 i.e. that the most sought after heat transfer coefficient could not be determined in this way. Furthermore, we were unable to develop this methodology to allow the determination of the “true integral heat transfer coefficients, $(k_R')_{252}^0$ ”. This particular methodology was therefore excluded from the ICARUS Systems and we have not used it in the intervening years. See Footnote (7).

Footnote 7) We note, however, that this particular method for determining the heat transfer coefficients requires further investigation. "Topping-up" of the cells with heated D_2O could be made to produce perturbations of the same amplitude as those achieved using the resistive heaters. This would improve the precision of the evaluation of $(k_R')^o_{251}$ which could then probably be determined at $t = t_2$. It might also allow the determination of $(k_R')^o_{252}$ and would certainly lead to a considerable simplification of the experiment design.

Figs. 8A, 8B and 9 illustrate the determination of $(k_R')^o_{261}$ and $(k_R')^o_{262}$ with the start and end of the integration procedures being set at $t = t_2$ and $t = t_1$ (for Figs. 8A and 9) and $t = T$ and $t = t_1$ (for Fig. 8B). It should be noted that the origin for the plots in Figs. 8A and 9 is well-defined near $t = t_2$ (where $d\Delta\theta/dt \approx 0$) which is the point in time at which we require the heat transfer coefficients. The small values of the abscissae should be especially noted as should be the degradation of the performance when setting the origin at $t = T$ (Fig. 8B) compared to $t = t_1$ (Fig. 8A). The evaluation of these heat transfer coefficients (with the origin set at $t = t_2$) became one of the targets of the ICARUS procedures; the values determined for these sets of measurements are listed in Columns 6-9 of Table 1. The values of $(k_R')^o_{261}$ determined in this way are somewhat larger than the values of $(k_R')_{21}$ determined at the same point in time listed in Column 10 of Table 1. This is expected as the extrapolations in these Figures determine $(k_R')_{11}$ at $t = t_2$ (rather than $(k_R')_{21}$).

We would expect the means of $(k_R')^o_{261}$ and $(k_R')^o_{262}$ (Columns 6 and 8 of Table 1) to be close to the means of $(k_R')_1$ and $(k_R')_2$, (Columns 2 and 3 of Table 1). Table 1 shows that this is indeed the case.

Fig. 10 illustrates the determination of $(k_R')_{271}^0$ and Columns 11 and 12 of Table 1 list the derived values. The determination of the heat transfer coefficient at $t = T$ is not of any particular significance and this particular method of evaluation was not included in the ICARUS package.

Figs. 11-14 illustrate the determination of $(k_R')_{361}^0$ and $(k_R')_{362}^0$ based on forward integration of the data from $t = t_1$. Here Figs. 11 and 12 use the first 33 data points adjacent to $t = t_1$ while Figs. 13 and 14 use the 33 data points adjacent to $t = T$. It can be seen that these evaluations are unsatisfactory from several different points of view. In the first place, the origin of the plots is not well-defined ($d\Delta\theta/dt \neq 0$ as $t \rightarrow t_1$); secondly, the range of the extrapolations required is too long (see especially Figs. 11, 13 and 14); thirdly, the values of the abscissae are large and comparable to the ordinates (see especially Fig. 12). It is not surprising therefore that the determination of the heat transfer coefficients using these particular procedures fails (see Columns 12-16 of Table 1). It was pointed out that evaluations near the end of the calibration pulse (Figs. 13 and 14 and Columns 17-20 of Table 1) would be more satisfactory than those based on the region close to the start of this pulse, $t = t_1$ (Figs. 11 and 12 and Columns 13-16 of Table 1). As the time at which the derived heat transfer coefficients might apply was uncertain, the procedures based on the forward integration of the data sets was excluded from the ICARUS Systems [see Footnote (8)]. However, the evaluation of $(k_R')_{31}^0$ near $t = t_2$, Column 21 of Table 1, was included to

Footnote (8) However, we believe that the evaluations carried out by the group at the New Hydrogen Energy Laboratories have been based on such forward integrations..

serve as a check on the evaluation procedures.

It is important to point out a major limitation of these data analyses. It can be seen that the time-dependence of the evaluated heat transfer coefficients e.g. see Figs. 3 and 6, is entirely in accord with the expected behaviour, equations (A.1) and (A.2). It was

therefore hoped that the derived values of the water equivalents, C_pM , could be used to provide the minor corrections to the level of the electrolyte required to allow the presentation of the derived heat transfer coefficients on a single plot versus the electrolyte content of the cells. However, this hope could never be realised; the water equivalents are derived from the slopes of the plots such as those in Fig. 7A-10. Inevitably, this introduces errors into the estimations of C_pM and the accuracy of these water equivalents is therefore insufficient to allow the corrections of the heat transfer coefficients for changes in the level of the electrolyte between the successive measurement cycles.

In view of this deficiency, a level controller was added to the ICARUS -1 system in the development of the further ICARUS -2 instrumentation. The principle of this level controller is illustrated in Fig. 15B and it was estimated that this would reduce the errors of the heat transfer coefficients between successive measurement cycles to $\sim 0.04\%$. However, these level controllers were never used. It was also apparent that it was necessary to control the level of the water baths surrounding the calorimeters, but such level controllers were never constructed.

Fig. 15B also illustrates a further feature of the instrumentation: the proposed use of the cell currents to drive the resistive calibration heaters. This aspect is discussed further below, see Fig. 20.

It is also necessary to assess the errors inherent in the various evaluations of the heat transfer coefficients which can be conveniently carried out by using the relevant standard deviations. Thus Fig. 16 shows the standard deviations of $10^9 (k_R')_{11}$ and $10^9 (\overline{k_R'})_{11}$ as a function of time for Days 1 and 2 of the measurement cycles. The second is lower than the first by about $(6)^{1/2}$ as would be expected if these differential coefficients show normally distributed random errors (due principally to errors in the temperature measurements cf. Fig. 4).

Next, Fig. 17 shows the standard deviations of the integral lower bound heat transfer coefficients $(k_R')_{21}$ and $(\overline{k_R'})_{21}$. Note first of all that $\sigma (k_R')_{21}$ is much smaller than $\sigma (k_R')_{11}$ which illustrates the benefits of using the integral rather than the differential

coefficients. However, we find that $\sigma(\overline{k_R'})_{21} > \sigma(k_R')_{21}$ which is clearly impossible. This result is, in fact, due to the systematic decrease of $(k_R')_{21}$ (and of all the other heat transfer coefficients) with time.

The effects of these systematic variations with time can be taken into account by evaluating the standard deviations about the median centre lines. The effects on the results in Fig. 16 are entirely negligible (of order 10^{-14} i.e. 0.00001 on the scale of Fig. 16) confirming that the fluctuations are due to random errors. The effects on the standard deviations of the integral heat transfer coefficients are shown in Fig. 18. We see that $\sigma(\overline{k_R'})_{21}$ is now of the same order as $\sigma(k_R')_{21}$. We would expect it to be much smaller but, evidently, we now reach the limit of the evaluation procedures: we cannot investigate random or systematic errors in these coefficients if these are less than $0.00001 \times 10^9 (k_R')$ as this is the cut-off limit of the interpretation. [see Footnote (9)]

Footnote (9) However, we see that the integral heat transfer coefficients in Figs. 6-10 are not statistically independent as the process of integration uses all the preceding values of the coefficients. Fig. 19 shows we can get round this difficulty in principle; we section the data (here into sectors of 28,650s duration) so that we obtain a series of statistically independent values of $(k_R')_{21}$. However, note that these values will converge onto the relevant plot of $(k_R')_{11}$ versus time. A realistic application of this methodology would require a raising of the rate of data acquisition (desirable for other reasons). A practical limit is set by the time-lags in the glass shields surrounding the thermistors-say ~ 10 s. This would allow the making of ~ 60 measurements of statistically independent values of $(k_R')_{21}$ over a two day period. However, it is debatable whether such an investigation would be useful as these values of $(k_R')_{21}$ would converge onto the $(k_R')_{11}$ median line.

An alternative way of testing the errors of the integral heat transfer coefficients is to apply equation (A.13) to the data and to then evaluate the standard deviations of the derived values of $(k_R')_{21}^\circ$. This method has the advantage that it simultaneously tests the

applicability of the differential equation modelling the calorimeters by testing whether the heat transfer coefficients can be represented by a single, time-independent value.

Fig. 20 gives the results for days 1 and 2 and for days 9 and 10 of the measurement cycles. If we exclude the first ~ 100 points in the integration procedure, we find that the relative standard deviations $\sigma (k_R')_{21} / (k_R')_{21}$ is just 0.0056% for the measurements on Days 1 and 2 (i.e. better than the specification 0.01% for the instrumentation). The comparable relative standard deviation for Days 9 and 10 is 0.015% which is actually better than the 0.1% which was specified for the instrumentation. However, closer inspection of the data in Fig. 20 shows that the results for $(k_R')_{21}$ actually fall into two groups separated by the cessation of the calibration pulse. The relative standard deviations on the two sides of this dividing line are 0.0023%. The mismatch of the kind observed for Days 9 and 10 is presumably due to errors in the power delivered by one or both of the polarising circuits used to drive the cell and the calibration heater. The circuit illustrated in Fig. 15B was therefore devised to use the same current supply to drive both the cell and the calibration heater. However, this feature of the switching boxes was never put into use.

We observe that notwithstanding the errors illustrated in Fig. 20, the relative standard deviations are so small that it should be possible to make thermal balances to within 0.1mW for a typical input of 1 W to the calorimeters. The analysis presented above indicates that such balances should be made using the integral heat transfer coefficients $(k_R')_{22}$ estimated at $t = 0$. Table 2 illustrates such a calculation made using the seven applicable measurement cycles. We can see that the rate of excess enthalpy generation shown in Column 8 is 0.0011 W. These rates, also shown in Figs. 5A and B in comparison with those calculated using the differential heat transfer coefficients $(k_R')_{12}$, are approximately equal to the rates which may be calculated for the reduction of electrogenerated oxygen present in the cell (compare [12]). It will be clear that we must regard the rates as being constant during each measurement cycle, an assumption which is evidently justified. The data shown in Column 8 of Table 2 confirm that such rates can be estimated to within ± 0.0001 W which requires that the accuracy of the true integral heat transfer coefficient is nearly equal to the precision of the lower bound values, i.e. that the errors are $\sim \pm 0.01\%$.

Discussion

We note first of all that the radiant surface area of the ICARUS-2 cell used in these experiments was 109.7cm^2 . Multiplying by the Stefan-Boltzmann coefficient $5.6703 \times 10^{-12}\text{Wcm}^{-2}\text{K}^{-4}$ we obtain $(k_R')_{262} = 0.622 \times 10^{-9}\text{WK}^{-4}$, which is close to the value determined by the calibrations, Table 1. The agreement of the predicted and measured values can be taken as a justification for the representation of heat transfer by equations such as (A.3) where the rate of radiative heat transfer is increased slightly from the value which applies to radiation alone to allow for a small term due to the effects of conductive heat transfer.

We also note that marked increases of the heat transfer coefficient from the value predicted from the Stefan-Boltzmann coefficient and the radiant surface area (which have been observed in numerous experiments) indicate a “softening” of the vacuum in the Dewar flasks (or faulty construction of the cells) and/or inappropriate experiment designs and methods of evaluation of the data as well as neglect of the effects of “positive feedback”.

The material presented in this paper shows that exact data analyses should be based on the evaluation of the true integral heat transfer coefficient, $(k_R')_{22}$, coupled to the integral lower bound heat transfer coefficient $(k_R')_{21}$. Accurate and precise estimates of these coefficients can be obtained from $(k_R')_{262}^0$ and $(k_R')_{261}^0$, the values that apply to the calibration period $t_1 < t < t_2$. The procedure which we have illustrated here was part of that incorporated in the ICARUS-Systems methodology (3).

The accuracy of $(k_R')_{22}$ and precision of $(k_R')_{21}$ are very nearly equal with errors of $\sim \pm 0.01\%$. Such errors can in fact be estimated from the errors in the temperature measurements coupled to the averaging procedures which have been described in this paper. The accuracy and precision which can be achieved should be compared to the rather wild statements have been made in the literature about the accuracy of this type of instrumentation. Such statements can be seen to be the outcome of inadequate experiments coupled to inadequate and incomplete interpretations.

It will be seen that the application of the integral heat transfer coefficients requires that the rates of any excess enthalpy generation be constant in time. In turn this requires that the experiments be carried out using suitable "blank systems". If the rates of excess enthalpy generation vary with time, we will inevitably conclude that the instrumentation has enhanced errors. Moreover, such a conclusion will apply to any calorimetric system which we might propose.

The wild statements made in the literature extend also to the effects of the rates of reduction of electrogenerated oxygen. These rates can be estimated perfectly adequately by carrying out suitable "blank experiments". We note that if the precision and accuracy of the experimentation is lowered to say 1%, it will then be impossible to measure such rates; equally, it will be impossible to monitor the build-up of excess enthalpy generation until this has reached specific rates in the range $0.1-1 \text{ Wcm}^{-3}$. Such deficiencies are no doubt at the root of many of the further confusing results and statements which have been made in the literature.

We observe also that the calibration of the cells could be based equally well on the determination of the lower bound heat transfer coefficients for suitable "blank experiments". The use of such heat transfer coefficients in the data analysis for Pd-based cathodes in D_2O -based electrolytes will then automatically discriminate against the contribution of the reduction of electrogenerated oxygen to the total rates of excess enthalpy generation.

Appendix

It has been established that at low to intermediate cell temperatures (say $30^\circ < \theta < 80^\circ$) the behaviour of the calorimeters is modelled adequately by the differential equation

$$C_p M (d\Delta\theta/dt) = [E_{\text{cell}}(t) - E_{\text{thermoneutral, bath}}]I + Q_f(t) + \Delta QH(t-t_1) - \Delta QH(t-t_2) - (3I/4F[P/\{P^*-P\}])[C_{p,D_2O,g} - C_{p,D_2O,l}]\Delta\theta + L] - (k_R^0)\theta_{\text{bath}}^3[1-\gamma t] \{f_1(\theta)/\theta_{\text{bath}}^3 + 4\phi\Delta\theta\}$$

change in the enthalpy content of the calorimeter
enthalpy input due to electrolysis
rate of excess enthalpy generation

calibration pulse
rate of enthalpy removal by the gas stream with $E_{\text{thermoneutral}}$ referred to the bath temperature

time dependent heat transfer coefficient
effect of radiation
effect of conduction

(A.1)

With the calorimeters supplied with the ICARUS Systems, the conductive contribution to heat transfer is very small. This term could therefore be “lumped” into the radiative term by allowing for a small increase in the radiative heat transfer coefficient:

$$\text{Radiative heat transfer} = (k_R')^0[1-\gamma t][(\theta_{\text{bath}} + \Delta\theta)^4 - \theta_{\text{bath}}^4] \quad (\text{A.2})$$

The values of the pseudoradiative “heat transfer coefficient, $(k_R')^0[1-\gamma t]$, derived are close to those calculated from the Stefan-Boltzmann coefficient and the radiative surface area. If the time dependence of the heat transfer coefficient is not included explicitly in equation (A.2) then

$$\text{Radiative heat transfer} = (k_R') [(\theta_{\text{bath}} + \Delta\theta)^4 - \theta_{\text{bath}}^4] \quad (\text{A.3})$$

where the pseudoradiative heat transfer coefficient, (k_R') , now shows a weak time-dependence.

The simplest starting point is to assume that there is no excess enthalpy generation in the calorimeter and to evaluate a corresponding “differential lower bound heat transfer coefficient” at a time just before the end of the calibration pulse, $t = t_2$:

$$(k_R')_1 = [(E_{\text{cell}}(t) - E_{\text{thermoneutral, bath}})I - \Delta H_{\text{evap}}(t) - C_p M (d\Delta\theta/dt) + \Delta QH(t-t_1)]/f_1(\theta) \quad (\text{A.4})$$

This was the first heat transfer coefficient used in our investigations, hence the designation $(k_R')_1$. It will be apparent that the differential lower bound heat transfer coefficient $(k_R')_{11}$, may be evaluated at other points of the measurement cycle, by changing the enthalpy input due to the calibration pulse to

$$\Delta QH(t-t_1) - \Delta QH(t-t_2) \quad (\text{A.5})$$

It is next necessary to evaluate a “true heat transfer coefficient”. The simplest procedure giving $(k_R')_2$ near the end of the calibration period at $t=t_2$ is obtained by including the calibration pulse

$$(k_R')_2 = \{ \Delta Q + [E_{\text{cell}}(\Delta\theta_2, t_2) - E_{\text{cell}}(\Delta\theta_1, t_2)]I - \Delta H_{\text{evap}}(\Delta\theta_2, t_2) + \Delta H_{\text{evap}}(\Delta\theta_1, t_2) - C_p M [(d\Delta\theta/dt)_{\Delta\theta_2, t_2} - (d\Delta\theta/dt)_{\Delta\theta_1, t_2}] \} / f_2(\theta) \quad (\text{A.6})$$

where we now have

$$f_2(\theta) = [\theta_{\text{bath}} + (\Delta\theta_2, t_2)]^4 - [\theta_{\text{bath}} + (\Delta\theta_1, t_2)]^4 \quad (\text{A.7})$$

It can be seen that we need to estimate the cell potential, the cell temperature and the differential of this temperature at the time $t=t_2$ which would have been reached in the absence of the calibration pulse [see footnote (A.1)]

Footnote (A.1) This evaluation was carried out in a somewhat different manner in the initial studies (1), (2) (7) in an attempt to avoid the disadvantages of such interpolation procedures. The values of $(k_R')_{11}$ and $(k_R')_2$ obtained were used as starting values for the non-linear regression procedure used at that time (2). As we could not make this procedure "user friendly" with the computing power then available to us and as, more especially, the methodology which we adopted was evidently not understood (8). (for a further example of such misunderstanding see (5)) we adopted the methodology described in the present paper. This methodology was also the basis of the ICARUS Systems (9).

As is explained in the main text, it is preferable to base the evaluation of the "raw data" on the integrals of the enthalpy input and of the temperature functions rather than to lower the precision and accuracy of the evaluations by using the differentials of the inherently noisy temperature-time series.

For the backward integrals starting from $t \simeq T$ we obtain

$$(k_R')_{21} = \frac{\int_T^t \text{net enthalpy input } (\tau) d\tau}{\int_T^t f_1(\theta) d\tau} - \frac{C_p M [\Delta\theta(t) - \Delta\theta(T)]}{\int_T^t f_1(\theta) d\tau} - \frac{Q_d [t - T]}{\int_T^t f_1(\theta) d\tau} \quad (\text{A.8})$$

while forward integration from the start of the measurement cycle

$$(k_R')_{31} = \frac{\int_0^t \text{net enthalpy input } (\tau) d\tau}{\int_0^t f_1(\theta) d\tau} - \frac{C_p M [\Delta\theta(t) - \Delta\theta(0)]}{\int_0^t f_1(\theta) d\tau} - \frac{Q_d [t]}{\int_0^t f_1(\theta) d\tau} \quad (\text{A.9})$$

The evaluation of the heat transfer coefficients applicable to particular time regions ($j = 5, 6, 7, 8$) simply requires changes in the lower limits of the relevant integrals.

The evaluation of the "true heat transfer coefficients" requires the combination of the enthalpy inputs in equations (A.8) and (A.9) with the thermal inputs made at one or a series of points. This can be carried out in a number of ways; we confine attention here to the procedure originally suggested in the Handbook for the ICARUS - 1 System (9). If we consider $(k_R')_{362}$ and if we make a thermal balance just before the application of the calibration pulse, then if the system has relaxed adequately so that we can set $d\Delta\theta/\approx 0$

$$0 = [\text{Net enthalpy input } (t_1)][t - t_1] + Q_f[t - t_1] - (k_R')_{32} \{[(\theta_{\text{bath}} + \Delta\theta(t_1))^4 - \theta_{\text{bath}}^4][t - t_1]\} \quad (\text{A.10})$$

Combination with equation (A.9) (with the appropriate change in the lower limit of the integration) gives

$$(k_R')_{362} = \frac{\int_{t_1}^t \text{net enthalpy input } (\tau) d\tau - [\text{net enthalpy input } (t_1)][t - t_1] - C_p M [\Delta\theta(t) - \Delta\theta(t_1)]}{\int_{t_1}^t f_1(\theta) d\tau} \quad (\text{A.11})$$

The corresponding equation for $(k_R')_{262}$ follows from (A.11) on replacing t_1 by t_2 . It is convenient to write all the equations for the determination of the relevant heat transfer coefficients in the "straight line form" e.g.

$$\left. \frac{\int_{t_2}^t \text{net enthalpy input } (\tau) d\tau - [\text{net enthalpy input } (t_1)][t - t_2]}{\int_{t_2}^t f_1(\theta) d\tau} \right\} y = C_p M [\Delta\theta(t) - \Delta\theta(t_2)] + (k_R')_{262}^0 \quad (\text{A.12})$$

where $(k_R')_{262}^0$ can be seen to be the value of the integral heat transfer coefficient at $t = t_2$. The value of t_2 should be chosen to be the mid-point of the measurement cycle as $(k_R')_{262}^0$ is the most useful (and well defined) value of the true heat transfer coefficient. It should be noted that extrapolations such as (A.12) automatically remove the effects of $C_p M$ on the value of the derived heat transfer coefficient (a desirable feature because the water equivalents of the cells have the highest errors).

The integral lower bound heat transfer coefficient, $(k_R')^{\circ}_{261}$ (equation (A.8) with T replaced by t_2) and the integral true heat transfer coefficient, $(k_R')^{\circ}_{262}$, (equation (A.12)) were the “target procedures” for the ICARUS -style evaluations of the experimental data (9).

It should be noted that the definitions of the integral heat transfer coefficients given in this Appendix have regarded these coefficients as being constant in time whereas we would, in fact, anticipate a weak time dependence e.g. equation (A.2) or Fig.6. This weak time-dependence causes an equally weak time-dependence of the derived heat transfer coefficients. Use of the more exact equation (A.2) gives for example for the derived values of $(k_R')_{21}$ in (A.8)

$$(k_R')_{21} = (k_R')^{\circ}_{21} [1 - \gamma(t-T) + \gamma \int_T^t \int_T^{\tau} f_1(\theta) d\tau d\theta / \int_T^t f_1(\theta) d\theta] \quad (A.13)$$

where $(k_R')^{\circ}_{21}$ is the value of $(k_R')_{21}$ at $t = T$. An ultimate test of the validity of the representation of the calorimeters by the differential equation (A.1) is therefore the question of whether the heat transfer can be represented by a single time-independent coefficient, here $(k_R')^{\circ}_{21}$. This question is discussed further in the main text.

We also note that if we regard $f_1(\theta)$ as being constant throughout the measurement cycle (which is a rough approximation for the case of the “lower bound heat transfer coefficients”) then (A.13) becomes

$$(k_R')_{21} = (k_R')^{\circ}_{21} [1 + \gamma(T - t)/2] \quad (A.14)$$

Similarly, we obtain

$$(k_R')_{31} = (k_R')^{\circ}_{31} [1 - \gamma t/2] \quad (A.15)$$

where $(k_R')^{\circ}_{31}$ is now the value of $(k_R')_{31}$ at $t = 0$. It follows that the slopes of the plots of $(k_R')_{21}$ and $(k_R')_{31}$ versus time are roughly one half of the plot of $(k_R')_{11}$ versus time (cf. Fig. 6)

For a more complete discussion see (10), (11).

References

- 1) M. Fleischmann, S. Pons and M. Hawkins, J. Electroanal Chem., 261 (1989) 301; 263 (1989) 187.
- 2) M. Fleischmann, S. Pons, M.W. Anderson, L.J. Li and M. Hawkins, J. Electroanal Chem., 287 (1990) 293
- 3) ICARUS -2; Isoperibolic Calorimetry : Acquisition, Research and Utilities System. Document Version 2.0 (February, 1995), TECHNOVA INC., 13th Floor, Fukoku Seimei Building, 2-2-2 Uchisaiwai-cho, Chiyoda-Ku, Tokyo 100, Japan.

The ICARUS -1 System is described in:

The ICARUS Systems; Isoperibolic Calorimetry : Acquisition, Research and Utilities System, Version 1 (December 1993), Low Power Measuring System for Three Cells, TECHNOVA INC., 13th Floor, Fukoku Seimei Building, 2-2-2 Uchisaiwai-cho, Chiyoda-Ku, Tokyo 100, Japan.

- 4) O. Levenspiel, "Chemical Reaction Engineering" (1972) Wiley, London.
- 5) Frederick T. Wagner, Thomas E. Moylan, Michael E. Hayden, Ulrike Narger and James L. Booth, J. Electroanal Chem., 295 (1990) 393.
- 6) Wilford N. Hansen, Proceedings of the Second Conference on Cold Fusion, Conference Proceedings of the Italian Physical Society, Editors: Tullio Bressani, Emilio Del Giudice, Giuliano Preparata, Como, Italy. 33 (1991) 491; ISBN 88-7794-045-X: see also Michael E. Melich and Wilford N. Hansen, Proceedings of the Third International Conference on Cold Fusion, Universal Academy Press, Frontiers of Science Series N° 4, Editor : H. Ikegami, Tokyo, Japan, (1993) 397; ISBN 4-946443-12-6.
- 7) M. Fleischmann and S. Pons, J. Electroanal Chem., 332 (1992) 33.
- 8) R.H. Wilson, J.W. Bray, P.G. Kosky, H.B. Vakil and F.G. Will, J. Electroanal Chem., 332 (1992) 1.
- 9) M. Fleischmann, S. Pons, Monique Le Roux and Jeanne Roulette, Trans. Fusion Technol., 26 (1994) 323.
- 10) M. H. Miles, M. Fleischmann and M. A. Inam, Report NRL / MR / 6320--01--8526, Naval Research Laboratory, Washington, DC 20375-5320, March 2001.

11) S. Szpak and P. A. Mosier-Boss, Technical Report 1862, Volume 2, SPAWAR Systems Centre, San Diego, February 2002.

12) Fritz G. Will, J. Electroanal Chem., 426 (1997) 177.

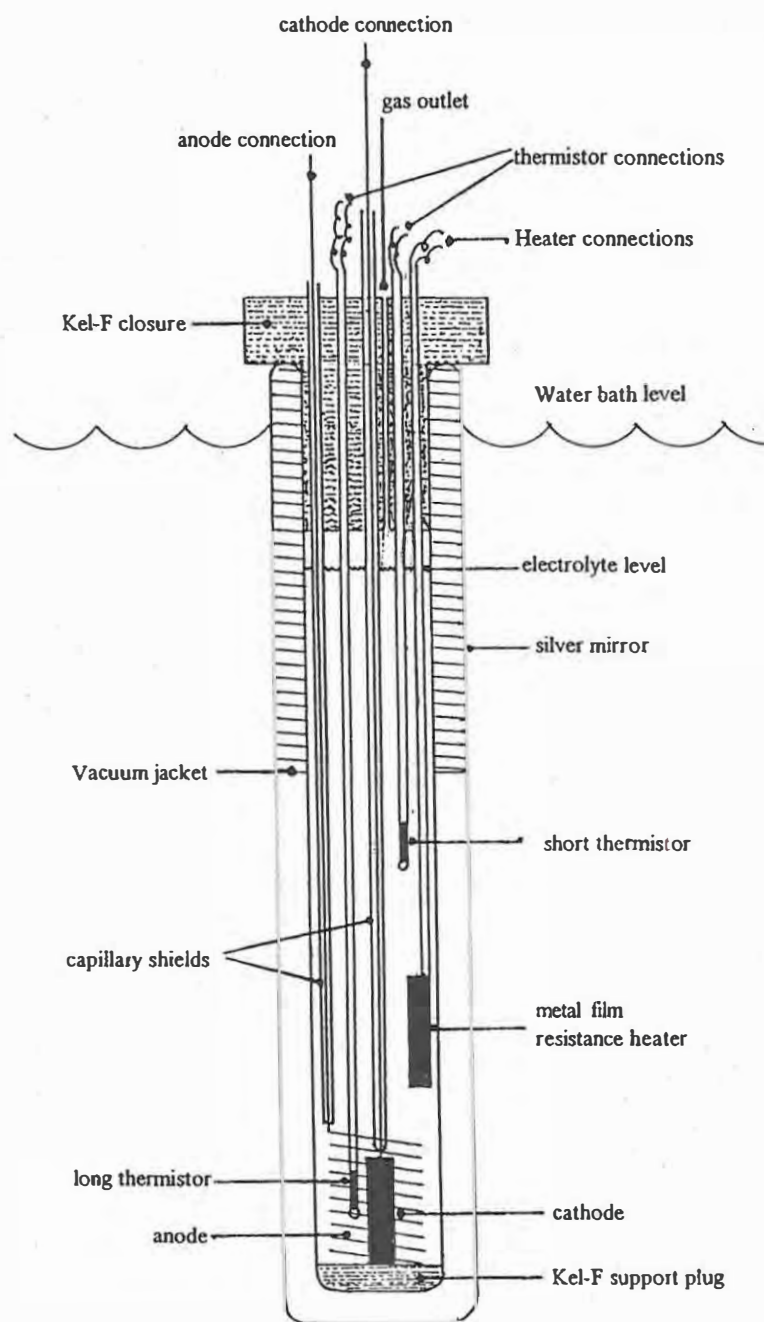


Fig. 1 The Isoperibolic Calorimetric Cell.

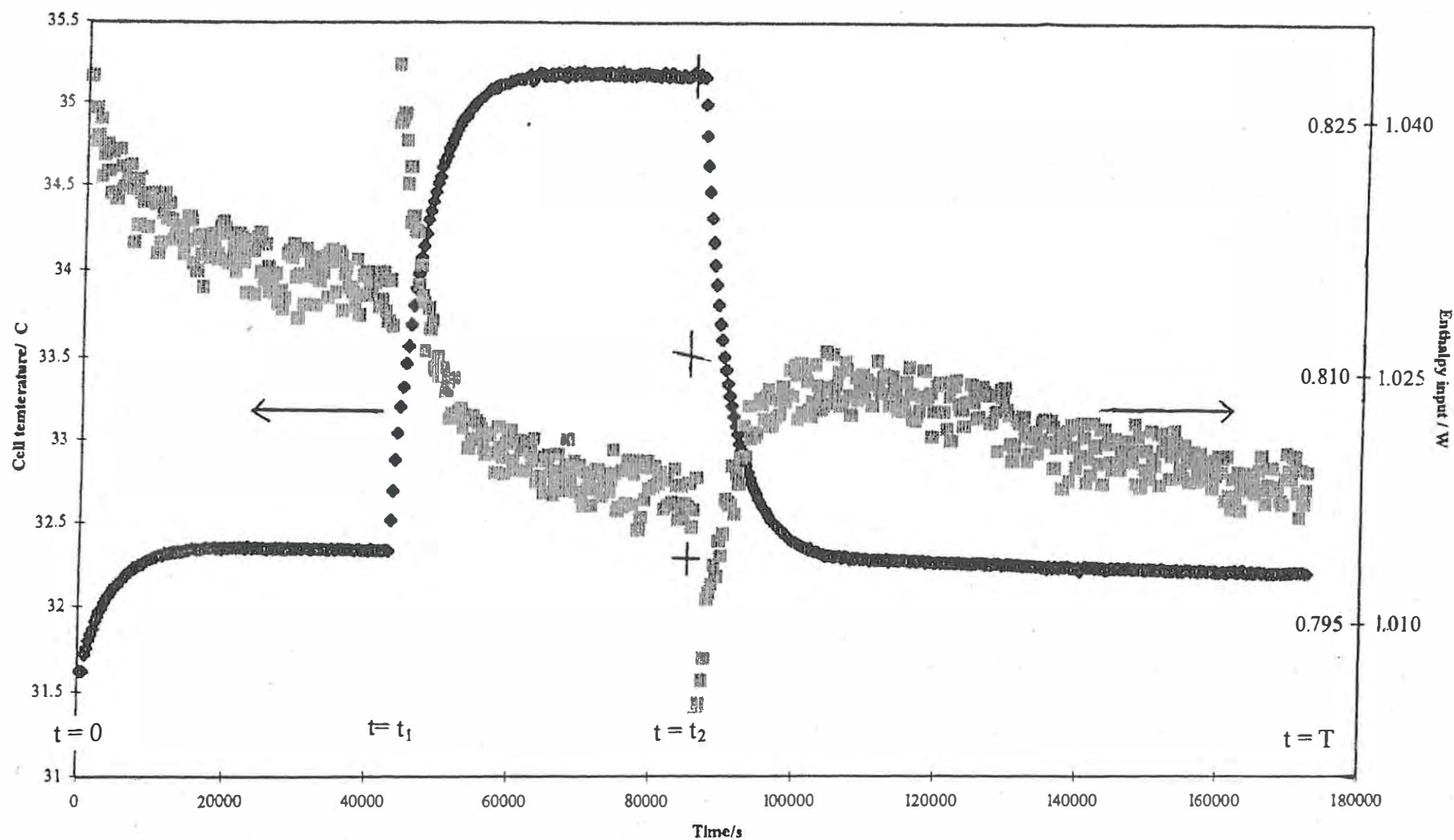


Fig. 2 Plot of the "raw data" for days 9 and 10 of the "blank experiment".
 Pt cathode ($\phi = 1\text{mm}$, $\ell = 2\text{cm}$) polarised at 0.2A in $0.1\text{ M LiOD/D}_2\text{O}$.
 Estimates of the pseudo-radiative lower bound heat transfer coefficient, $(k_R')_1$, and of the pseudo-radiative true heat transfer coefficient, $(k_R')_2$, can be made near the end of the calibration period at $t = t_2$.

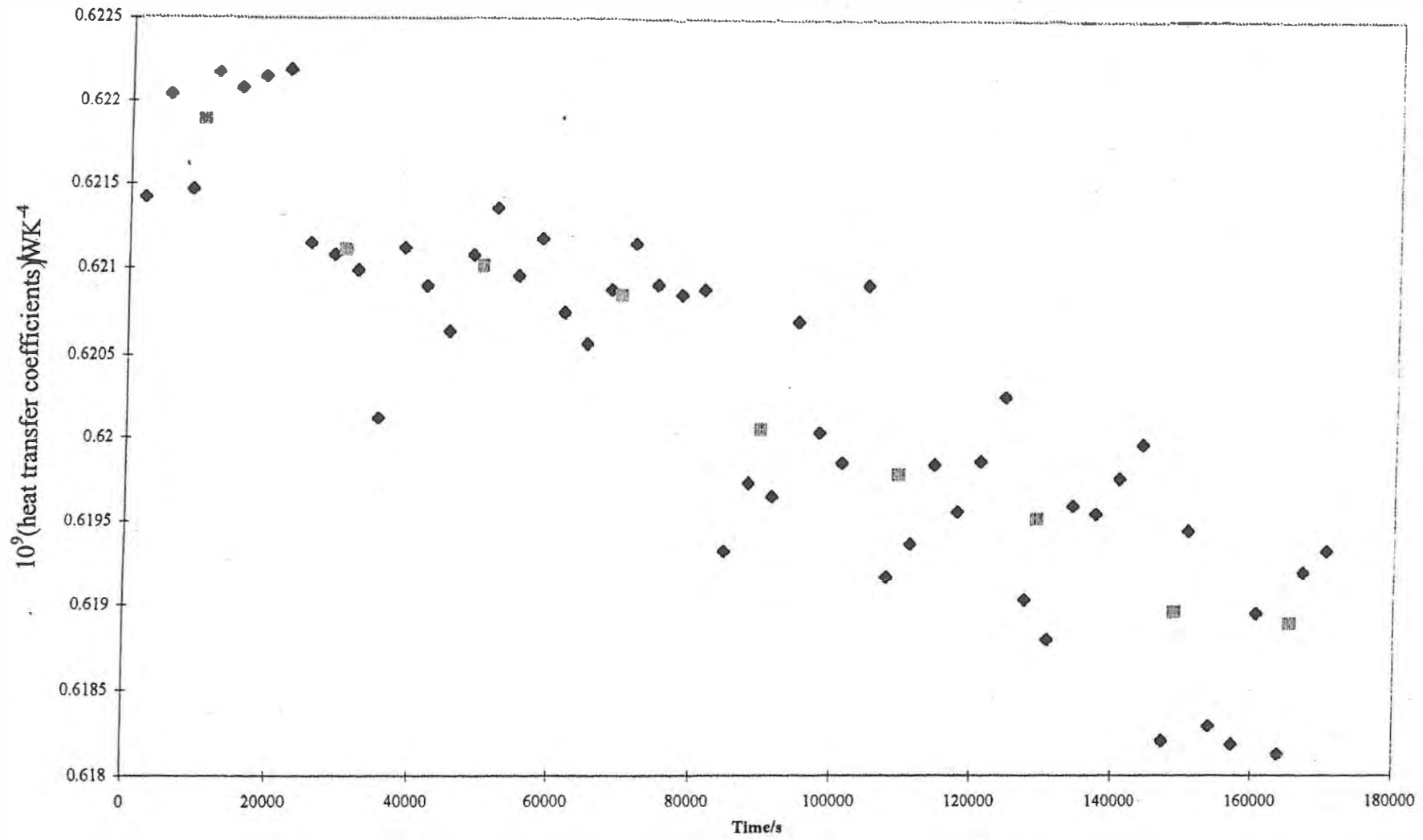


Fig. 3 The values of $(\overline{k_R})_{I1}$ \blacklozenge , and of $(\overline{k_R})_{II}$ \square , for days 1 and 2 of the measurement cycles.

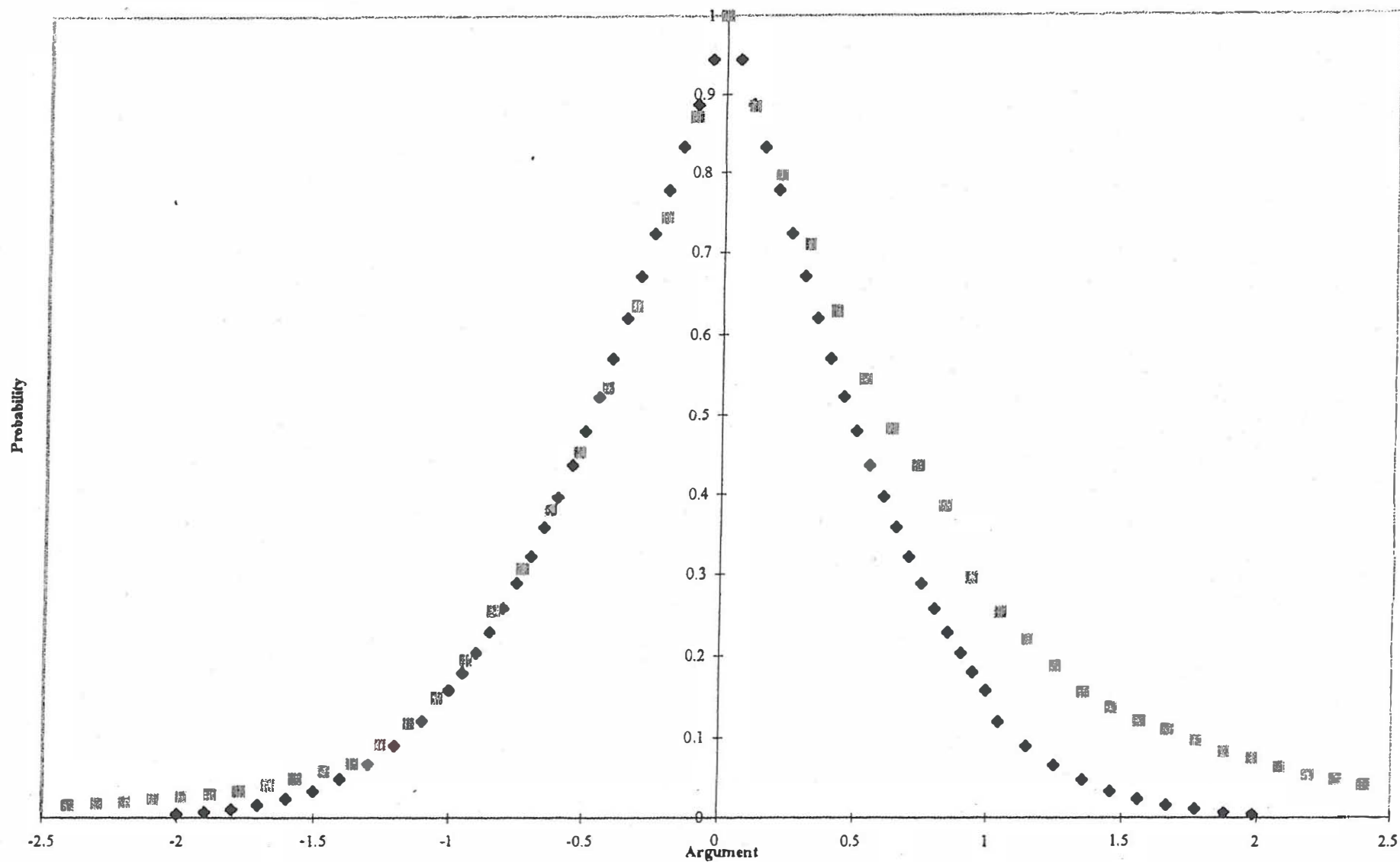


Fig. 4 The upper and lower tail distributions of the differential rates of excess enthalpy generation for days 3-16 of the measurement cycles, \boxtimes ; comparison with a normal distribution of errors, \blacklozenge .

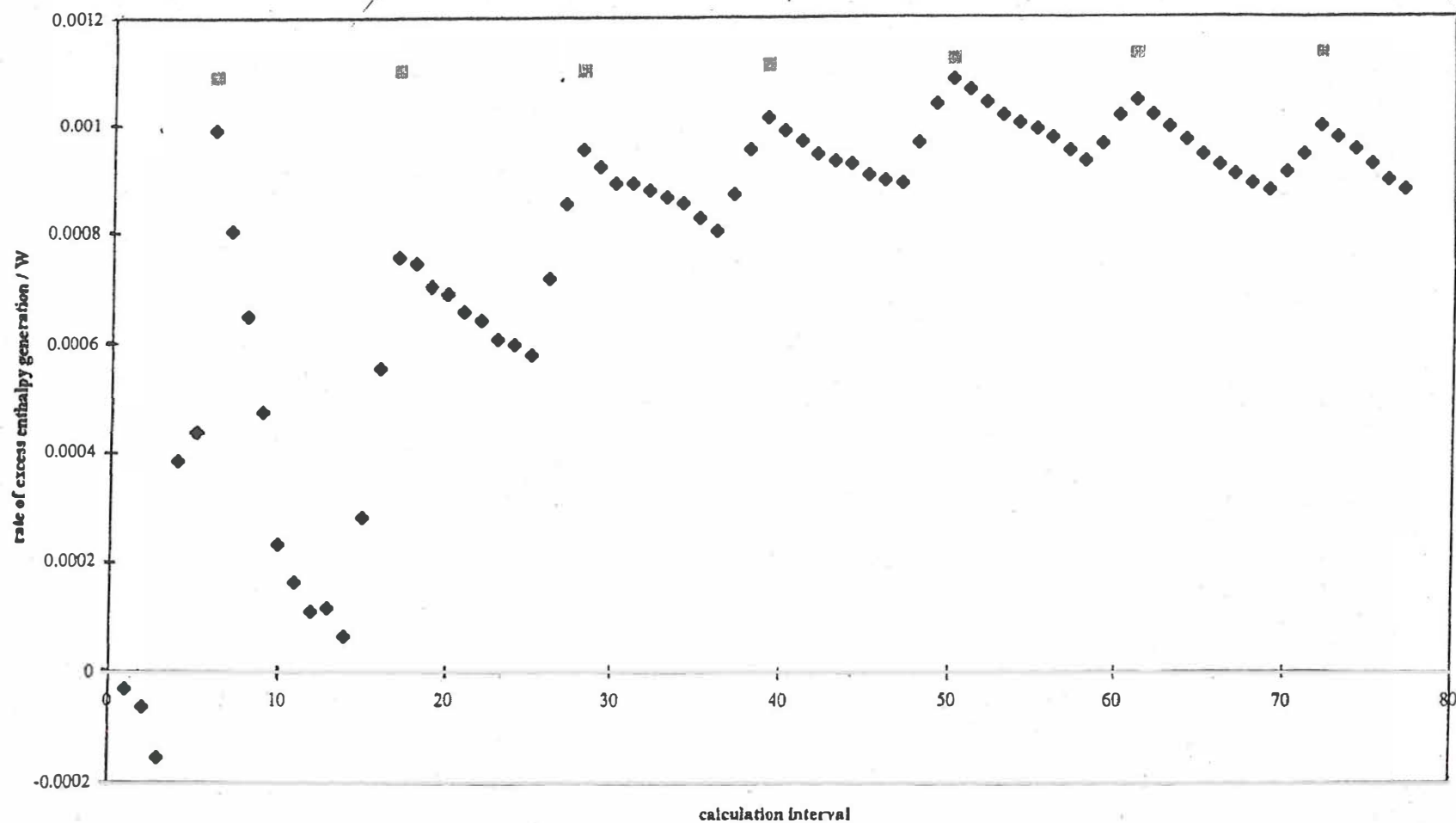


Fig. 5A The differential rates of excess enthalpy generation calculated with a true heat transfer coefficient varying with time, ◆. The figure also shows rates calculated using the integral value of the heat transfer coefficient ◻, see table 2 below.

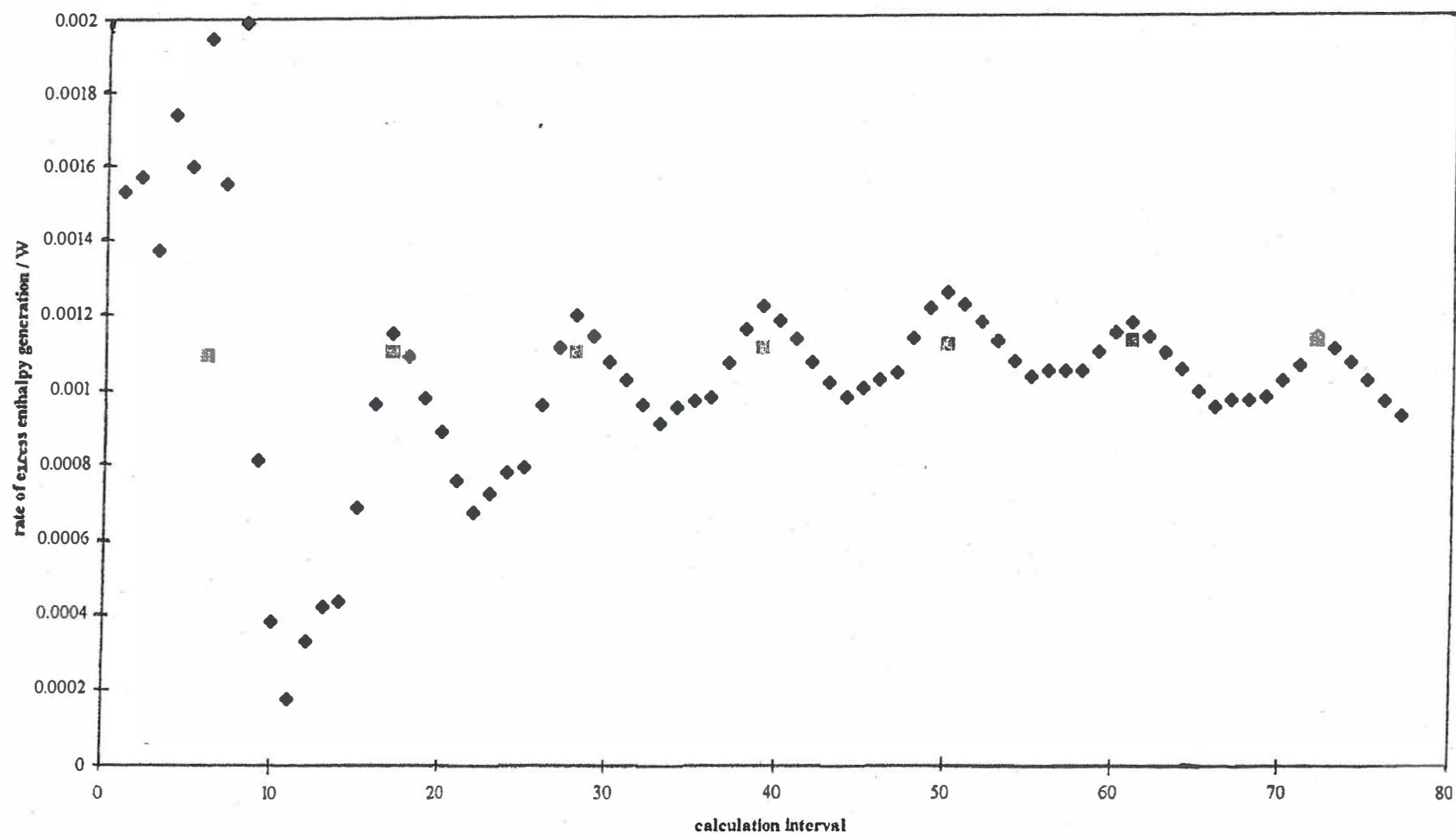


Fig. 5B The differential rates of excess enthalpy generation calculated using a single value of the true heat transfer coefficient at $t = 86,400s$, ◆. The figure also shows rates calculated using the integral value of the heat transfer coefficients, ◻, see Table 2 below.

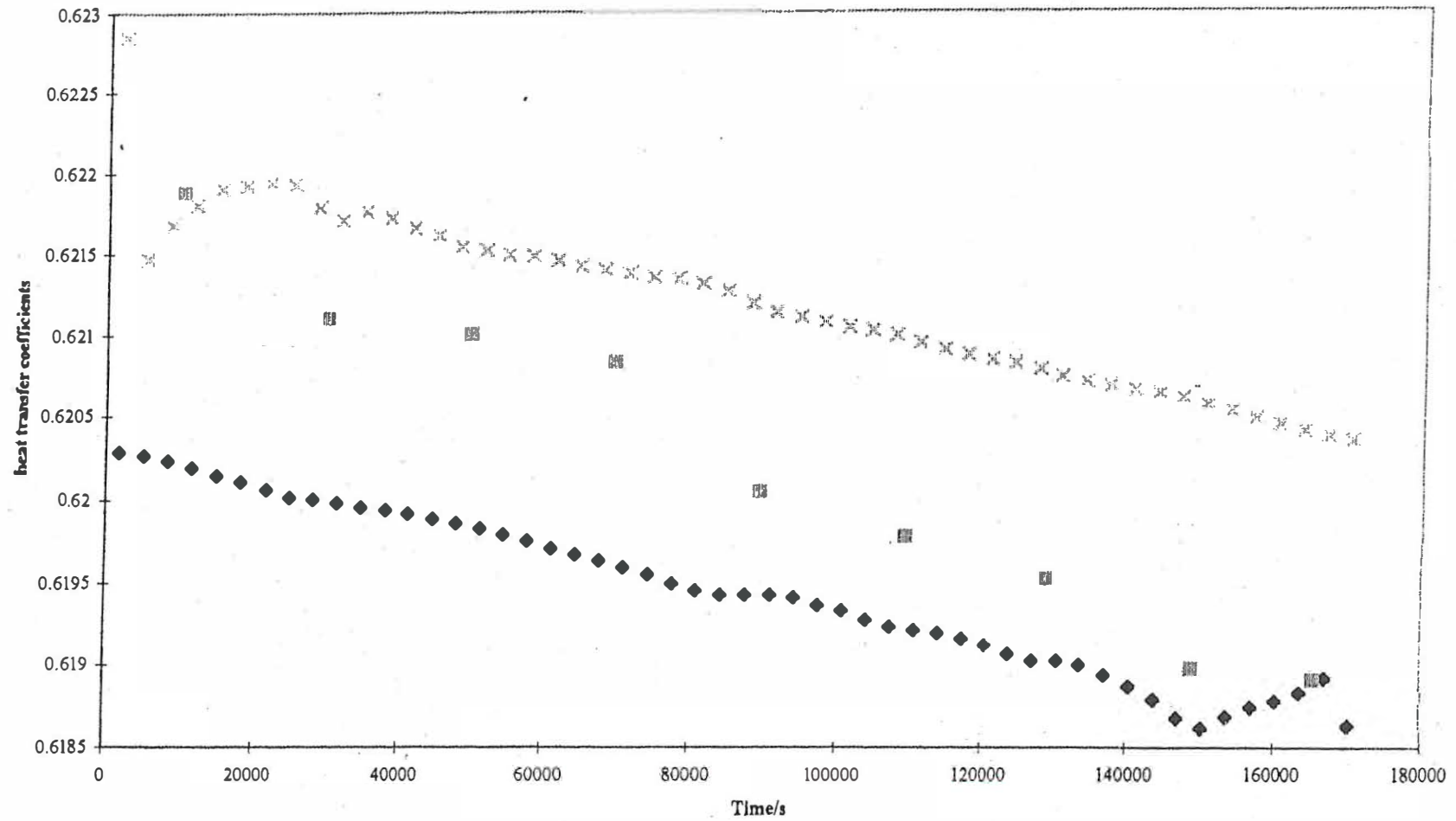
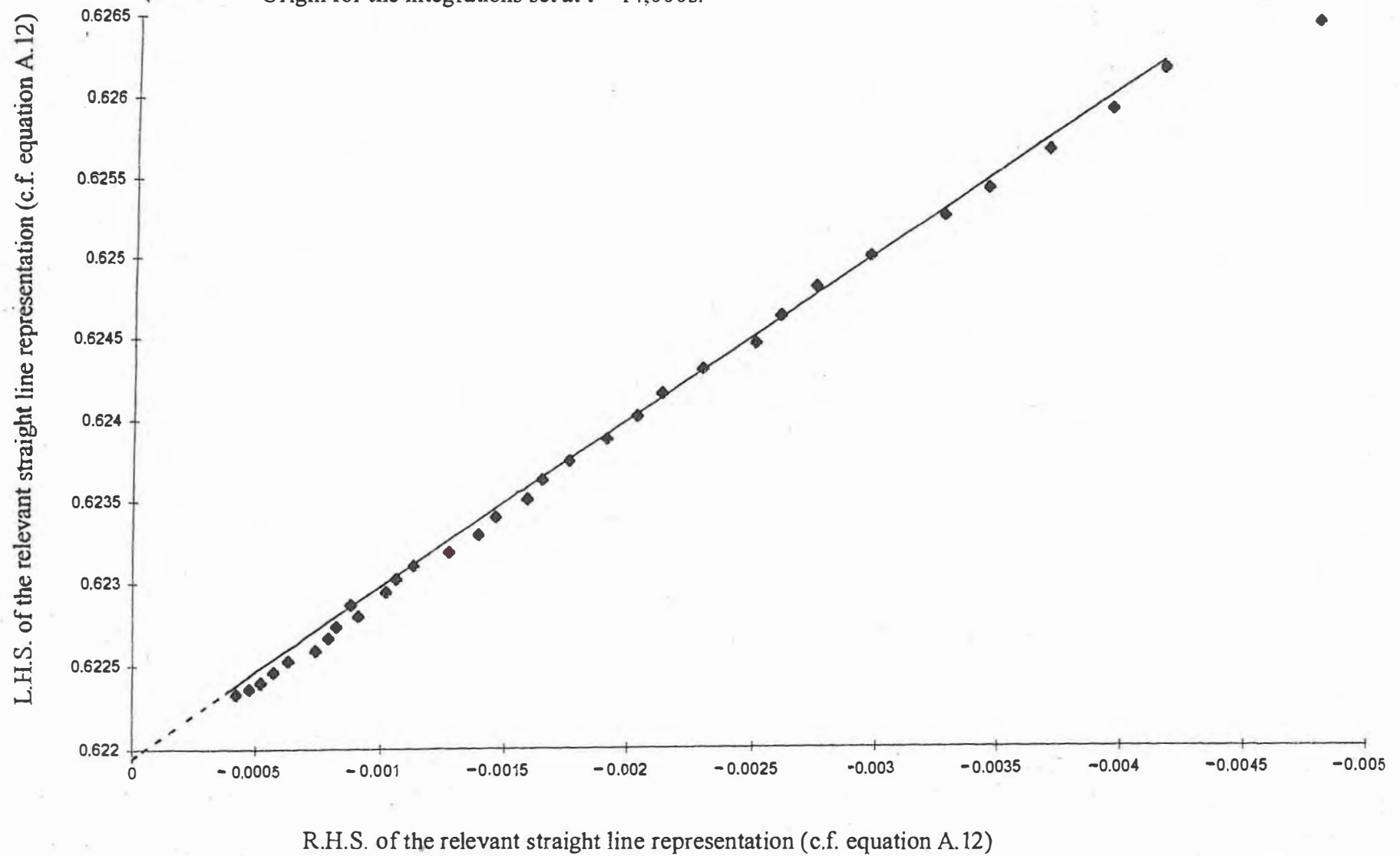


Fig. 6 Comparison of the variation with time of the integral heat transfer coefficients, $(k_R')_{31}$ and $(k_R')_{21}$ x, ♦, with the differential lower bound heat transfer coefficient, $(k_R)_{11}$ ■ Days 1 and 2 of the measurement cycles.

Fig. 7A Evaluation of $(k_R')^0_{251}$ and C_{pM} for Days 9 and 10 of the measurement cycles.
Origin for the integrations set at $t = 14,000s$.



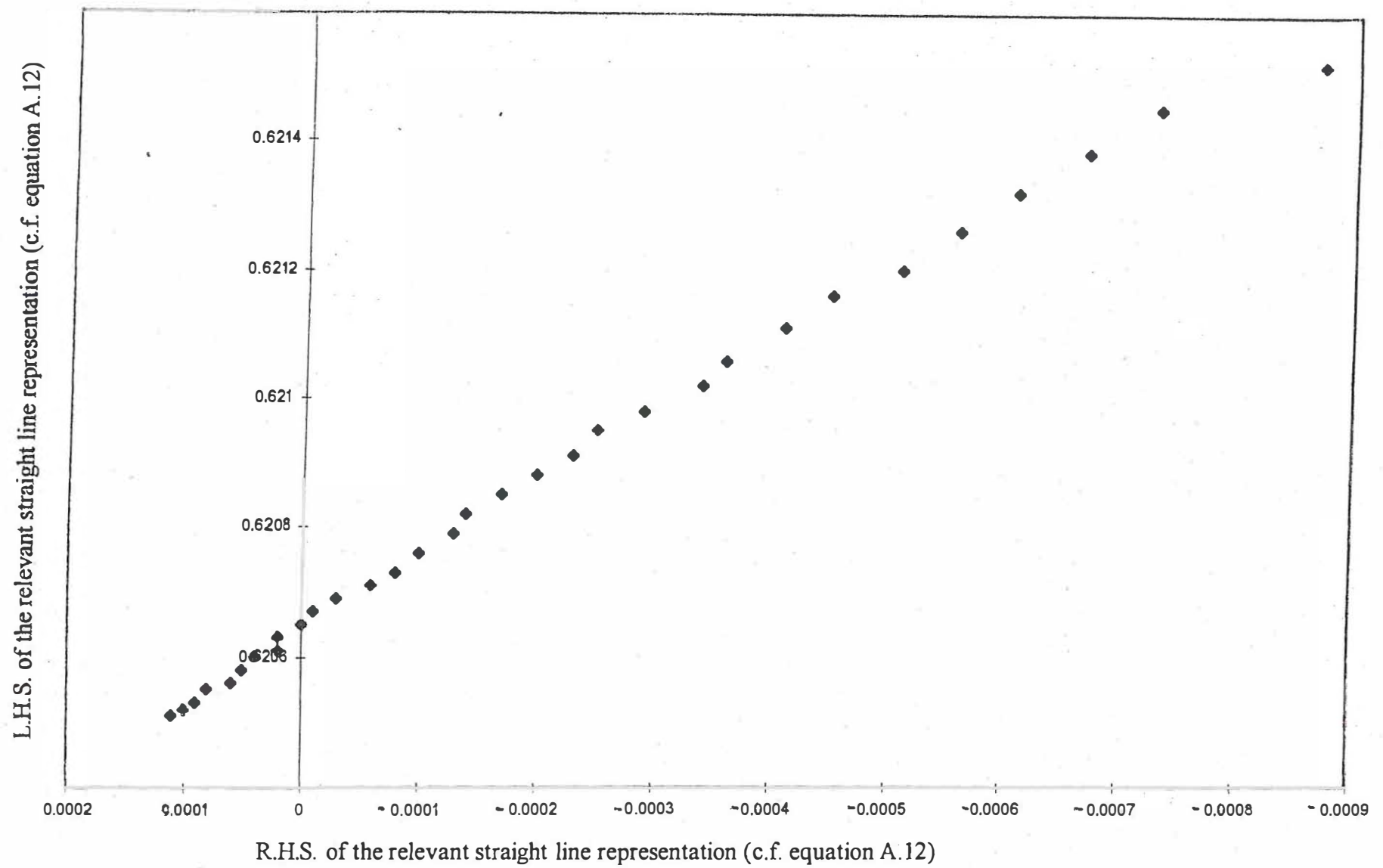


Fig. 7B Evaluation of $(k_R')_{251}^0$ and CpM for Days 9 and 10 of the measurement cycles. Origin for the integrations set at $t = T$.

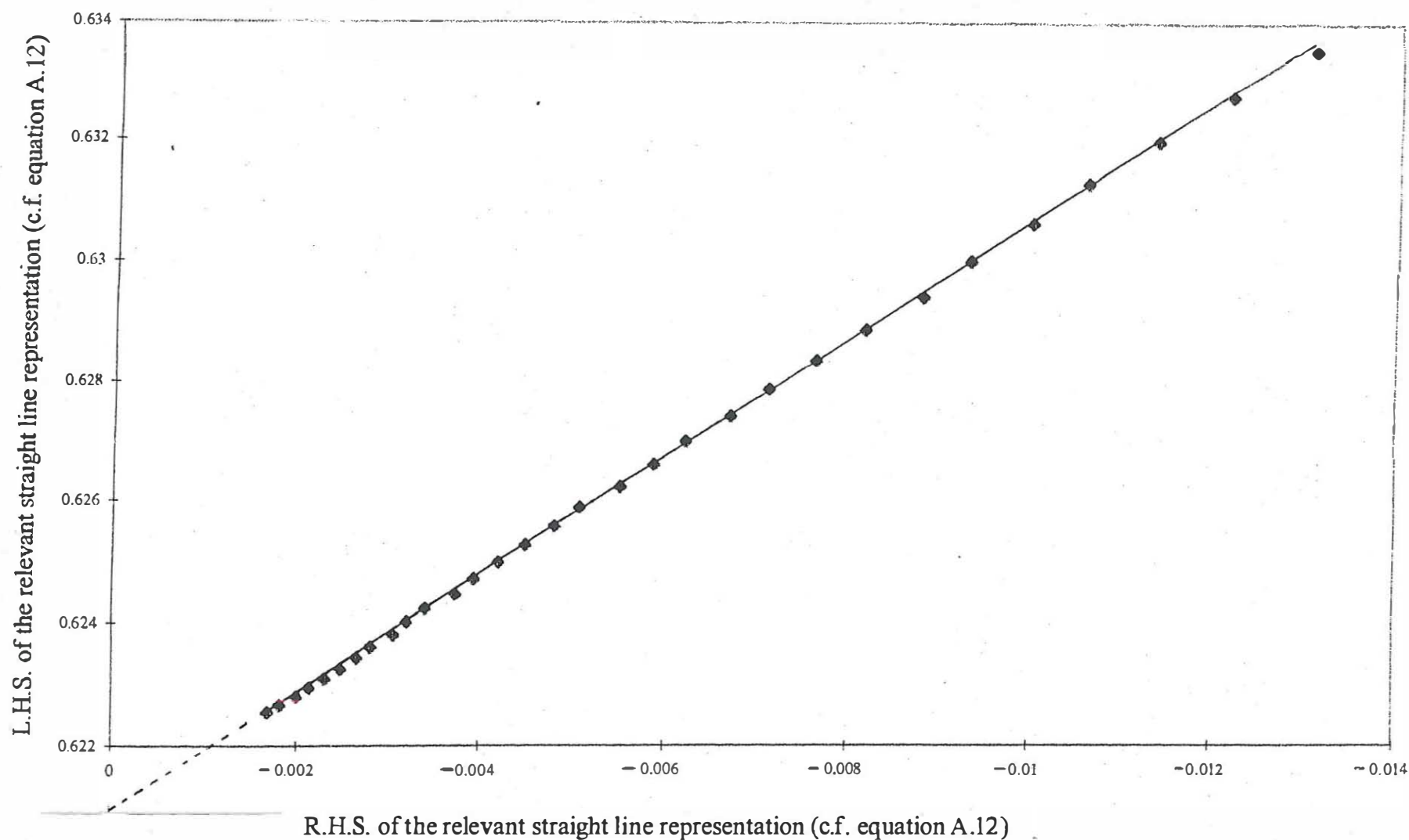


Fig. 8A Evaluation of $(k_R')_{261}^{\circ}$ and C_pM for Days 9 and 10 of the measurement cycles. Origin for the integrations set at $t = t_2$.

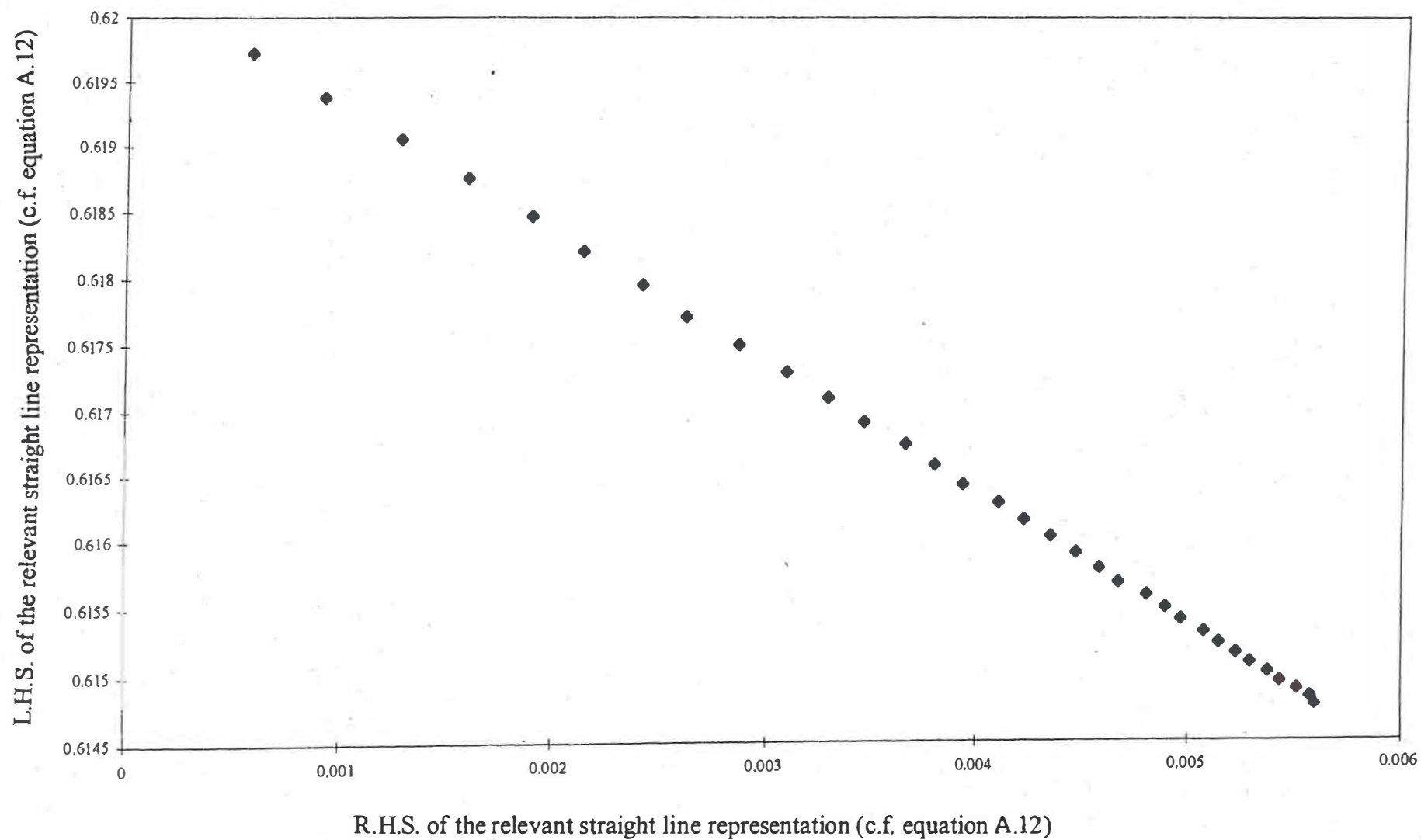


Fig. 8B Evaluation of $(k_R')_{261}^0$ and C_pM for Days 9 and 10 of the measurement cycles.
Origin for the integrations set at $t = T$.

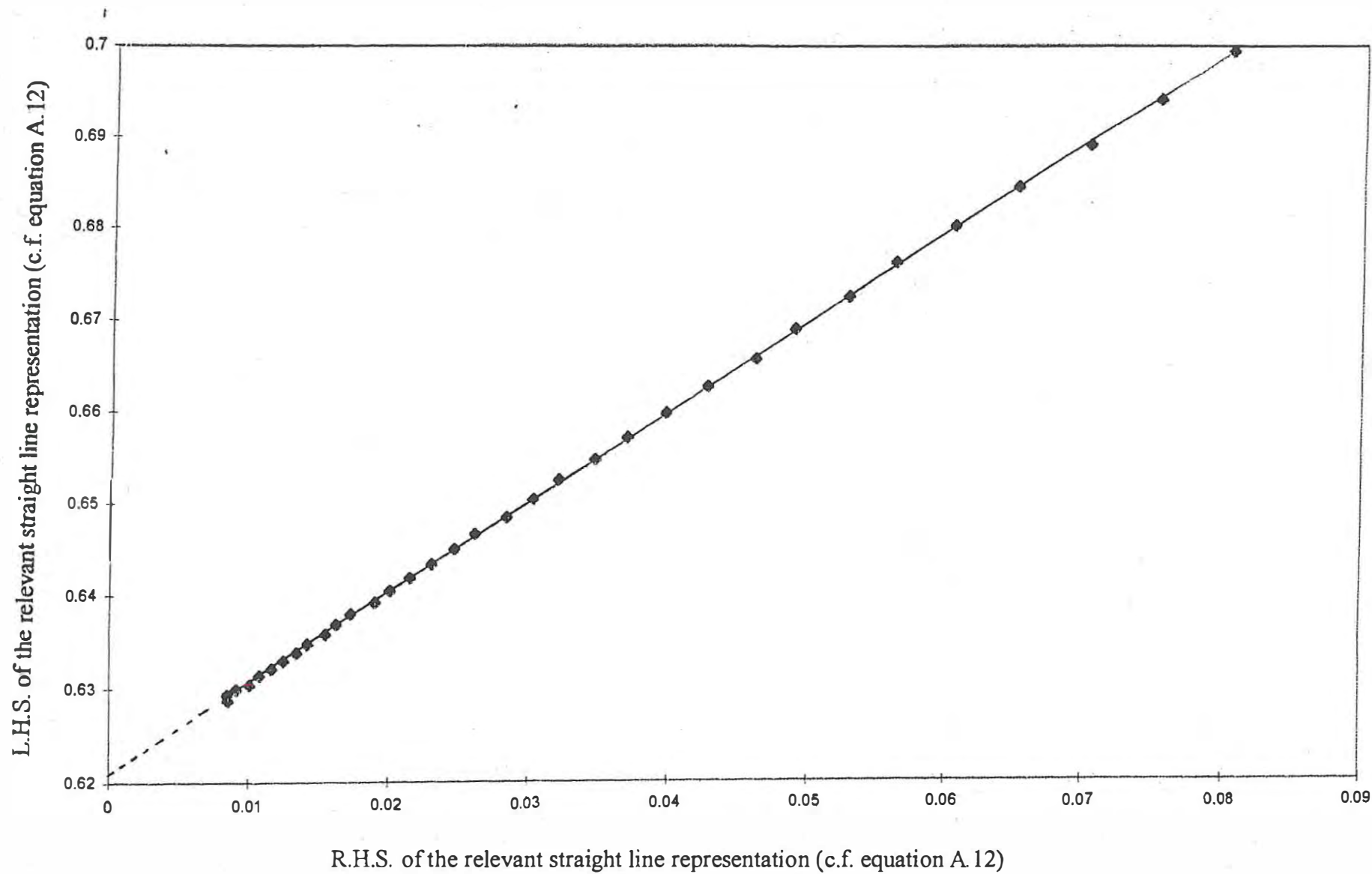


Fig. 9 Evaluation of $(k_R')_{262}^\circ$ and C_pM for Days 9 and 10 of the measurement cycles. Origin for the integrations set at $t = t_2$.

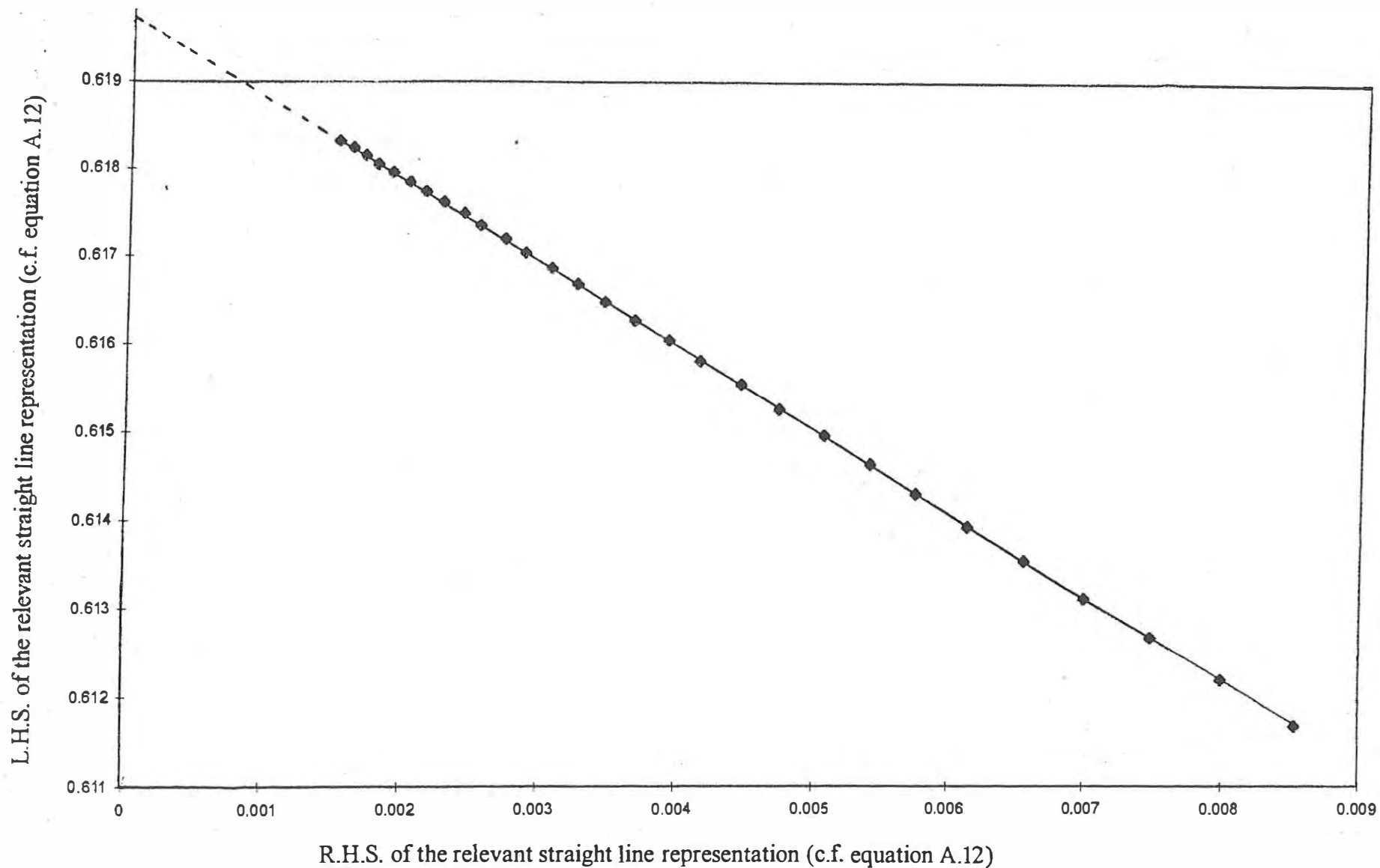


Fig. 10 Evaluation of $(k_R')_{271}^\circ$ and C_pM for Days 9 and 10 of the measurement cycles. Origin for the integrations set at $t = T$.

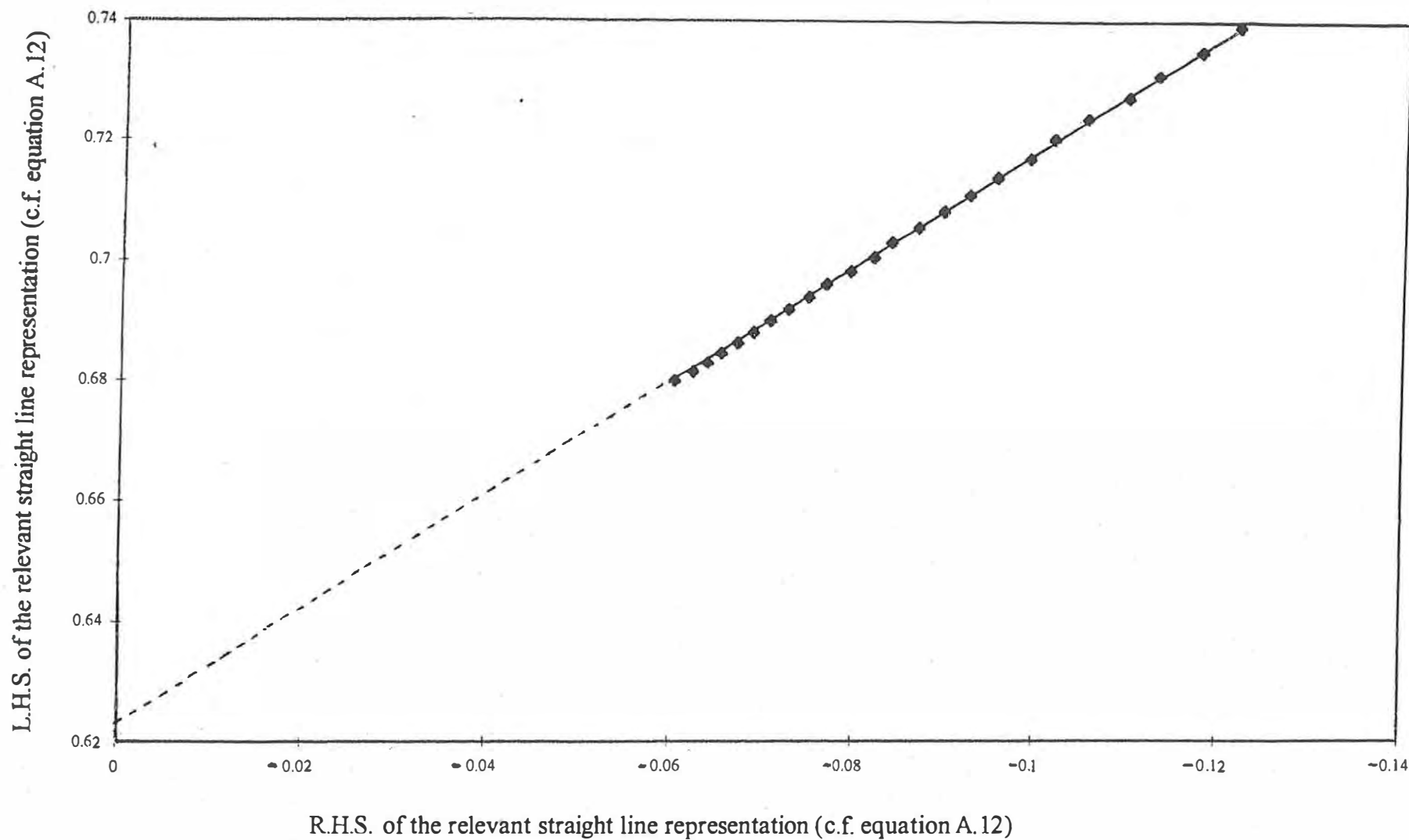


Fig. 11 Evaluation of $(k_R')_{361}^0$ and $C_p M$ for days 9 and 10 of the measurement cycles origin for the integrations set at $t = t_1$. Use of the 33 measurement intervals adjacent to $t = t_1$

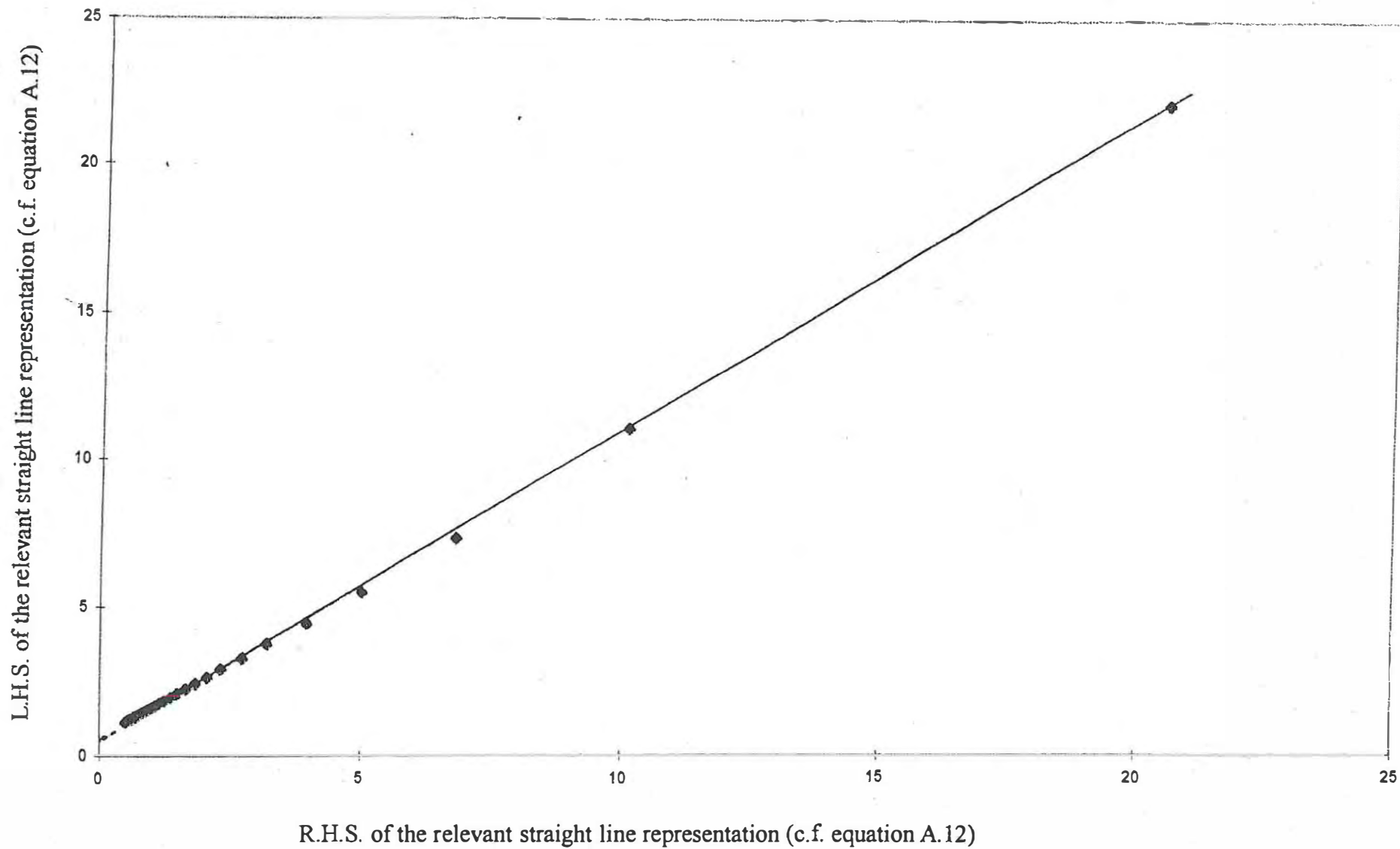


Fig. 12 Evaluation of $(k_R')_{362}^{\circ}$ and $C_p M$ for days 9 and 10 of the measurement cycles origin for the integrations set at $t = t_1$. Use of the 33 measurement intervals adjacent to $t = t_1$.

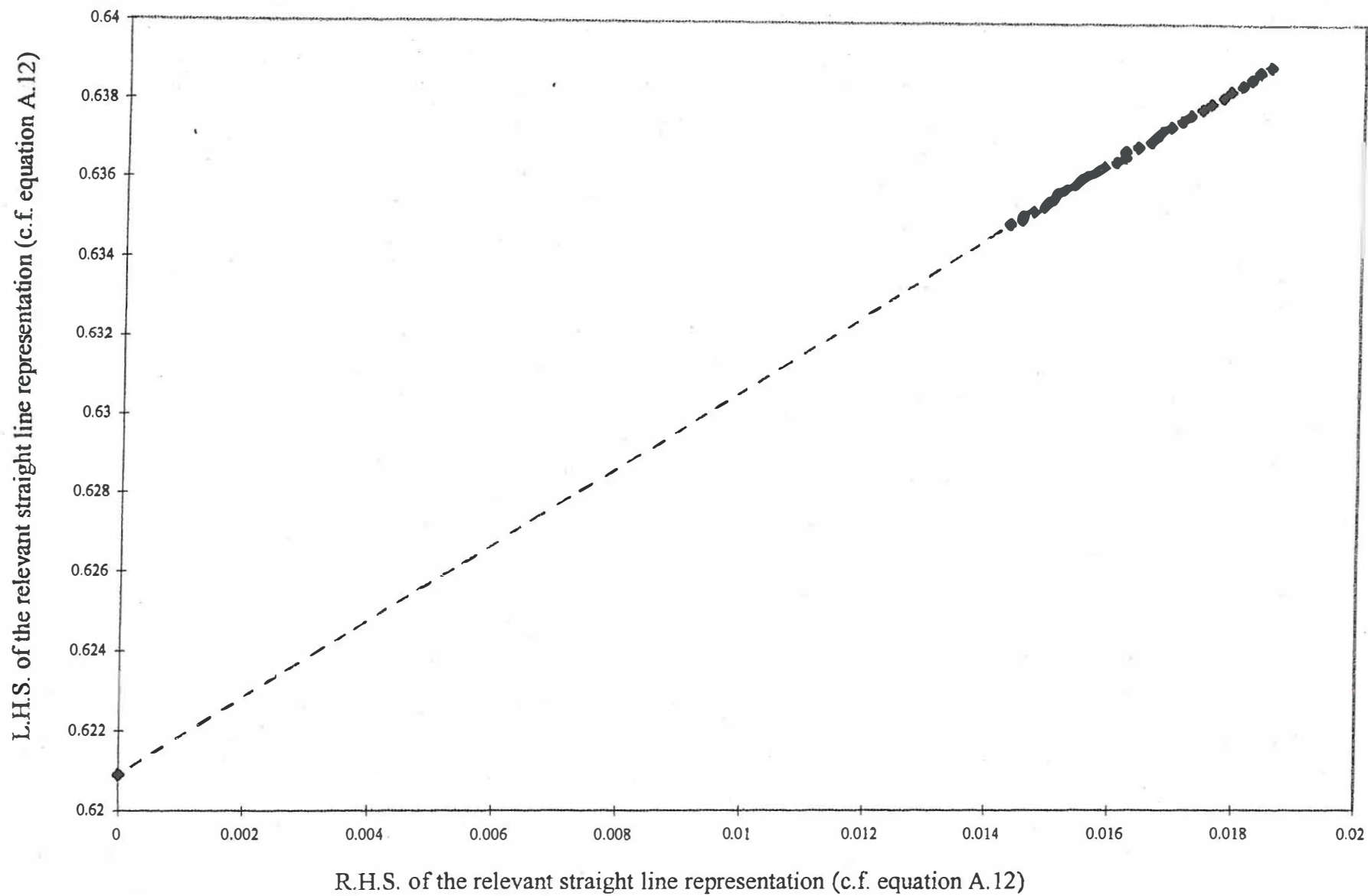


Fig. 13 Evaluation of $(k_R')_{361}^0$ and $C_p M$ for days 9 and 10 of the measurement cycles
origin for the integrations set at $t = t_1$. Use of the 33 measurement intervals adjacent to $t = t_2$

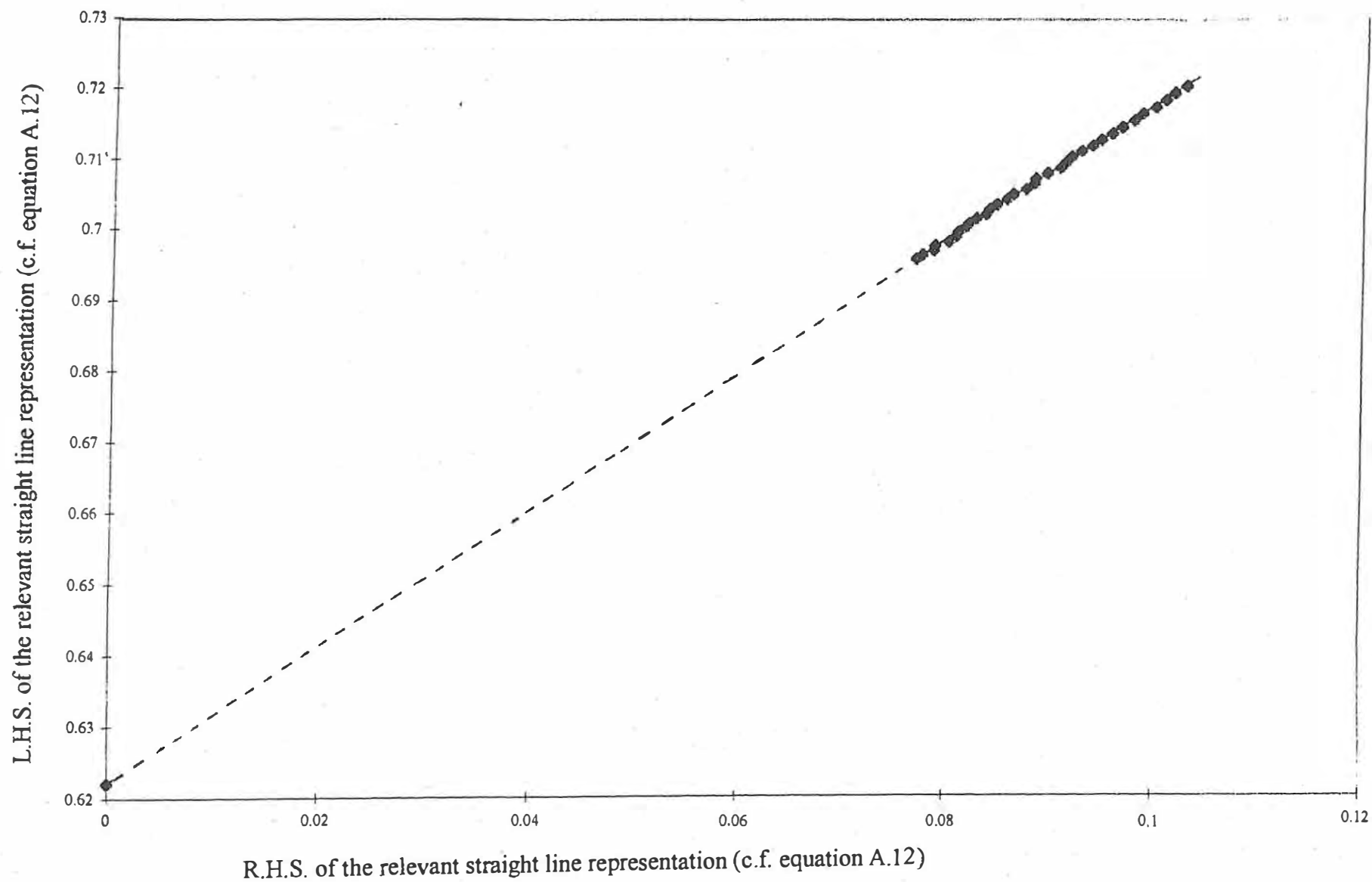


Fig. 14 Evaluation of $(k_R')_{362}^0$ and $C_p M$ for days 9 and 10 of the measurement cycles origin for the integrations set at $t = t_1$. Use of the 33 measurement intervals adjacent to $t = t_2$

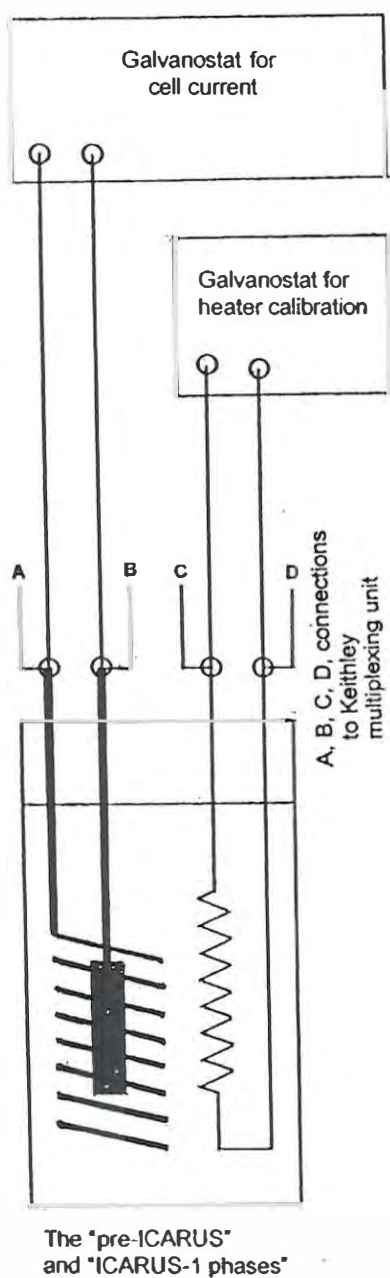


Fig. 15A Schematic of the polarising circuit used with the ICARUS -1 System.

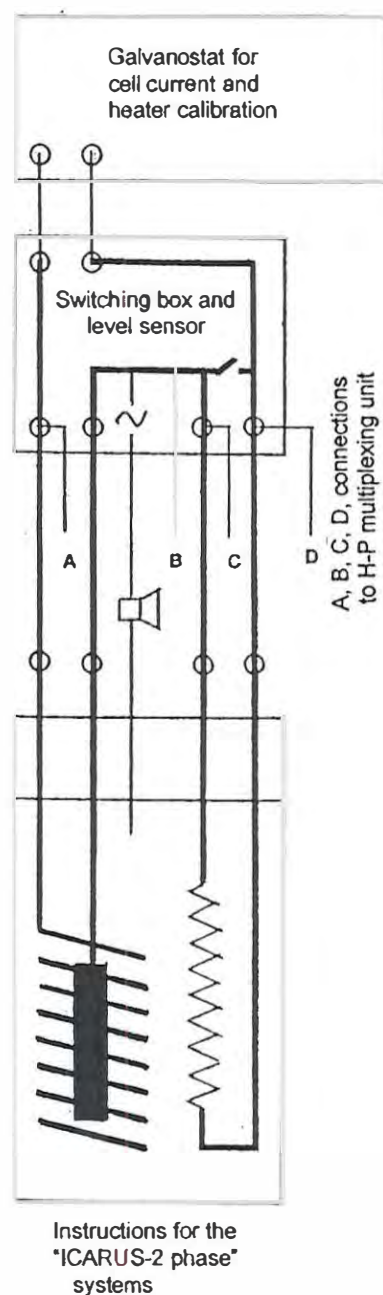


Fig. 15B Schematic of the polarising circuit used with the ICARUS -2 System. The figure shows the provision of the means of using the cell current to calibrate the system as well as the means for testing the level of the electrolyte in the cell.

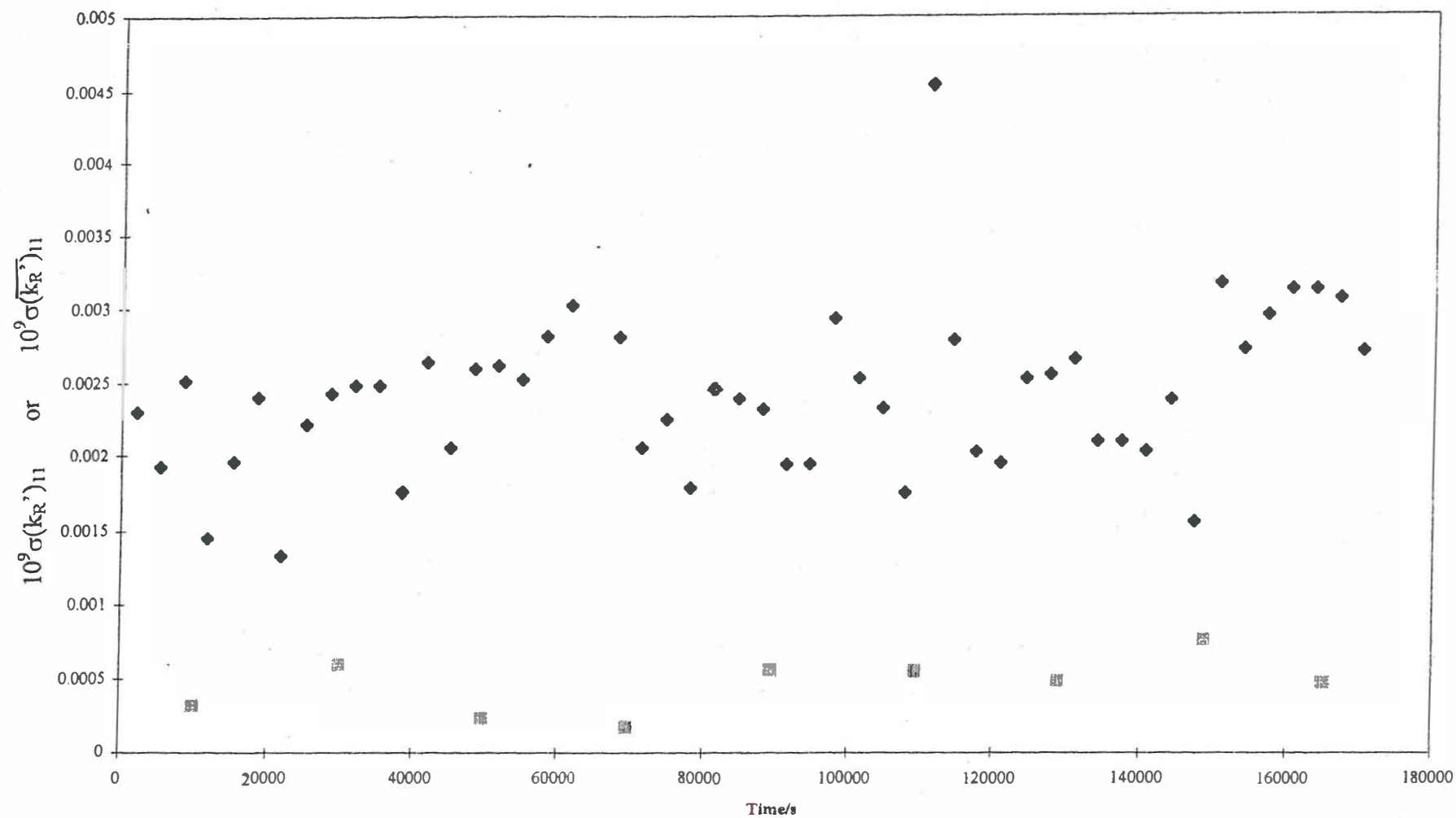


Fig. 16 The standard deviations of the differential lower bound heat transfer coefficients $10^9 (k_R')_{11}$, ◆, and $10^9 (\overline{k_R}')_{11}$, ■, Days 1 and 2 of the measurement cycles.

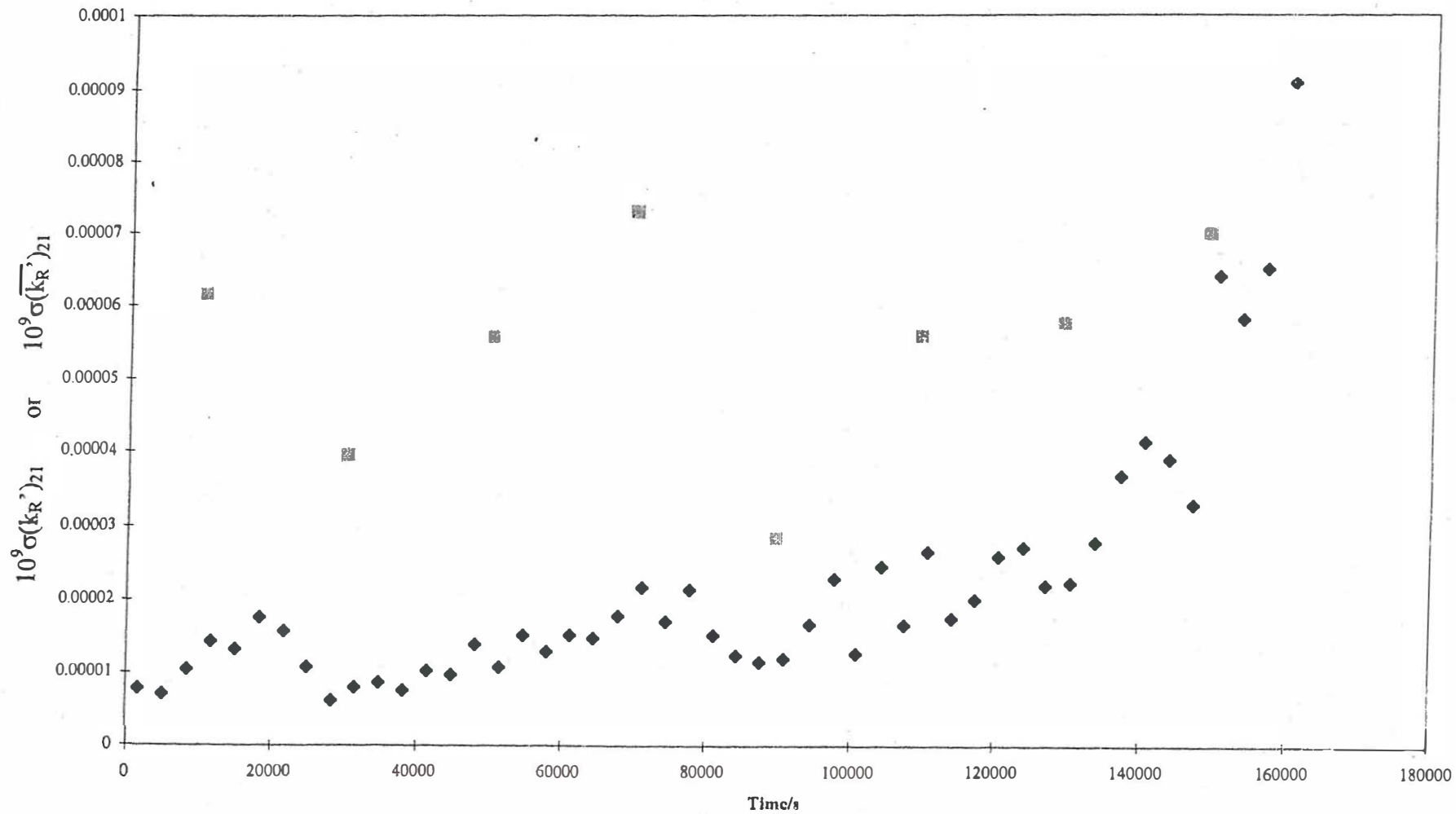


Fig. 17 The standard deviations of the integral lower bound heat transfer coefficients $10^9 \sigma(k_R')_{21}$, ◆, and $10^9 \sigma(\overline{k_R}')_{21}$, ■, Days 1 and 2 of the measurement cycles.

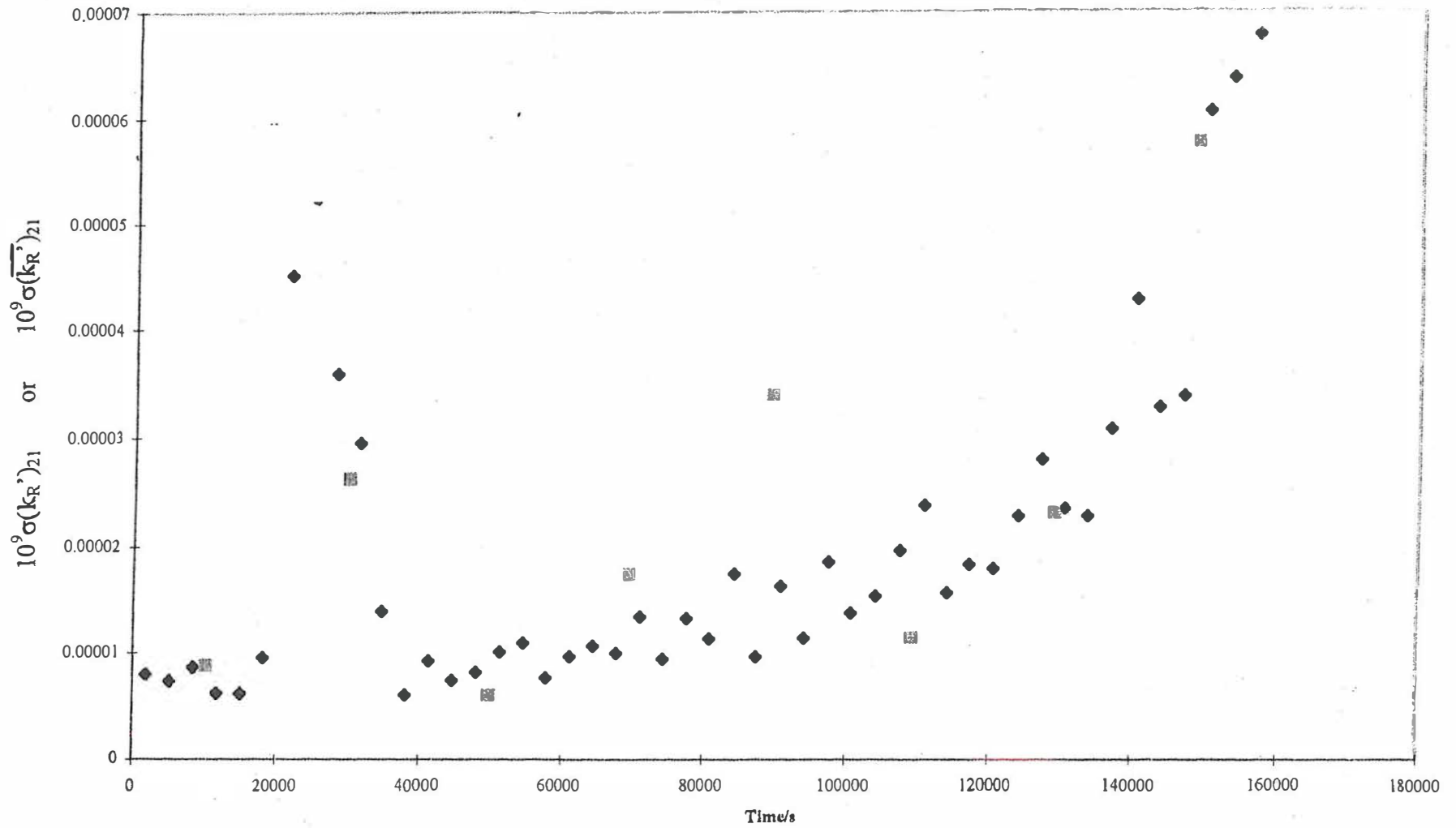


Fig. 18 The standard deviations of the integral lower bound heat transfer coefficients $10^9 (k_R')_{21}$, ◆, and $10^9 (\overline{k_R'})_{21}$, ■, evaluated about the median centre lines. Days 1 and 2 of the measurement cycles.

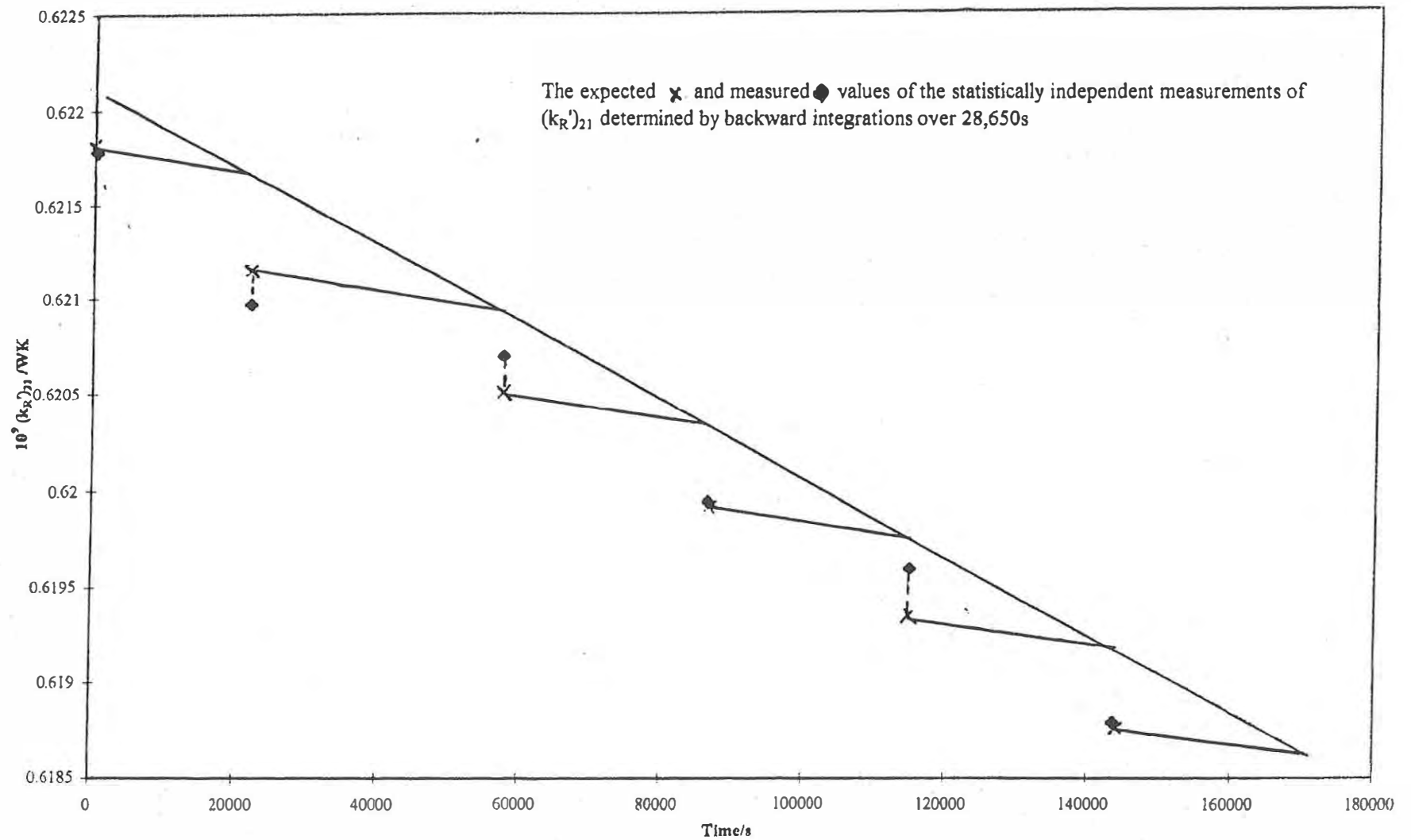


Fig. 19 The expected, \times , and measured \blacklozenge values of the statistically independent measurements of $(k_R')_{21}$, determined by backward integrations over 28,650s time intervals.

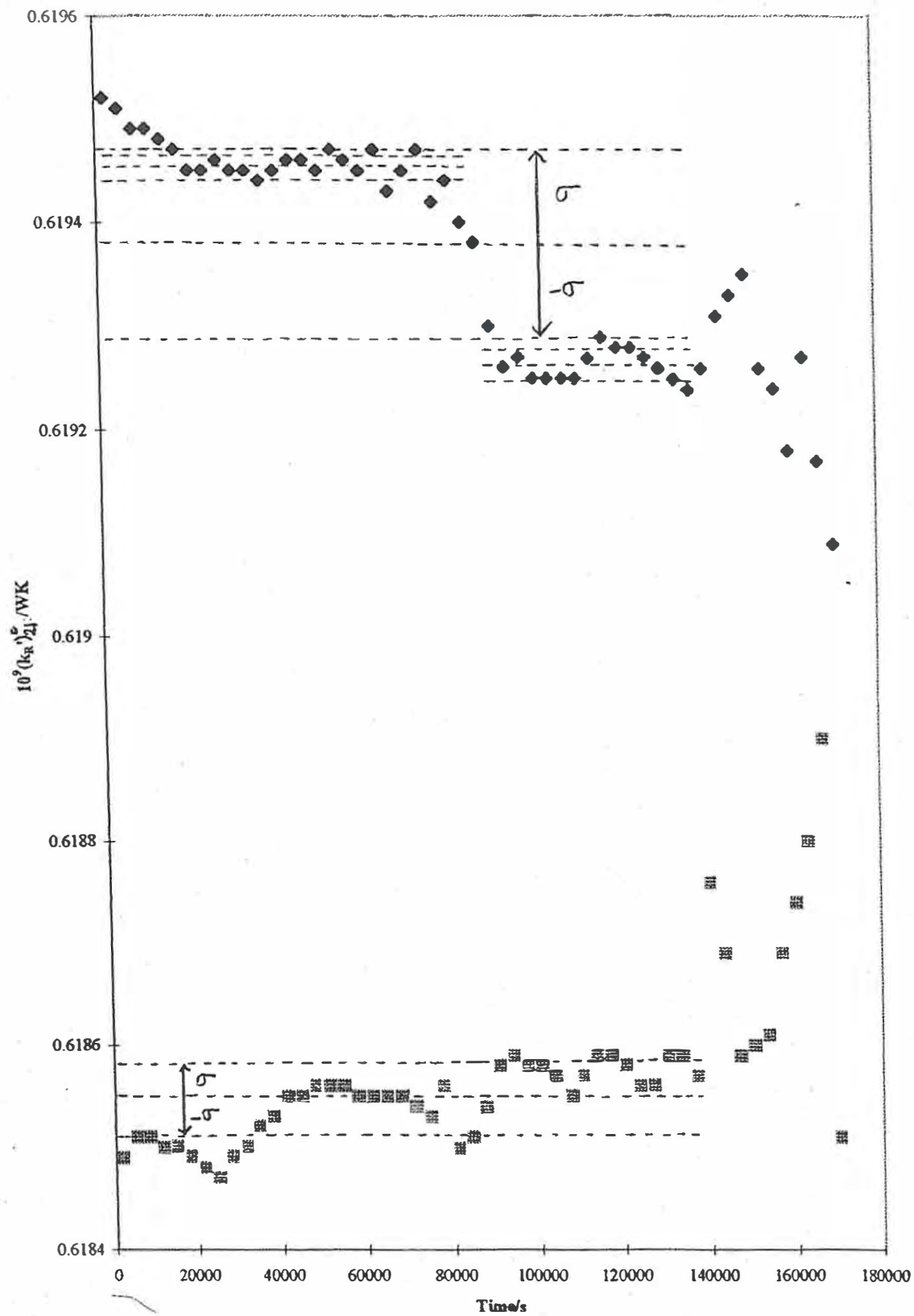


Fig. 20 The variation of derived value of $(k_R')_{21}$, with time (equation (A.13)). Data for days 9 and 10, ♦, and for days 1 and 2, ■

TABLE 1 Summary of some important values of the heat transfer coefficients.														
	ICARUS	METHOD				ICARUS	METHOD							
1	2	3	4	5	6	7	8	9	10	11	12	13	14	15
	$10^9(k_R)_1$	$10^9(k_R)_2$	$10^9(k_R)^0_{251}$	$C_p M$	$10^9(k_R)^0_{261}$	$C_p M$	$10^9(k_R)^0_{262}$	$C_p M$	$10^9(k_R)^0_{21}$	$10^9(k_R)^0_{271}$	$C_p M$	$10^9(k_R)^0_{361}$	$C_p M$	$10^9(k_R)^0_{362}$
Days	/WK ⁻⁴	/WK ⁻⁴	/WK ⁻⁴	/JK ⁻¹	/WK ⁻⁴	/JK ⁻¹	/WK ⁻⁴	/JK ⁻¹	/WK ⁻⁴	/WK ⁻⁴	/JK ⁻¹	/WK ⁻⁴	/JK ⁻¹	/WK ⁻⁴
	near t=t ₂	near t=t ₂	near t=0	r	near t=t ₂	r	near t=t ₂	r	at 129,000s		r	evaluation	r	evaluation
												near t=t ₁		near t=t ₁
1 and 2			0.6215	-349.8					0.619035					
				-0.99961										
3 and 4	0.61913	0.61706	0.62179	-331.6	0.61953	-348.6	0.6196	-397.4	0.618326	0.61884	-322.5	0.63367	-282.1	0.8132
				-0.99955		-0.99975		-0.99977			-0.99993		-0.98786	
5 and 6	0.62056	0.62016	0.62177	-348.2	0.62115	-340.2	0.62124	-339.1	0.619428	0.61976	-327.7	0.62719	-310.2	0.70098
				-0.99961		-0.99991		-0.99993			-0.99999		-0.99862	
7 and 8	0.62043	0.62202	0.62205	-349.6	0.62123	-340.7	0.62111	-340.2	0.61979	0.61916	-326.8	0.64828	-211.4	1.15002
				-0.99987		-0.99993		-0.99992			-0.99998		-0.88512	
9 and 10	0.62049	0.62446	0.62192	-356.9	0.62087	-341.1	0.62085	-341.1	0.619579	0.61977	-330	0.62242	-341.2	0.53265
				-0.99838		-0.99993		-0.99994			-0.99999		-0.98509	
11 and 12	0.62075	0.62139	0.62207	-355.6	0.62135	-339.8	0.62133	-339.7	0.619157	0.61951	-329.7	0.63371	-273.5	0.94799
				-0.9998		-0.9999		-0.99991			-0.99998		-0.9667	
13 and 14	0.61972	0.6185	0.62172	-362.3	0.62071	-337.5	0.62101	-336.1	0.61874	0.61913	-325	0.64916	-205.2	0.94681
				-0.9995		-0.99994		-0.99994			-0.99997		-0.96089	
15 and 16	0.61985	0.62051	0.62172	-348.3	0.62065	-339	0.62064	-338.9	0.618502	0.61885	-321.8	0.61047	-408.6	-0.33424
				-0.99964		-0.9999		-0.99994			-0.99907		-0.90565	
	mean	mean			mean		mean							
	0.62013	0.62059			0.62078		0.62083							

					ICARUS METHOD
16	17	18	19	20	21
$C_p M$ /JK ⁻¹	$10^9 (k_R)^0_{361}$ /WK ⁻⁴	$C_p M$ /JK ⁻¹	$10^9 (k_R)^0_{362}$ /WK ⁻⁴	$C_p M$ /JK ⁻¹	$10^9 (k_R)^0_{31}$ /WK ⁻⁴
r	evaluation near $t=t_2$	r	evaluation near $t=t_2$	r	near $t=t_2$
-281.4	0.62032	-321.6	0.62331	-323.4	0.61886
-0.99827		-0.99891		-0.99914	
-310.9	0.62094	-341.1	0.62017	-340.6	0.62028
-0.9997		-0.99927		-0.99941	
-181.1	0.62086	-347.9	0.61934	-347.5	0.62063
-0.969		-0.99782		-0.99819	
-363.3	0.62099	-338.7	0.62131	-339.4	0.62102
-0.99973		-0.99951		-0.99952	
-242.5	0.62094	-375.7	0.61925	-375	0.62704
-0.99231		-0.99921		-0.99933	
-211	0.62041	-328.9	0.62007	-320	0.61704
-0.98956		-0.99926		-0.99808	
-580.7	0.62044	-329.9	0.61872	-332.6	0.61734
-0.98163		-0.99978		-0.99964	

Table 2									
Thermal balances using the integral heat transfer coefficient based on backward integration of the data sets.									
1	2	3	4	5	6	7	8		
Days	input $d\tau$	$10^{-9} f_i(\theta)d\tau$	$10^9(k_R')_{262}$	$10^9(k_R')_{262}$	thermal	output	equivalent		
	/J	K^4s	$/WK^{-4}$	$/WK^{-4}$	output	- input $d\tau$	excess rate		
			near $t=t_2$	near $t=0$	/J	/J	/W		
3 and 4	140501.1	226640.2	0.6187	0.6195	140403.6	181.313	0.00109		
5 and 6	141849	228529.4	0.62034	0.62114	141948.8	182.824	0.00110		
7 and 8	141774.4	228484.3	0.62021	0.62101	141891	182.788	0.00110		
9 and 10	143166.6	230672.1	0.61995	0.62075	143189.7	184.538	0.00111		
11 and 12	143956.7	231844.2	0.62043	0.62123	144028.6	185.476	0.00112		
13 and 14	145003.8	233772.4	0.62011	0.62091	145151.6	187.018	0.00113		
15 and 16	144858	233584.8	0.61974	0.62054	144948.7	186.868	0.00113		

Dr. Melvin H. Miles
807 W. Mamie Ave.
Ridgecrest, CA 93555
Phone: 760-375-9258 home
Cell Phone: 760-608-3093
E-mail: melmiles1@juno.com

Martin Fleischmann

Blundel

Dave Nagel
Matt McCann
Mike McCann
Talbot Chubb
Scott Chubb

Pam Boss

September 5, 2006

Jed Rothwell, Steve Krantz, Charles Beaudette,
Ed Storms

Dear Cold Fusion Authors,

I have tried very hard to get an important manuscript that was written by Martin Fleischmann to be published by the Journal of Physical Chemistry. This manuscript is a more detailed version of the paper in ICCF-10 Proceedings, pp. 247-268. The Editor (George C. Schatz) sent this manuscript out for review, but he obviously selected only cold fusion critics. The publication of this manuscript in a major journal would be a major step in gaining acceptance for cold fusion calorimetry and the earlier work of Fleischmann and Pons.

I asked the Editor outright if he would publish this manuscript if I could completely refute the reviewer's comments, but his response was that this battle would likely not work for this manuscript. Nevertheless, I submitted my full rebuttal of the reviewer comments. The Editor sent my rebuttal to the reviewers, but he informed them that they need not respond to my rebuttal. Therefore, no response has been received. I would like to make my battle with these reviewers public because I am certain that they cannot defend their negative comments regarding this manuscript by the use of any scientific principles.

Please let me know how to proceed to make this matter public. Furthermore, you may use this material in any manner you want. Should I post this to the CMNS group?

The following are attached:

1. November 1, 2005 letter to George C. Schatz with manuscript. November 8, 2005 – received email response assigning Manuscript #JP058292J.
2. March 6, 2006 comments from Reviewers 65 and 69. I am forwarding the email of the reviewer comments.
3. My March 14, 2006 reply to the editor to point out the unfair bias of the two reviewers selected.
4. March 30, 2006 reply by the two reviewers to what I thought was a private letter to the editor.
5. April 17, 2006 reply of this editor to my asking if this was a winnable battle.
6. My June 4, 2006 letter to the editor along with my full rebuttal to each reviewer.
7. My July 16, 2006 email asking for the reviewers to respond to my rebuttal.

8. The July 24, 2006 reply from the editor informing me that he had told the reviewers that they did not need to respond to my rebuttal and that the matter was closed.

Dr. Melvin H. Miles

Dr. Melvin H. Miles
Department of Chemistry
University of La Verne
1950 3rd Street
La Verne, California 91750
909-593-3511 Ext. 4646
mmiles@ulv.edu work
Work Fax: 909-392-2754

November 1, 2005

George C. Schatz
Editor, The Journal of Physical Chemistry
Department of Chemistry
Northwestern University
Evanston, IL 60208-3113

Dear Dr. Schatz,

Enclosed are three copies of a manuscript titled "The Precision and Accuracy of Isoperibolic Calorimetry as Applied to the Pt/D₂O System" to be considered for publication in the Journal of Physical Chemistry B. Although Martin Fleischmann (Fellow Royal Society) is the main author, I have studied this manuscript extensively and agree that the reported calorimetry is correct and accurate as stated. Therefore, this calorimetry should be of interest for the study of a variety of electrochemical reactions. Please note that I have previously reported on related calorimetric studies (J. Phys. Chem., Vol. 98, No. 7, pp. 1948-1952, 1994).

Although editors and reviewers may want to reject this manuscript based on the dreaded words "cold fusion", please note that these words are seldom used in this manuscript, and there are no claims of excess heat or other anomalous effects. Therefore, the authors hope that this manuscript can be evaluated simply on known principals of physical chemistry. When the correct data analysis is applied, then the accuracy of this calorimetry should approach the accuracy of the temperature measurements, i.e. about 99.99%. Similar to the differential equations of chemical kinetics, it should be obvious that integration gives more accurate constants than the use of the differential equation.

I hope that this manuscript can be divorced from the paranoia of cold fusion and evaluated purely on its scientific correctness.

Sincerely,

Dr. Melvin H Miles
Visiting Professor
University of LaVerne

encl.

From: Davine – Journal of Physical Chemistry

To: mmiles@ulv.edu

Date: Mon. 06 Mar 2006 17:59:58 -0600

Dear Dr. Fleischmann:

Enclosed are two reviews of your manuscript. As you can see, the reviewers are very critical concerning the technical details of your experiment, and the analysis of your results. In view of this, I have decided to reject your paper.

Sincerely,

George C. Schatz
Editor-in-Chief

Reviewer 65 - See attached pdf file.

Reviewer 69

JP058292J-28-594

Remarks on M. Fleischmann and M.H. Miles, "The precision and accuracy of isoperibolic calorimetry...", This paper is far too long and if indeed to be published, should be roughly halved in length. It has a number of problems, as outlined below. All in all, the paper is very unreadable, as much seems to be assumed understood rather than specified. Is it a report of new results? Is it a reanalysis of old results? This should be made clear. The statement on page 1, that the "experiments reported in this paper are closely related to those which we have reported previously" does not tell us.

1. There is no indication of where the data comes from. Is this recycling of 1990 data or if not, where were the measurements taken? There is virtually no detail on the experimental conditions, materials, control circuitry etc. On p.4, NMR results are named to confirm the absence of isotope separation (which will be a surprise to electrochemists); where are these results from? Carried out by the present authors in the course of this work, or where?
2. P.2. point (i): Heat transfer is said to be controlled by radiation, but there are other known heat paths, by conduction, and a major heat transport contribution by the effluent gases is entirely ignored. Can it be justified to assume even "pseudo" pure radiation heat transfer behaviour? This needs at least to be justified. Even the detailed analysis in ref (2) mentions conductance as significant.
3. P.3 point (v), uniform temperature. This reviewer has checked through Britz's Cold Fusion Bibliography, currently containing 1356 entries, of papers in refereed journals. A quick search through this finds at least four papers in which temperature gradients in such cells as were used here were noted. The authors of the present paper do show two thermistors in Fig. 1, but they are

not referred to otherwise. If the two thermistors always agreed perfectly, this should be stated. More likely, there were temperature fluctuations at both thermistors, but at least the means and standard deviations should be shown to be the same, within the error.

4. P.4 point (viii), no parasitic reactions? At least one comes to mind, the deposition of Li. There is a good number of papers (again to be found by a search through the bibliography) of papers reporting such deposition, up to about 1%at. This may not contribute significantly to heat generated, but that should be mentioned and discounted with reasons given.

5. On the same page, point (ix), it is stated that effluent gases show close to 100% current efficiency, and also that the heavy water that needed to be added also showed the same. This was surely much less accurate a measurement? How was it made, within what precision?

6. p.5, Measurements and interpretation: Fig. 2 shows "raw data"; as asked for above, from what experiments? Old work, or newly performed work by the authors? It seems also unfortunate that a Pt cathode is used to calibrate the system. The authors are no doubt aware that Storms has claimed that excess heat can also happen on Pt cathodes (this can be seen on the LENR CANR website). This should at least be mentioned and reasons given why this does not matter here. This applies also to "blank systems" on p.17. Also, the perturbations mentioned have not been described. Are they current steps, or what? In fact, it does not seem that it has been mentioned anywhere whether current or potential was controlled, except perhaps in the word "galvanostat" in a later figure. Will all readers of this journal know what that is?

7. P. 9 equation (3), the symbol is introduced, but this reviewer finds nowhere a definition of it.

8. P. 9 eqn (A14) and (A15) on page 10. These are copies of the same equations in the Appendices, and should simply be referred to here, not reproduced.

9. Figs. 5, why the sawtooth shape? More unspecified perturbations?

10. Figs. 7-14 seem too many similar figures. Here is one place where much bulk can be saved, by presenting just one, and simply describing the results of the others. The intercepts these figures produce can be tabled, along with their SD values.

11. P.12 et al; a largish number of possible methods are described and discounted. It seems to this reviewer that they need only be briefly mentioned as possibilities, without detailed description, equations or results, and focus can then be directed on the one method that was found to be best. This would again save much bulk.

12. P. 12 Footnote (8) Where are these Hydrogen Energy Laboratories? They do not appear anywhere else in the paper.

13. P. 13, Fig. 15 is not really needed either; a few words would suffice, along with mention of Fig.1. Likewise, Fig. 16 could be replaced by a simple statement that the error takes the value 0.002, rather steady with time.

14. P.15 line 3 from "We observe..." How does the very precise figure 0.1 mW relate to the error introduced by heat carried out by effluent gases? One suspects that it should be much larger.

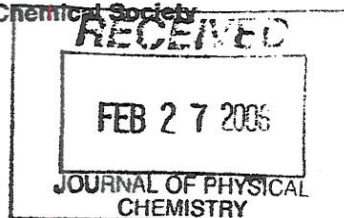
15. Pp.16, 17: "Wild statements have been made..." Where have these been made? References are needed. Bland statements like this are themselves wild.

16. Reduction at the cathode of oxygen produced at the anode is mentioned, and the paper by Will is referred to. There have however been some papers by Shanahan in *Thermochim. Acta*, suggesting that the very good mixing of the cell's contents can result in merging of deuterium and oxygen bubbles and their transport to the electrodes, there to recombine, catalysed by the electrode metals. This possibility was not included in the Will paper. The authors should address this possibility.



THE JOURNAL OF PHYSICAL CHEMISTRY

Published by the American Chemical Society



Reviewer: 69

Ms. No.: JP058292J-28-594

Author(s): Martin Fleischmann*, M. H. Miles*

Title: The Precision and Accuracy of Isoperibolic Calorimetry as Applied to the $\text{Pt/D}_2\text{O}$ System

PLEASE RETURN SIGNED ORIGINAL WITH MANUSCRIPT AND ONE ANONYMOUS COPY BY: **FEB 28, 2006**

Instructions to reviewers: Your frank answers to the items below will assist the editors greatly. Detailed criticisms of the manuscript should be placed in the spaces provided.

Specific suggestions regarding minor points in style, grammar, etc. may be made in pencil directly on the manuscript. If such suggestions are made, please note below on which pages these occur.

Your specific comments, keeping in mind the following criteria, would be appreciated.

CRITERIA: New physical insights or extremely important results

Conclusions adequately supported by data

Clarity

Length

Number and quality of illustrations and tables

Appropriate referencing

COMMENTS: (Use additional pages, if necessary)

See attached.

Recommendations regarding this manuscript:

1. ☐ This paper represents a significant new contribution, and should be published either as is, or subject to minor revisions as indicated below.
2. ☐ The paper is probably publishable, but should be reviewed again in revised form before it is accepted.
3. ☒ This paper is not recommended because:
a) it does not provide new physical insights ___; or
b) the material is not appropriate for *The Journal of Physical Chemistry* ___; more appropriate journals are:

Poor execution of experimental work, incorrect analysis, and wrong conclusions.

PLEASE SIGN ORIGINAL ONLY :

In this field, I believe this paper fell within the top 20% ___; top 50% ___; bottom 50% ___; bottom 25% ___.

The precision and accuracy of isoperibolic calorimetry as applied to the Pt/D₂O system.

This paper promulgates the same calorimetric measurement error made by Pons and Fleischmann in their original work. To make accurate measurements of heat rates with a heat conduction calorimeter, the temperature difference between the system and surroundings must be measured across the major path for heat transfer. (The authors need to read some of the classic works by Tian and Calvet and Wadso.) In the original work Pons and Fleischmann measured temperatures inside their Dewar (similar to this study) standing in a dishpan of water, and assumed the rate of heat production inside the Dewar was a function of the temperature difference between the water in the dishpan and inside the Dewar. They thus assumed the major heat transfer path was through the walls of the Dewar into the water. However, the main path was through the electrical leads. The water temperature in the dishpan was essentially irrelevant to the rate of heat production inside the Dewar.

The calorimeter system described in this paper is a poorly designed and incorrectly analyzed, isoperibol, heat-conduction calorimeter. The basic assumption made in analyzing the data is that the main path of heat transfer from the system (the solution inside the Dewar) to the surroundings (the water bath) is through radiative heat transfer, i.e. “the conductive contribution to heat transfer is very small.” (Appendix) No evidence to support this assumption is given other than that the result “is close to the value determined by the calibrations.” Although no data are given on the dimensions of the silver on the Dewar, electrical leads and other connections between the system and surroundings, or the room temperature, I suspect a simple calculation of thermal conductivities of these paths would show they are more significant than radiant transfer. (The authors need to read a paper by Christensen and Izatt in *Scientific Instruments* and another by Wadso on the effects of Dewar design on the apparent time constant of thermal conductivity between the inside of the Dewar and the surroundings.)

Clarity. The clarity of the paper is poor. The word "isoperibol" means constant surroundings, and does not describe the principle used for heat measurement. The measurement method is based on heat conduction and follows the law for heat transfer, i.e. $dQ/dt = \kappa \Delta T$ + Tian correction during transients or the Stefan-Boltzmann law if heat transfer is solely by radiant energy (a condition that is very difficult to achieve).

Length. From page 5 on, the paper is far too long and confusing. Henry Eyring once said research was like finding a path through the woods. First, you cut down all the trees, find the path, map the path, put all the trees back up, and then write a paper describing the path. These authors want to tell us about every tree they cut down, not just where the path is. Twenty figures is indigestible. And, to submit a table with handwritten notes! The purpose seems to be to overwhelm the reader with so much data, that they forget where they are going. Convince me with logic and reason, not with masses of numbers and incorrect statistical analyses. The authors need to try for clarity, not obfuscation. The claim of 99.99% precision and accuracy is unbelievable.

Referencing. The references are inadequate. References 3, 6, 10, and 11 are not readily available. No references to any papers critical of cold fusion are given, nor are there any references to classical works on calorimetry.

Specifics.

Isoperibolic calorimetry in the title means little since it only says the calorimeter is in a constant environment. What is the heat measurement principle? Temperature rise, heat conduction, and power compensation (including phase change) are the only possibilities.

It is doubtful that the contents of the calorimeter are always at a uniform temperature considering the large heat inputs and evaporative losses in the gas flow,

The heat sink consists not only of the water bath, but also the lid a room. How are the leads, etc. thermally connected to the room? What temperature is the room?

How does the electrolyte used ensure that there were no parasitic reactions?

How was it confirmed that the volumes of the gases evolved agreed to within 1% of those calculated?

Item (x) makes me wonder if the system was operated and analyzed as a steady state system, or as a transient system? The analysis appears to be a mixture, but it is certainly not clear.

Item (xii) indicates the lead wires were insulated from the room, so the heat sink for these heat transfer paths are the connections to the power supply, etc.

Use of T for time is a poor symbol.

Kel-F is electrochemically active, being used as the anode in some batteries. Is this a problem?

Since the wrong model (radiation only) was used to analyze the data, the remainder of the paper needs no further comment.

Dr. Melvin H. Miles
Department of Chemistry
University of La Verne
1950 3rd Street
La Verne, California 91750
909-593-3511 Ext. 4646
mmiles@ulv.edu work
Work Fax: 909-392-2754

March 14, 2006

Email: Davine – Journal of Physical Chemistry

Dear Dr. Schatz

I have studied your reviewer's comments and agree with some of them. The paper was too long, but I thought that many of the figures could be published as supplementary materials. The clarity of this paper could also be improved. However, many reviewer comments are simply wrong. The following is a list of some of these erroneous comments. I will call them Reviewer 1 and Reviewer 2 because it is not clear to me which comments belong to Reviewers 65 and 69.

Reviewer 1

1. The major heat transport contribution by the effluent gases was not ignored. This term is clearly defined in Equation A.1 of the Appendix. This major false statement alone should disqualify this reviewer. The entire paper is based on this differential calorimetric equation. I have published a very similar differential calorimetric equation in *J. Phys. Chem.* **98**, 1948-1952 (1994).
2. The NMR results do not confirm the absence of isotope separation. Instead, NMR results confirm the isotope separation that preferentially removes H rather than D to remove unwanted H₂O contamination from the heavy water. This helps to maintain the isotopic purity of the system.
3. Correct cell designs yield uniform temperatures. These were long and narrow cells in contrast to short and broad cells that yield non-uniform temperatures. Both thermistors yield identical results. Tests using sixteen thermistors placed throughout these cells show uniform temperatures during electrolysis.
4. Storms is alone in left field with his claim of excess heat using Pt cathodes. Any real excess heat found by Storms likely resulted from dissolution of his Pd anode and then with this Pd plating out on his Pt cathode.

Reviewer 2

1. Calling a precisely thermostatted water bath a "dishpan of water" is unprofessional and demeaning. The temperature in this bath was controlled to better than $\pm 0.01^\circ\text{C}$. This comment alone shows this reviewer's unscientific prejudice, hence his comments should be tossed. Obviously, the rate of heat production inside the Dewar is independent of the constant temperature of the bath.
2. The close agreement of the experimental heat transfer coefficients with values theoretically calculated using the Stefan-Boltzmann constant (p. 3) proved that the heat transfer occurs mainly by radiation (not conduction).

I have read previous false statement by Steve Jones of BYU stating that Kel-F is electrochemically active. If you selected either Steve Jones or Lee Hansen of BYU as reviewers, then you guaranteed yourself a very negative review. Apparently, this is the easy way out for editors who receive cold fusion papers. Quite different reviews could be obtained from Dr. David J. Nagel of The George Washington University, Dr. Michael Melich of the Naval Postgraduate School, Dr. Michael McKubre of SRI International, Dr. Peter L. Hagelstein of MIT, Dr. John Dash of Portland State University, Dr. Scott R. Chubb of the Naval Research Laboratory and many others. Please try to prove me wrong by sending this manuscript to some of these scientists who may actually understand the basic calorimetric equation that is the focus of this paper.

Sincerely,

Dr. Melvin H. Miles

From: Davine – Journal of Physical Chemistry

To: mmiles@ulv.edu

Date: Thu. 30 Mar 2006 14:06:57 -0600

Dear Dr. Miles:

Enclosed are comments from the two reviewers of your manuscript. As you can see, neither reviewer feels you have enough of a case to proceed. After looking this over, I have decided not to consider your paper further.

Sincerely,

George C. Schatz
Editor-in-Chief

Reviewer 65

Well he got me on the first point; there was indeed a heat term in (A1) from evolved gases, which I had overlooked (I plead length and organization of the paper). In the text, however, it says that radiation controls heat transfer, so it seems that this term is thrown out after getting mentioned, without much explanation given.

On the NMR point, the text is at best confusing, seeming to state that the isotopic composition of the water is preserved. This implies no separation, which would gradually change the composition - as is indeed made use of in industry, I believe.

All in all, Miles has not made much of an effort here. He does not address most of the points I made, and where he does, and partially agrees, makes no promises of altering the paper accordingly. He sticks to rubbishing the referees and asks for others, clearly all people who have promoted cold fusion.

Reviewer 66

Agreement between the calculated Stefan-Boltzmann heat transfer coefficient and the measured heat transfer coefficient does not prove that radiation is the major mode of heat transfer. It is only fortuitous that the constants for radiation and conductance come out about the same. The authors made no attempt to even calculate the conductance. The "basic calorimetric equation" used to describe the system in this paper is simply wrong, and playing games with reviewers will not correct that error no matter how much Miles wishes it to be.

To: Mel and Linda Miles <melmiles1@juno.com>

Date: Mon. 17 Apr 2006 10:44:06 -0500

Dr. Miles:

I appreciate your frank discussion. To be honest, I feel this battle is probably not going to work for this manuscript.

Sincerely,

George C. Schatz
Editor-in-Chief

Dear Dr. Schatz

My previous brief comments to you were simply to show that, in my opinion, the two reviewers were not qualified to review this manuscript based on some of their statements. My comments to you were intended to be private and were not to be considered as my rebuttal to the reviewers.

However, it was my mistake to not have stated this clearly. As a matter of fact, I am quite willing to write a full rebuttal for the two reviewers. I am confident that I can completely refute nearly all their statements by using basic principles found in physical chemistry textbooks. However, my recent bout with cancer makes me realize that life is too short to waste time fighting unwinnable battles. I understand perfectly why you may not want to publish any manuscripts related to cold fusion. Therefore, I would like to know that you would actually publish a shortened revised manuscript after I win this battle with the reviewers. Martin Fleischmann is a genius, a Fellow of the Royal Society, and a man ahead of his times. Very few people understand correctly his calorimetric equations and complicated data analyses methods, but that does not make them wrong. Contrary to erroneous reviewer statements, the rate of enthalpy loss due to the evolved gases is included throughout these calculations. Professor Fleischmann's end result of 1.1 mW power due to the reduction of the electrogenerated oxygen agrees with theoretical calculations for this system. There is no cold fusion occurring in this Pt/D₂O system.

If you can honestly assure me that this is not an unwinnable battle, then I will prepare full rebuttals for these two reviewers.

Sincerely,

Dr. Melvin H. Miles

**Dr. Melvin H. Miles
Department of Chemistry
University of La Verne
1950 3rd Street
La Verne, California 91750
909-593-3511 Ext. 4646
mmiles@ulv.edu work
Work Fax: 909-392-2754**

June 4, 2006

Dear Dr. Schatz,

I realize that due to the political nature of the subject matter of Manuscript JP058292J that it will probably never be published by the Journal of Physical Chemistry. Nevertheless, for the record I should be entitled to give formal rebuttals to the comments of the two reviewers and to receive their responses. My previous brief comments were intended as private comments to you relating to the bias of the referees selected.

Please transmit my full rebuttal to the reviewers and ask them to respond. The reviewers should respond to the specific comments using scientific principles rather than stating generalities.

Sincerely,

Dr. Melvin H. Miles

Major heat transport contribution by the effluent gases is entirely ignored.

The rate of enthalpy removal by the gas stream is clearly identified in Equation A.1 (Appendix). The most important contribution is the enthalpy of evaporation of D₂O, L. Therefore, this term is defined as

$$\Delta H_{\text{evap}} = \frac{3I}{4F} [P/(P^* - P)] [(C_{p,D_2O(g)} - C_{p,D_2O(l)}) \Delta \theta + L]$$

The term is present in Equations A.4 and is included in every equation where “net enthalpy input” is shown. Therefore, this reviewer’s later statement that this term is thrown out after getting mentioned is completely false.

The exact expression for the rate of enthalpy transfer due to the D₂, O₂, and D₂O gas stream is given by Eq. 2 in J. Phys. Chem., Vol. 98, p. 1949 (1994). Quoting from my previous publication: “accurate results require the evaluation of all terms in the differential equation governing the calorimeter”. This differential equation is Eq. 1 in the 1994 publication and Eq. A.1 in this present manuscript. It is unreasonable for the reviewer to assume that the heat transport by the effluent gases is entirely ignored when both authors have always emphasized the importance of this term in previous publications such as J. Phys. Chem., Vol. 98, pp. 1948-1952 (1994). Reducing calorimetric errors to ±0.01% (±0.0001 W) as reported in this manuscript would certainly not be possible if heat transport by the effluent gases were ignored as claimed by this reviewer.

Because the reviewer apparently does not understand the basic calorimetric differential equation, I would like to point out that integration of the data, such as shown in Equation A.12, yields much better results. This should be obvious from differential equations encountered in chemical kinetics. Furthermore, Equation A.12 is in “straight line form” where “y” is the first term, $(k_R')_{262}^0$ is the intercept “a”, and the slope “b” equals C_pM. Now look at the excellent straight line for the experimental data in Fig. 9 that proves that accurate values for $(k_R')_{262}^0$ and C_pM can be obtained from this integration of the experimental data. Once again, the rate of enthalpy removal by the gas stream was included in these calculations. This reviewer needs to show exactly what errors, if any, were made by this use of Equation A.12.

Temperature gradients in such cells as were used

Uniform cell temperatures are certainly important and this will depend on the cell geometry. Stirring only by the gas evolution would be a serious problem for short, fat cells used by MIT, Caltech and others in early studies. Problems of temperature gradients in cells used by other laboratories does not directly translate to problems for our cells. The long and narrow design described on p. 3 eliminates this problem. The measured radial and axial mixing times of 3 seconds and 20 seconds compared with the thermal relaxation time of 5000 seconds proves that temperature gradients are not a problem. We have placed as many as 16 thermistors throughout the cell to prove this point. Each cell always contains at least two thermistors. Identical temperatures are measured with thermistors that are properly calibrated. The same calorimetric results are always obtained with the data from either thermistor. Finally, Figure 2 present actual

measurements of the cell temperature and the fluctuations are small. Averaging procedures (p. 16) reduce even this small error in temperature measurements to yield final calorimetric errors of only $\pm 0.01\%$.

Heat transfer is said to be controlled by radiation, but there are other known heat paths. Can it be justified to assume even “pseudo” pure radiation heat transfer behavior?

We have already covered the heat transport by the effluent gases represented by ΔH_{evap} . This leaves only heat transport by radiation and conduction because the cell is in a thermostatted bath where convection is not a factor. In terms of power, P , in J/S or W

$$P = k_R (T_{\text{cell}}^4 - T_{\text{bath}}^4) + k_C (T_{\text{cell}} - T_{\text{bath}}) = k'_R (T_{\text{cell}}^4 - T_{\text{bath}}^4)$$

Obviously, as $k_C \rightarrow 0$, then $k'_R \rightarrow k_R$. Based on the Stefan-Boltzmann coefficient and radiant surface area as discussed on p. 16

$$k_R = 5.6703 \times 10^{-12} \text{ Wcm}^{-2}\text{K}^{-4} (109.7\text{cm}^2) = 0.6220 \times 10^{-9} \text{ WK}^{-4}$$

It should be obvious that $P_R/P = k_R/k'_R$ where P_R is the power transferred by radiation and P_C is the power transferred by conduction. If only 50% of the power were transferred by radiation, then k'_R would be twice as large as k_R . The close agreement of the experimental k'_R values shown in Table 1 with k_R calculated above proves that the heat transfer by conduction is quite small compared with the heat transfer by radiation ($P_C \ll P_R$).

NMR results are named to confirm the absence of isotope separation.

As stated on p. 4, the operation of the cells in the “open mode” imposes continuous isotopic separation of ordinary hydrogen. It is well known that water electrolysis preferentially removes H rather than D. Early methods of preparing heavy water consisted of multi-stages of electrolysis. This open cell will preferentially remove H rather than D to improve the isotopic purity of the D_2O . For a closed system using a recombiner, any H_2O contamination will remain in the cell throughout the experiment. This reviewer has it backwards. NMR measurements can be used to confirm the presence of this isotopic separation in open cells.

The authors are no doubt aware that Storms has claimed that excess heat can also happen on Pt Cathodes.

I have a recent email from Ed Storms stating that his results were obtained using a palladium anode. Storms agrees that the dissolution of his palladium anode and the deposition of this palladium onto his Pt cathode explains his results. The simultaneous deposition of palladium ions and deuterium from D_2O solutions onto an inert substrate (co-deposition, see S. Szpak and P. Mossier-Boss) is one of the best methods for the production of excess heat.

Fig. 5, why the sawtooth shape? More unspecified perturbations?

Again, the reviewer has not carefully read p. 8 that explains this shape. The sawtooth shape is due to the use of the differential equation rather than integration of the data and assumptions

made about the time dependence of the true heat transfer coefficients. Due to electrolysis and the decreasing electrolyte levels, the heat transfer coefficients change with time (see Equations A.2 and A.3 as well as J. Phys. Chem., 98, 1948-1952, 1994). Abrupt changes occur with D₂O additions to the cell. Fig. 5 clearly shows the advantage of integration of the data (square shaded symbols). There are no sawtooth shapes and the rate of excess enthalpy generation is steady at about 0.0011 W.

There have however been some papers by Shanahan in *Thermochim. Acta* suggesting that very good mixing of the cell's contents can result in merging of deuterium and oxygen bubbles and their transport to the electrodes, there to recombine, catalyzed by the electrode metals.

The authors are aware of the Shanahan papers. One major purpose of our paper is to experimentally measure the extent of any recombination. The experimental result is clearly 0.0011 W produced by all forms of recombination (see Figs. 5A and 5B). Therefore, recombination can be ruled out as a major error source, as shown previously by Will. The experimental result is consistent with theoretical calculations based on oxygen diffusion and reduction at the cathode. It is well known that H₂ or D₂ is not oxidized at a platinum oxide anode. Even if deuterium and oxygen bubbles merge, they will not react at the anode, thus only oxygen reduction at the cathode is important. There is already a rich mix of deuterium gas at the cathode, thus any merging should be insignificant at this electrode. The results on the recombination controversy provided by this paper should be a strong argument for its publication.

I believe this addresses all of the major points raised by this reviewer. The additional comments can be readily addressed in the revision of this manuscript.

REVIEWER 69

A precise thermostated bath was always used in these experiments to control the bath temperature to within $\pm 0.01^\circ\text{C}$. A “dishpan of water” has never been used in any study by either author. This insulting and inaccurate comment clearly shows the bias of this reviewer. The water temperature in the thermostated bath (not dishpan) is obviously constant and therefore irrelevant to the rate of heat production inside the Dewar in any given experiment.

The heat transfer path through the electrical leads is readily calculated from known thermal conductivities (Pt, $0.730 \text{ W cm}^{-1}\text{K}^{-1}$). For a Pt lead of 0.5 mm diameter and 10 cm length, this yields 0.000014 W/K . For a cell temperature of 32.3°C (Fig. 2) and a room temperature of 25.0°C , we calculated an enthalpy transfer rate of 0.00015 W . This electrical lead effect is obviously much smaller than the radiative heat transfer pathway for this cell (up to 0.8 W). Furthermore, such electrical lead effects are nearly constant and can be readily included in the pseudo-radiative heat transfer coefficient. Insulation at the top of the cell prevents any power losses greater than the small value calculated for the two electrical leads. What does this leave as the major heat transfer pathway? The answer is the radiative heat transfer through the walls of the Dewar cell as stated in this manuscript.

Mathematical arguments also prove that the heat transport by radiation (P_R) is much larger than heat transport by conduction (P_C) for this Dewar calorimeter. In terms of total power (P) in W

$$P = k_R (T_{\text{cell}}^4 - T_{\text{bath}}^4) + k_C (T_{\text{cell}} - T_{\text{bath}}) = k'_R (T_{\text{cell}}^4 - T_{\text{bath}}^4)$$

Obviously, as $k_C \rightarrow 0$, then $k'_R \rightarrow k_R$. Based on the Stefan-Boltzmann coefficient and radiant surface area as discussed on p. 16

$$k_R = 5.6703 \times 10^{-12} \text{ Wcm}^{-2}\text{K}^{-4} (109.7\text{cm}^2) = 0.6220 \times 10^{-9} \text{ WK}^{-4}$$

It should be obvious that $P_R/P = k_R/k'_R$ where P_R is the power transferred by radiation and P_C is the power transferred by conduction. If only 50% of the power were transferred by radiation, then k'_R would be twice as large as k_R . The close agreement of the experimental k'_R values shown in Table 1 with k_R calculated above proves that the heat transfer by conduction is quite small compared with the heat transfer by radiation ($P_C \ll P_R$).

Comments regarding clarity and referencing can be addressed in the revision of this manuscript. Why is the claim of 99.99% precision and accuracy unbelievable? In a well-stirred calorimetric system, the precision and accuracy are limited mainly by the temperature measurements. Temperature measurements more accurate than $\pm 0.01^\circ\text{C}$ are possible. Accurate temperature measurements should result in similar accurate calorimetric results.

It is well known that Dewar vessels minimize heat transport by conduction. Thus the heat measurement principle is based on the rate of enthalpy transport via radiation through the Dewar walls into the bath. The phase change of D_2O from liquid to gas is given by “L” in Eq. A.1 (Appendix). This is the only phase change.

As many as 16 thermistors have been placed in similar Dewar cells to prove that the contents of these calorimeters are always at a uniform temperature. Furthermore, the raw data shown in Fig.

2 for cell temperature measurements every 300 seconds proves that the temperature fluctuations within the cell are small. Averaging procedures (p. 16) greatly reduce the calorimetric errors due to cell temperature measurements to $\pm 0.01\%$.

The LiOD electrolyte yields only Li^+ and OD^- ions in the D_2O solution. The only possible electrochemical reaction other than the D_2 and O_2 evolution reactions is the reduction of Li^+ . Thermodynamically, the reduction of Li^+ cannot occur in H_2O or D_2O solutions. If any lithium metal were formed electrochemically, it would immediately react with the D_2O to produce LiOD and D_2 gas ($\text{Li} + \text{D}_2\text{O} \rightarrow \text{LiOD} + 0.5 \text{D}_2$). In fact the LiOD for these experiments is generally produced by reacting lithium metal with D_2O .

The volumes of gases evolved have been measured by the direct gas displacement of water in an inverted calibrated buret. The volume of gas evolved can also be calculated by the makeup additions of D_2O .

For anyone that has followed the cold fusion calorimetry of open systems, it should be obvious that there is no steady state for these calorimetric measurements (see J.Chem.Phys. Vol. 98, p. 1948-1952, 1994). Quoting "There is no steady state in electrochemical calorimetry, so accurate results require the evaluation of all terms in the differential equation governing the calorimeter". The calorimetric analysis is based on the fundamental differential equation, Eq. A.1 in the Appendix.

The lead wires were chemically isolated from gases in the head space to prevent any recombination of the evolved gases. Glass tubing or shrink Teflon can be used to cover the bare wires. Thermal insulation was not the goal. However, the connection of these wires to the warmer power supply should help to further minimize the small heat transfer from the Dewar cell by the electrical leads.

My background is in battery research, and I have never heard of Kel-F being used as the anode in any battery. I have searched my battery books and there is no mention anywhere of Kel-F used in batteries. Kel-F is a chemically and electrochemically inert material under these experimental conditions.

Since the correct model (heat transfer by radiation) **WAS** used to analyze the data, the remainder of this paper stands as written. In summary, this calorimetric design and data analysis shows that only 0.0011 W is produced by recombination in the Pt/ D_2O system. This result on the recombination controversy should be a strong argument for the publication of this manuscript.

From: Davine – Journal of Physical Chemistry

To: "melmiles1@juno.com" <melmiles1@juno.com>

Date: Mon. 24 Jul 2006 14:46:25 -0500

Dear Dr. Miles:

I did forward your comments as requested but I left the option of replying to the reviewers. I have not received any response. I do not plan to reopen the file.

Sincerely,

George C. Schatz
Editor-in-Chief

From: Davine – Journal of Physical Chemistry

To: Mel and Linda Miles <melmiles1@juno.com>

Date: Wed, 19 Jul 2006 12:18:46 -0500

At 05:42 PM 7/16/2006 you wrote:

Dr. Schatz,

I am very interested in any scientific response to my comments that the reviewers can muster. Please remind them to reply. A non-reply will indicate that they have no rebuttal for my comments, hence this manuscript should be published if ordinary rules apply.

Dr. Miles

On Thu, 15 Jun 2006 14:58: 18 -0500 Davine – Journal of Physical Chemistry writes:

Dear Dr. Miles:

We will send your comments to the reviewers.

Thanks,

George C. Schatz
Editor-in-Chief